



## File Name:

## EPBC Referral Report No. 8 - Boskalis Cambridge Gulf - APPENDICES

Appendix A - Model Calibration and Validation Plots

Appendix B - Hydrodynamic and Wave Impact Plots

Appendix C - Sediment Transport Impact Plots

Appendix D - Sediment Plume Modelling Results

 $\underline{\textbf{Proposed action}} : \textbf{Boskalis Cambridge Gulf Marine Sand Proposal}, \textbf{Western Australia}.$ 

Proponent: Boskalis Australia Pty Ltd.

Contacts: steve@eco-strategic.com (040 9909 422), peter.boere@boskalis.com (041 9987 158)



## Appendix A – Model Calibration and Validation Plots



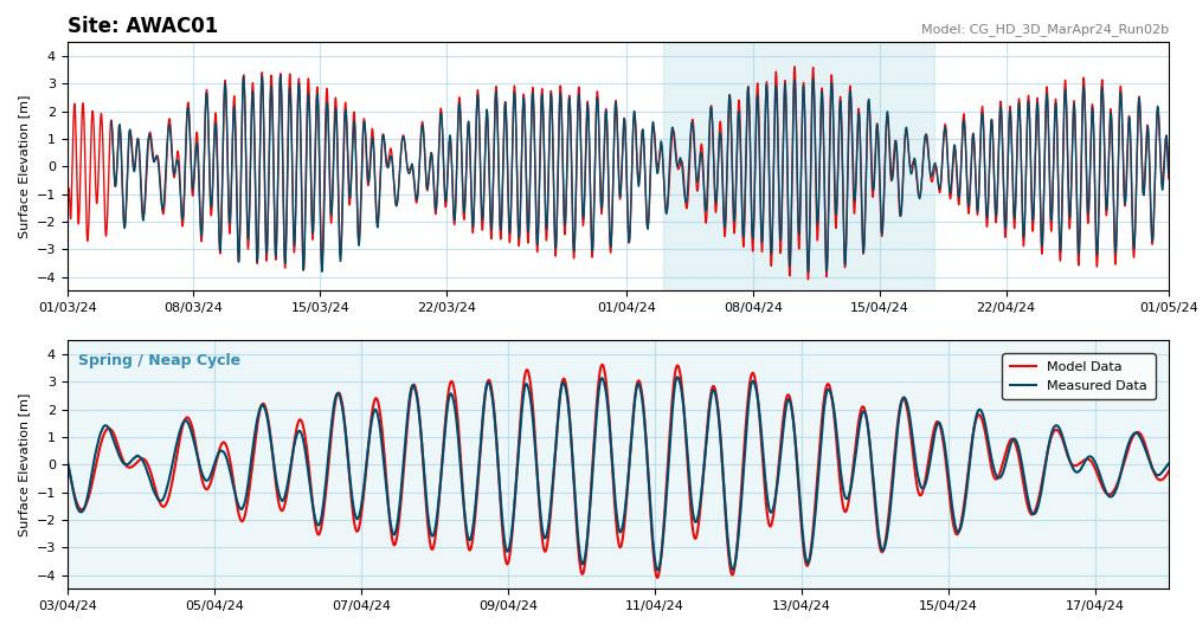


Figure A1. Modelled and measured water level at AWAC-01 over the model calibration period and selected calibration spring / neap cycle period.

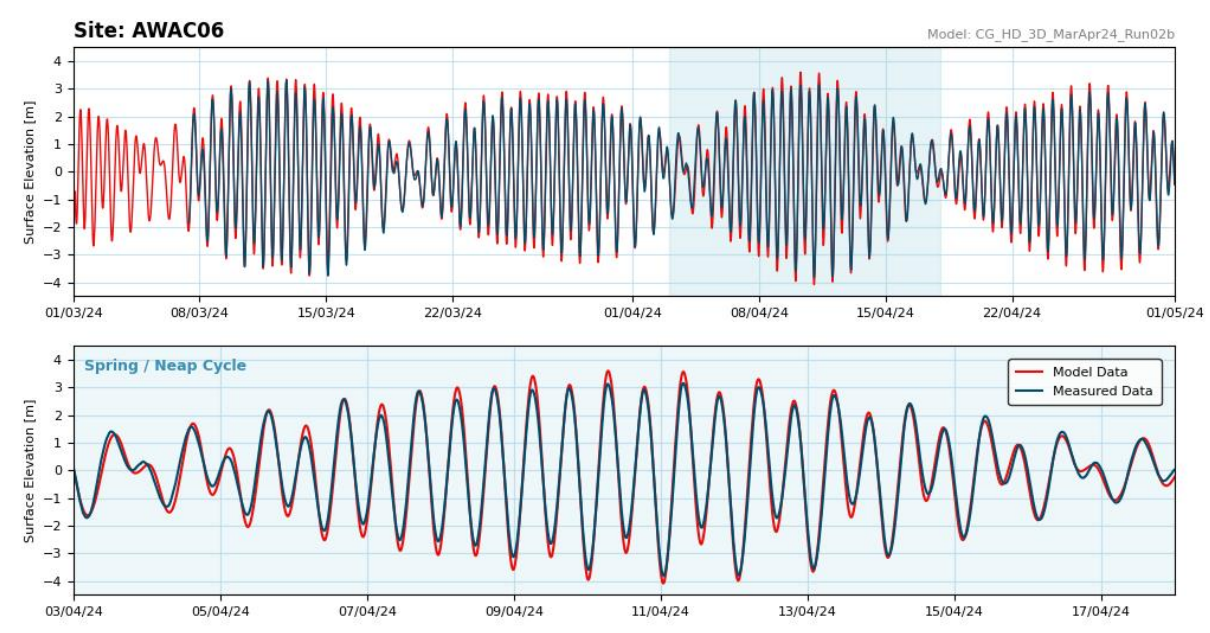


Figure A2. Modelled and measured water level at AWAC-06 over the model calibration period and selected calibration spring / neap cycle period.



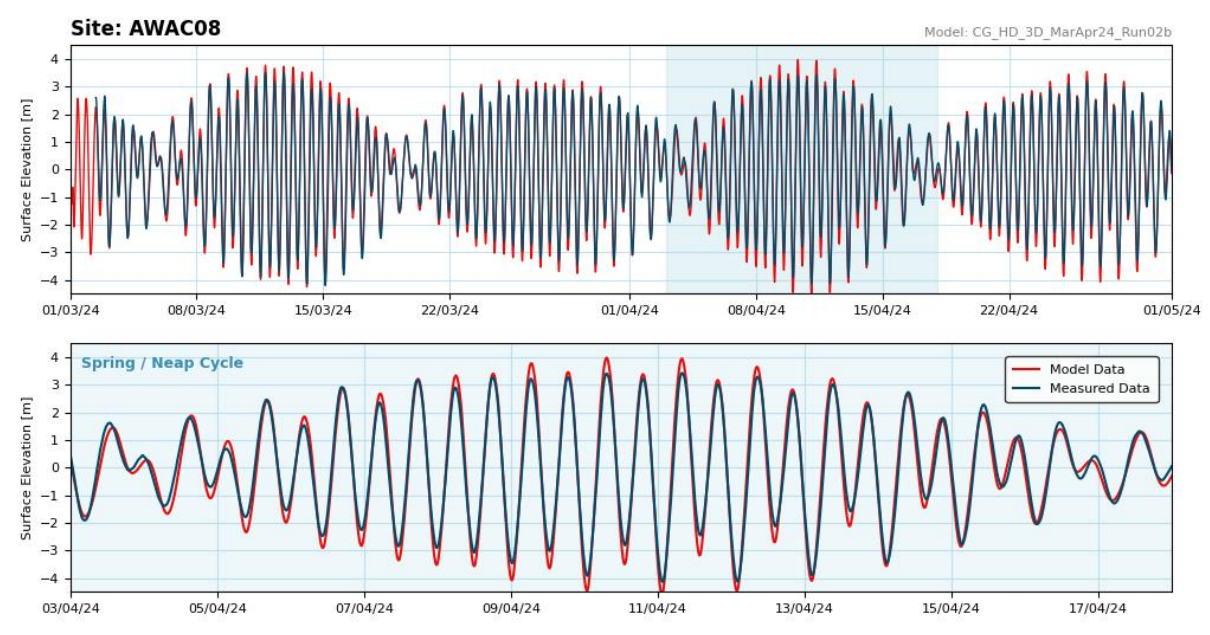


Figure A3. Modelled and measured water level at AWAC-08 over the model calibration period and selected calibration spring / neap cycle period.

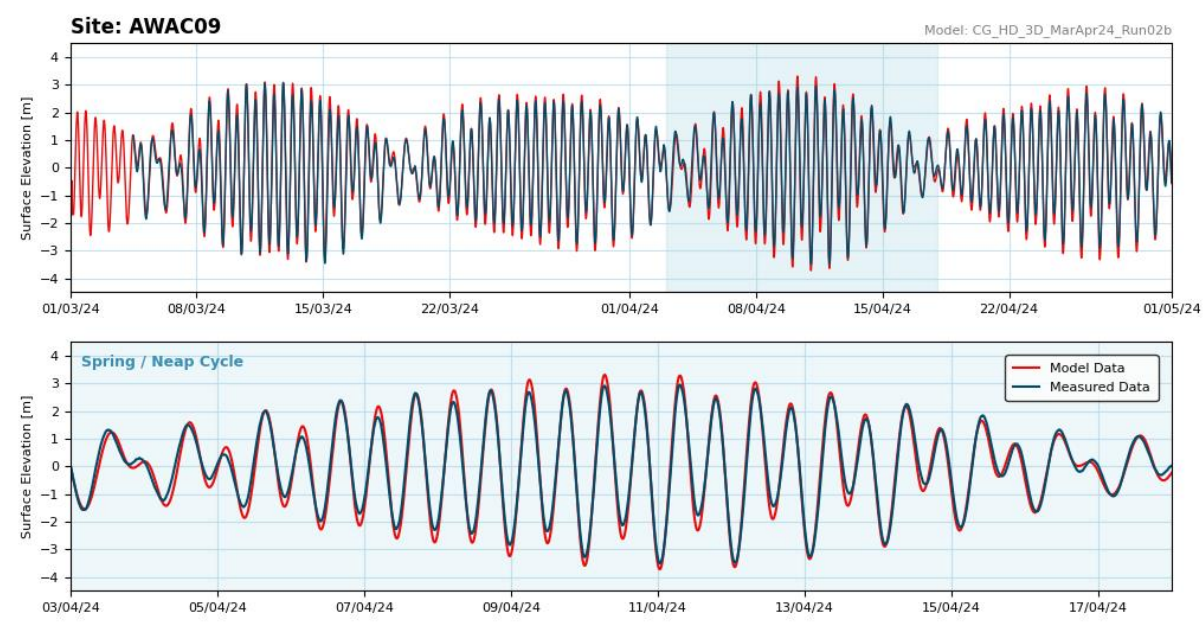


Figure A4. Modelled and measured water level at AWAC-09 over the model calibration period and selected calibration spring / neap cycle period.



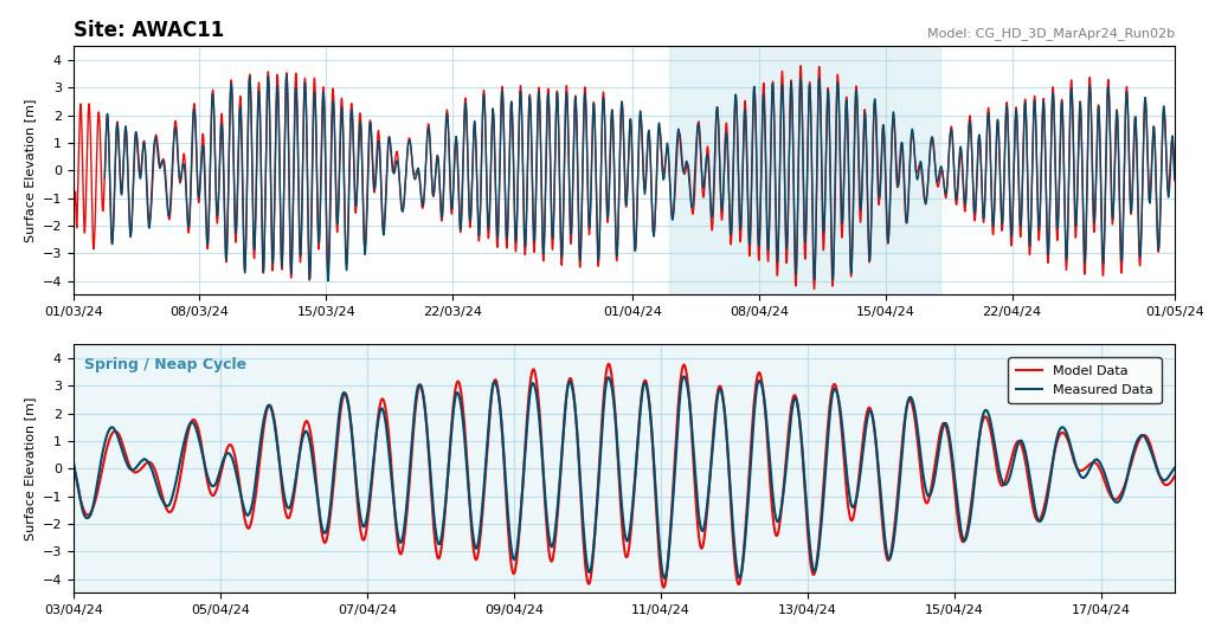


Figure A5. Modelled and measured water level at AWAC-11 over the model calibration period and selected calibration spring / neap cycle period.



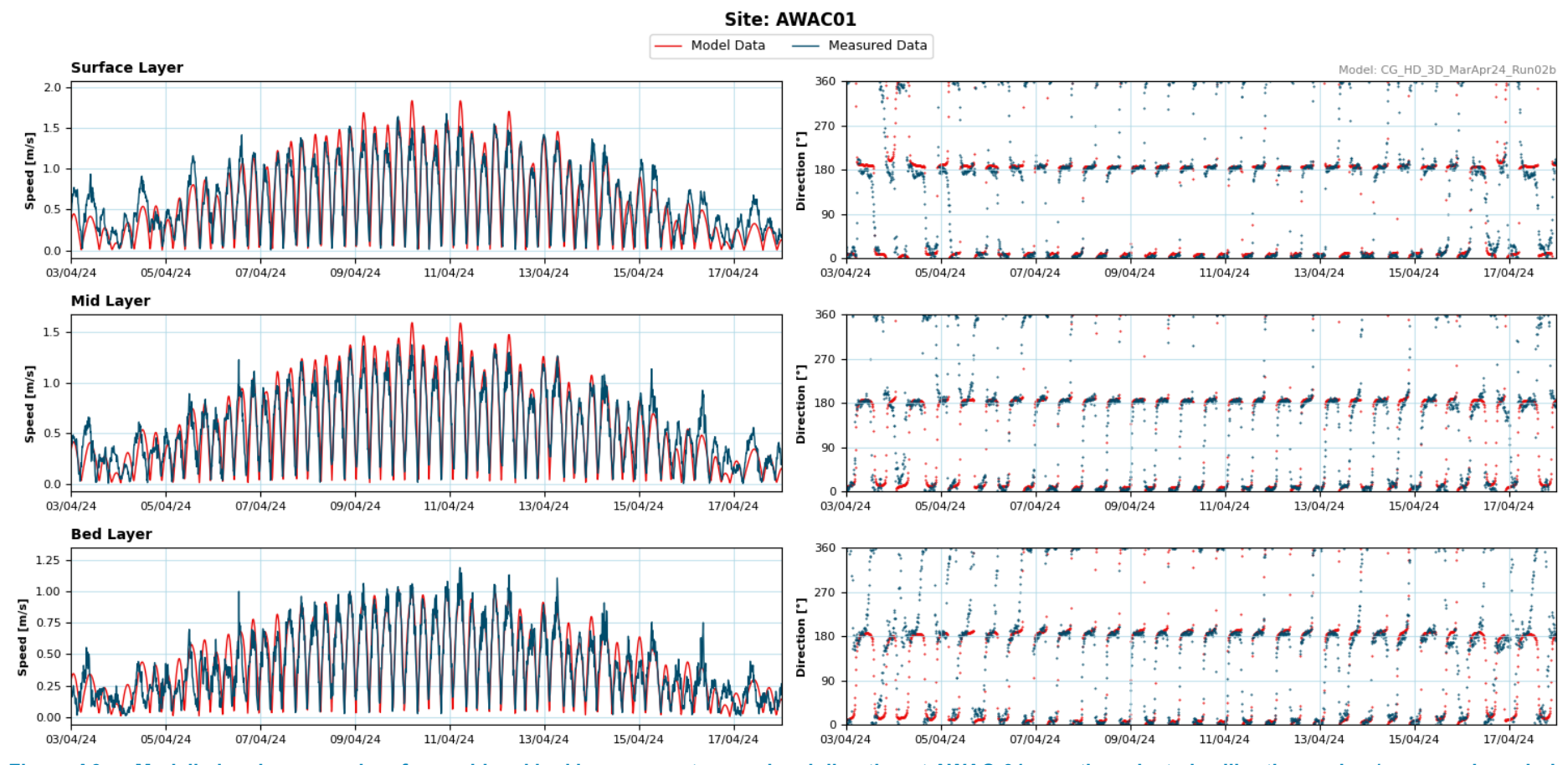


Figure A6. Modelled and measured surface, mid and bed layer currents speed and direction at AWAC-01 over the selected calibration spring / neap cycle period.



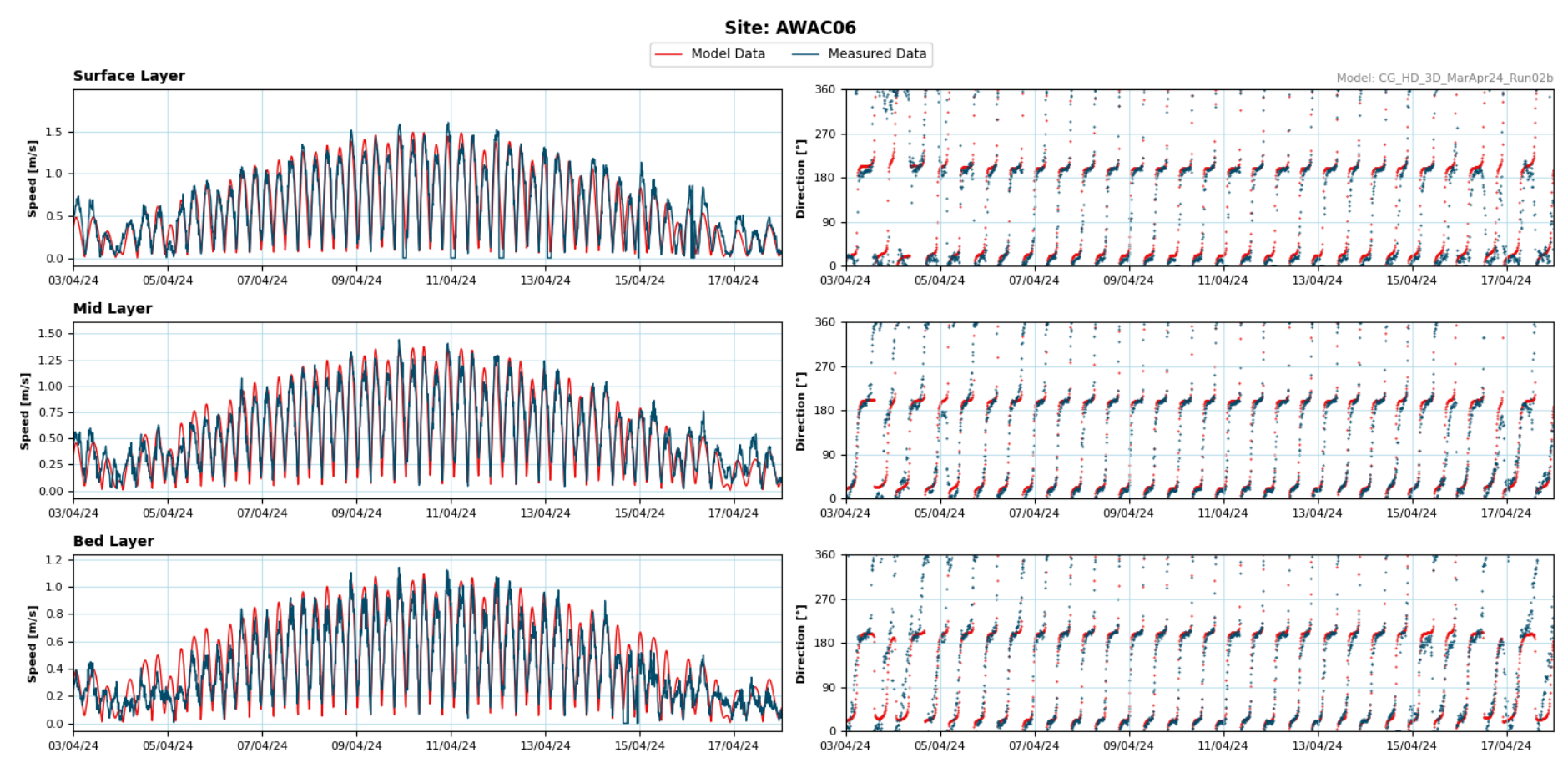


Figure A7. Modelled and measured surface, mid and bed layer currents speed and direction at AWAC-06 over the selected calibration spring / neap cycle period.



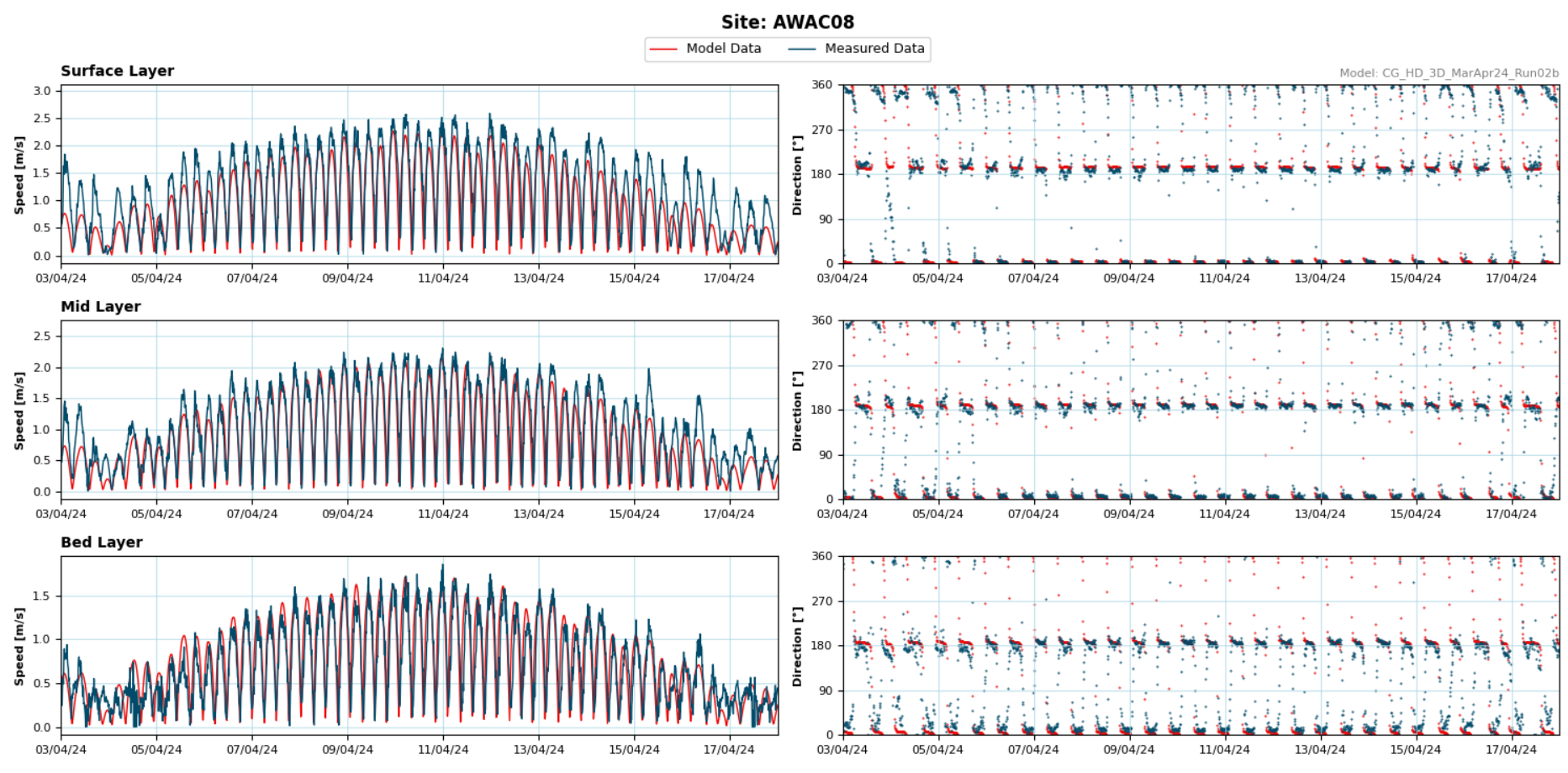


Figure A8. Modelled and measured surface, mid and bed layer currents speed and direction at AWAC-08 over the selected calibration spring / neap cycle period.



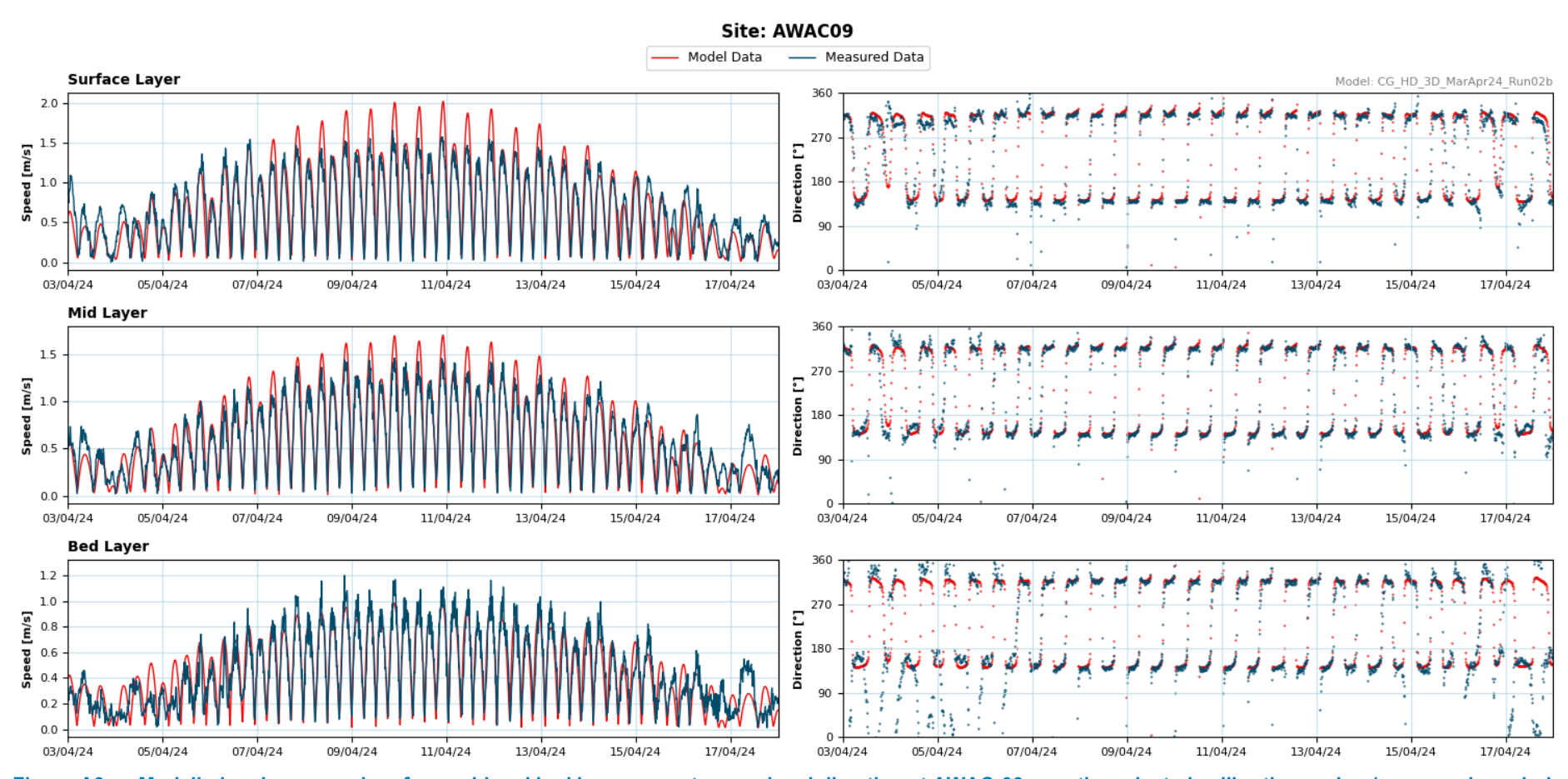


Figure A9. Modelled and measured surface, mid and bed layer currents speed and direction at AWAC-09 over the selected calibration spring / neap cycle period.



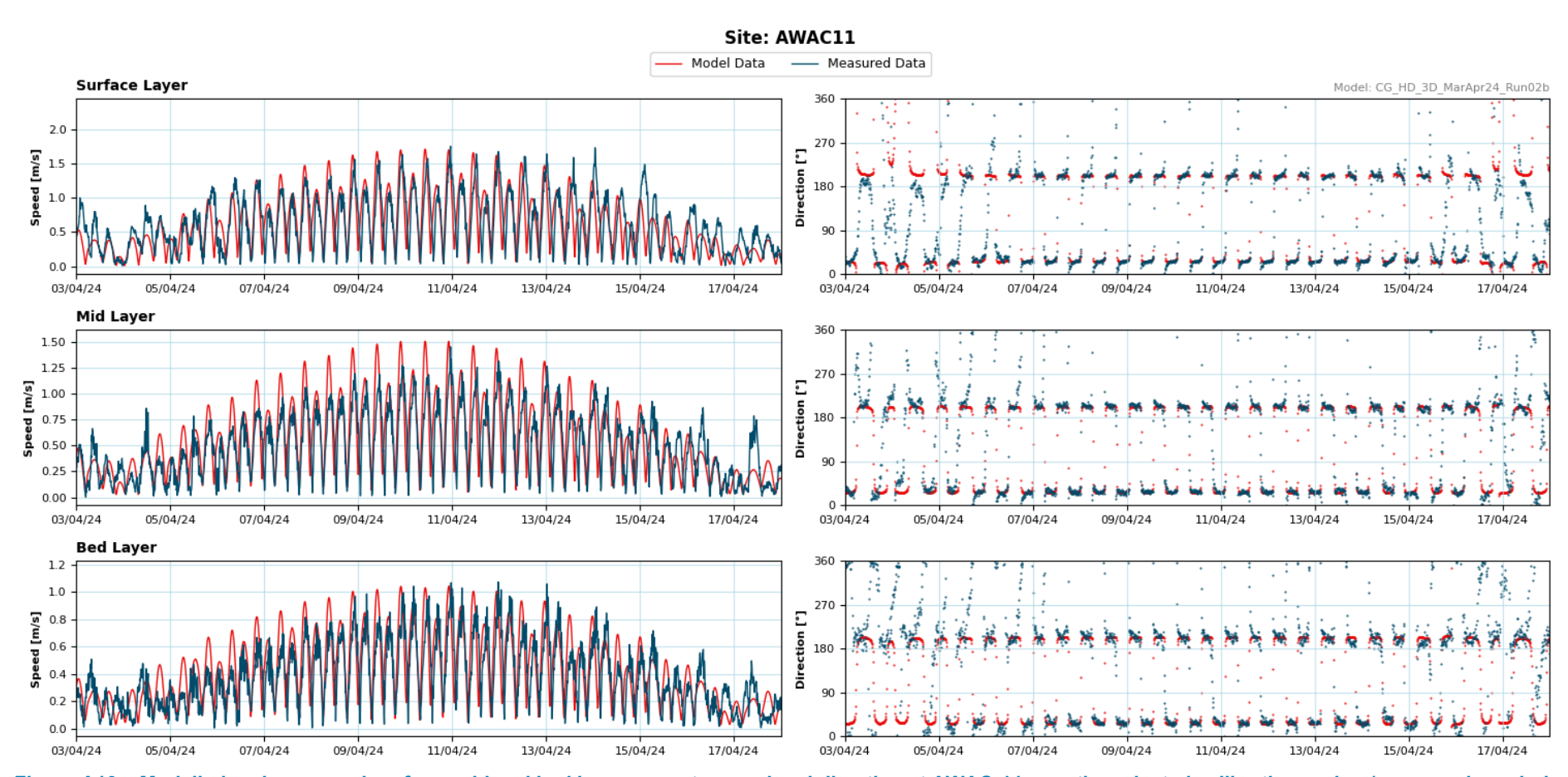


Figure A10. Modelled and measured surface, mid and bed layer currents speed and direction at AWAC-11 over the selected calibration spring / neap cycle period.



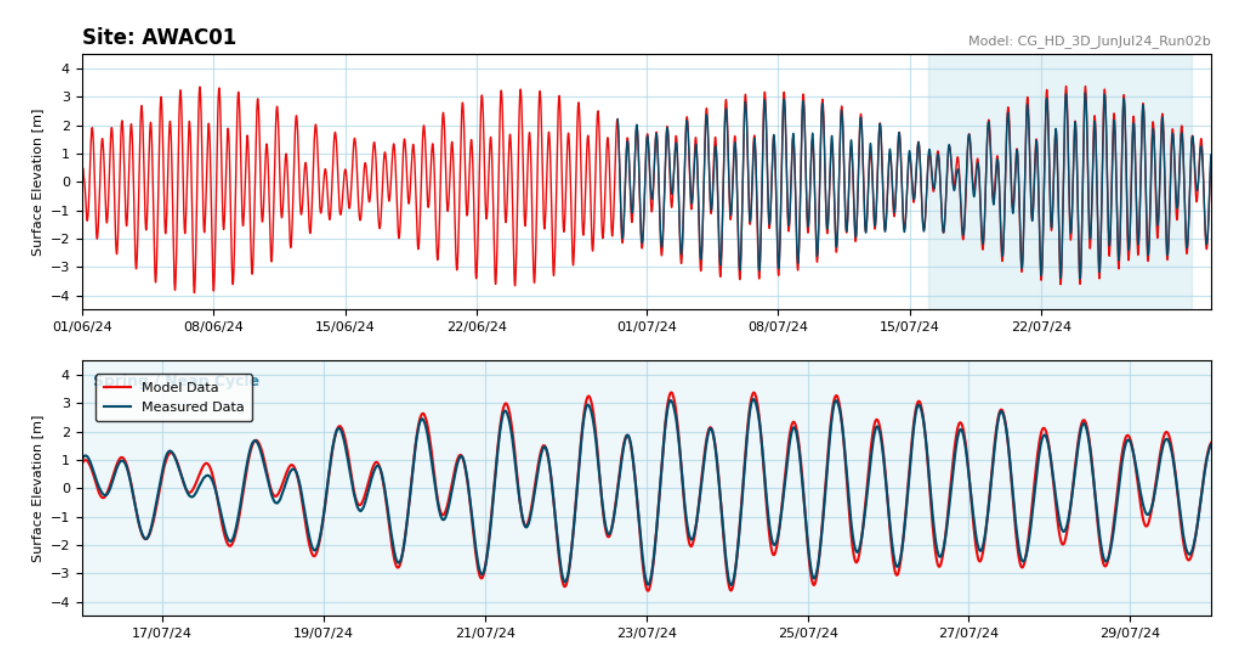


Figure A11. Modelled and measured water level at AWAC-01 over the model validation period and selected calibration spring / neap cycle period.

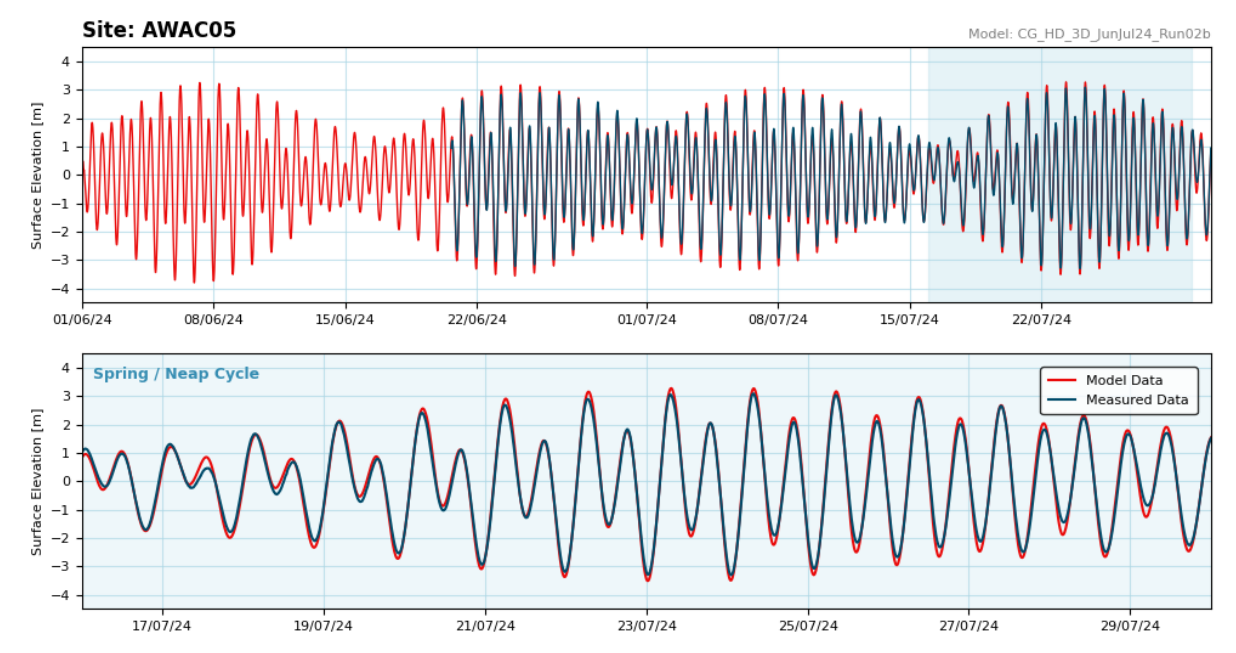


Figure A12. Modelled and measured water level at AWAC-05 over the model validation period and selected calibration spring / neap cycle period.



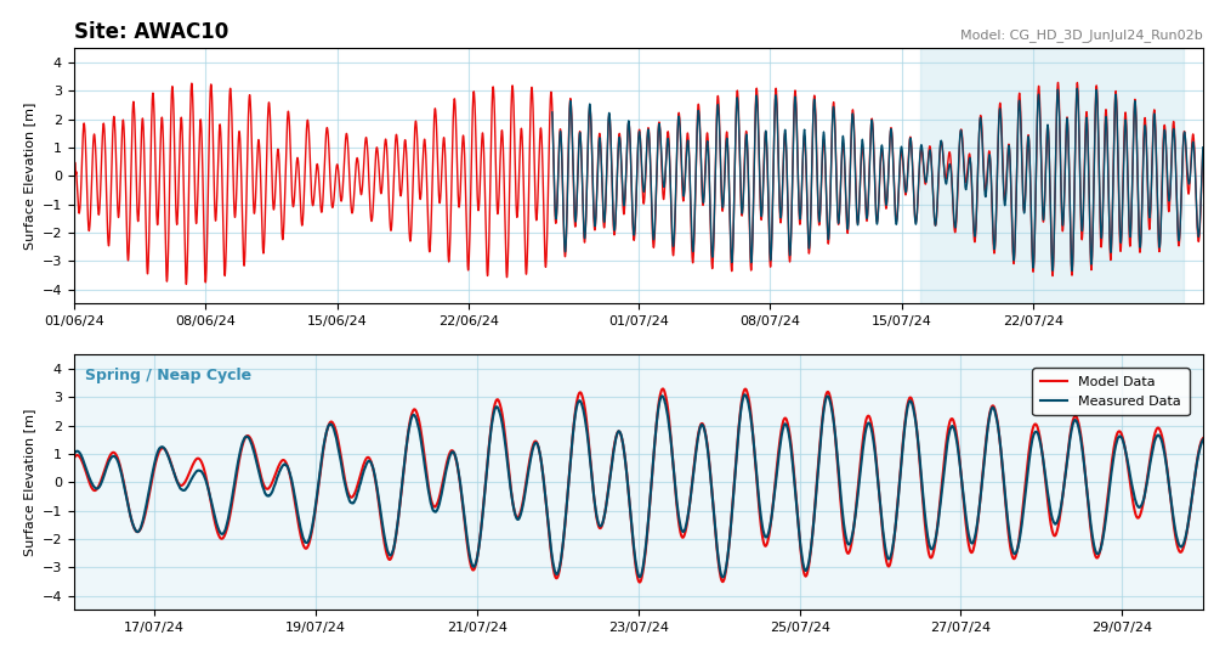


Figure A13. Modelled and measured water level at AWAC-10 over the model validation period and selected calibration spring / neap cycle period.

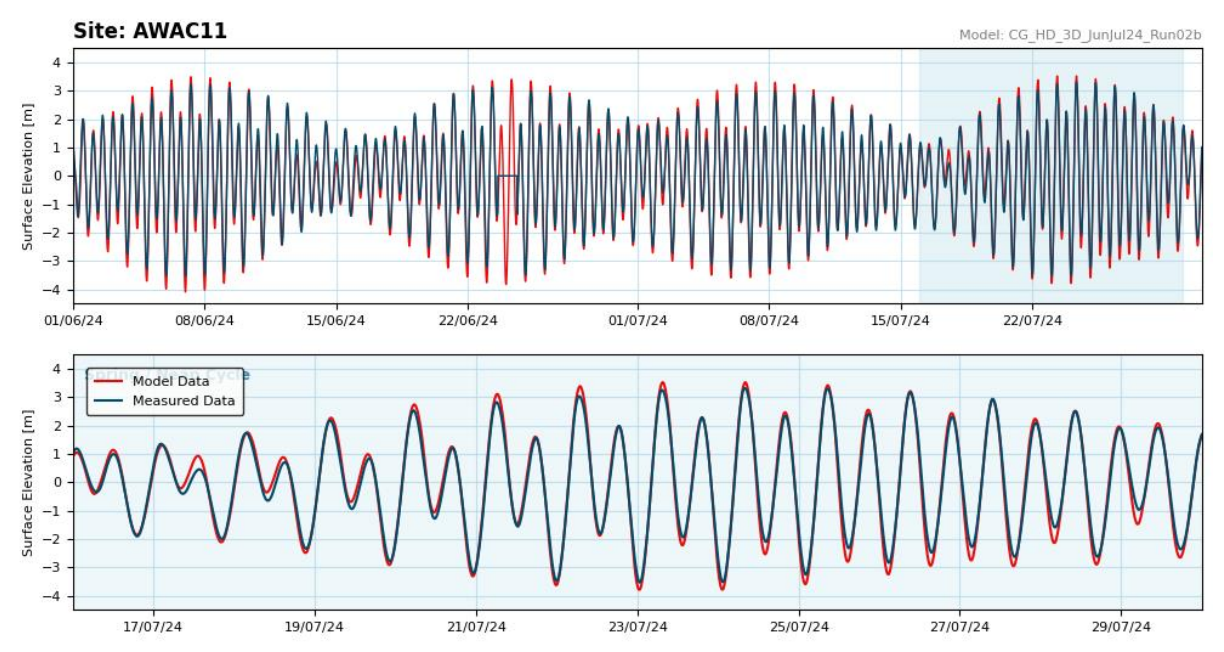


Figure A14. Modelled and measured water level at AWAC-11 over the model validation period and selected calibration spring / neap cycle period.



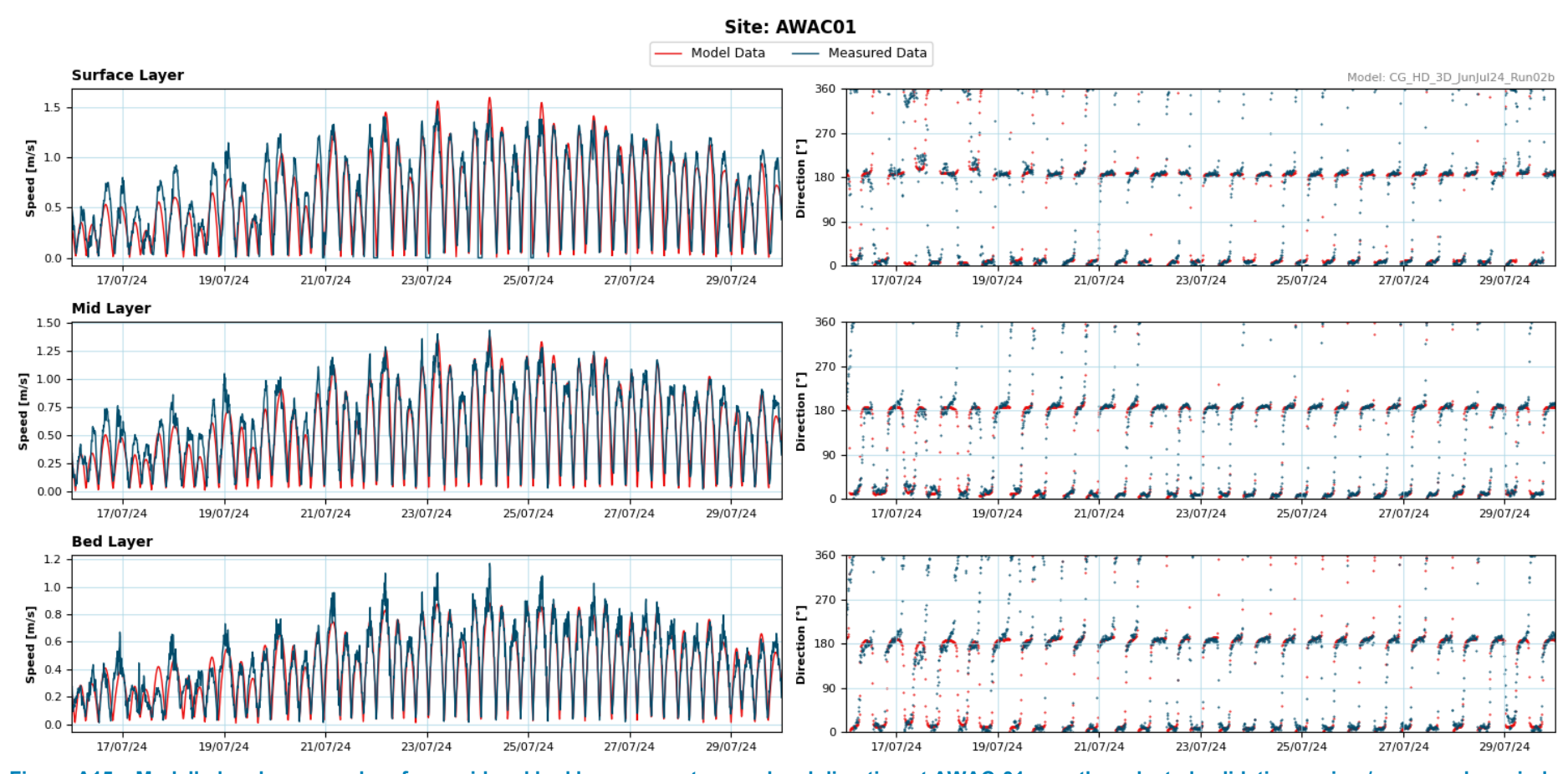


Figure A15. Modelled and measured surface, mid and bed layer currents speed and direction at AWAC-01 over the selected validation spring / neap cycle period.



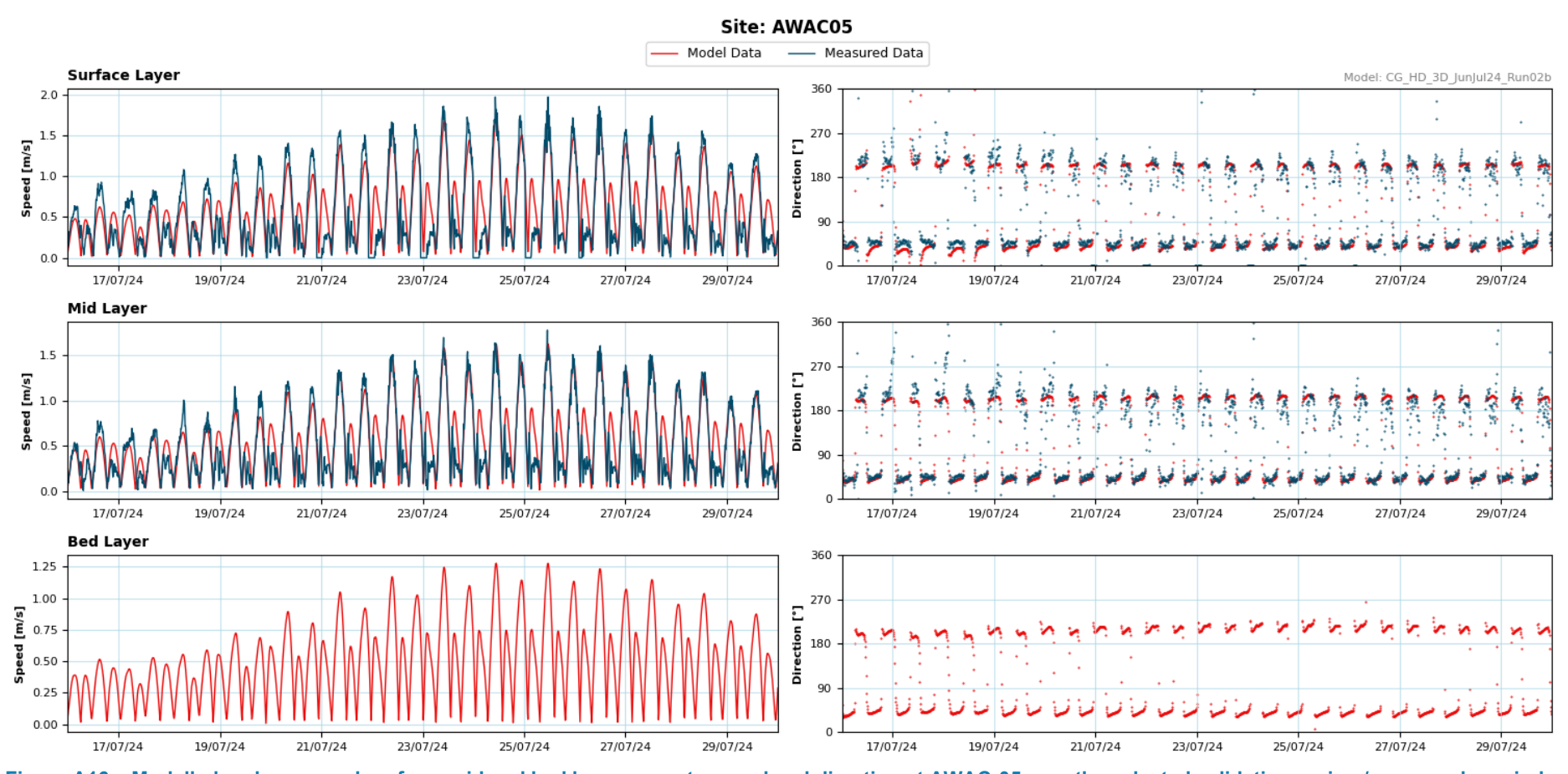


Figure A16. Modelled and measured surface, mid and bed layer currents speed and direction at AWAC-05 over the selected validation spring / neap cycle period.



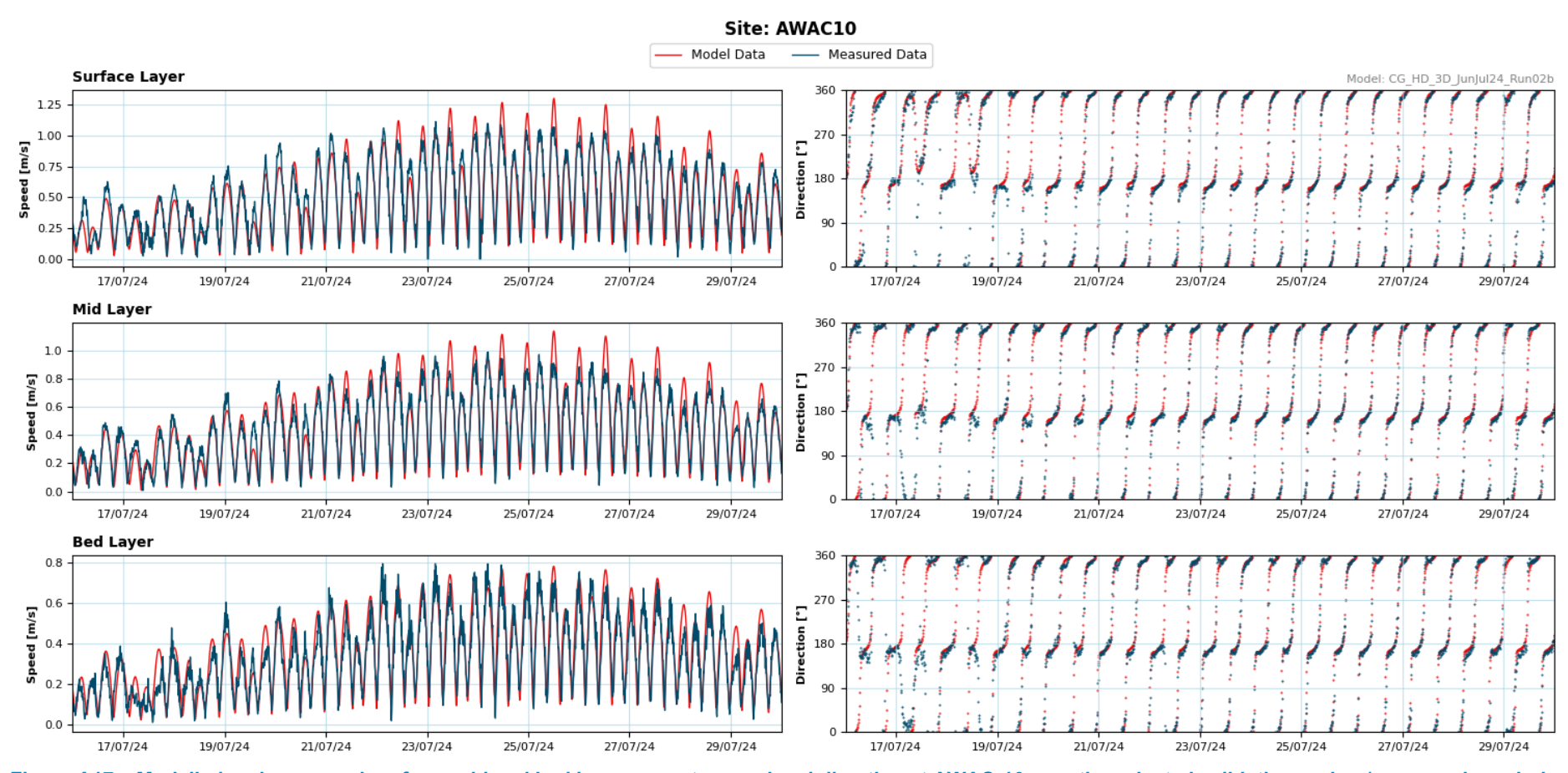


Figure A17. Modelled and measured surface, mid and bed layer currents speed and direction at AWAC-10 over the selected validation spring / neap cycle period.



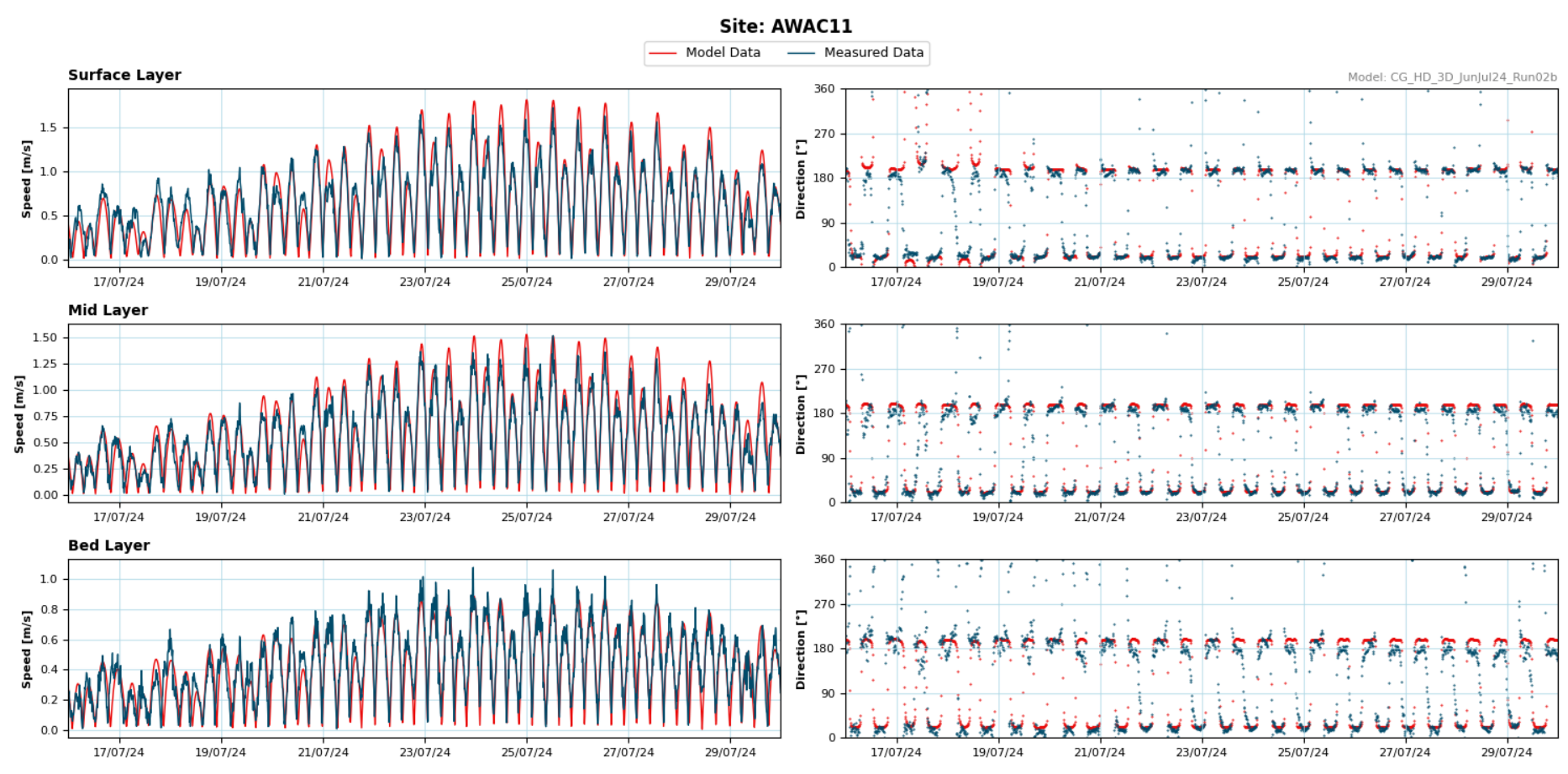


Figure A18. Modelled and measured surface, mid and bed layer currents speed and direction at AWAC-11 over the selected validation spring / neap cycle period.



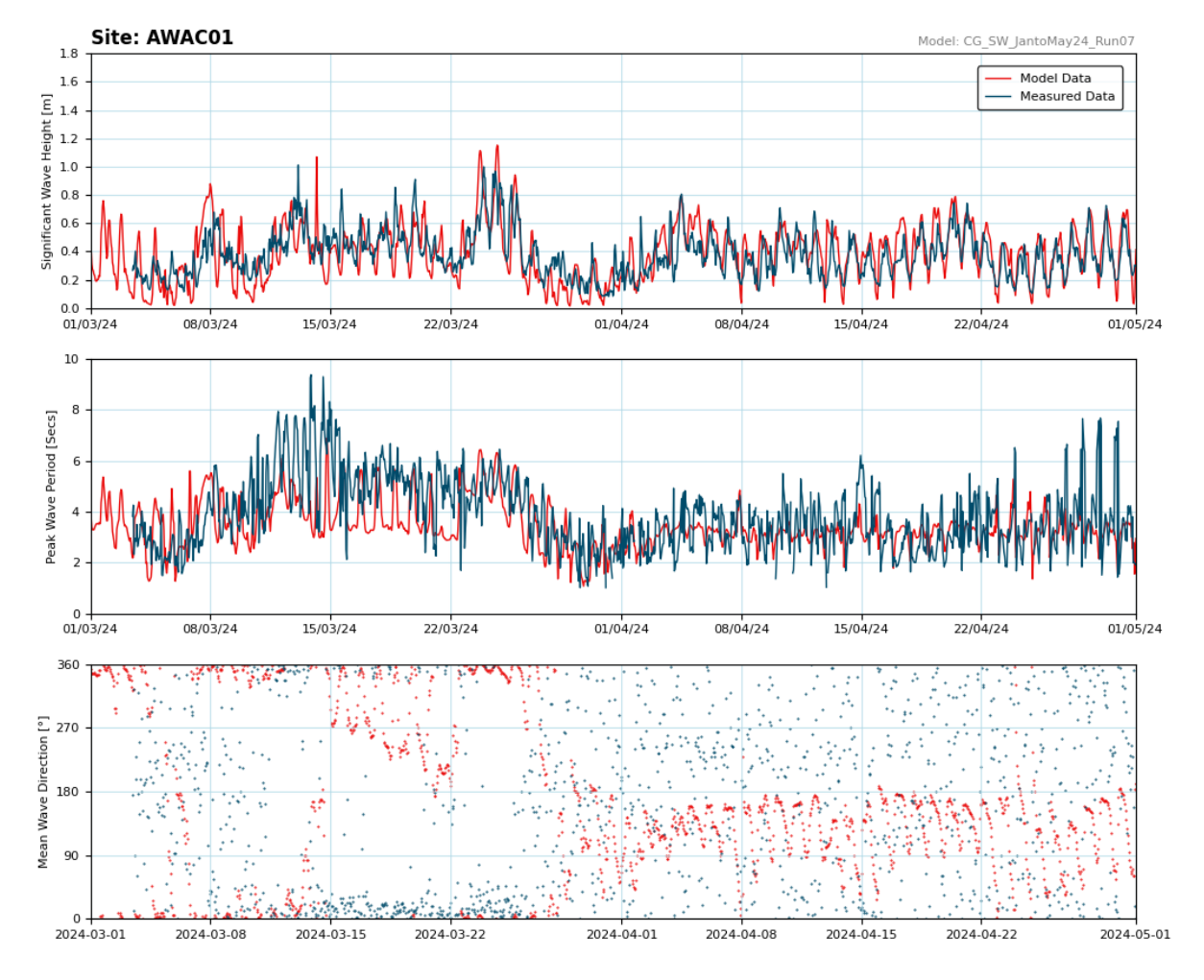


Figure A19. Modelled and measured significant wave height, peak wave period and mean wave direction at AWAC-01 over the model calibration period.



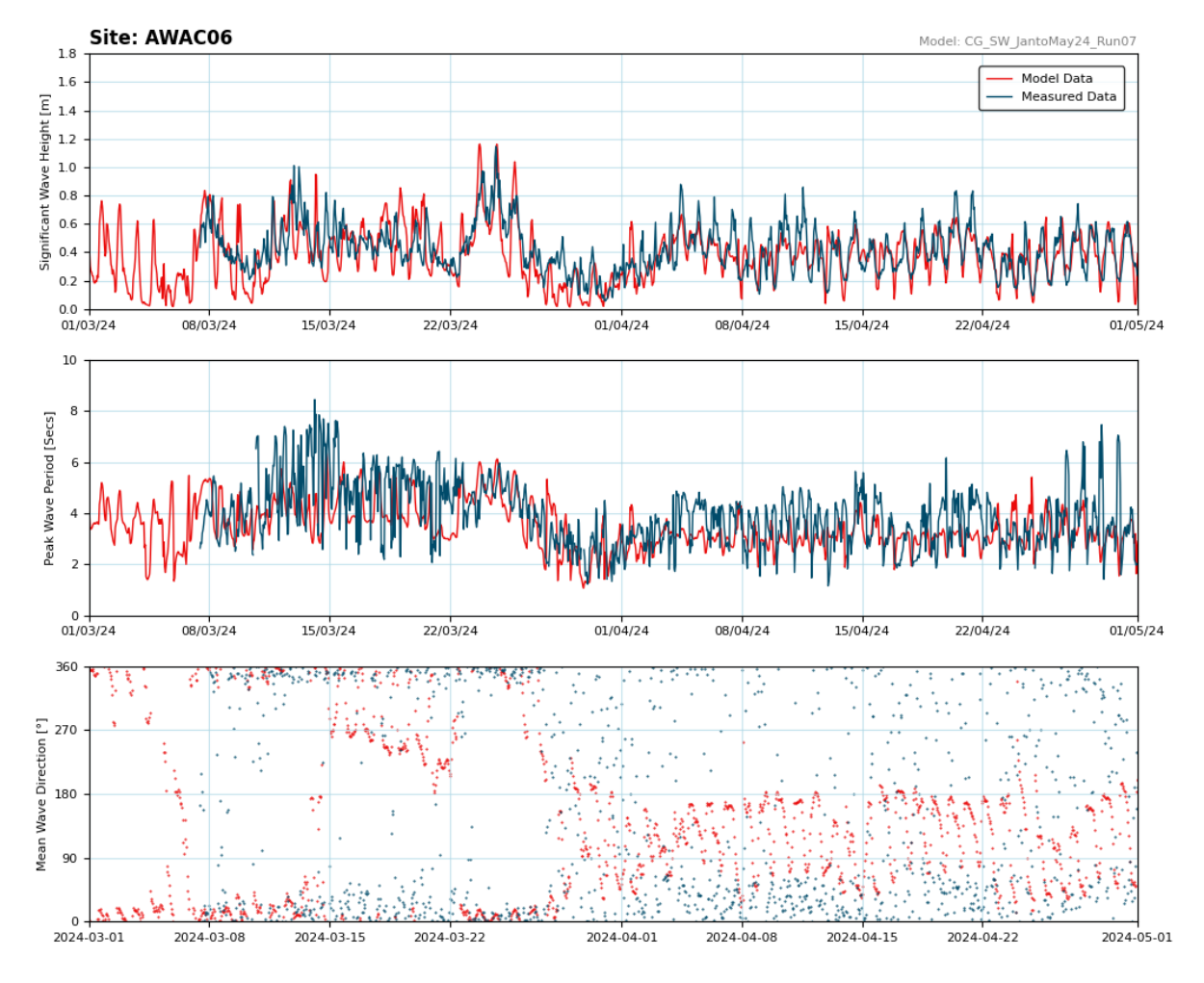


Figure A20. Modelled and measured significant wave height, peak wave period and mean wave direction at AWAC-06 over the model calibration period.



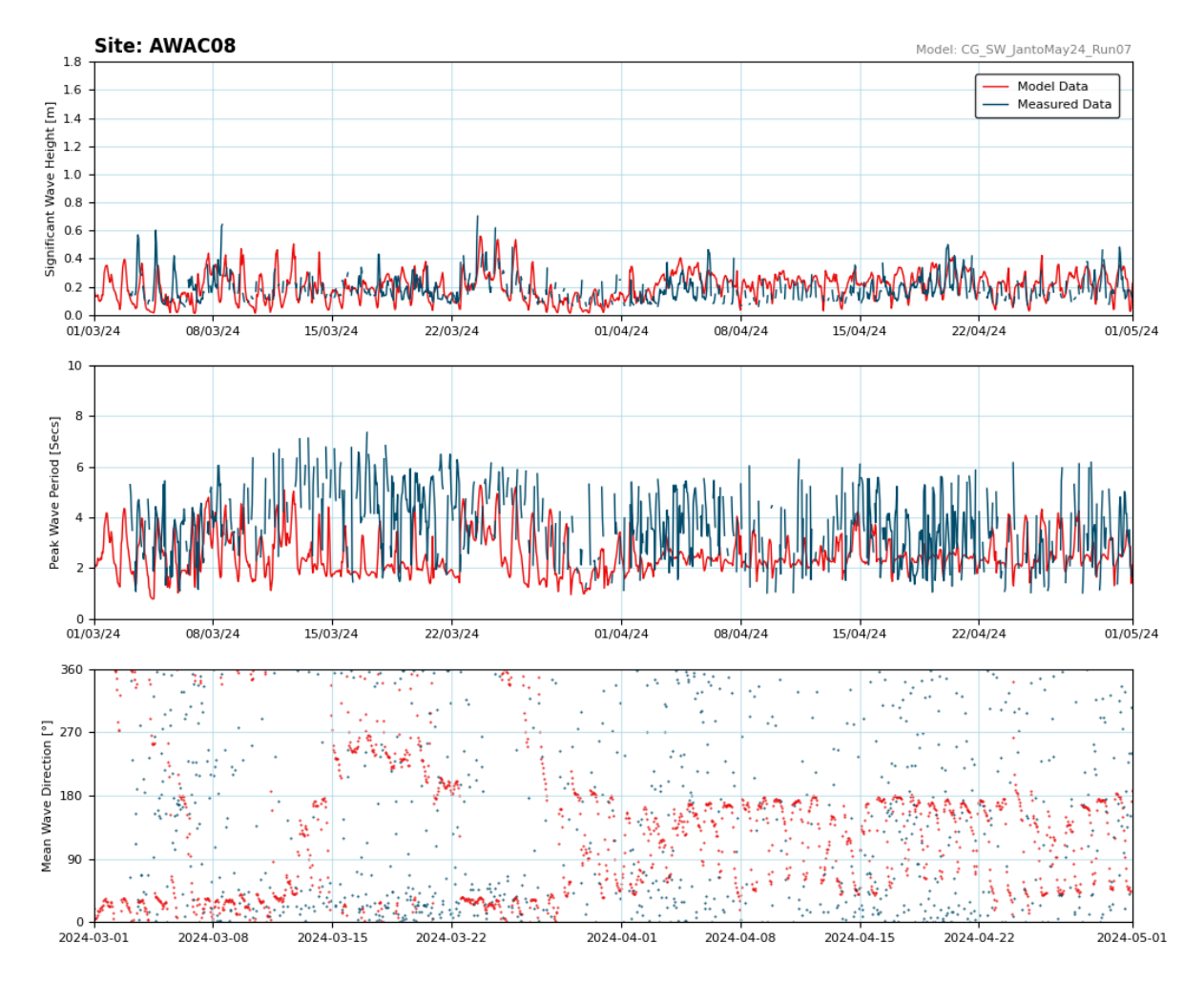


Figure A21. Modelled and measured significant wave height, peak wave period and mean wave direction at AWAC-08 over the model calibration period.



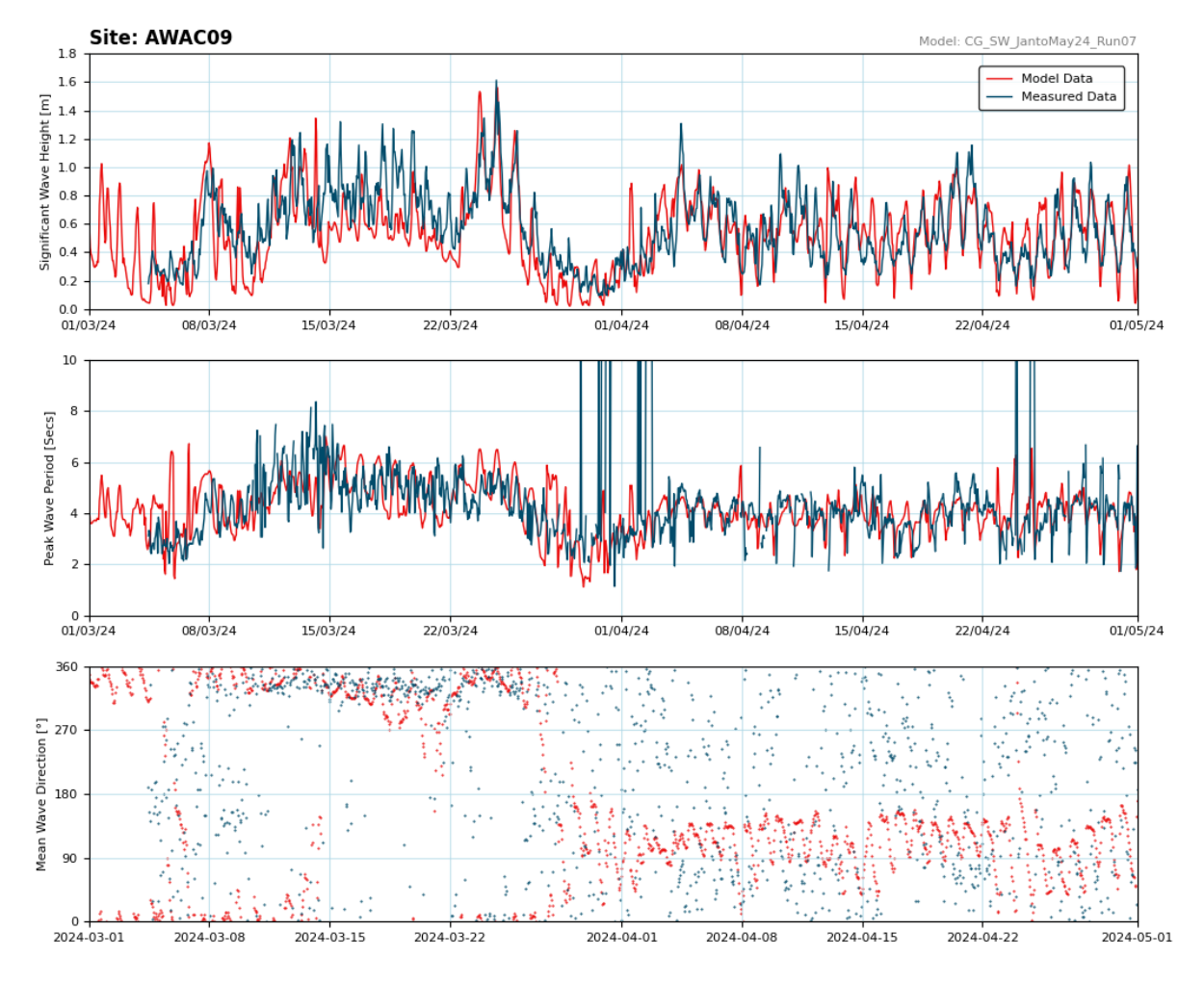


Figure A22. Modelled and measured significant wave height, peak wave period and mean wave direction at AWAC-09 over the model calibration period.



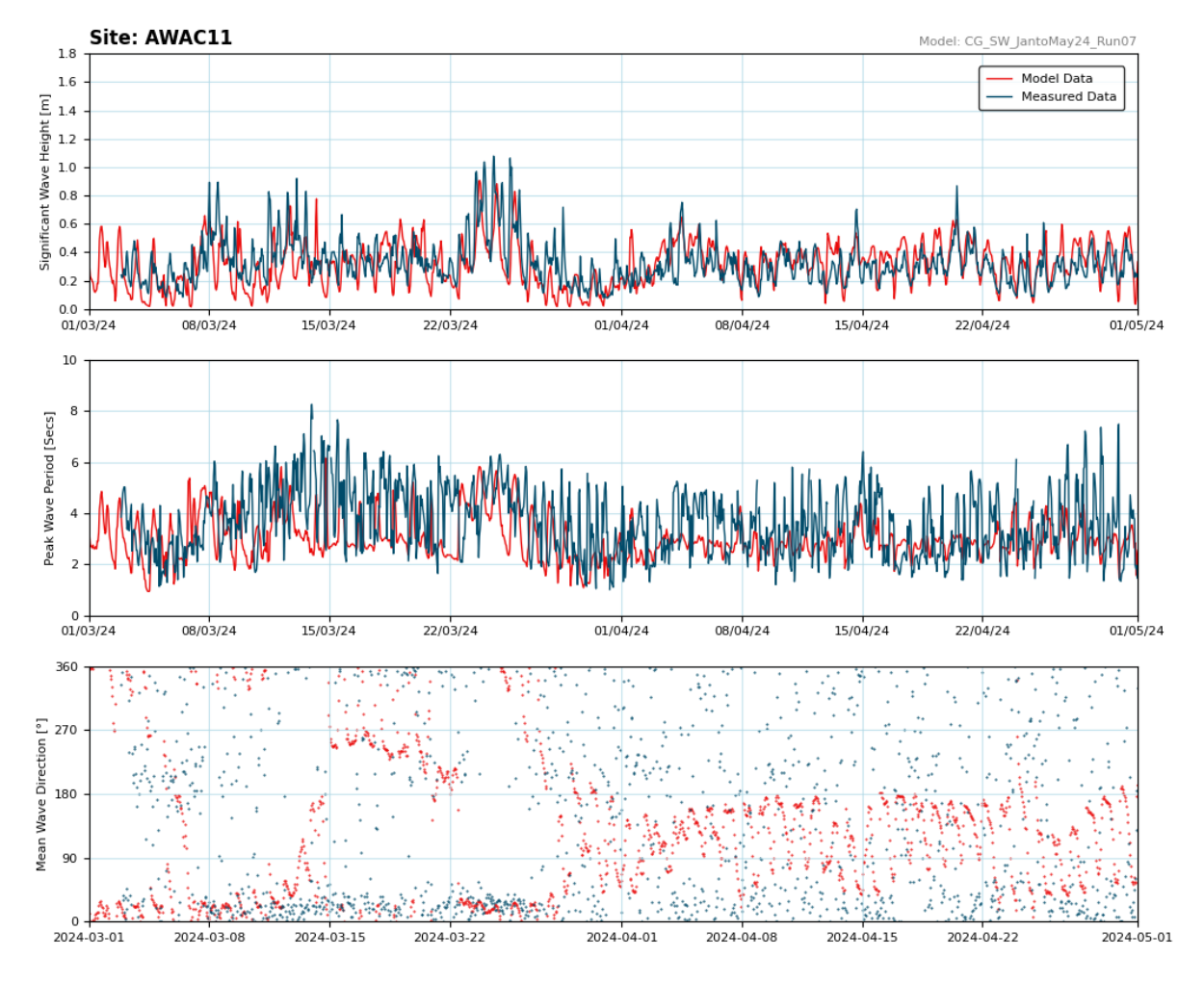


Figure A23. Modelled and measured significant wave height, peak wave period and mean wave direction at AWAC-11 over the model calibration period.



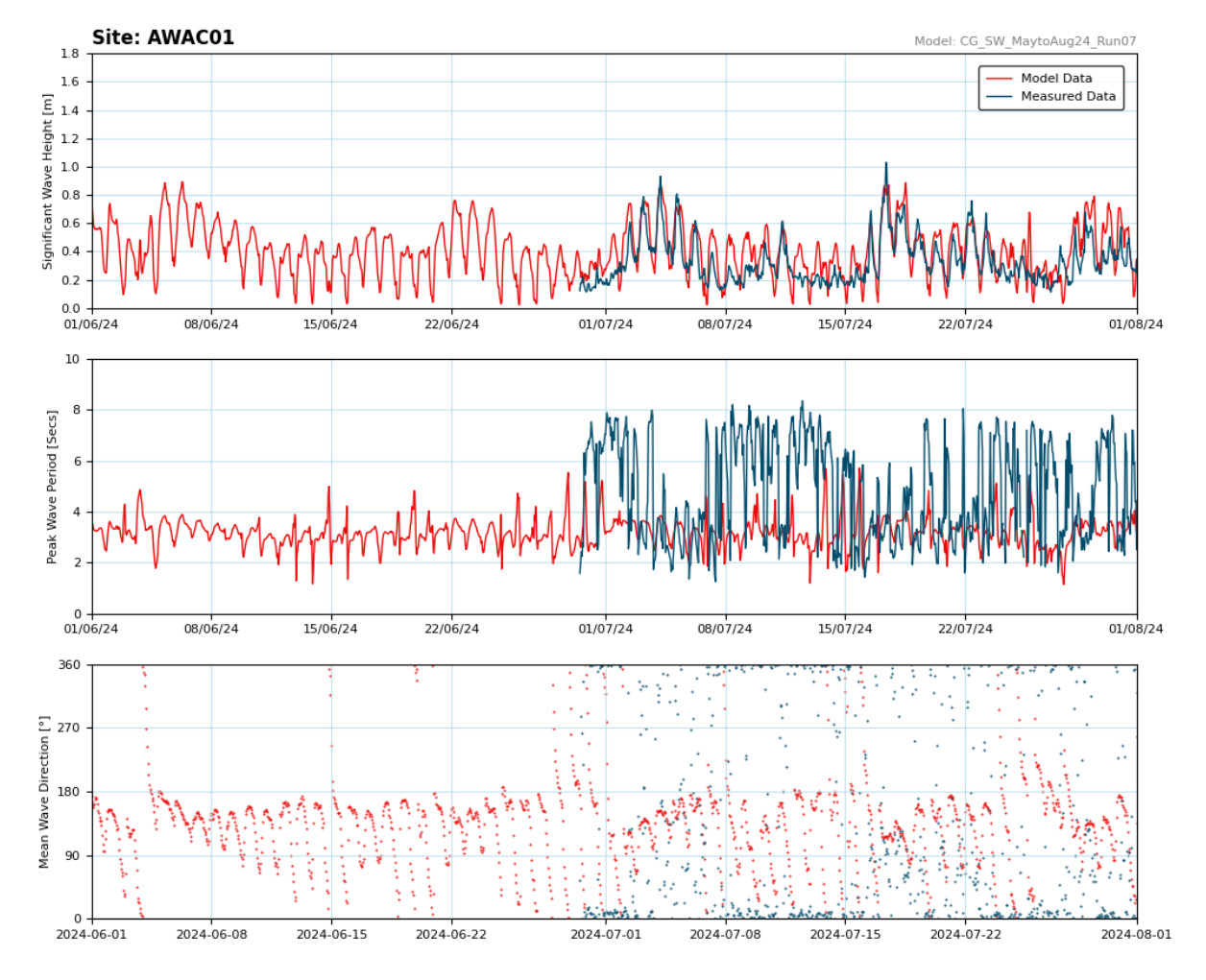


Figure A24. Modelled and measured significant wave height, peak wave period and mean wave direction at AWAC-01 over the model validation period.



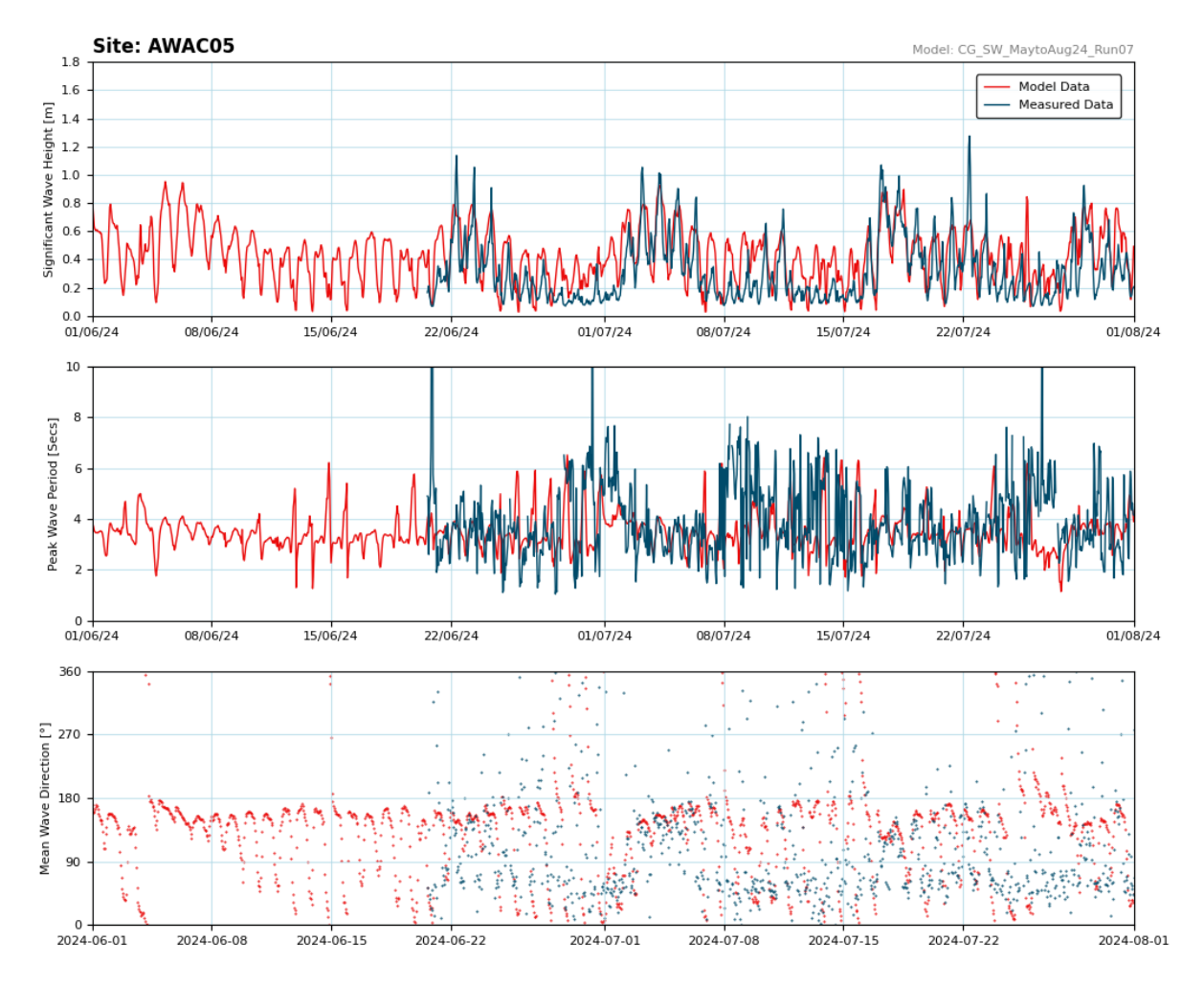


Figure A25. Modelled and measured significant wave height, peak wave period and mean wave direction at AWAC-05 over the model validation period.



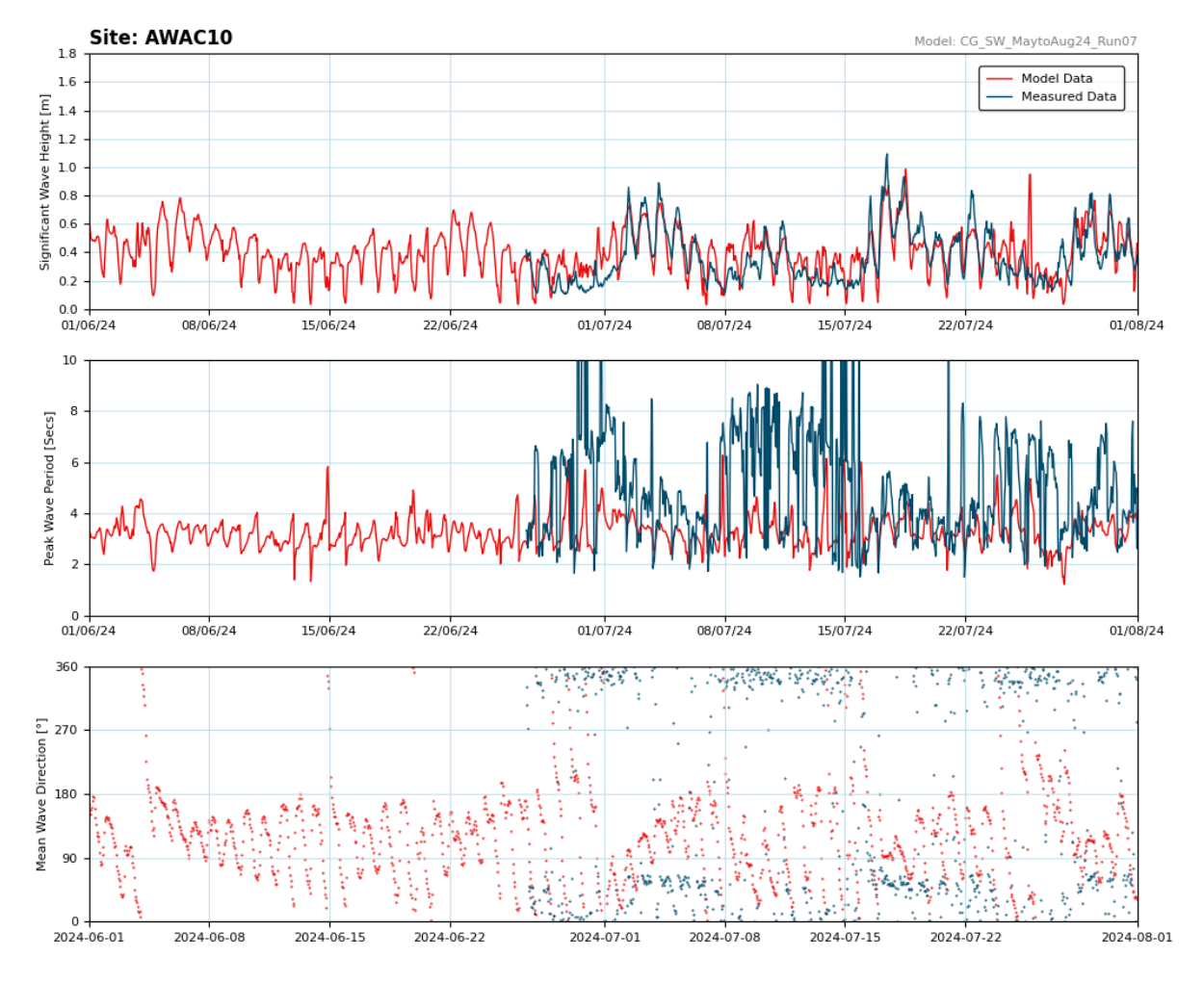


Figure A26. Modelled and measured significant wave height, peak wave period and mean wave direction at AWAC-10 over the model validation period.



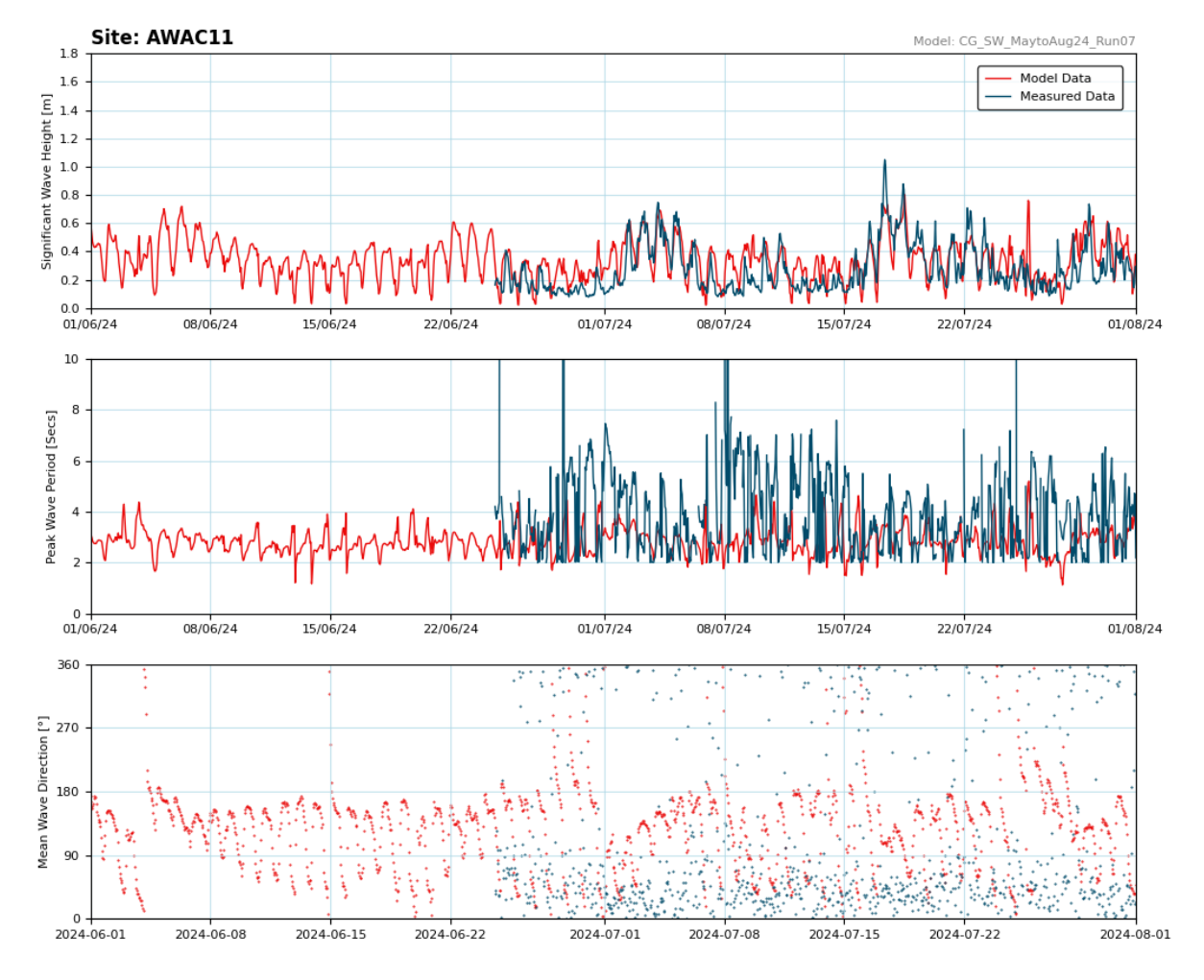


Figure A27. Modelled and measured significant wave height, peak wave period and mean wave direction at AWAC-11 over the model validation period.



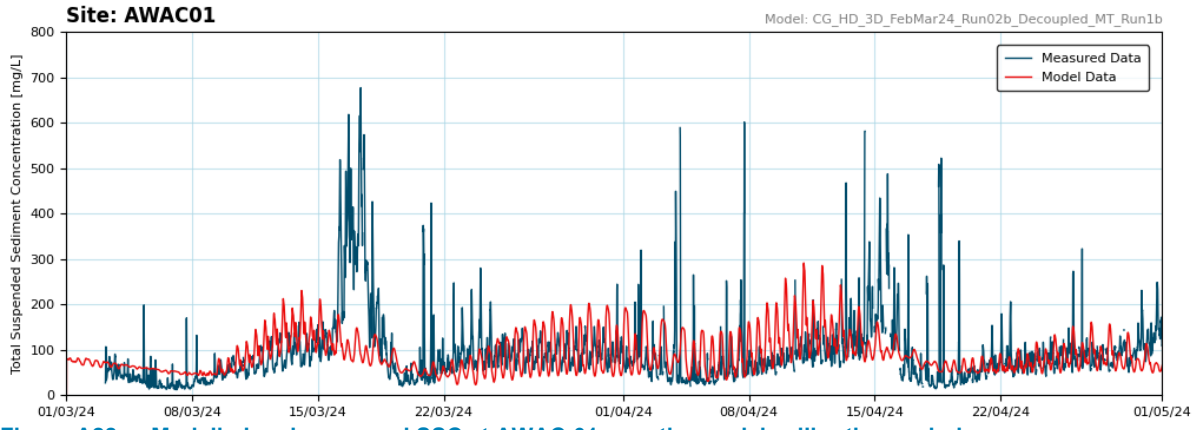


Figure A28. Modelled and measured SSC at AWAC-01 over the model calibration period.

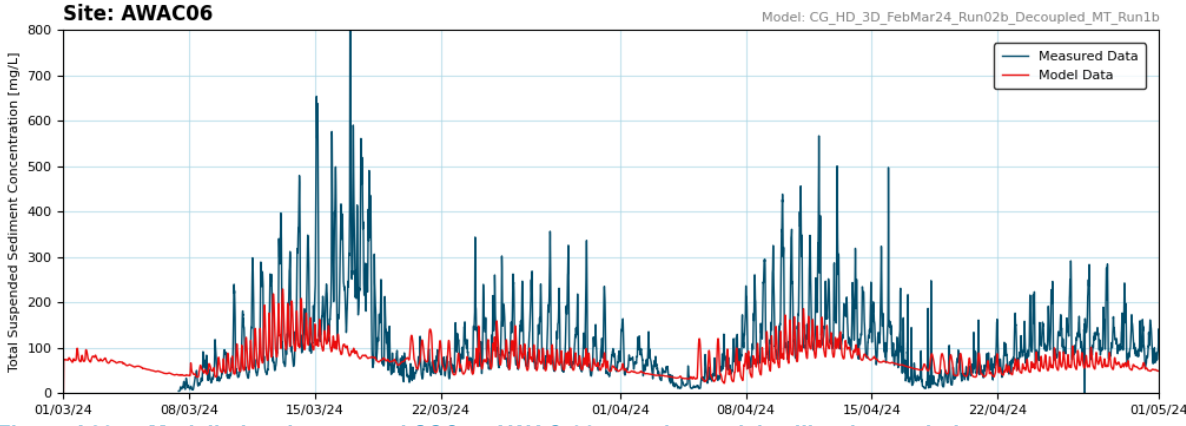


Figure A29. Modelled and measured SSC at AWAC-06 over the model calibration period.

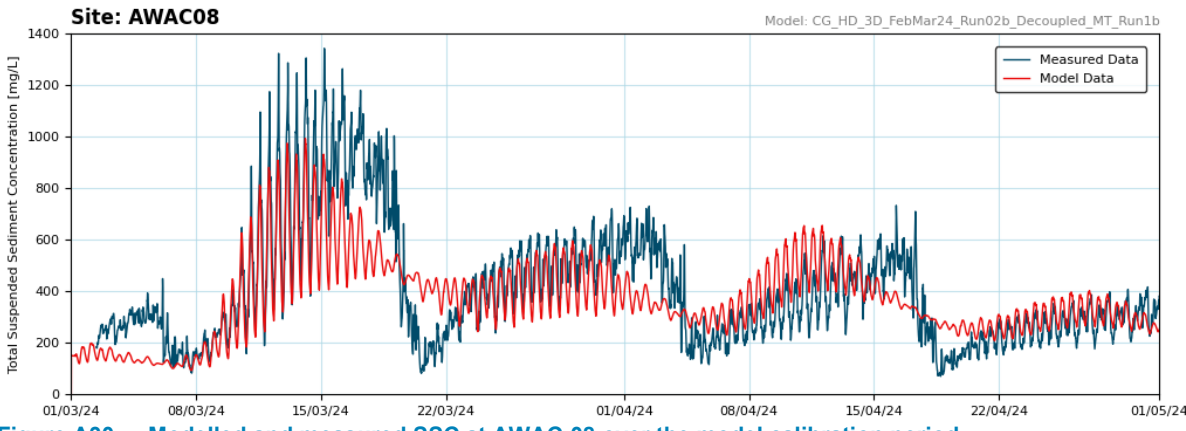


Figure A30. Modelled and measured SSC at AWAC-08 over the model calibration period.

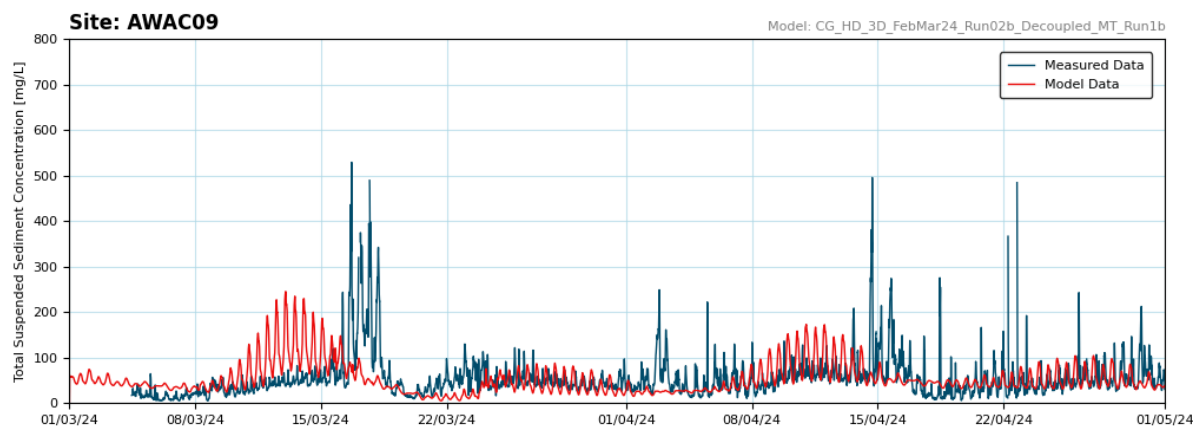


Figure A31. Modelled and measured SSC at AWAC-09 over the model calibration period.



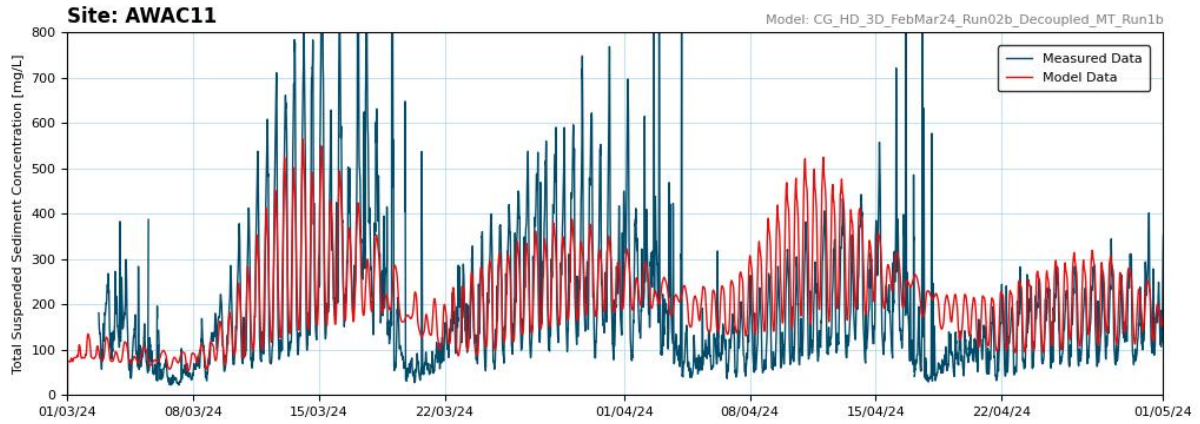


Figure A32. Modelled and measured SSC at AWAC-11 over the model calibration period.

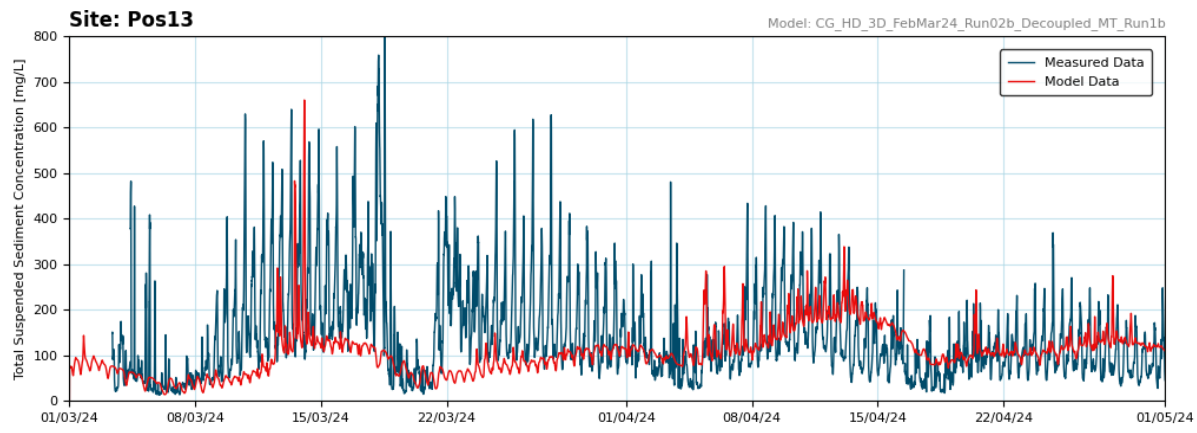


Figure A33. Modelled and measured SSC at Pos 13 over the model calibration period.

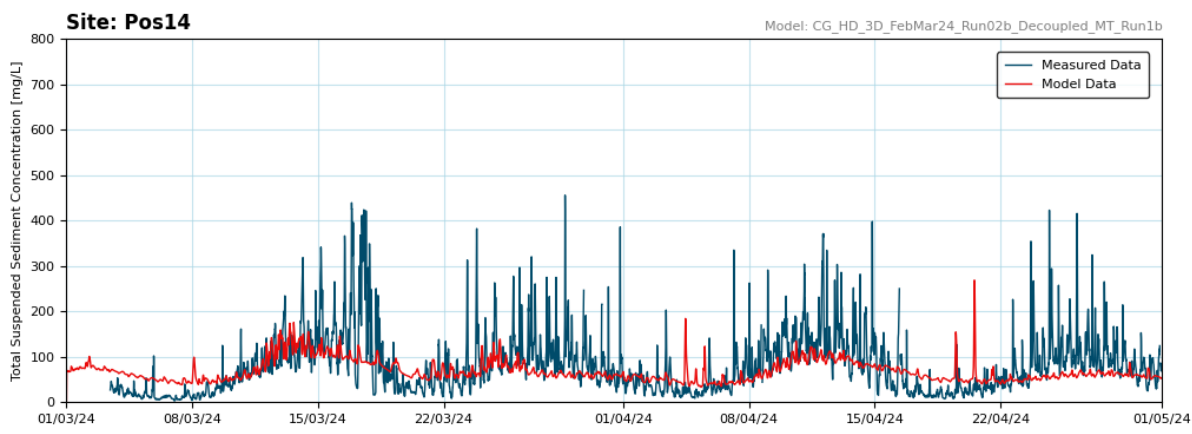


Figure A34. Modelled and measured SSC at Pos 14 over the model calibration period.

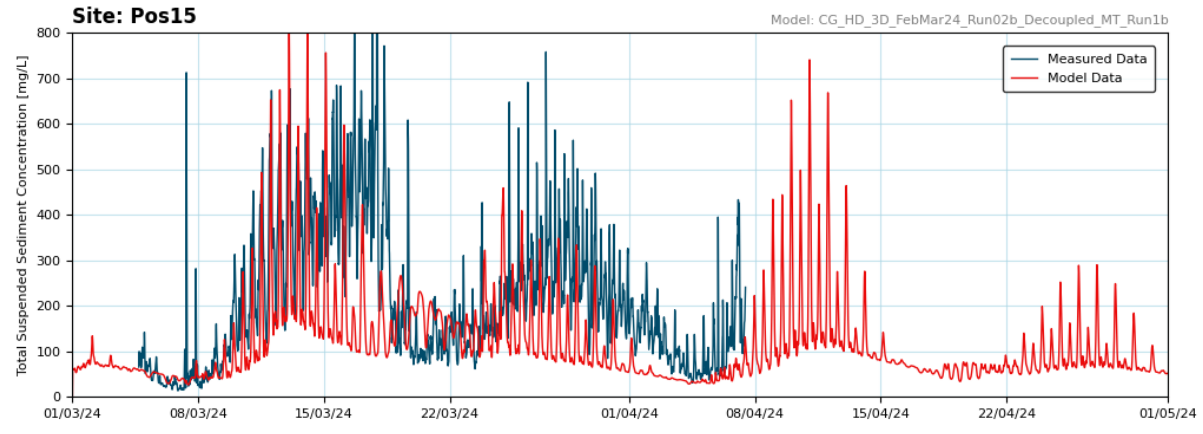


Figure A35. Modelled and measured SSC at Pos 15 over the model calibration period.



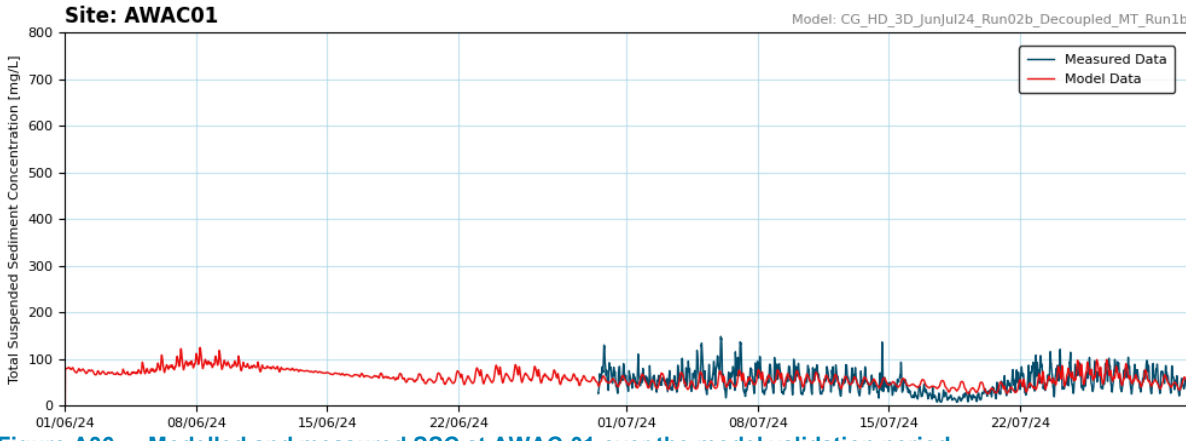


Figure A36. Modelled and measured SSC at AWAC-01 over the model validation period.

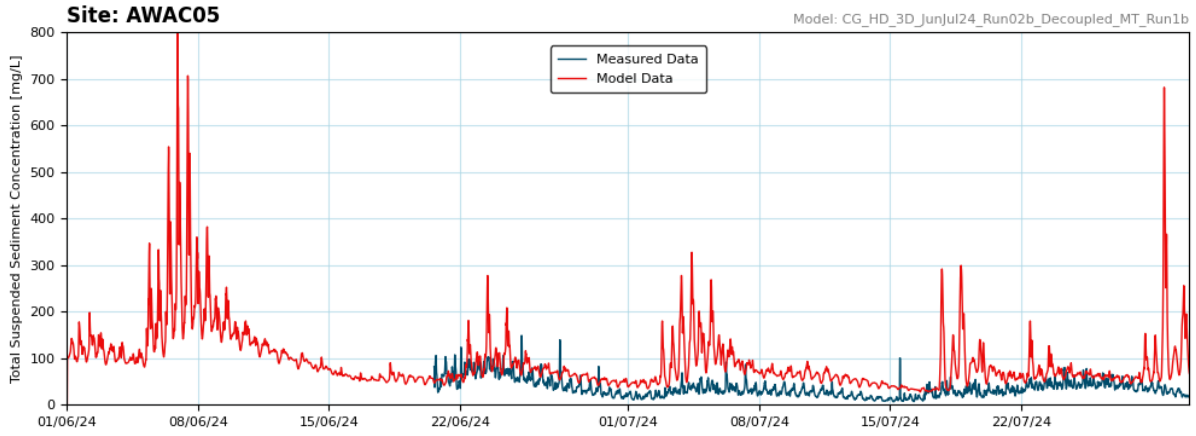


Figure A37. Modelled and measured SSC at AWAC-05 over the model validation period.

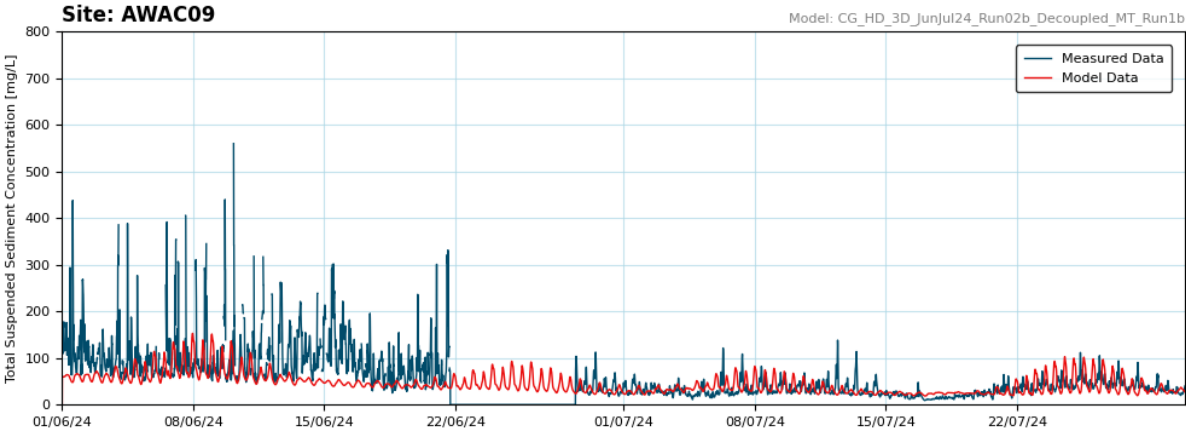


Figure A38. Modelled and measured SSC at AWAC-09 over the model validation period.

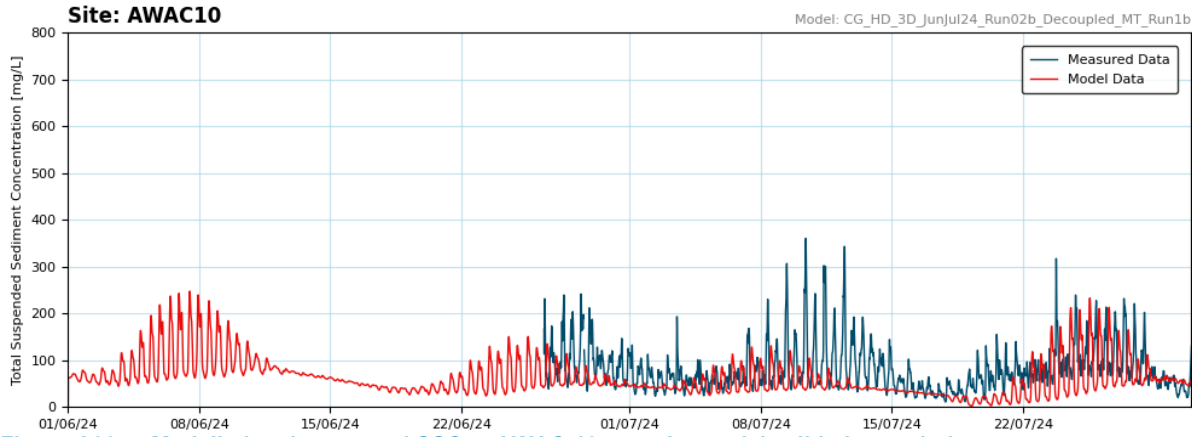


Figure A39. Modelled and measured SSC at AWAC-10 over the model validation period.



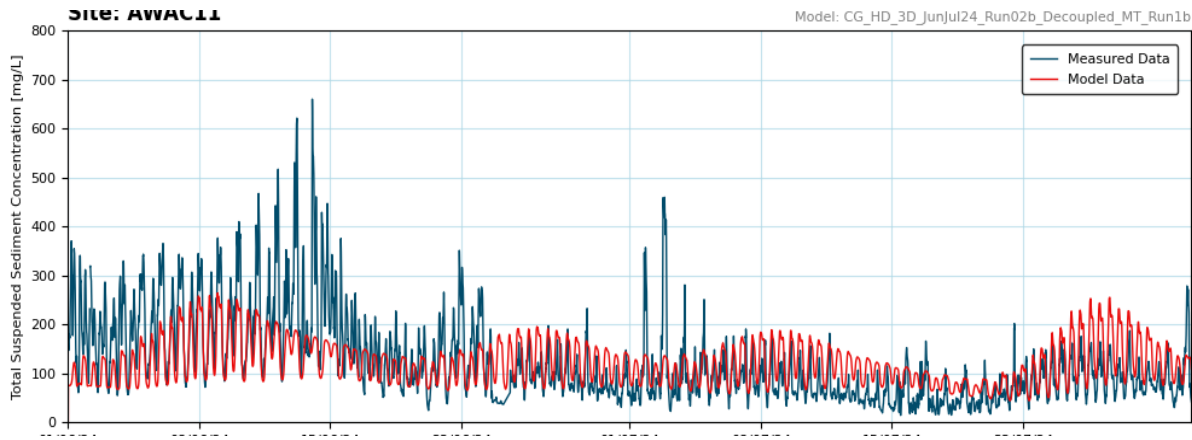


Figure A40. Modelled and measured SSC at AWAC-11 over the model validation period.

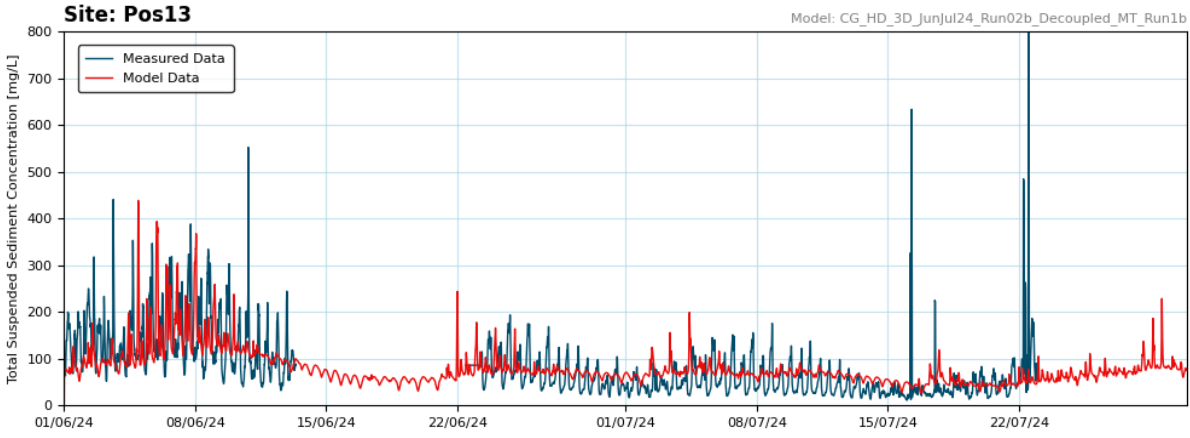


Figure A41. Modelled and measured SSC at Pos 13 over the model validation period.

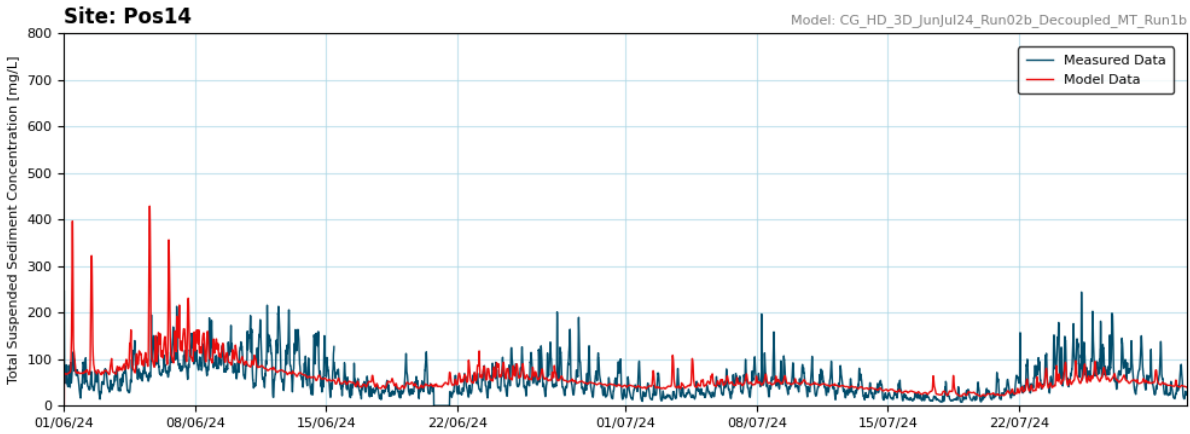


Figure A42. Modelled and measured SSC at Pos 14 over the model validation period.

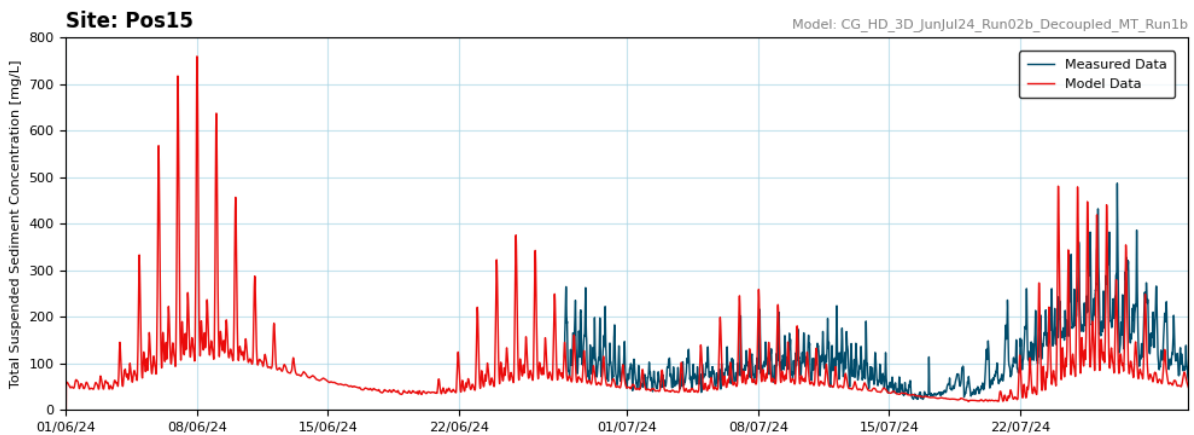


Figure A43. Modelled and measured SSC at Pos 15 over the model validation period.



## Appendix B – Hydrodynamic and Wave Impact Plots



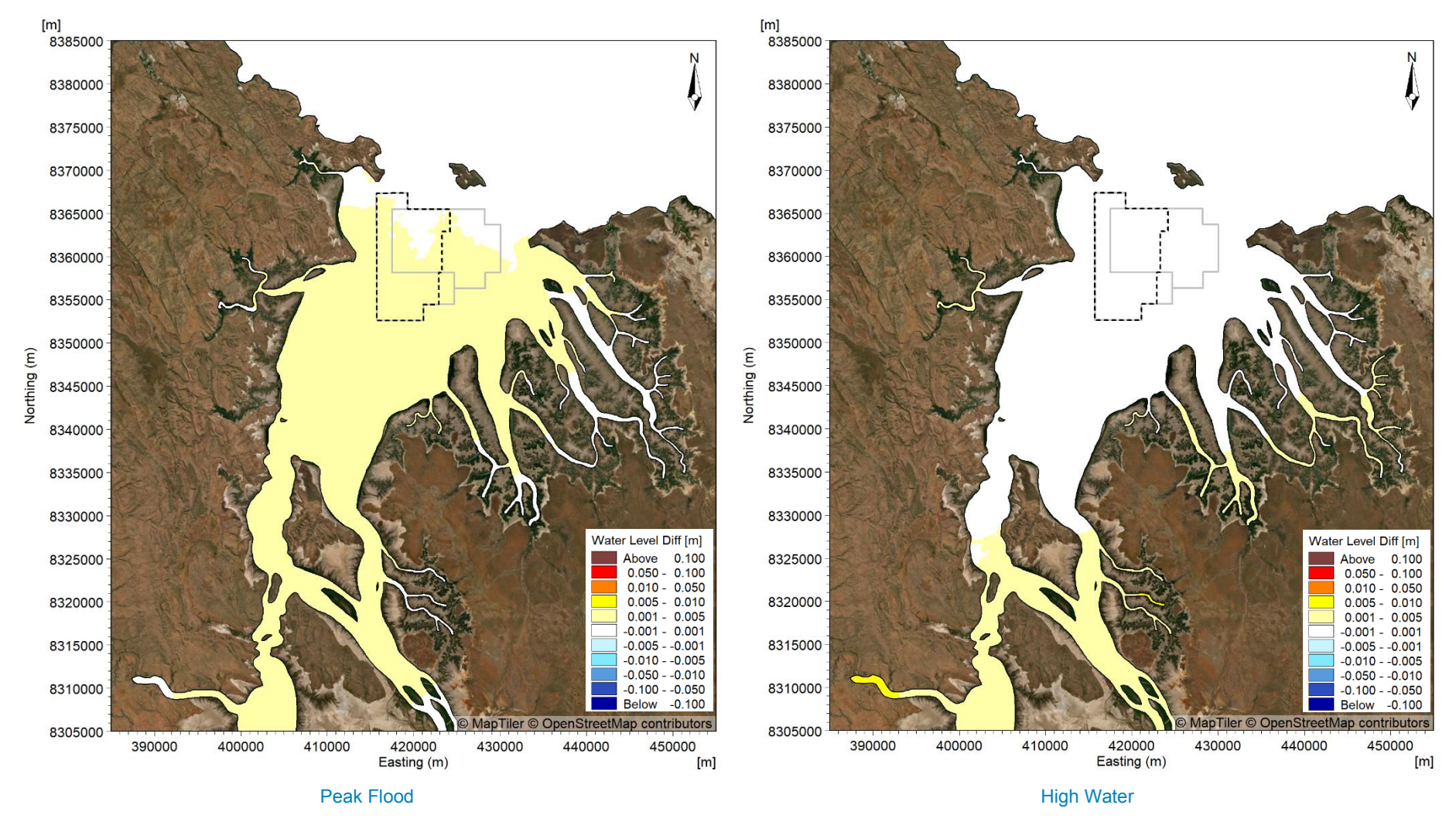


Figure B1. Modelled change in water level at peak flood (left) and high water (right) after 5 years of sand sourcing during a spring tide in the wet season.



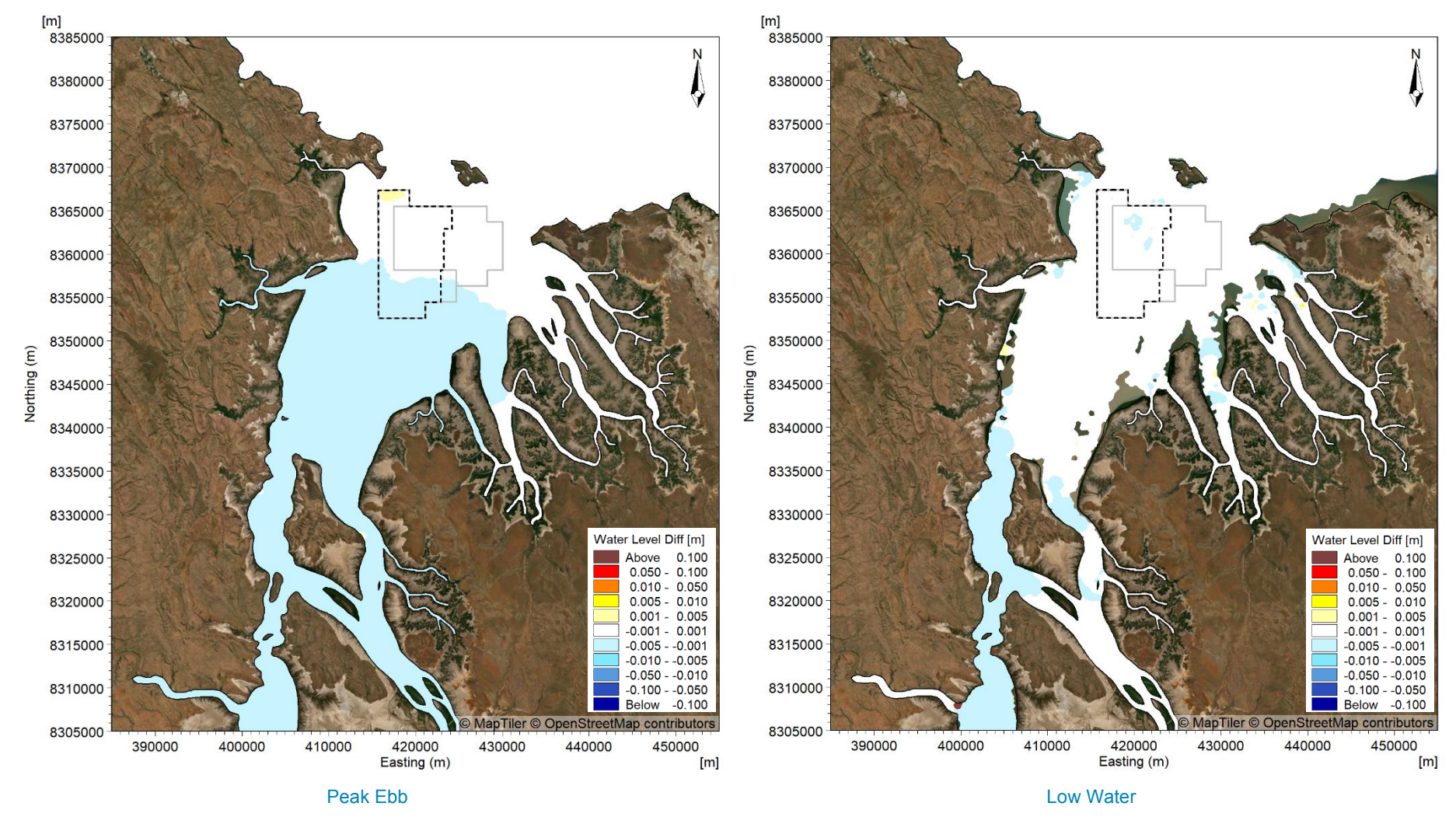


Figure B2. Modelled change in water level at peak ebb (left) and low water (right) after 5 years of sand sourcing during a spring tide in the wet season.



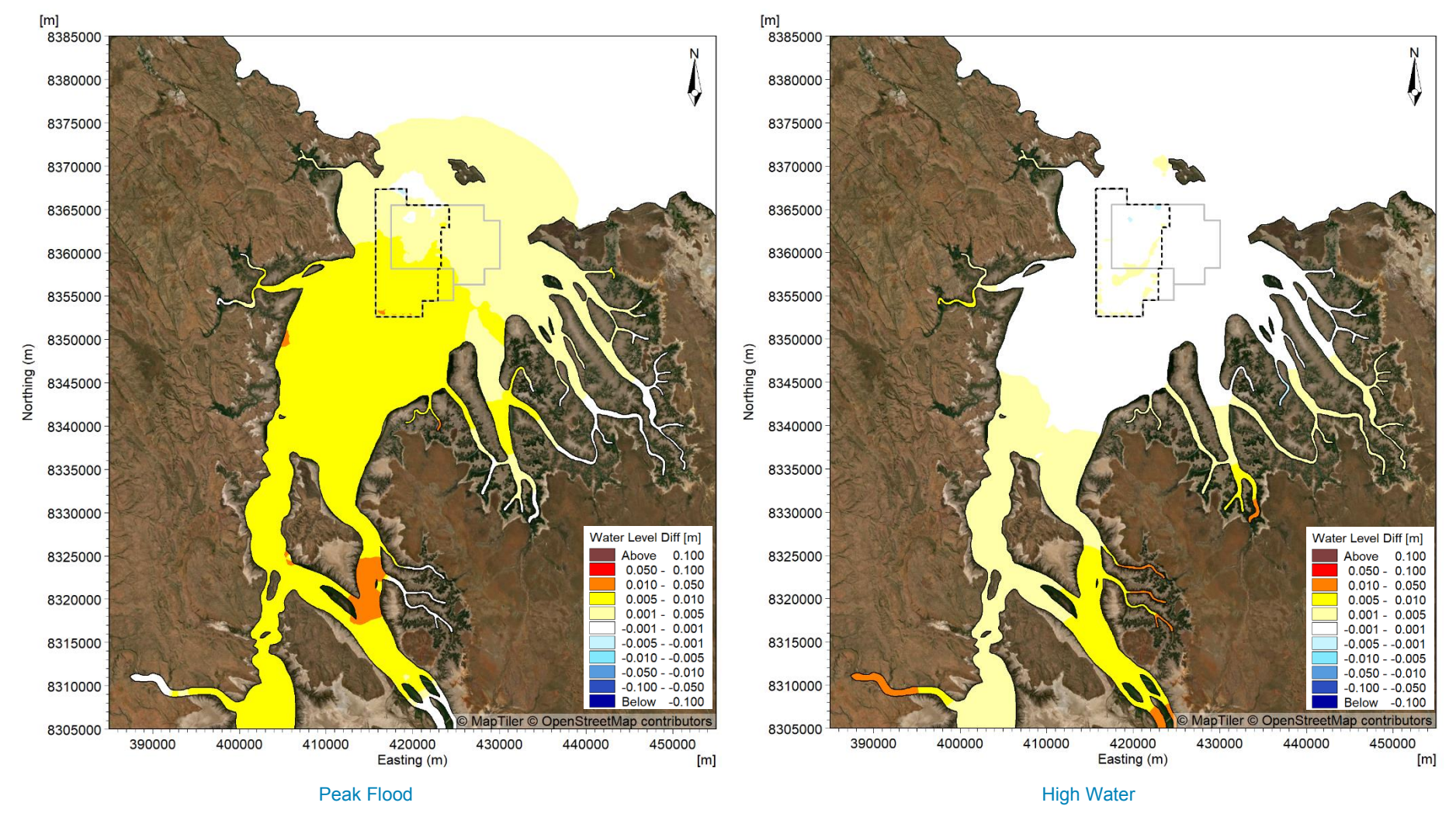


Figure B3. Modelled change in water level at peak flood (left) and high water (right) after 15 years of sand sourcing during a spring tide in the wet season.



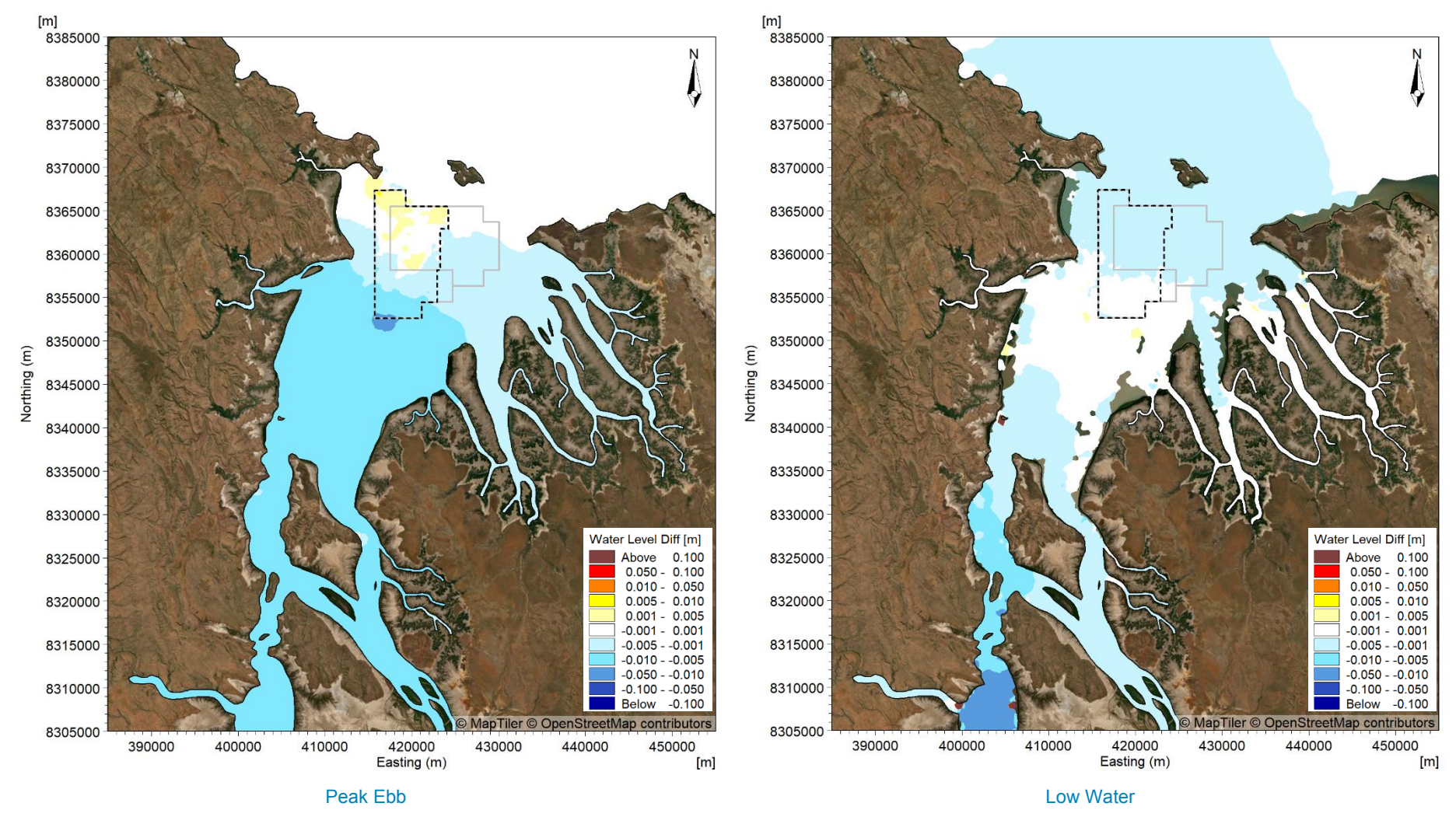


Figure B4. Modelled change in water level at peak ebb (left) and low water (right) after 15 years of sand sourcing during a spring tide in the wet season.



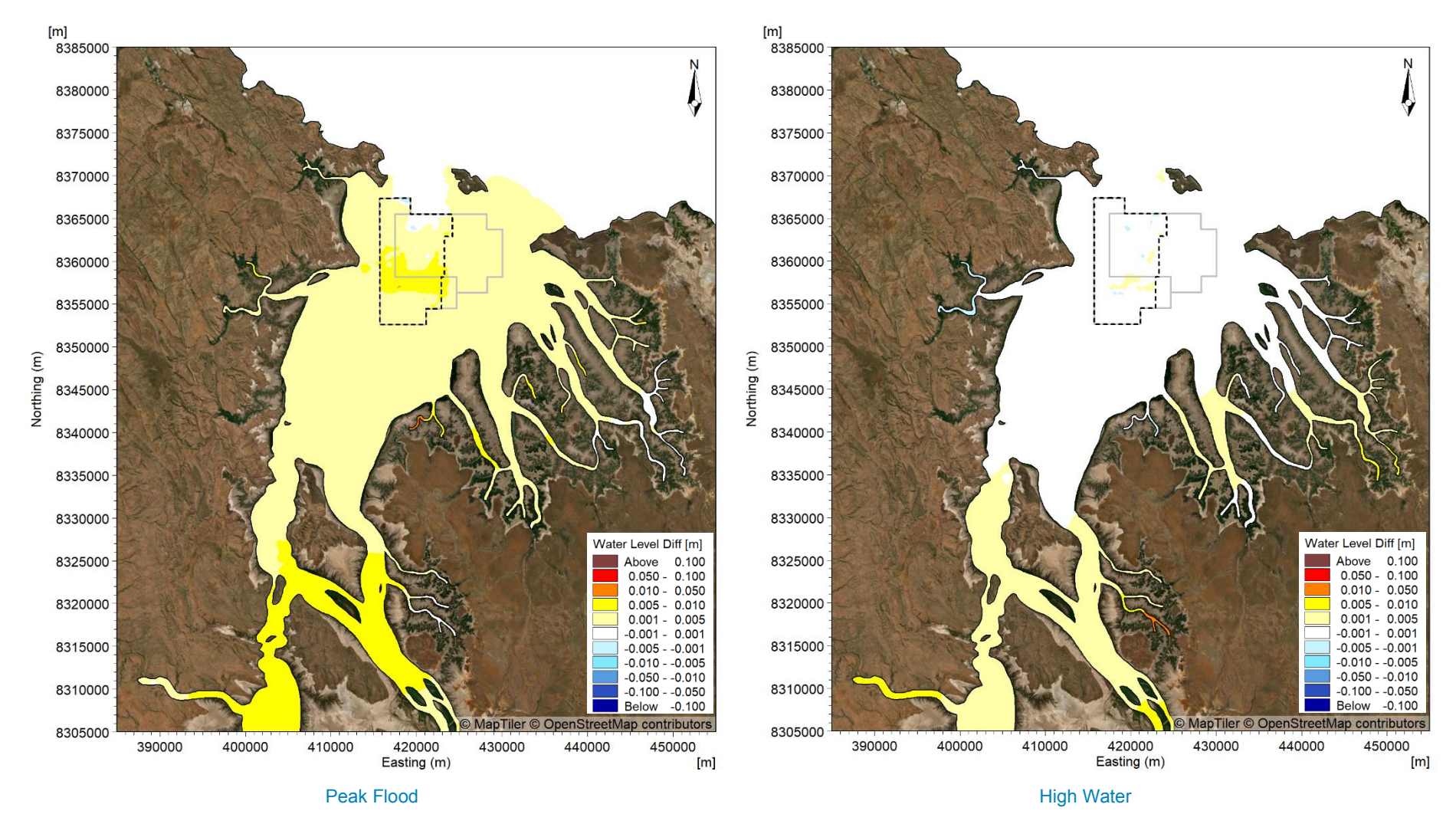


Figure B5. Modelled change in water level at peak flood (left) and high water (right) in 100 years time after 15 years of sand sourcing during a spring tide in the wet season.



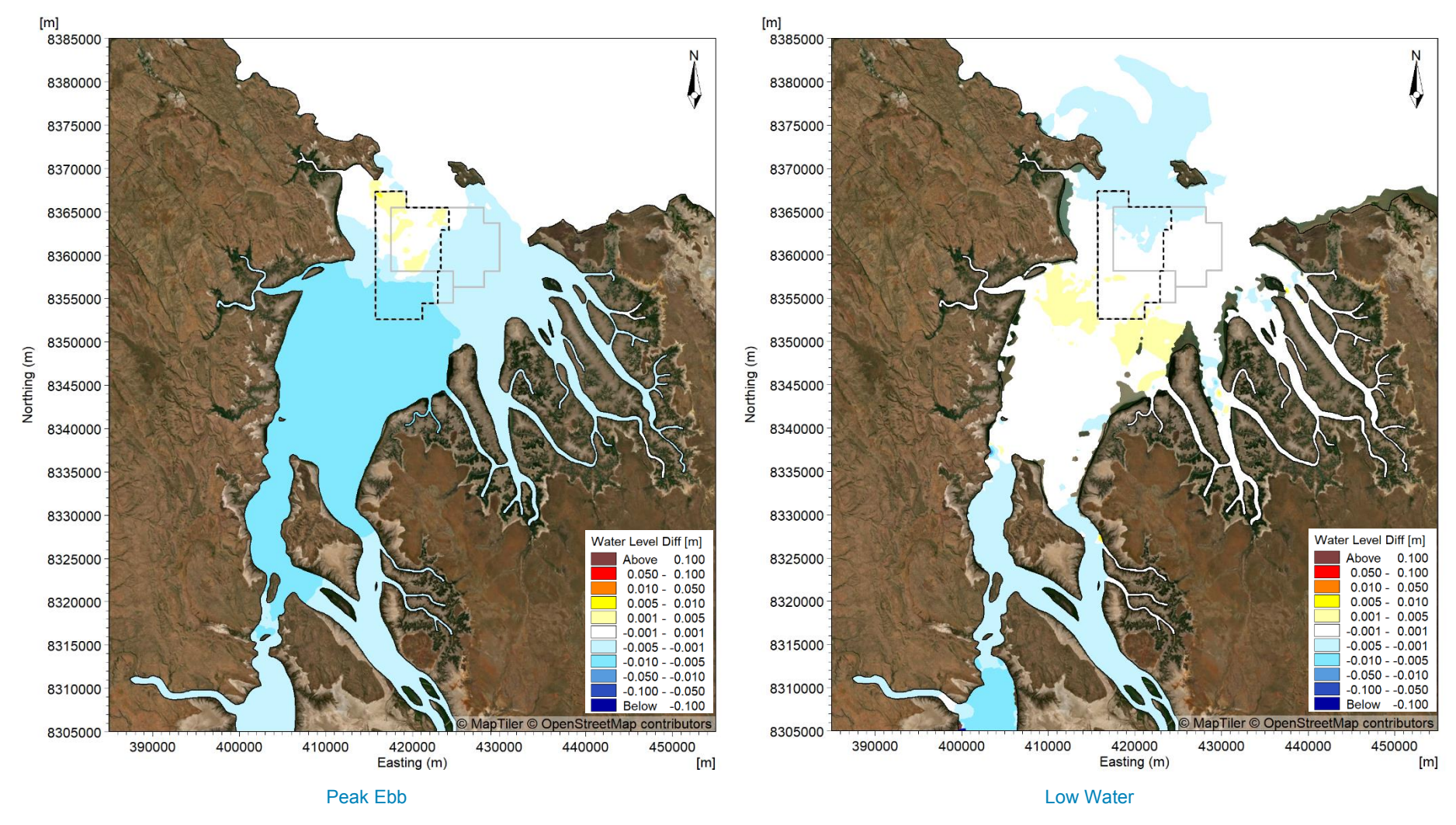


Figure B6. Modelled change in water level at peak ebb (left) and low water (right) in 100 years time after 15 years of sand sourcing during a spring tide in the wet season.



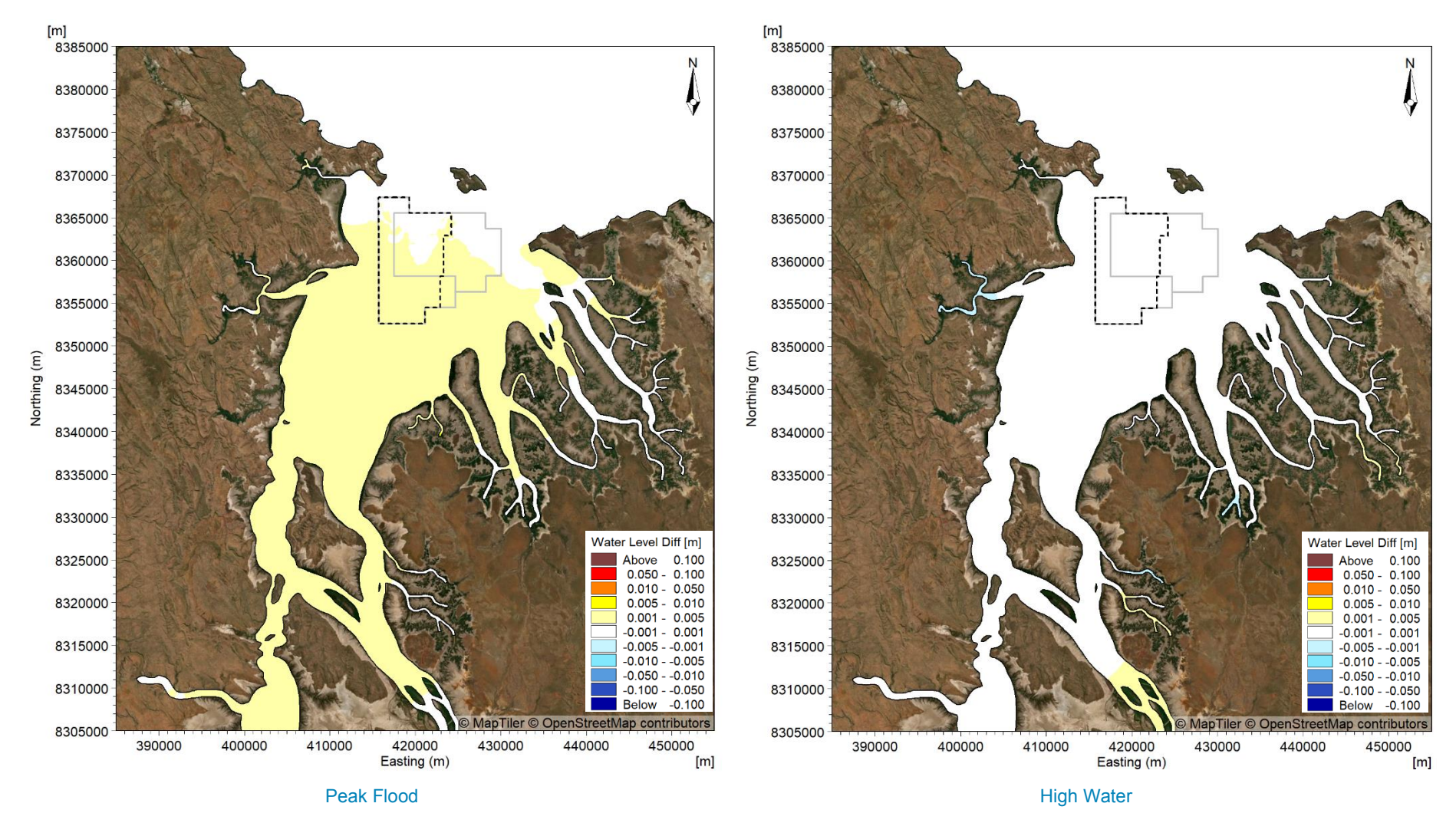


Figure B7. Modelled change in water level at peak flood (left) and high water (right) after 5 years of sand sourcing during a spring tide in the dry season.



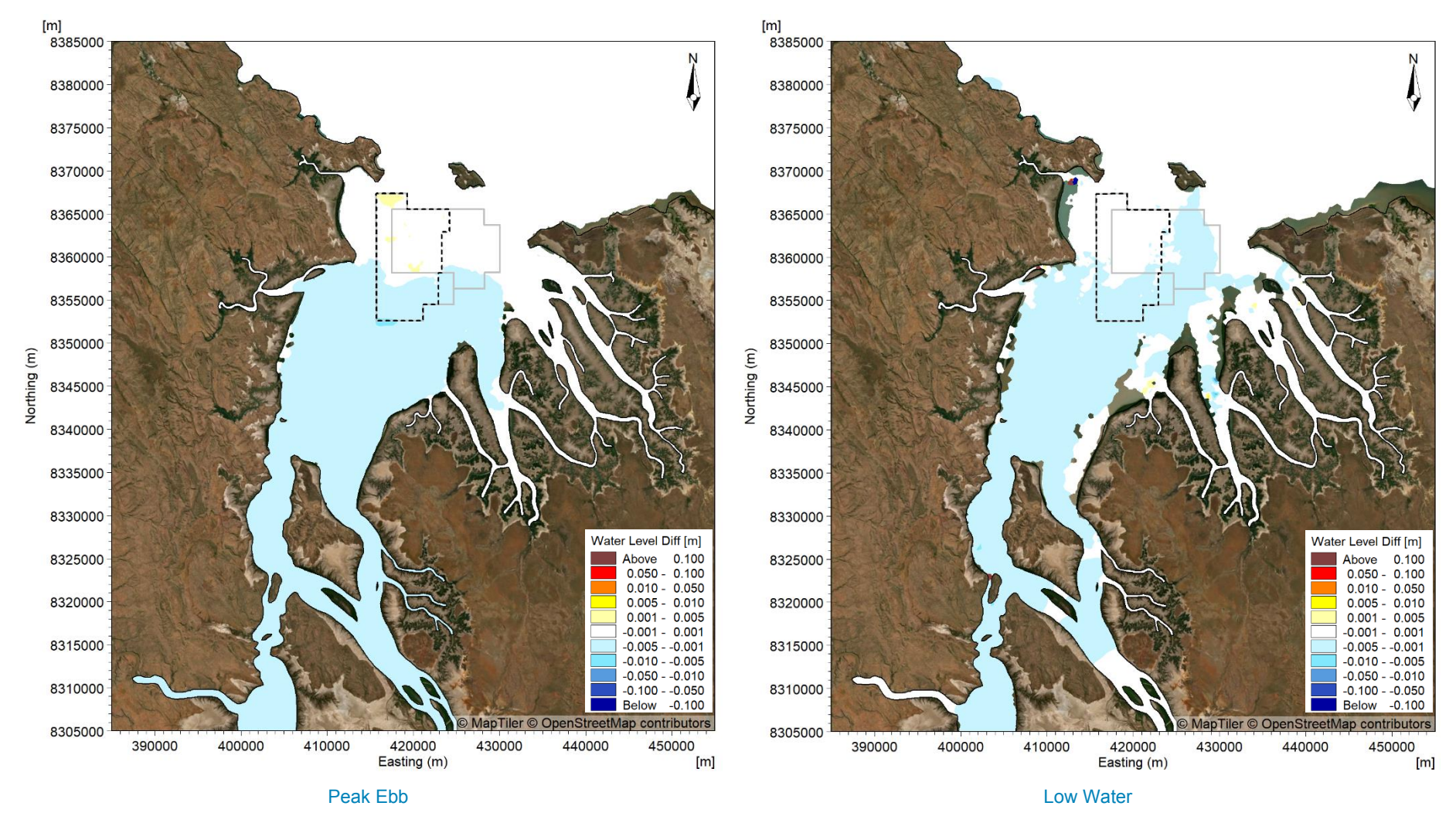


Figure B8. Modelled change in water level at peak ebb (left) and low water (right) after 5 years of sand sourcing during a spring tide in the dry season.



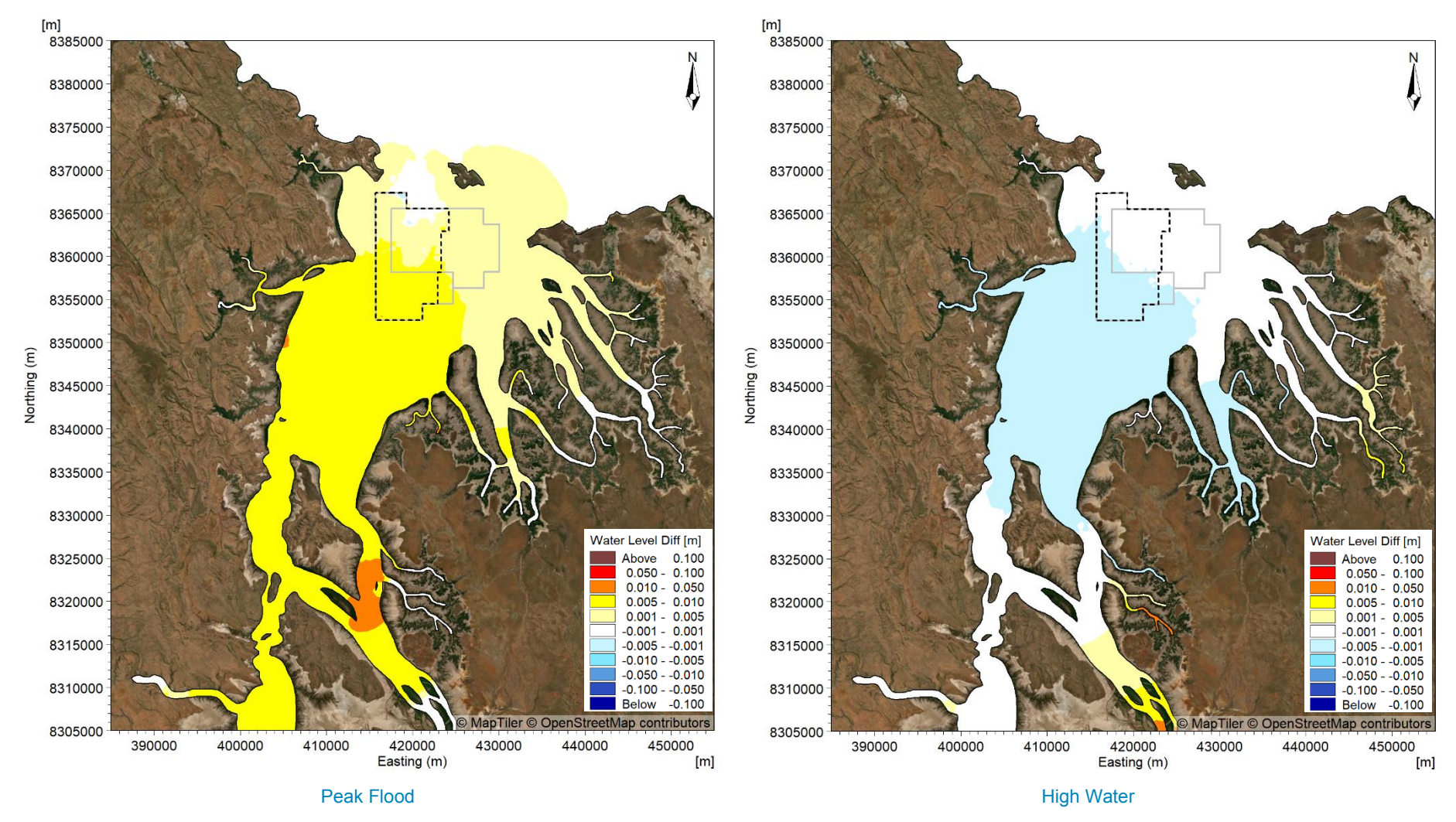


Figure B9. Modelled change in water level at peak flood (left) and high water (right) after 15 years of sand sourcing during a spring tide in the dry season.



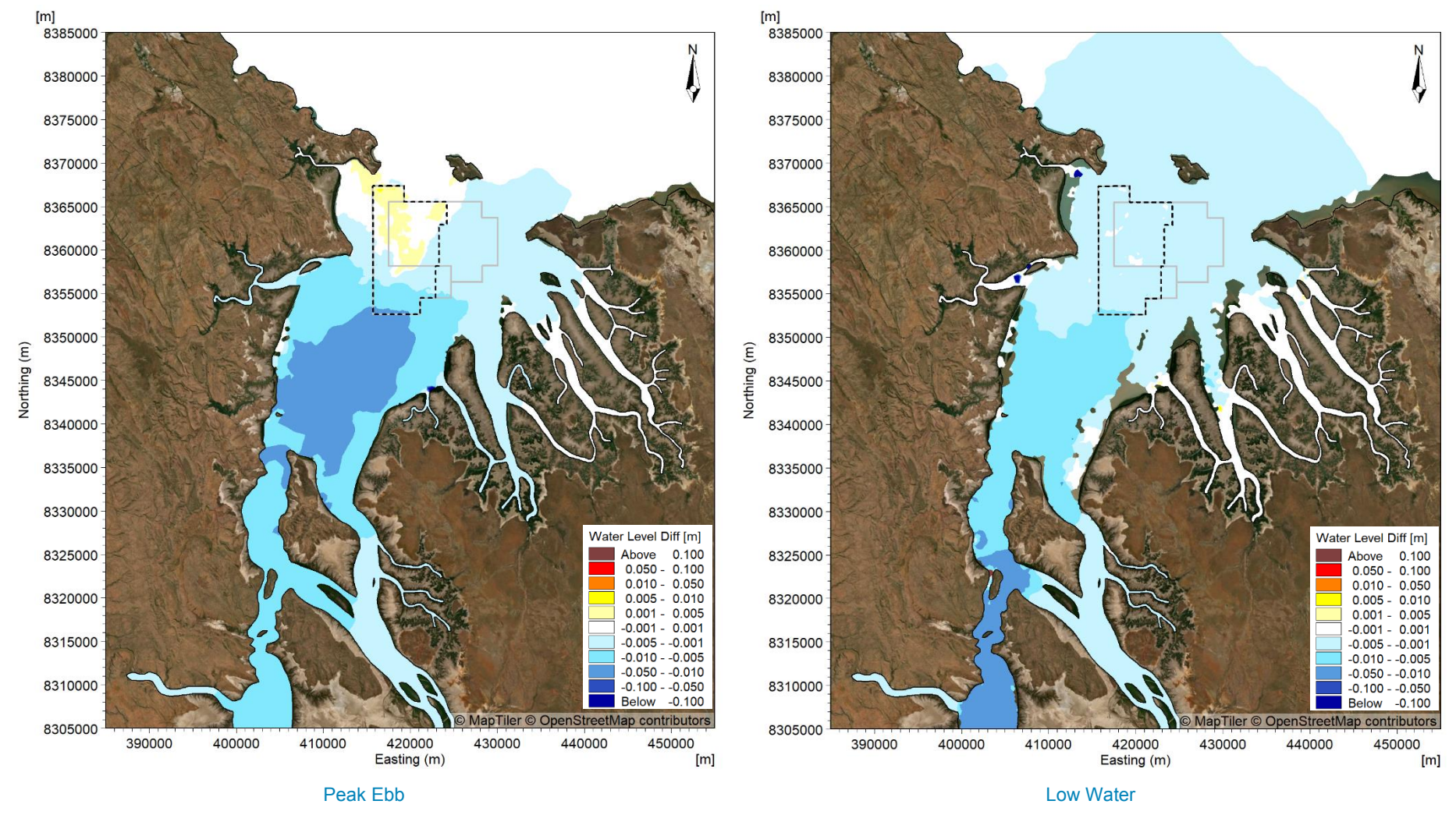


Figure B10. Modelled change in water level at peak ebb (left) and low water (right) after 15 years of sand sourcing during a spring tide in the dry season.



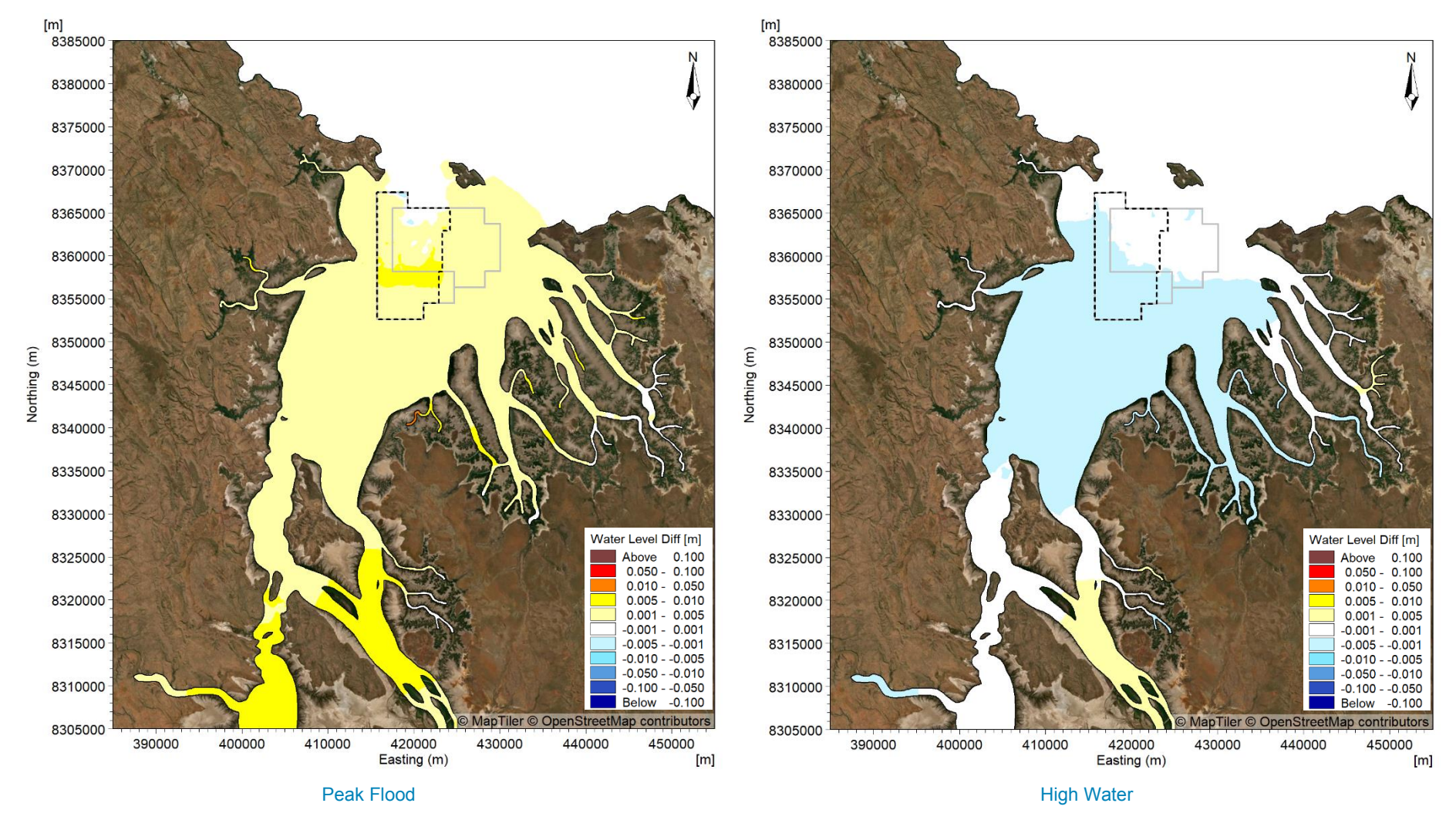


Figure B11. Modelled change in water level at peak flood (left) and high water (right) in 100 years time after 15 years of sand sourcing during a spring tide in the dry season.



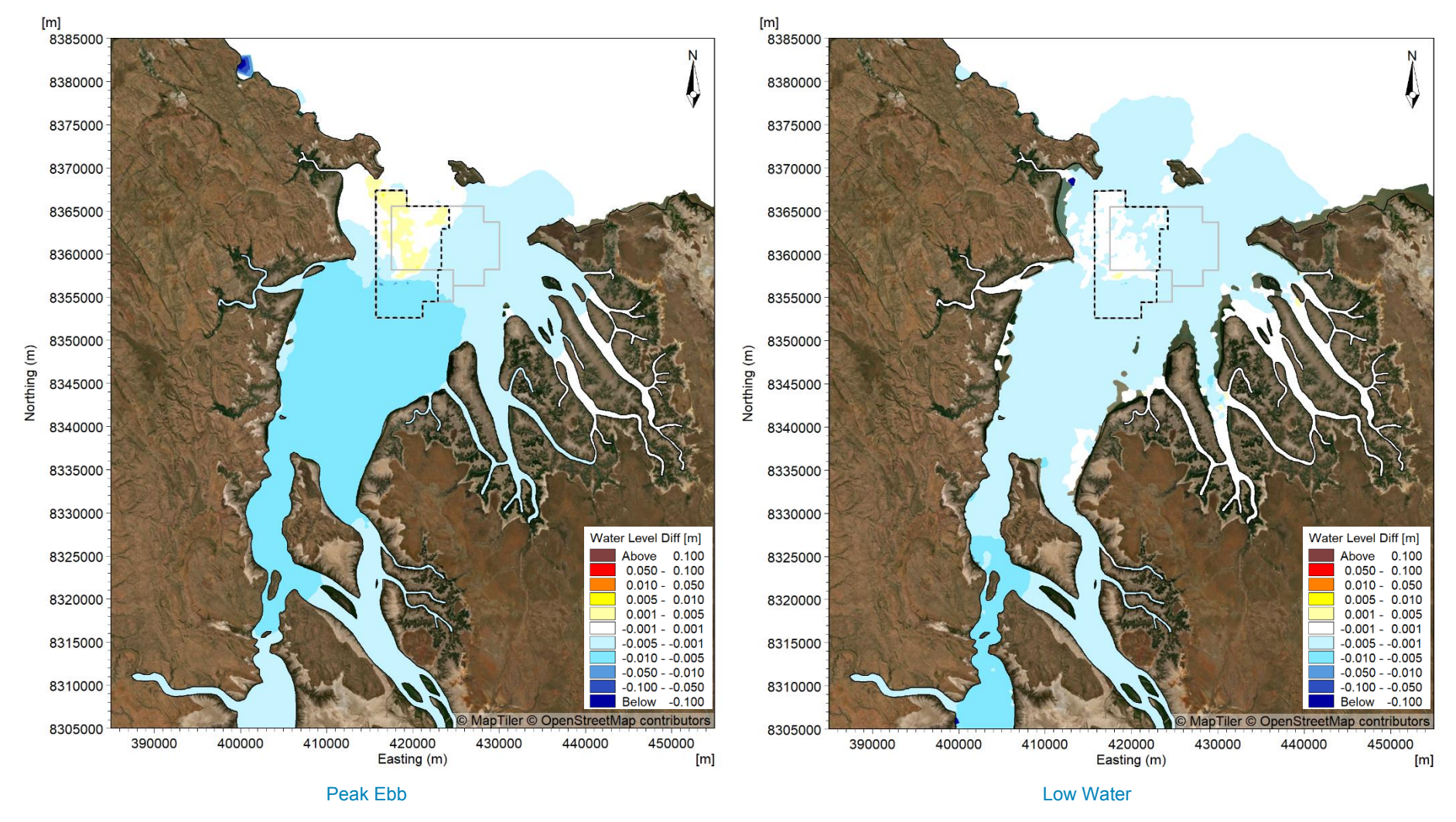


Figure B12. Modelled change in water level at peak ebb (left) and low water (right) in 100 years time after 15 years of sand sourcing during a spring tide in the dry season.



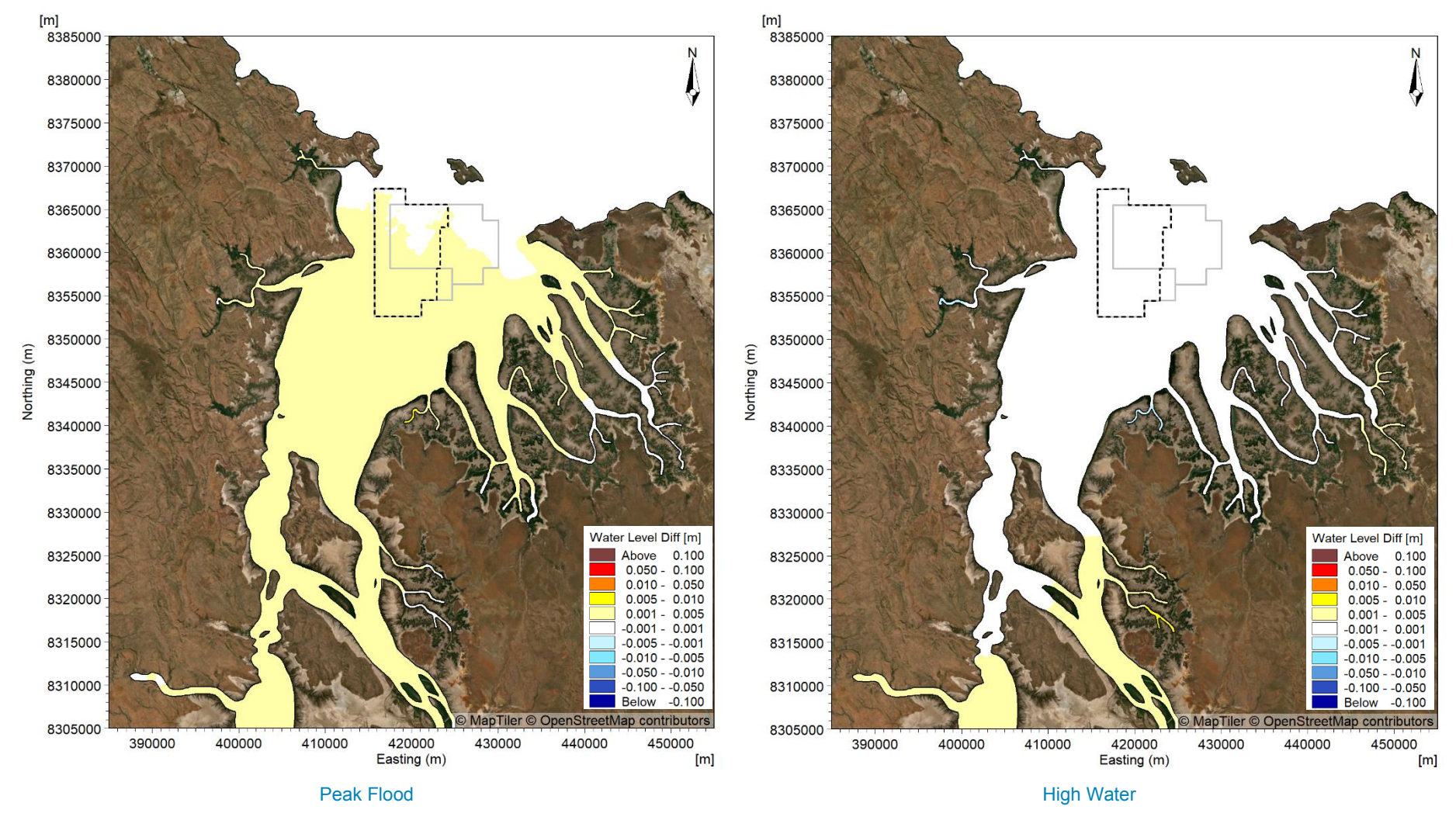


Figure B13. Modelled change in water level at peak flood (left) and high water (right) after 5 years of sand sourcing during a spring tide in the transitional season.



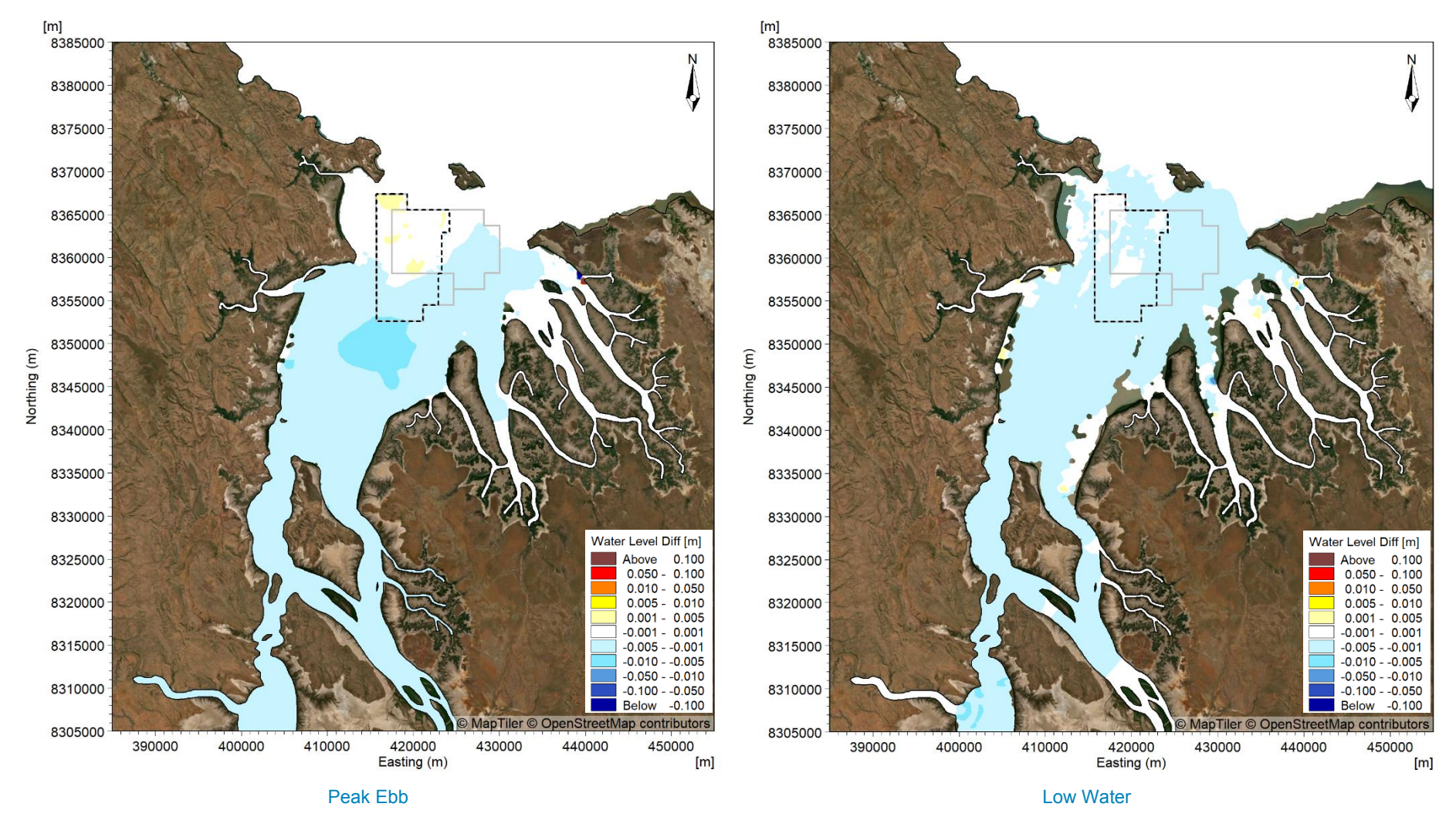


Figure B14. Modelled change in water level at peak ebb (left) and low water (right) after 5 years of sand sourcing during a spring tide in the transitional season.



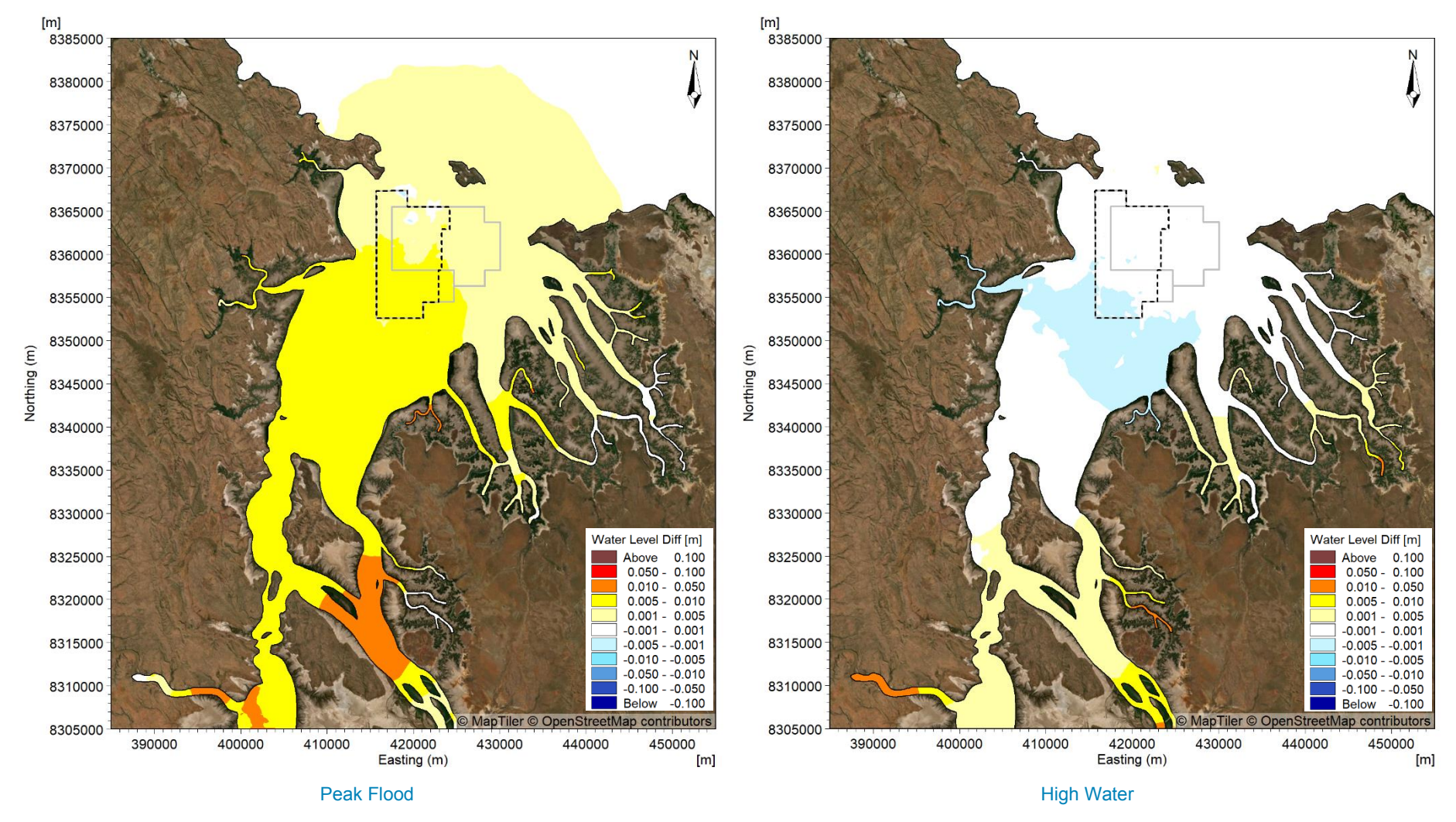


Figure B15. Modelled change in water level at peak flood (left) and high water (right) after 15 years of sand sourcing during a spring tide in the transitional season.



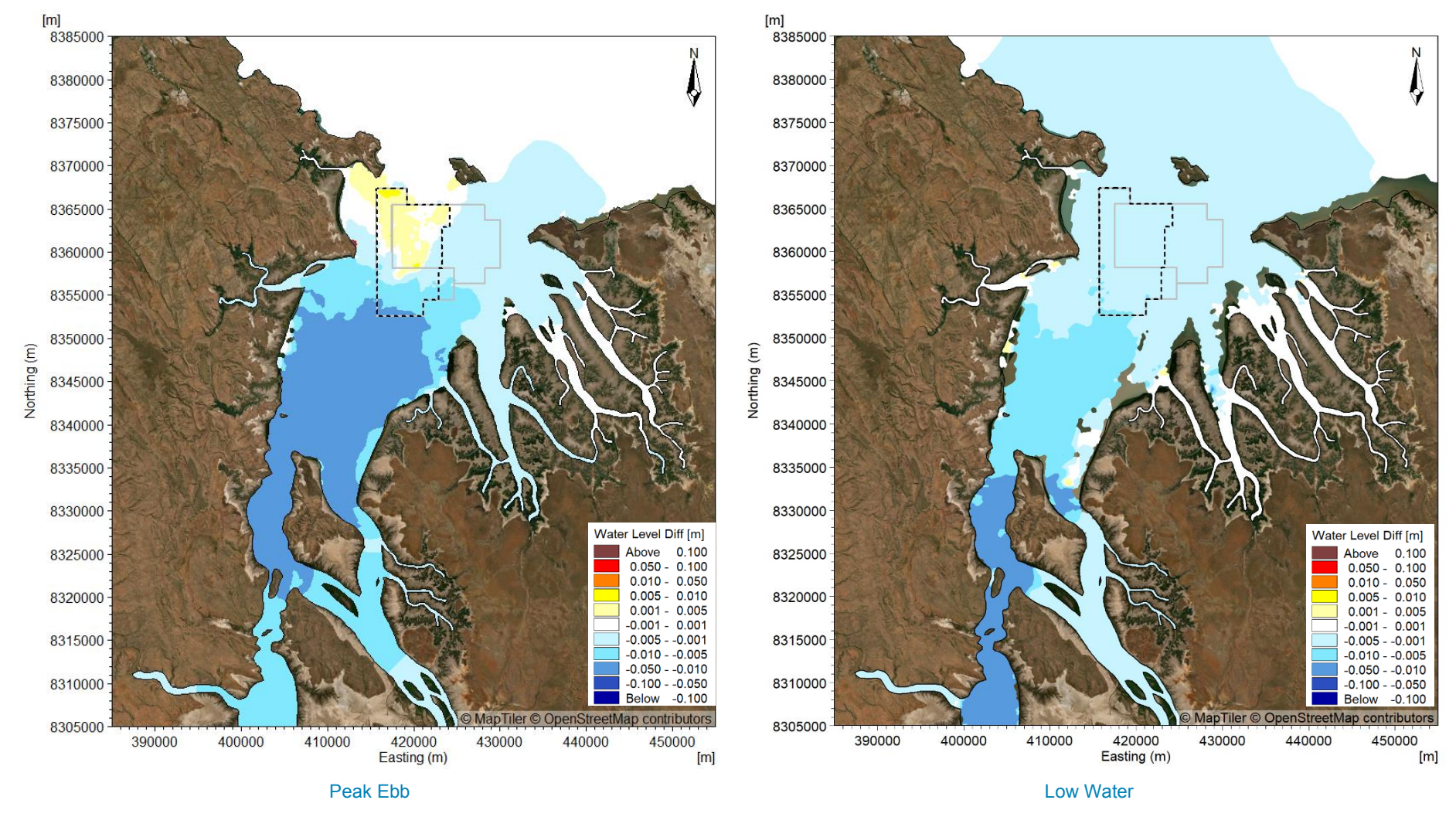


Figure B16. Modelled change in water level at peak ebb (left) and low water (right) after 15 years of sand sourcing during a spring tide in the transitional season.



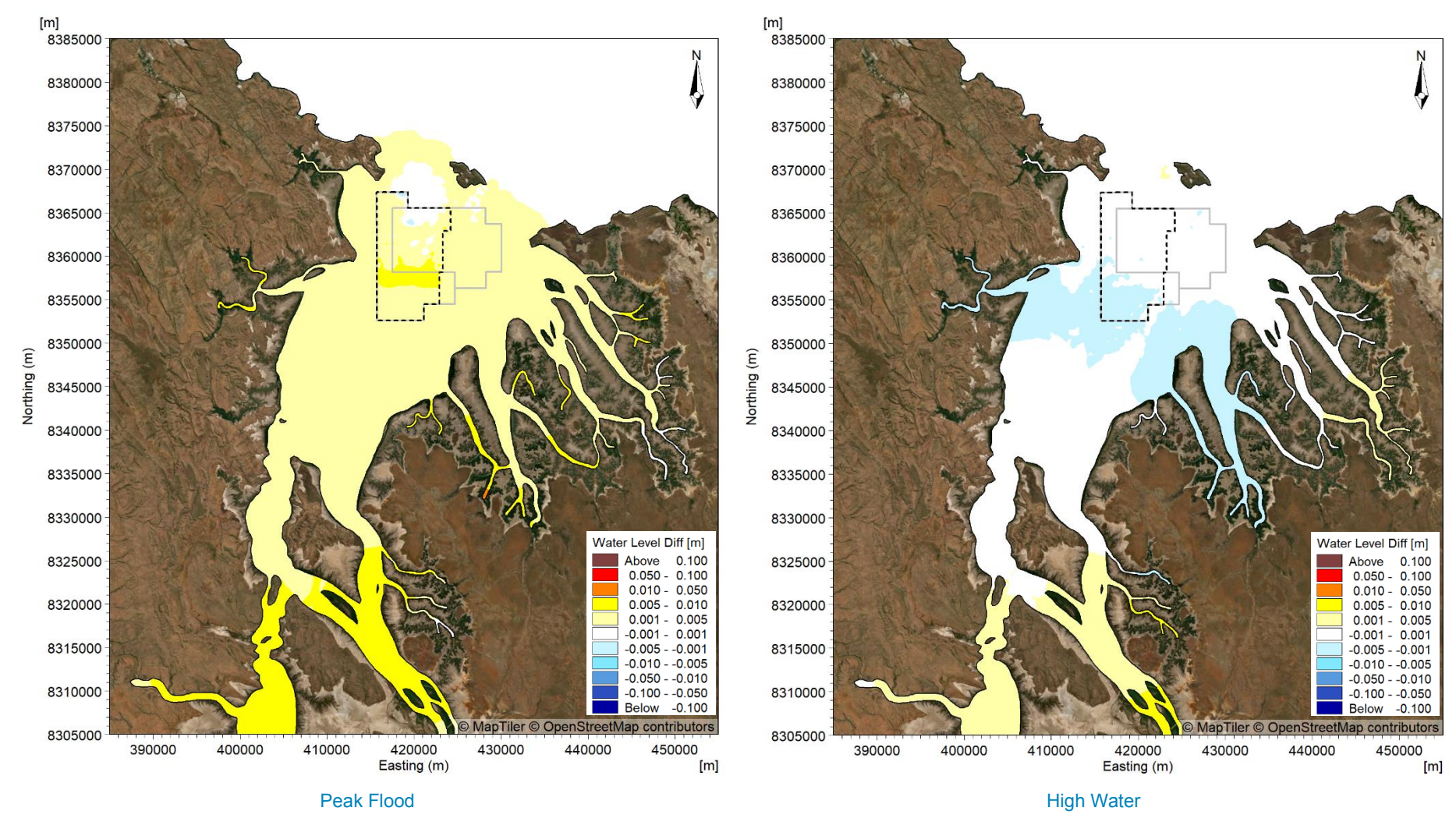


Figure B17. Modelled change in water level at peak flood (left) and high water (right) in 100 years time after 15 years of sand sourcing during a spring tide in the transitional season.

B18



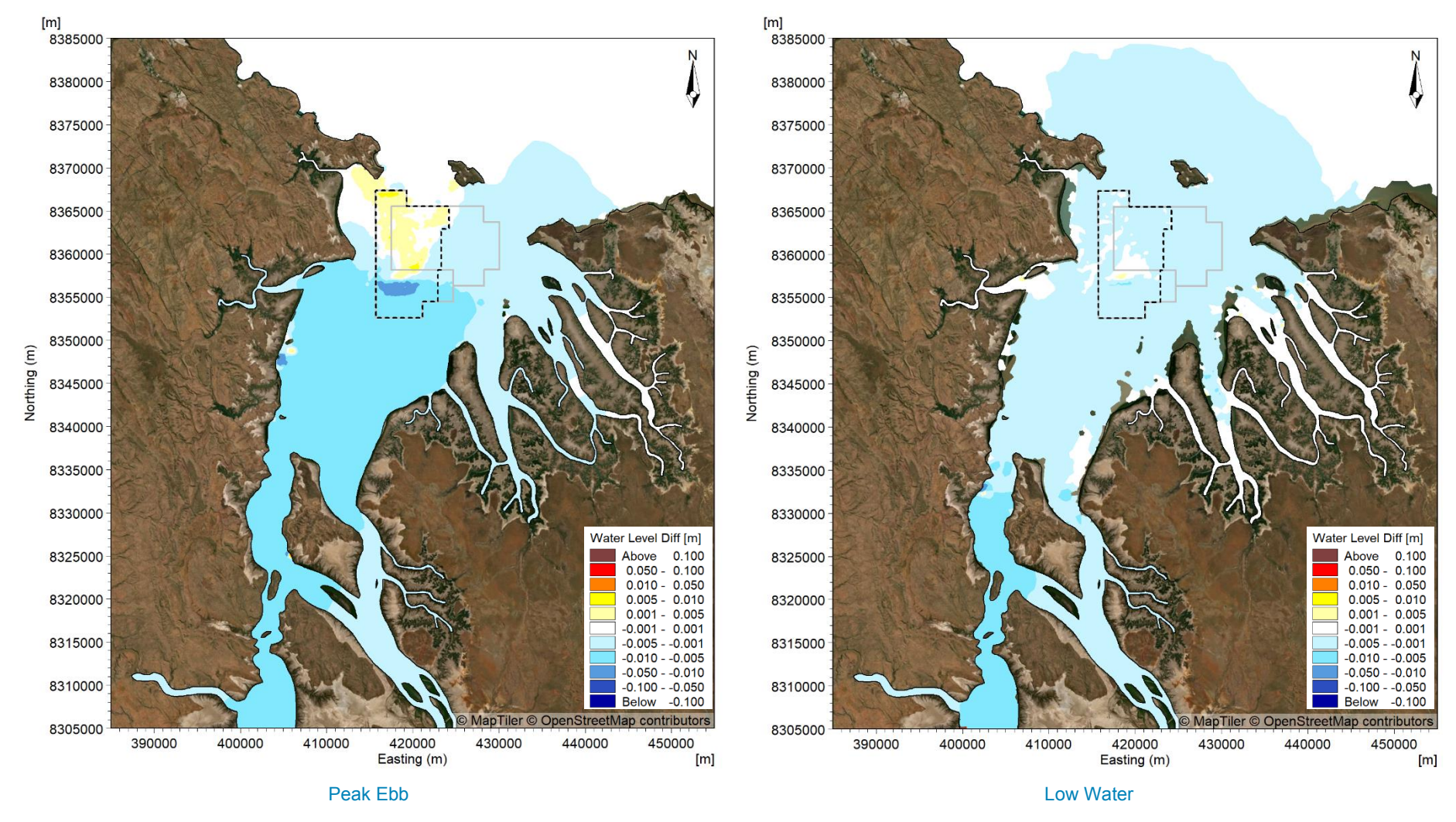


Figure B18. Modelled change in water level at peak ebb (left) and low water (right) in 100 years time after 15 years of sand sourcing during a spring tide in the transitional season.



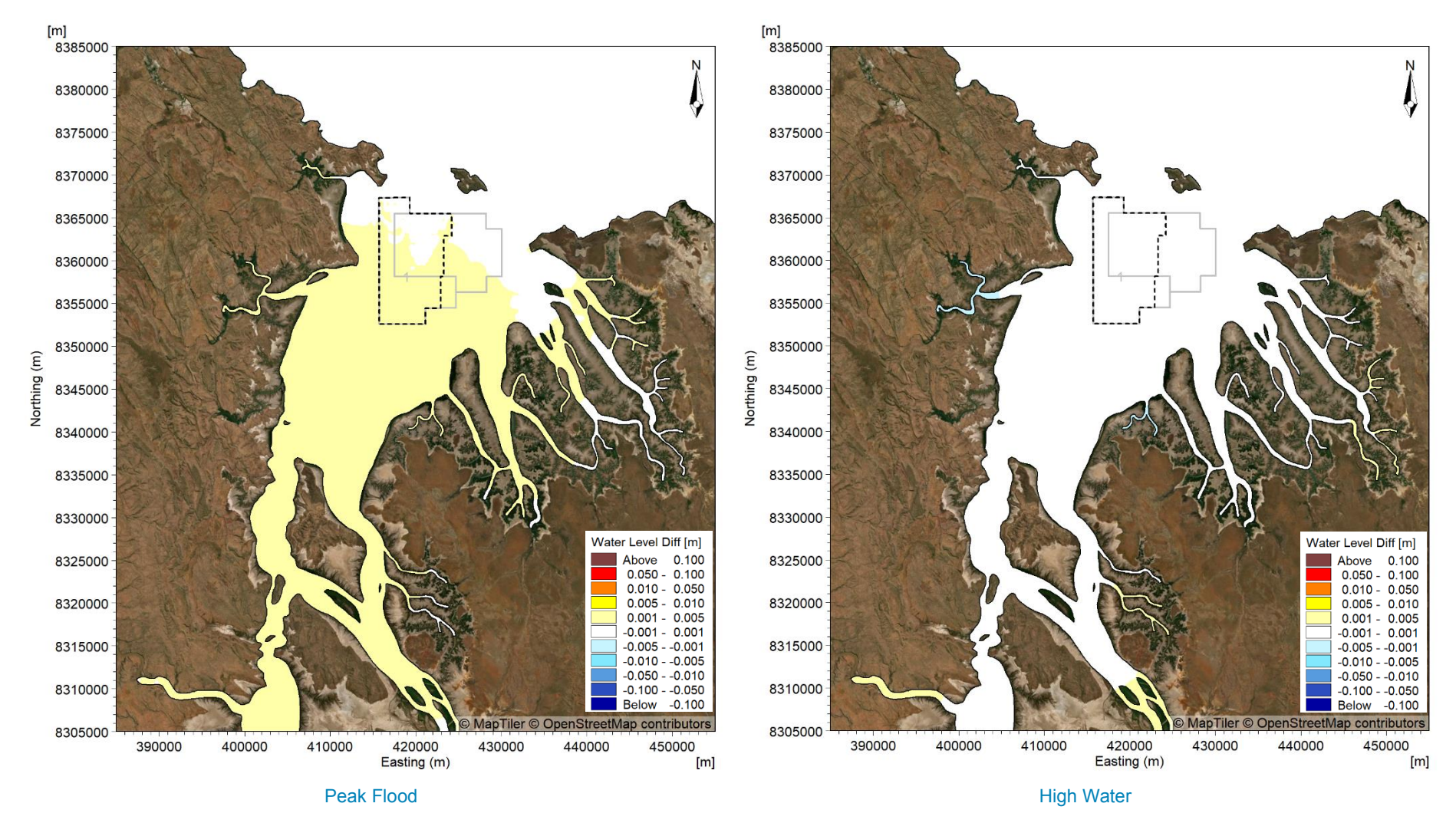


Figure B19. Modelled change in water level at peak flood (left) and high water (right) after 5 years of sand sourcing during TC Marcus.



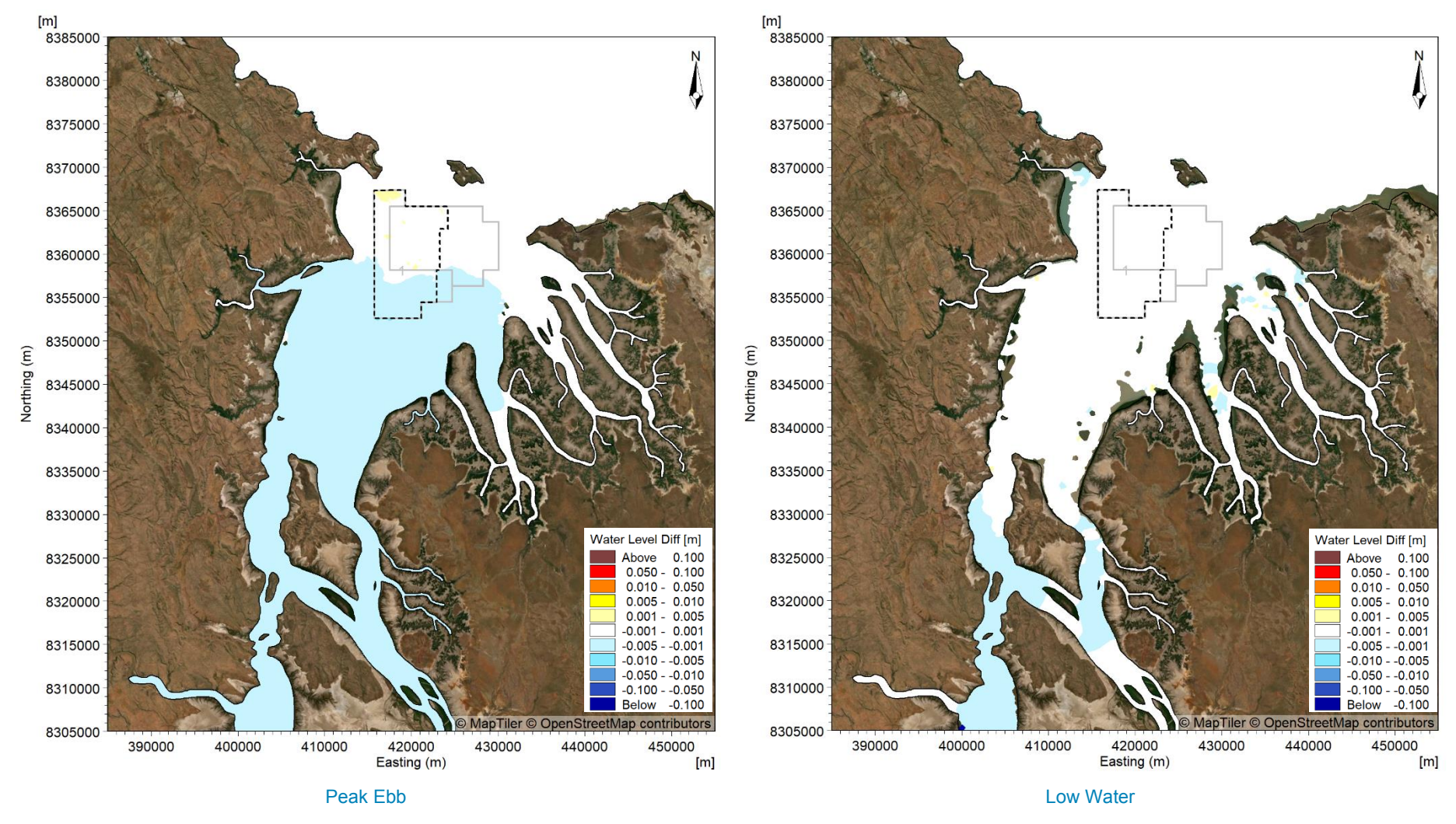


Figure B20. Modelled change in water level at peak ebb (left) and low water (right) after 5 years of sand sourcing during TC Marcus.



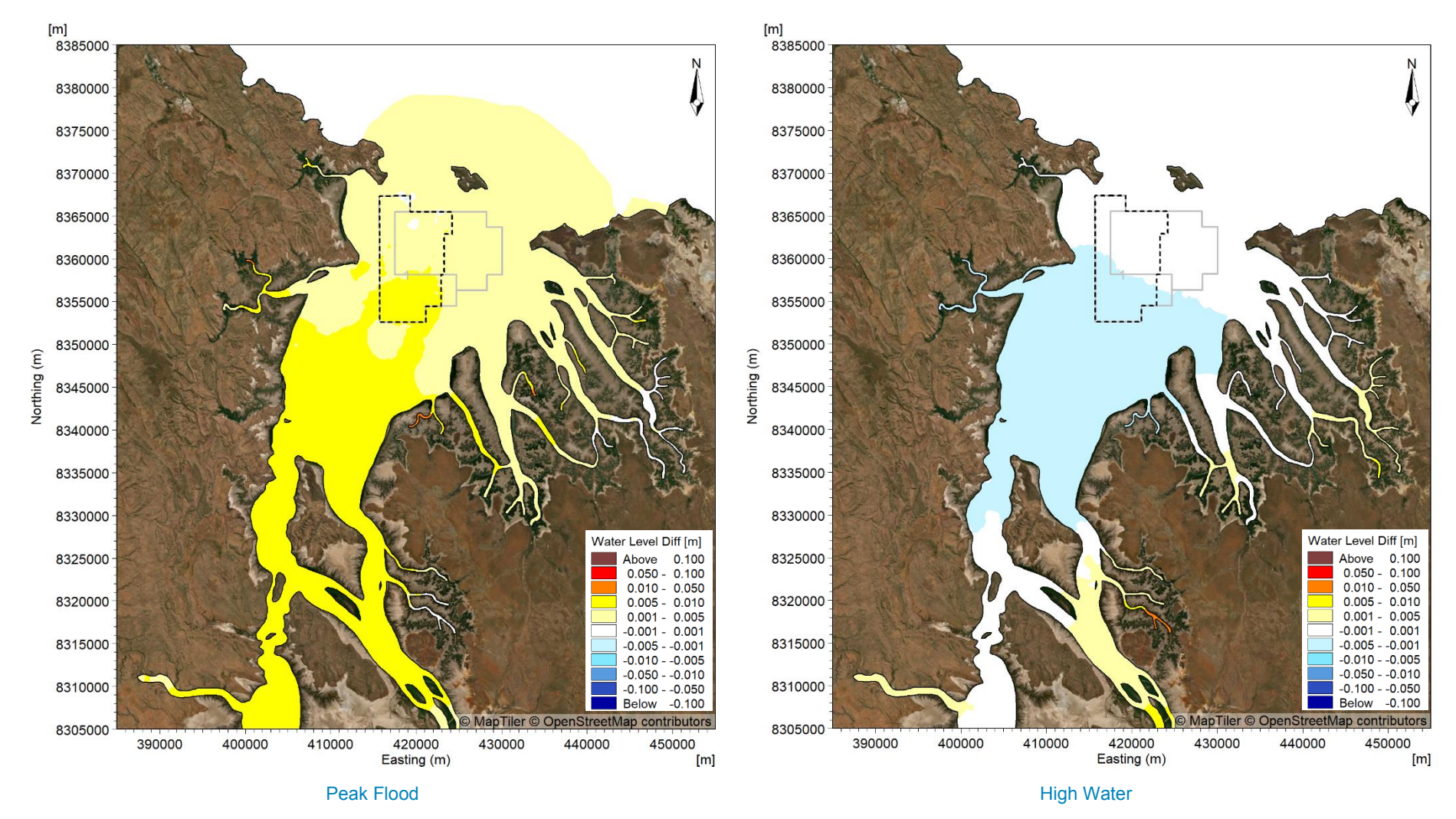


Figure B21. Modelled change in water level at peak flood (left) and high water (right) after 15 years of sand sourcing during TC Marcus.



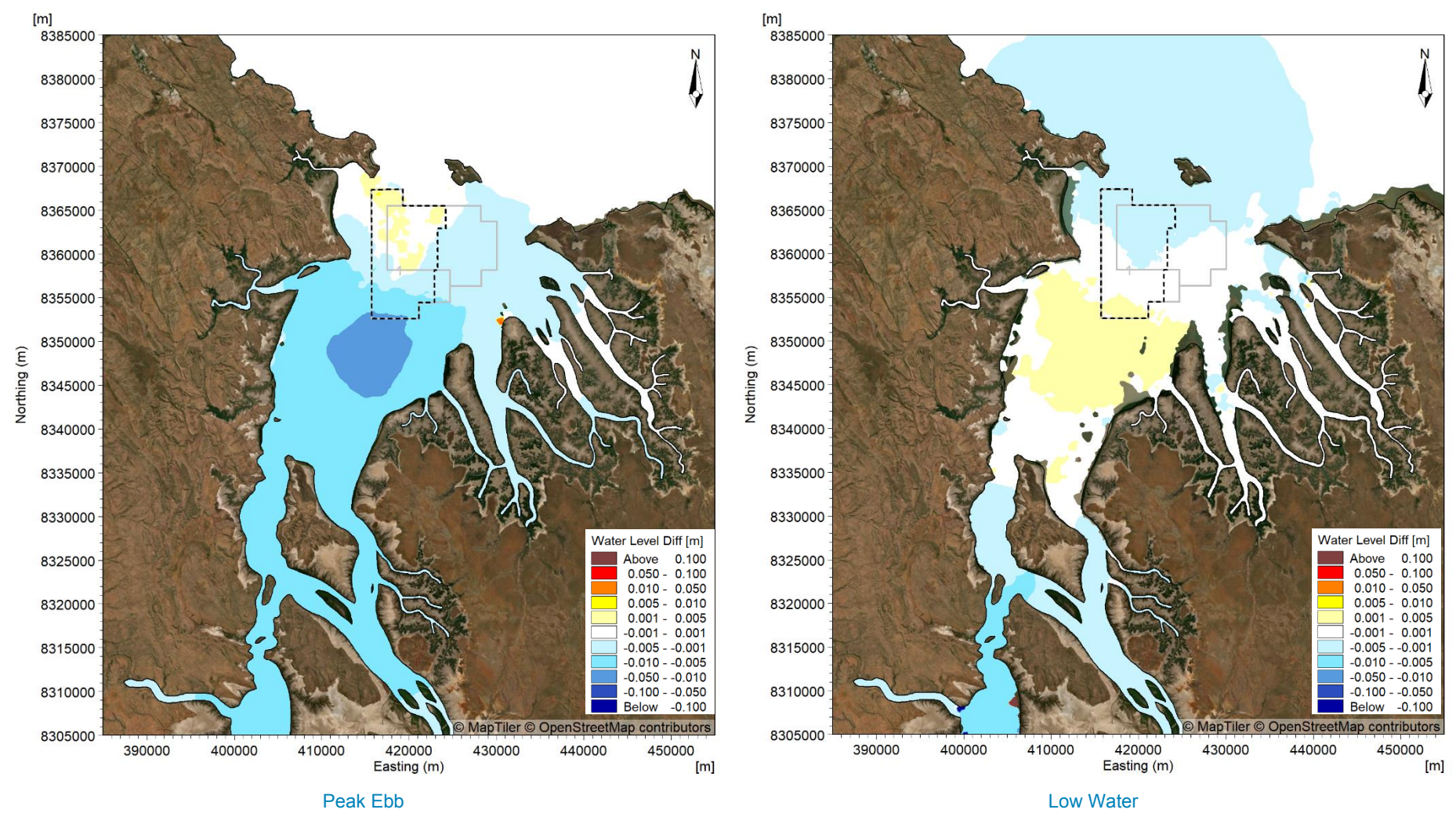


Figure B22. Modelled change in water level at peak ebb (left) and low water (right) after 15 years of sand sourcing during TC Marcus.



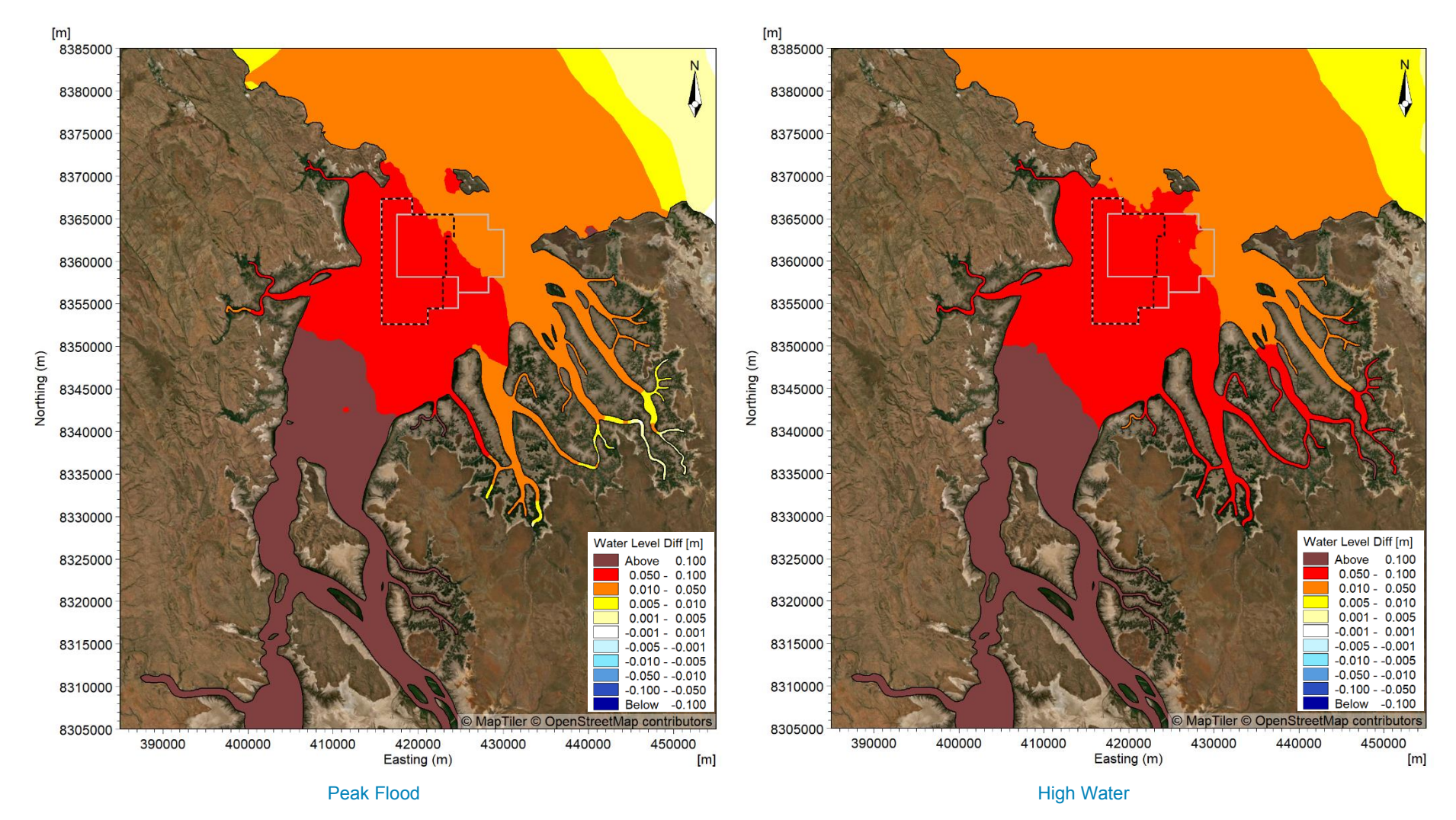


Figure B23. Modelled change in water level at peak flood (left) and high water (right) for the Pre-European Settlement scenario during a spring tide in the wet season during a high discharge event.



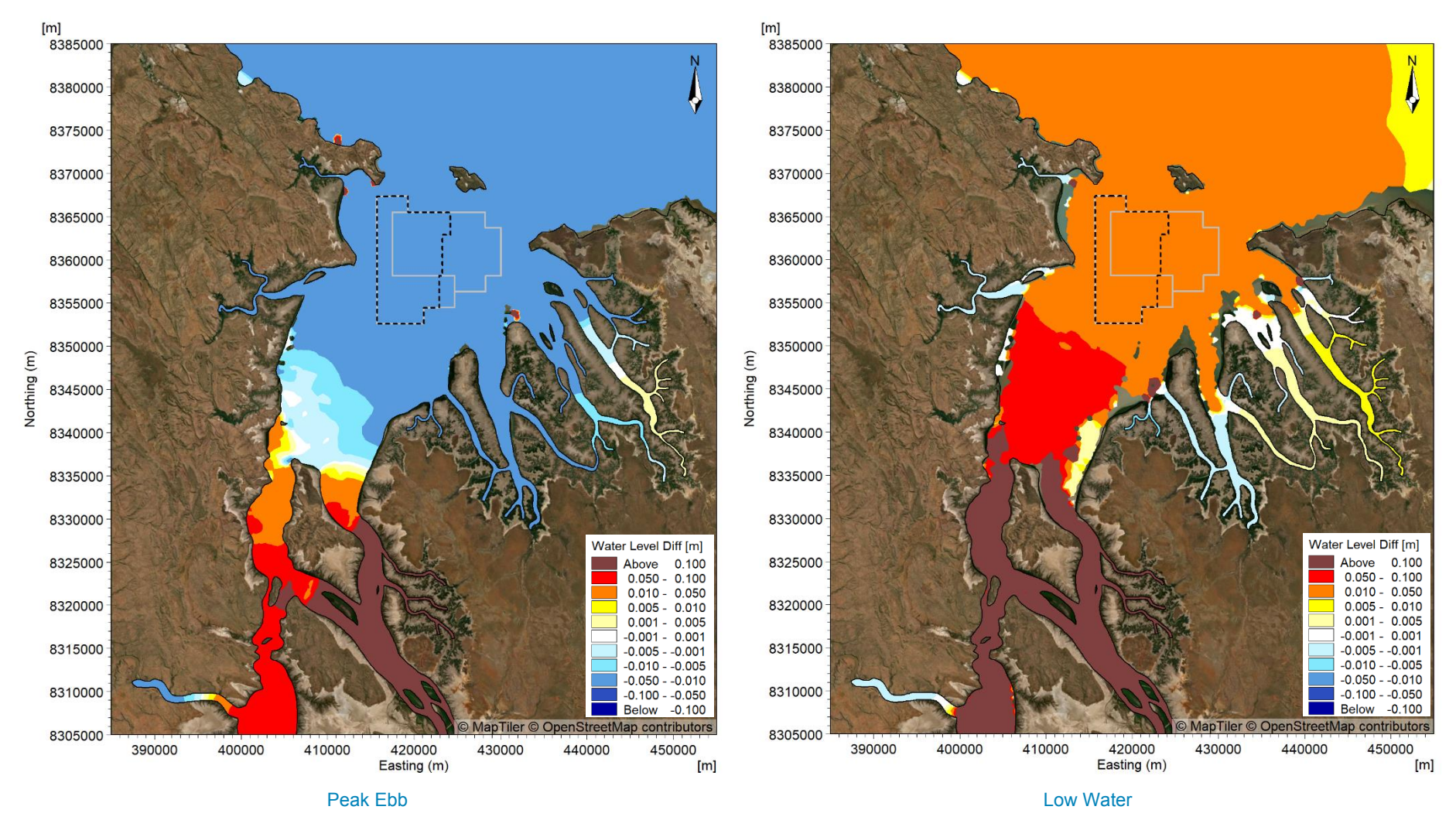


Figure B24. Modelled change in water level at peak ebb (left) and low water (right) for the Pre-European Settlement scenario during a spring tide in the wet season during a high discharge event.



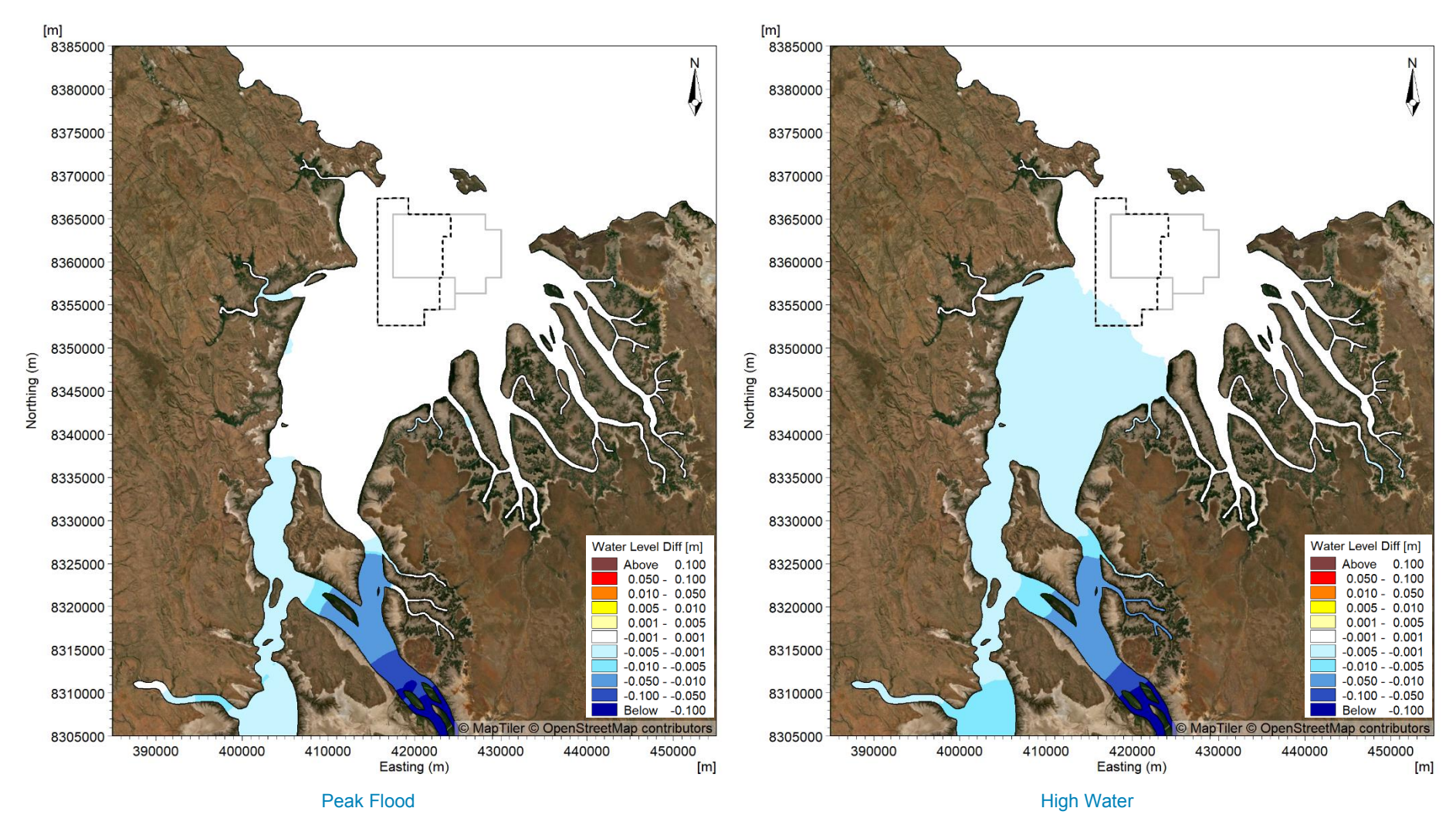


Figure B25. Modelled change in water level at peak flood (left) and high water (right) for the Pre-European Settlement scenario during a spring tide in the dry season.



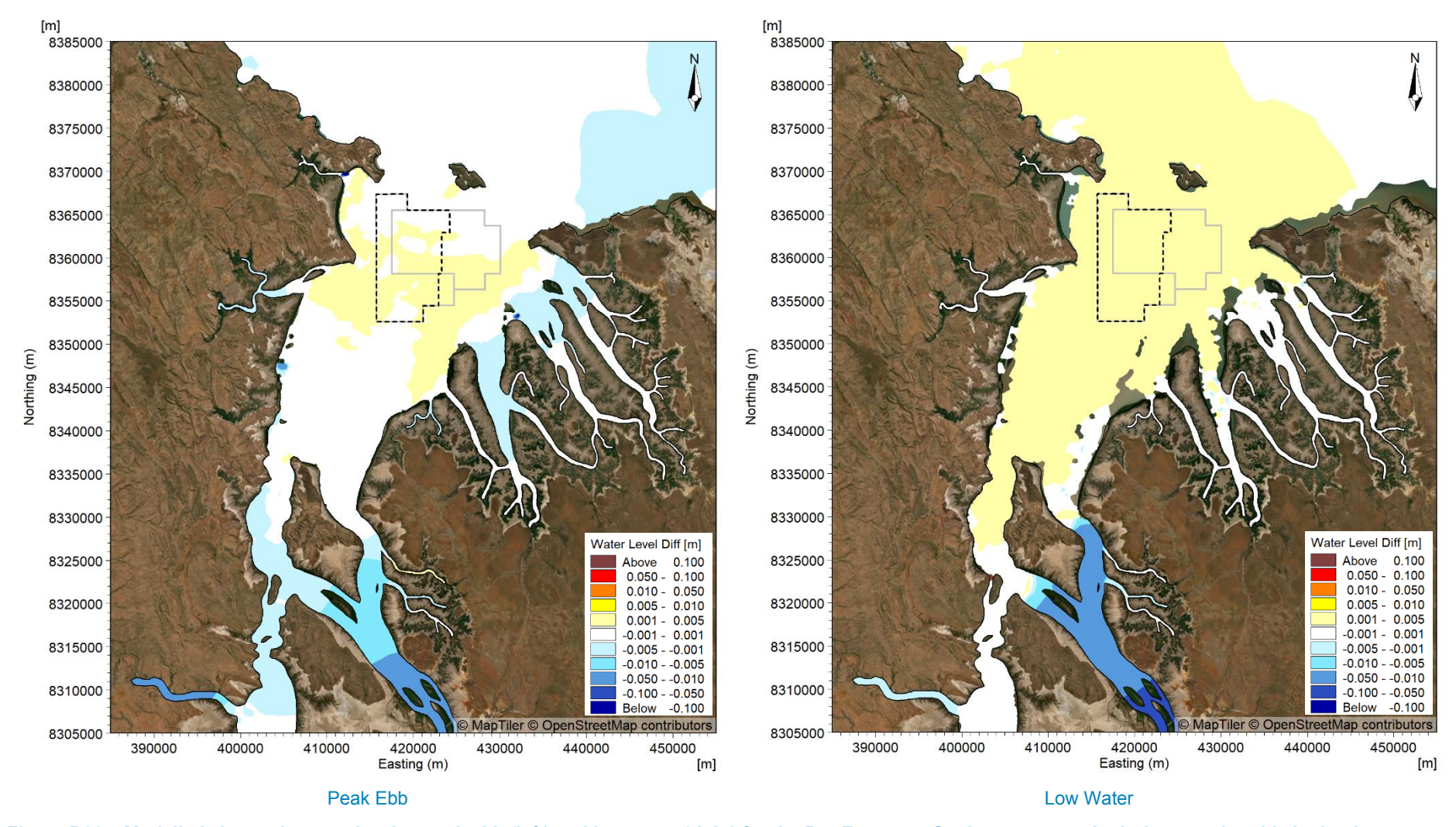


Figure B26. Modelled change in water level at peak ebb (left) and low water (right) for the Pre-European Settlement scenario during a spring tide in the dry season.



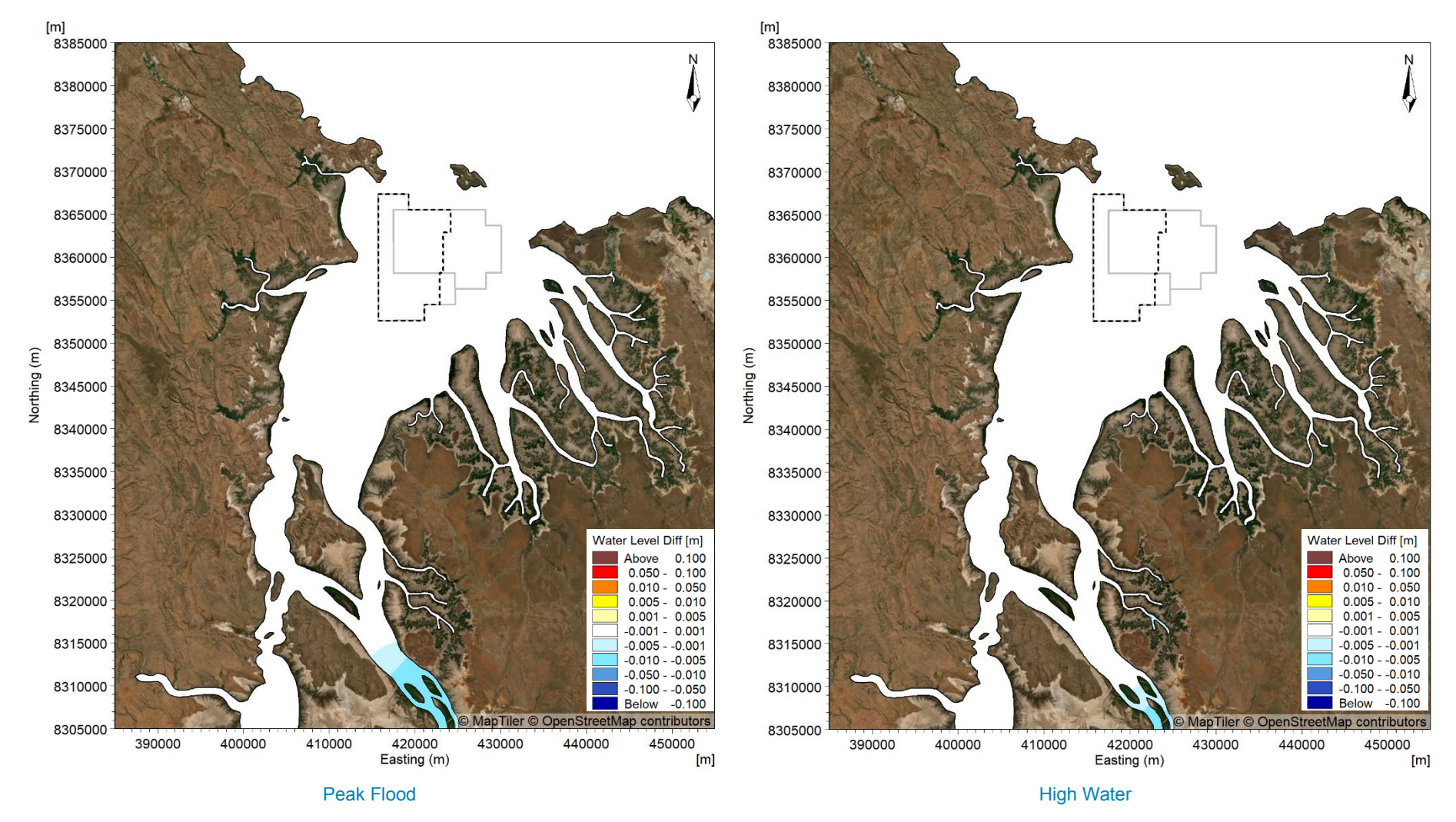


Figure B27. Modelled change in water level at peak flood (left) and high water (right) for the Pre-European Settlement scenario during a spring tide in the transitional season.



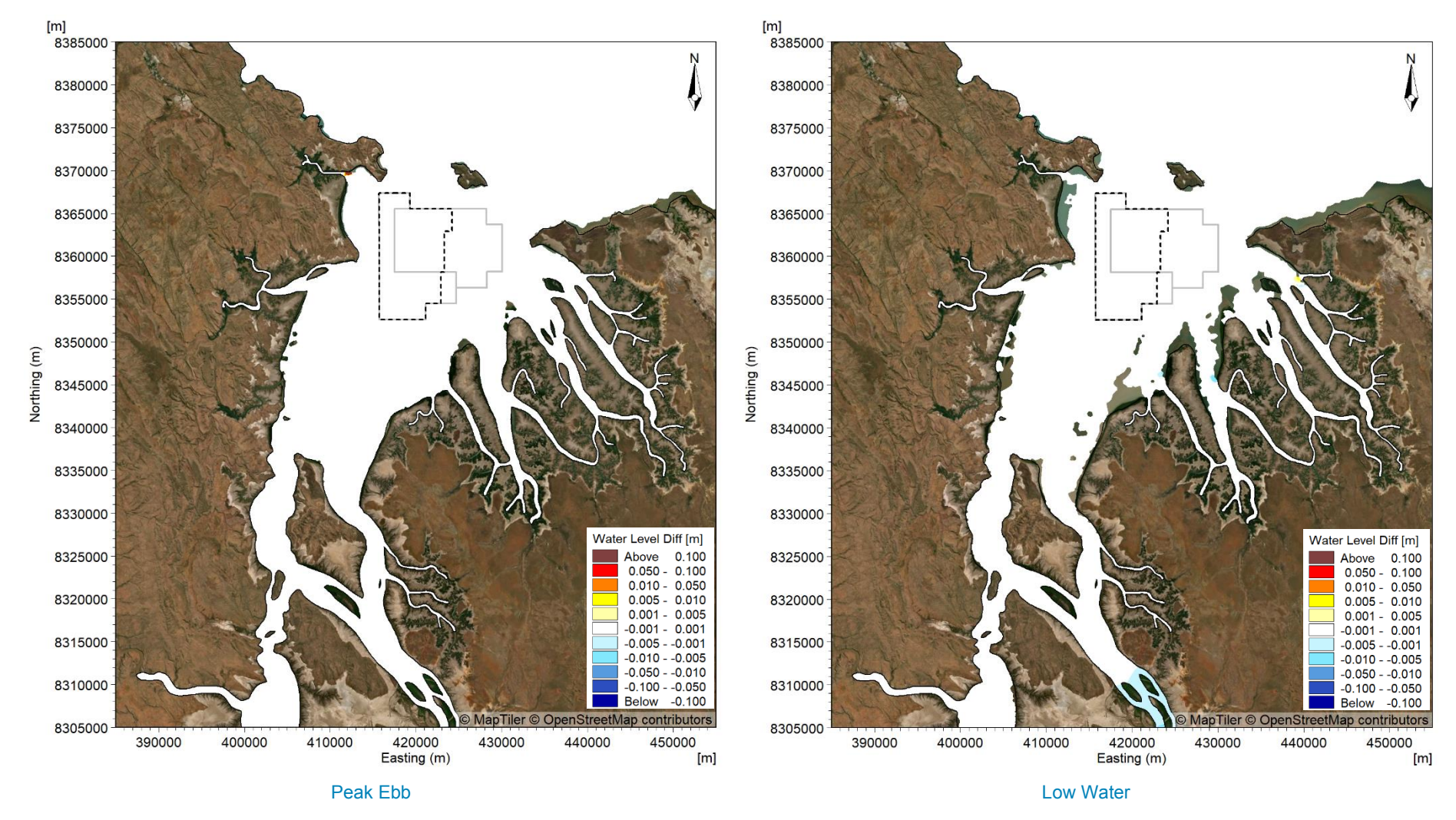


Figure B28. Modelled change in water level at peak ebb (left) and low water (right) for the Pre-European Settlement scenario during a spring tide in the transitional season.



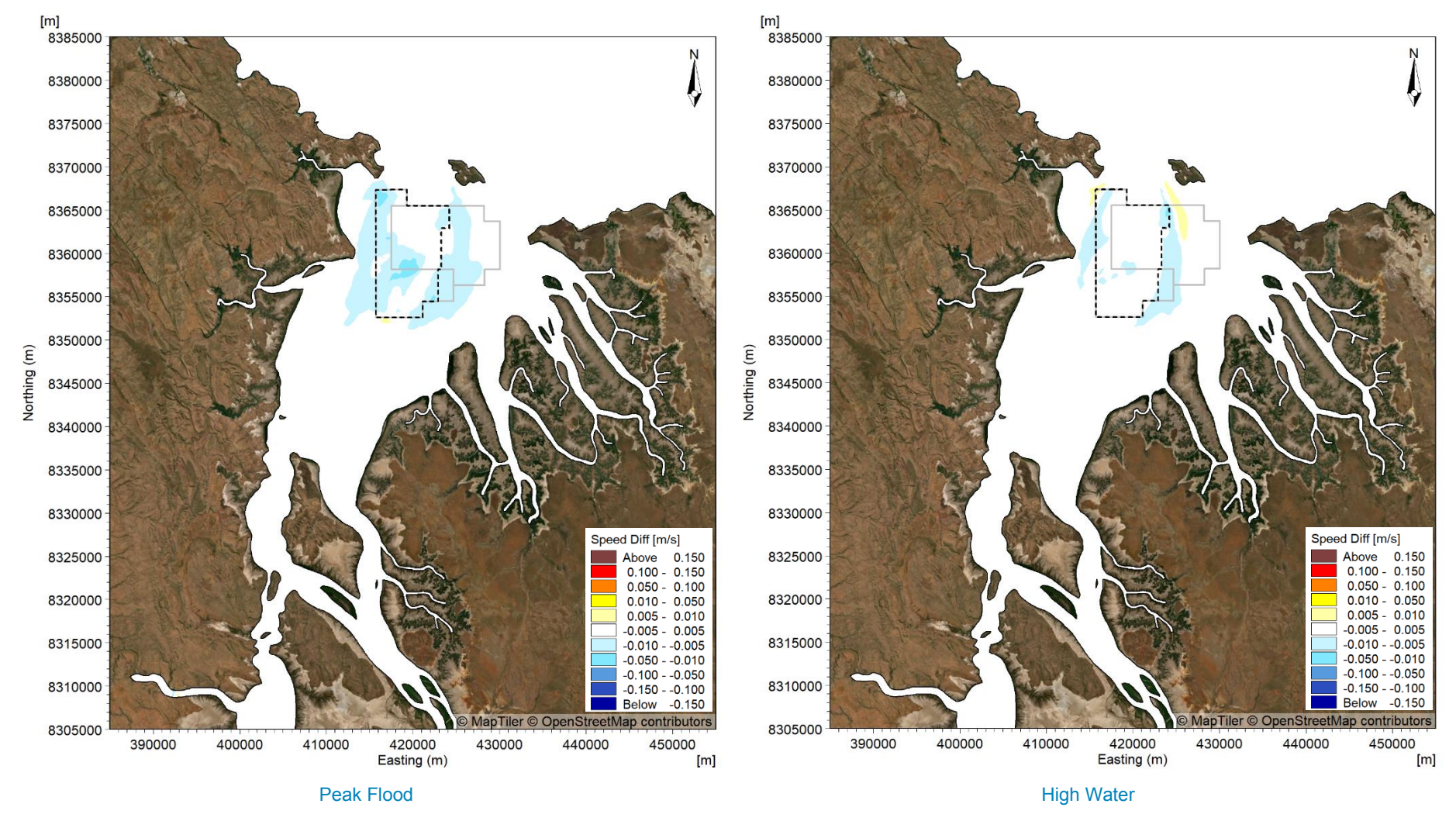


Figure B29. Modelled change in current speed at peak flood (left) and high water (right) after 5 years of sand sourcing during a spring tide in the wet season.



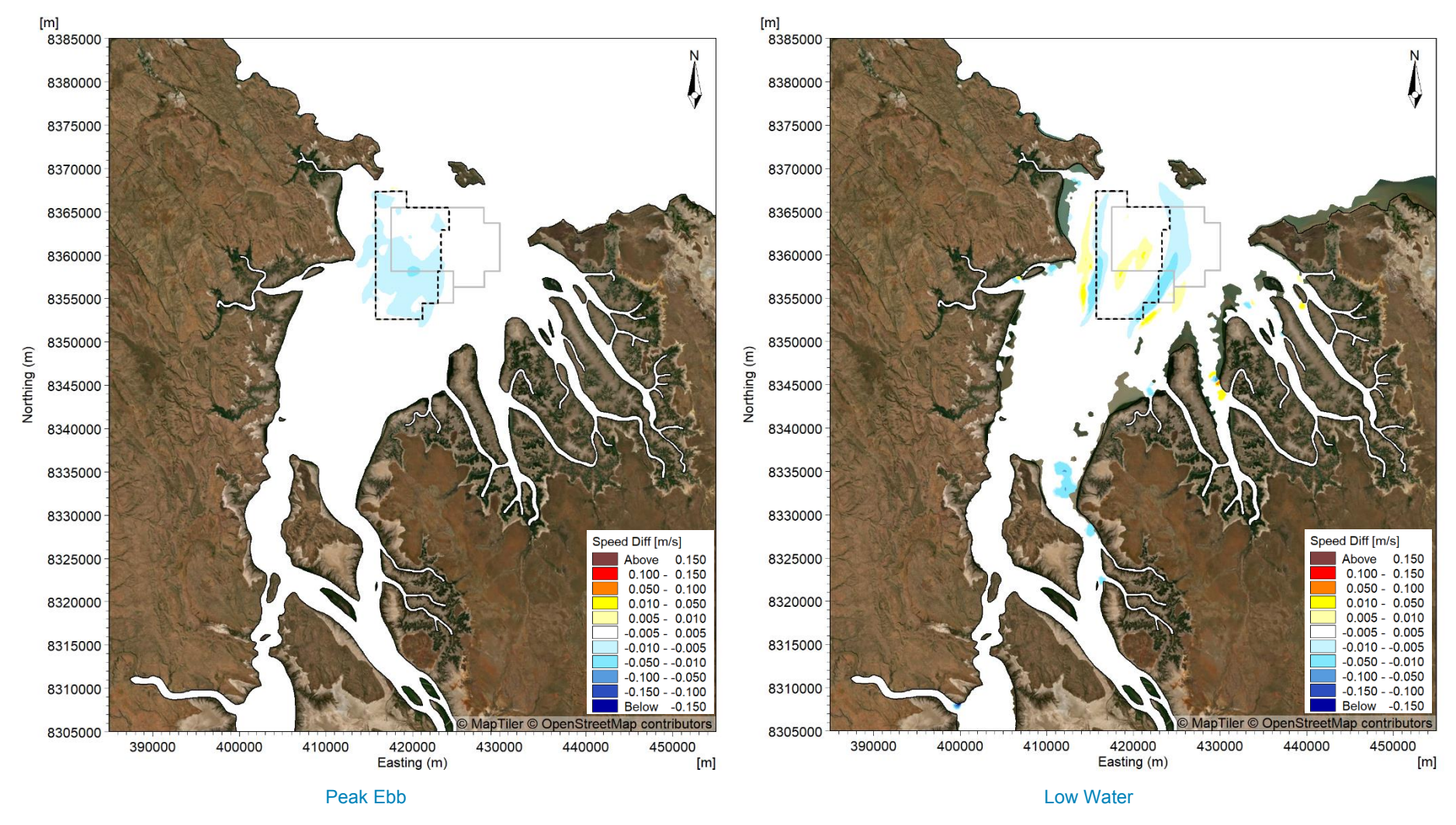


Figure B30. Modelled change in current speed at peak ebb (left) and low water (right) after 5 years of sand sourcing during a spring tide in the wet season.



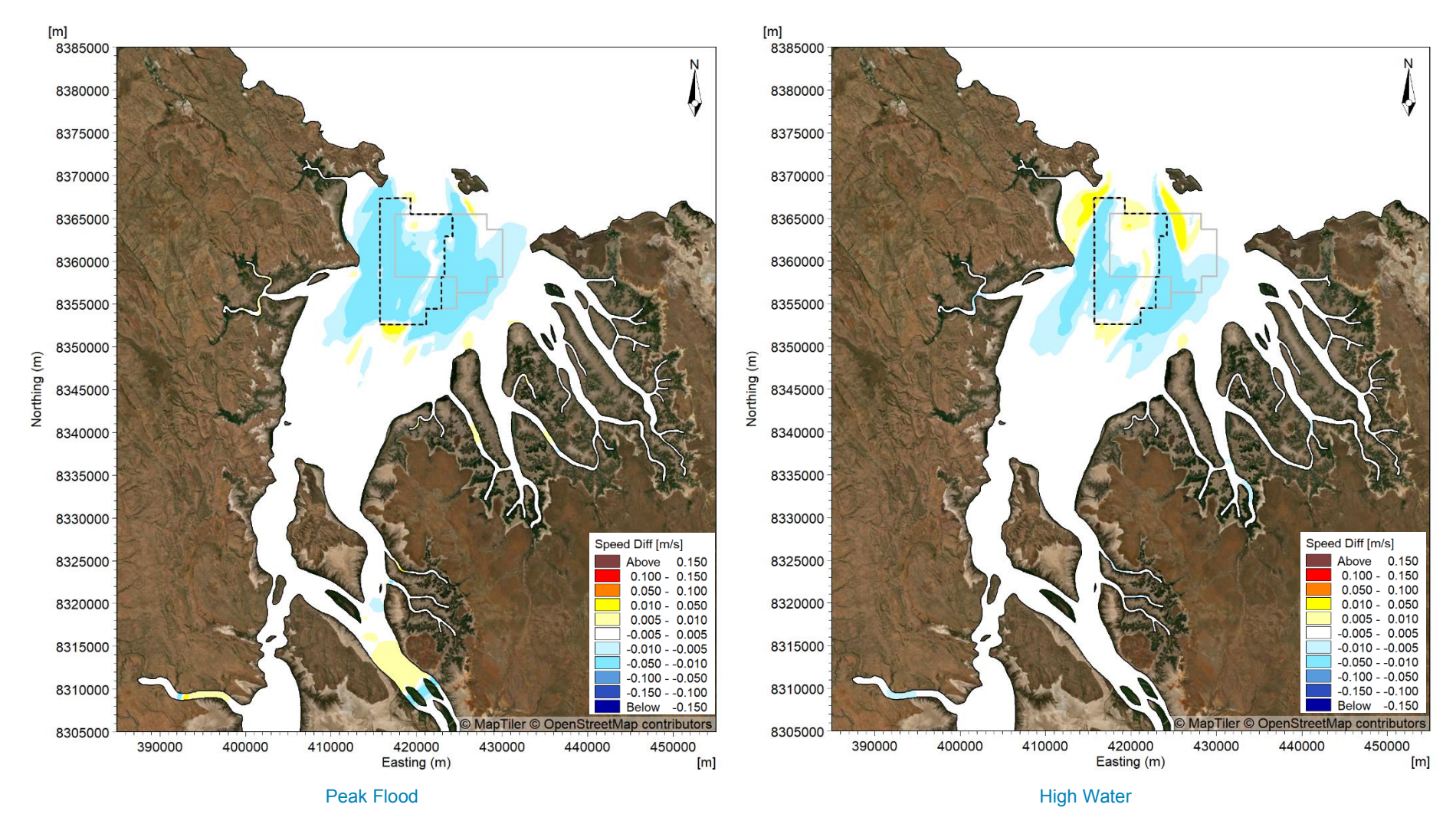


Figure B31. Modelled change in current speed at peak flood (left) and high water (right) after 15 years of sand sourcing during a spring tide in the wet season.



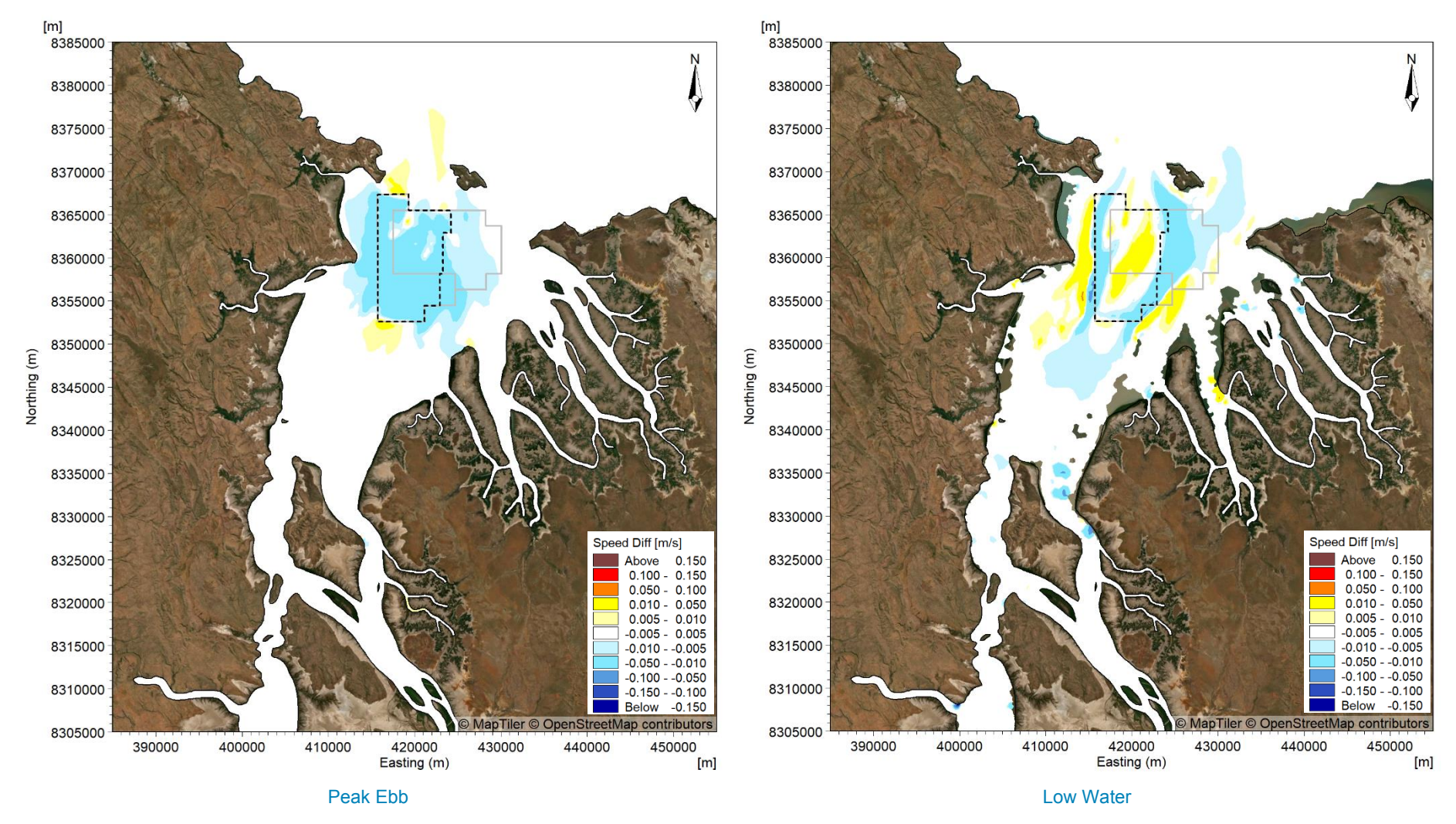


Figure B32. Modelled change in current speed at peak ebb (left) and low water (right) after 15 years of sand sourcing during a spring tide in the wet season.



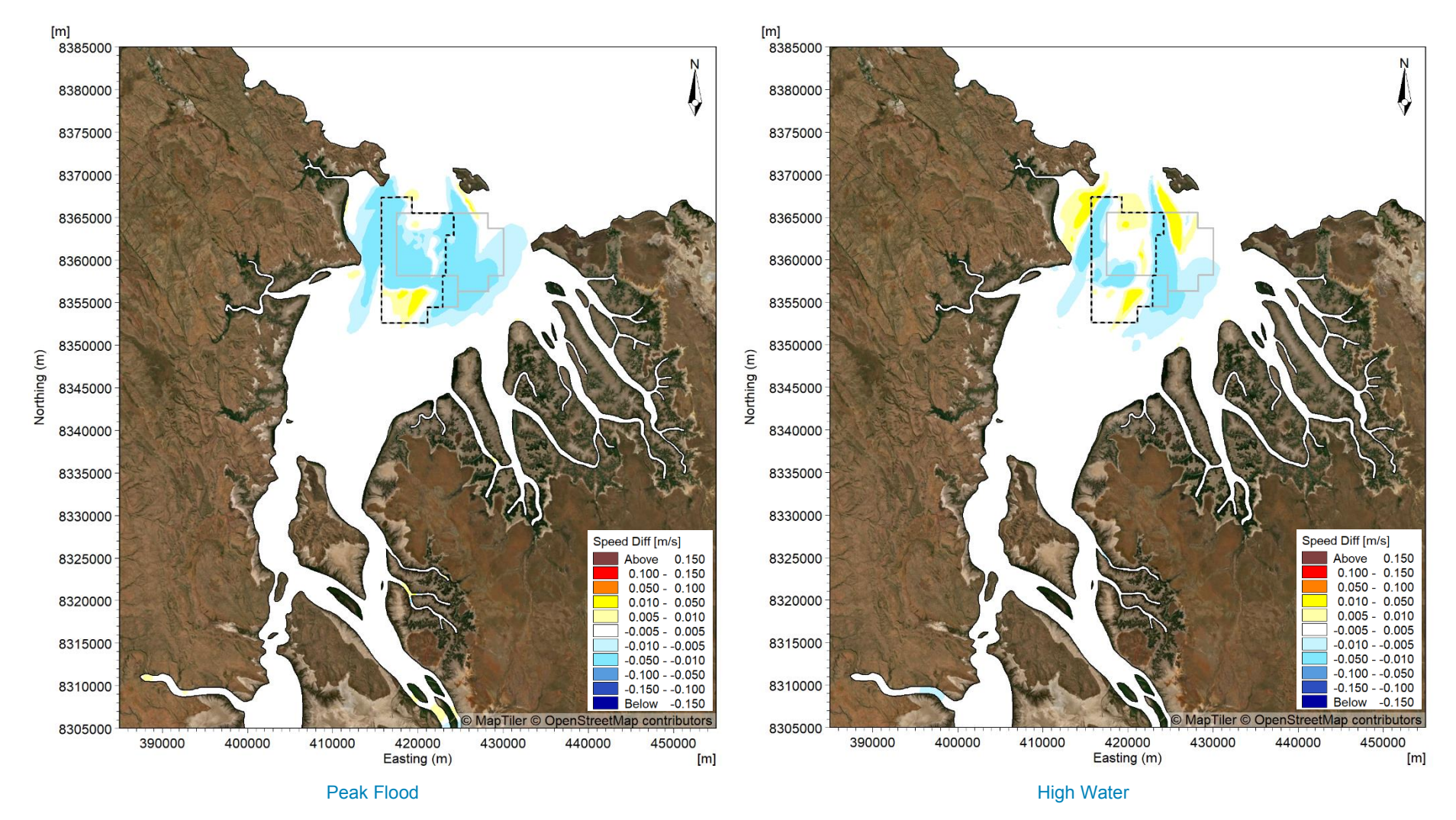


Figure B33. Modelled change in current speed at peak flood (left) and high water (right) in 100 years time after 15 years of sand sourcing during a spring tide in the wet season.



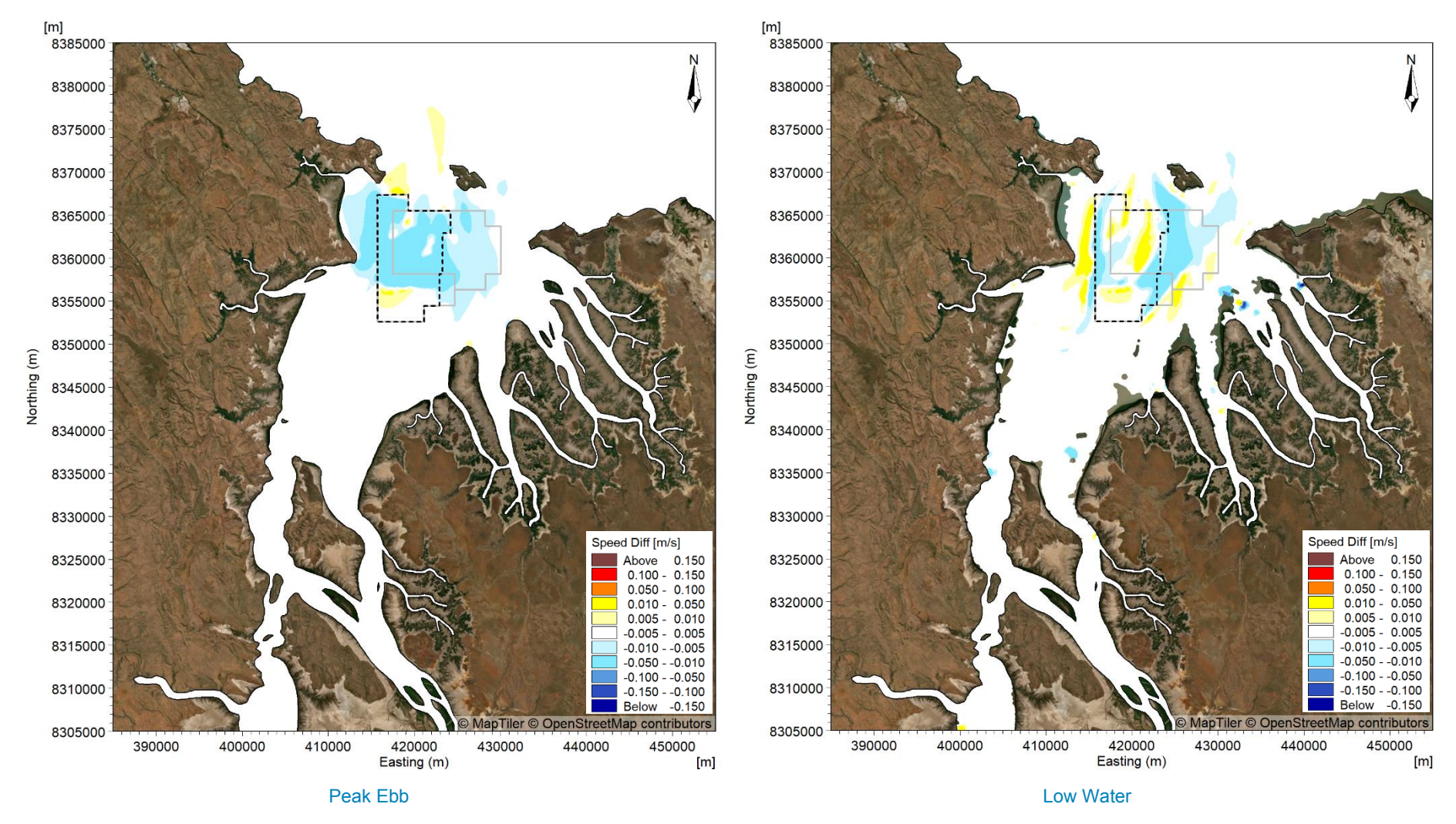


Figure B34. Modelled change in current speed at peak ebb (left) and low water (right) in 100 years time after 15 years of sand sourcing during a spring tide in the wet season.



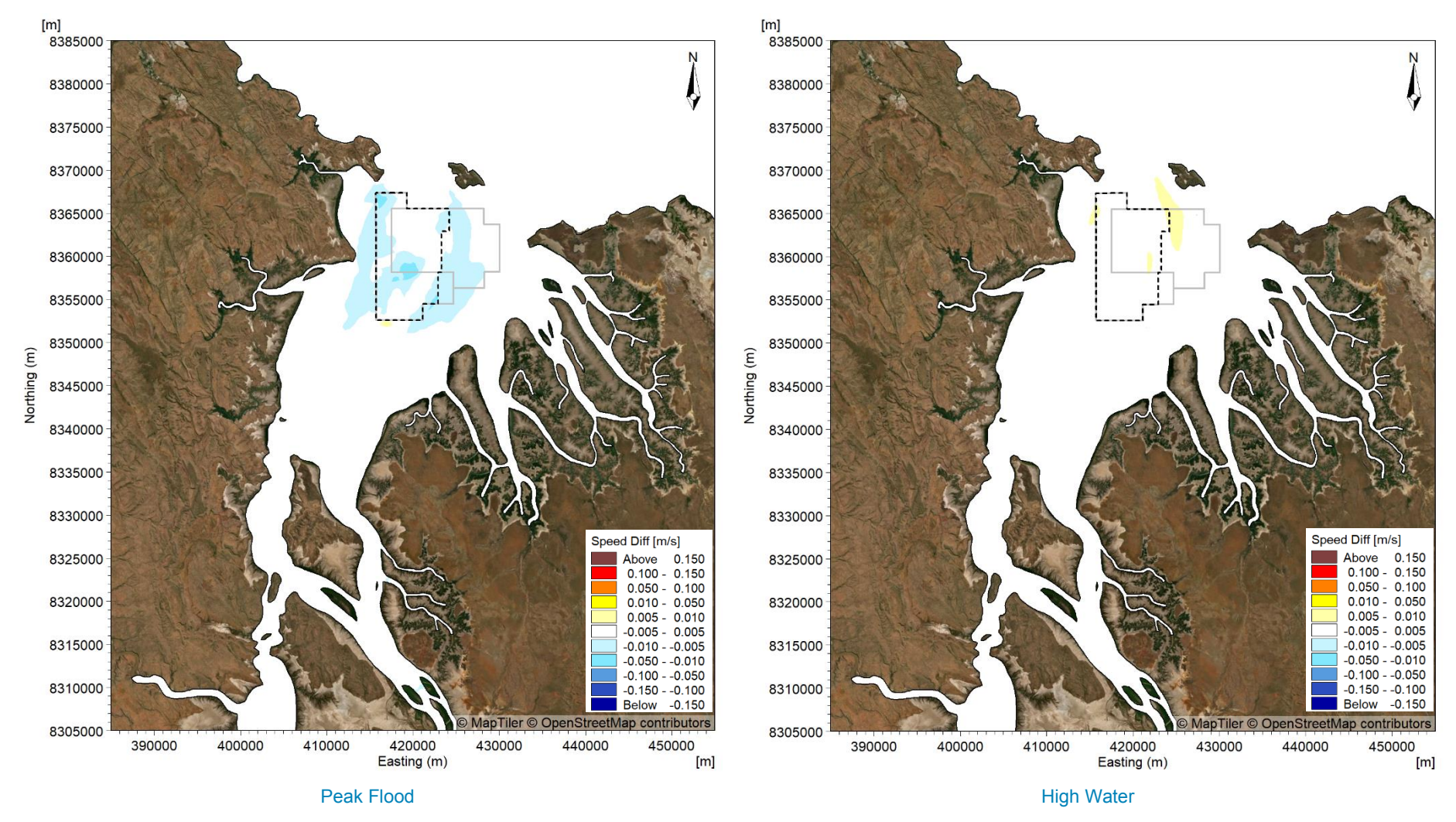


Figure B35. Modelled change in current speed at peak flood (left) and high water (right) after 5 years of sand sourcing during a spring tide in the dry season.



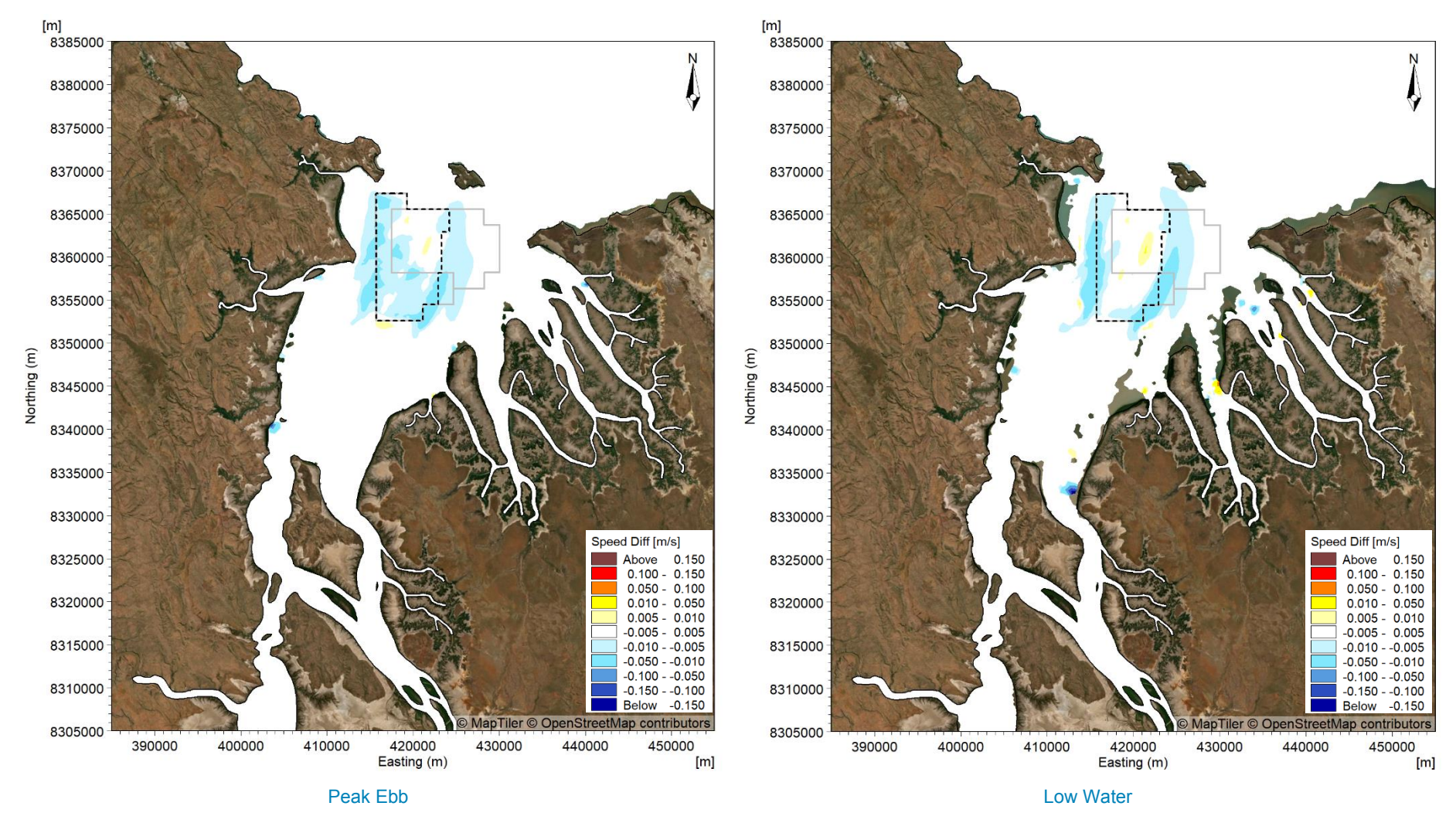


Figure B36. Modelled change in current speed at peak ebb (left) and low water (right) after 5 years of sand sourcing during a spring tide in the dry season.



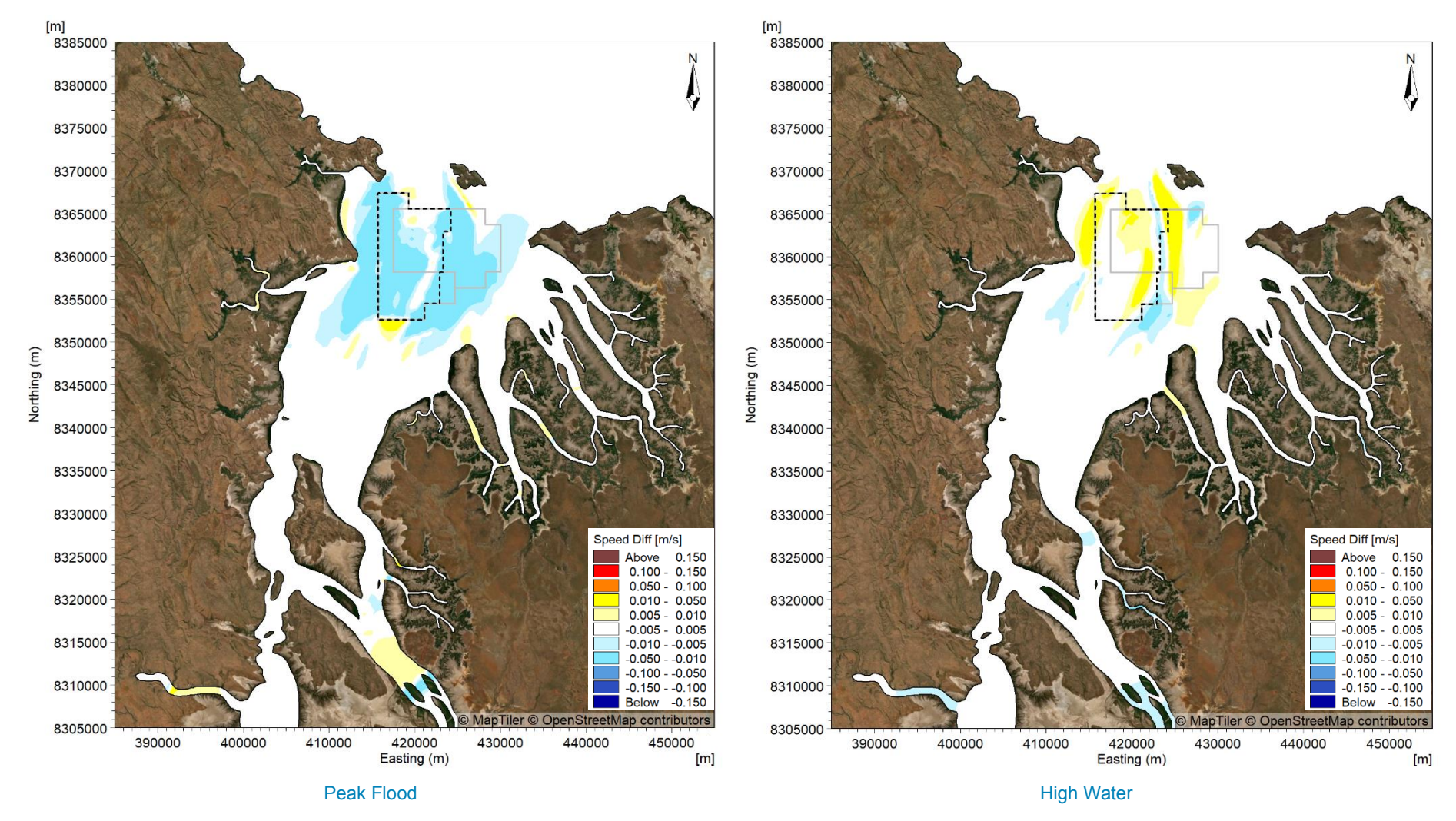


Figure B37. Modelled change in current speed at peak flood (left) and high water (right) after 15 years of sand sourcing during a spring tide in the dry season.

B38



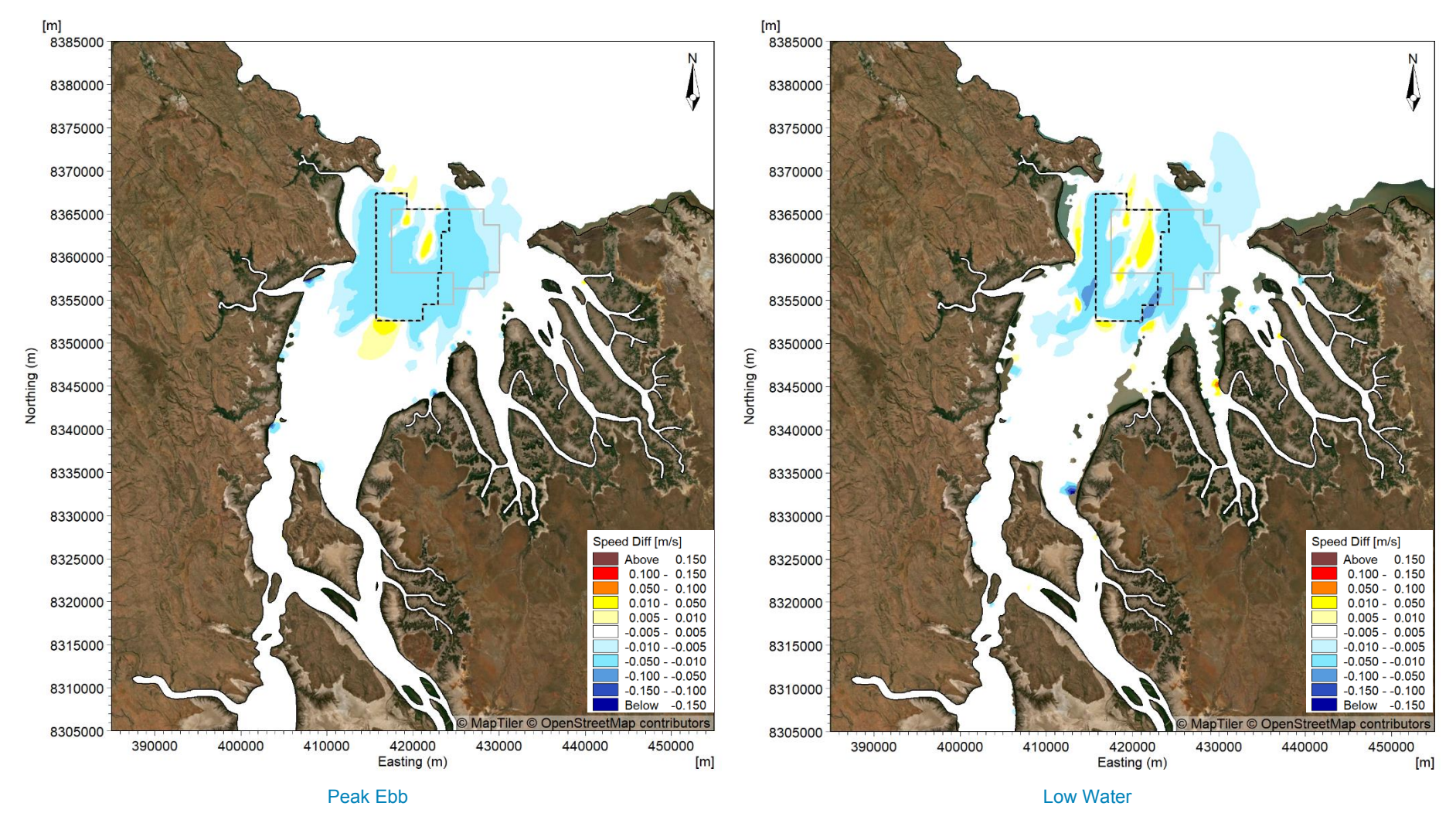


Figure B38. Modelled change in current speed at peak ebb (left) and low water (right) after 15 years of sand sourcing during a spring tide in the dry season.



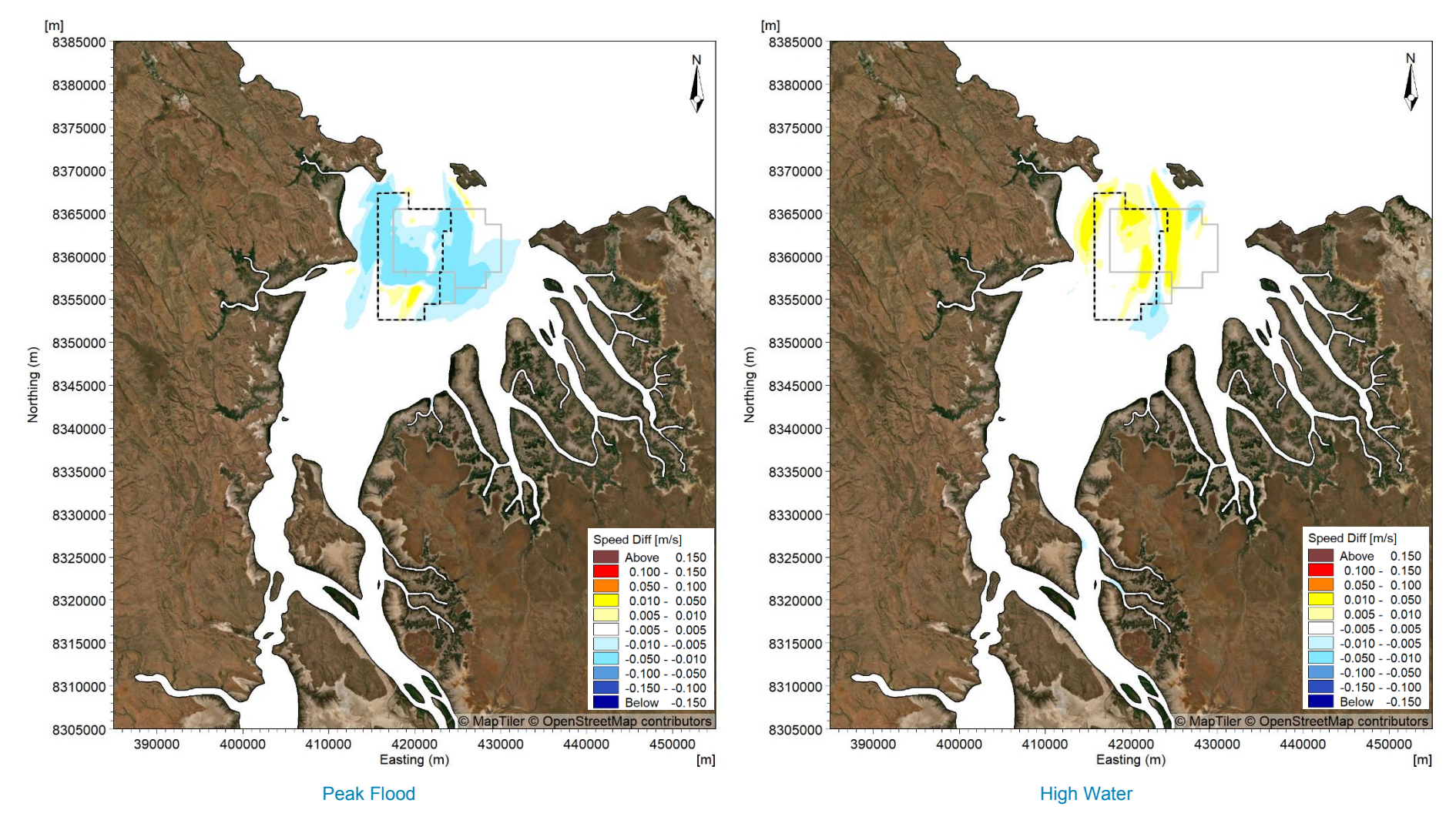


Figure B39. Modelled change in current speed at peak flood (left) and high water (right) in 100 years time after 15 years of sand sourcing during a spring tide in the dry season.



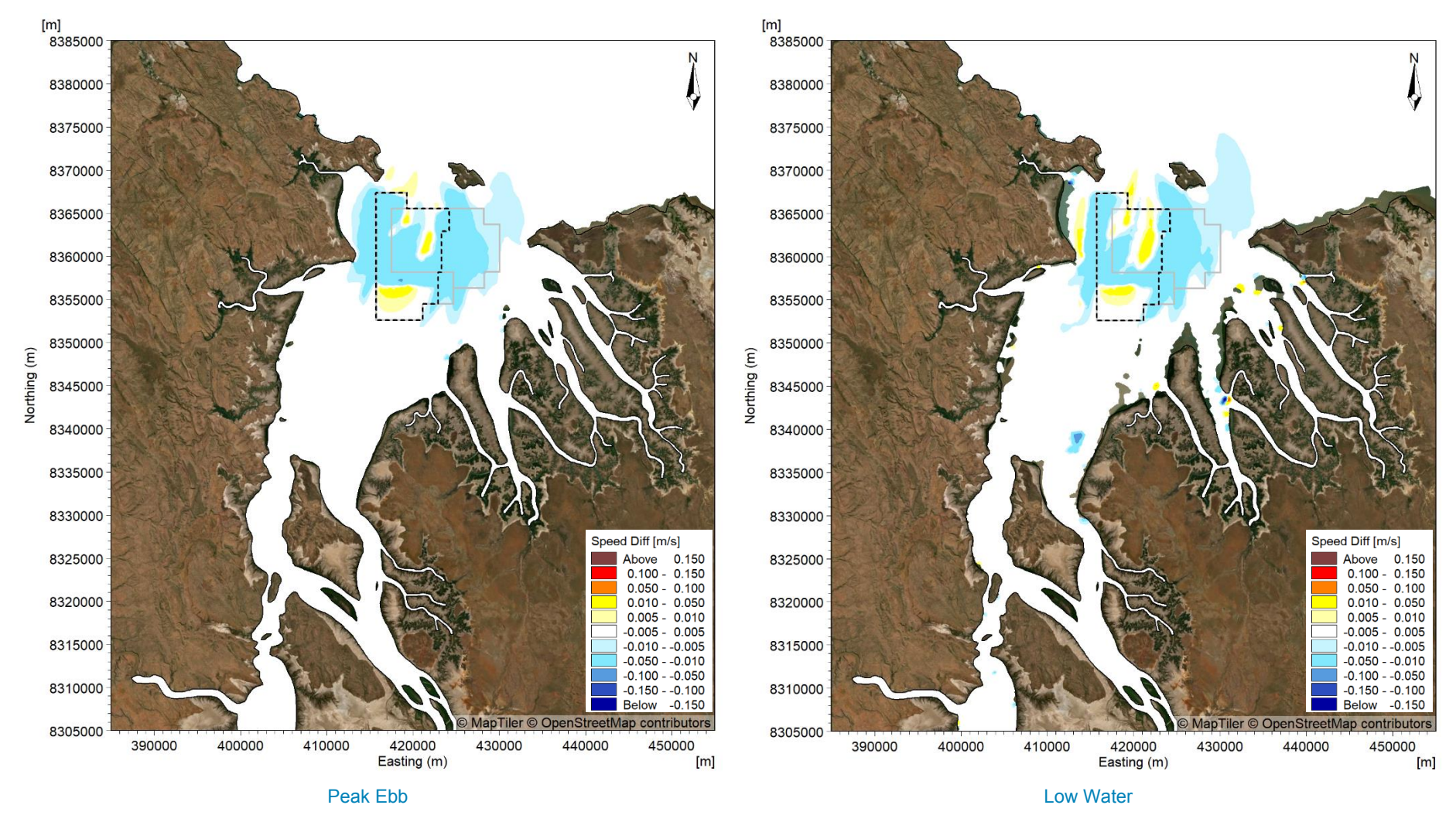


Figure B40. Modelled change in current speed at peak ebb (left) and low water (right) in 100 years time after 15 years of sand sourcing during a spring tide in the dry season.



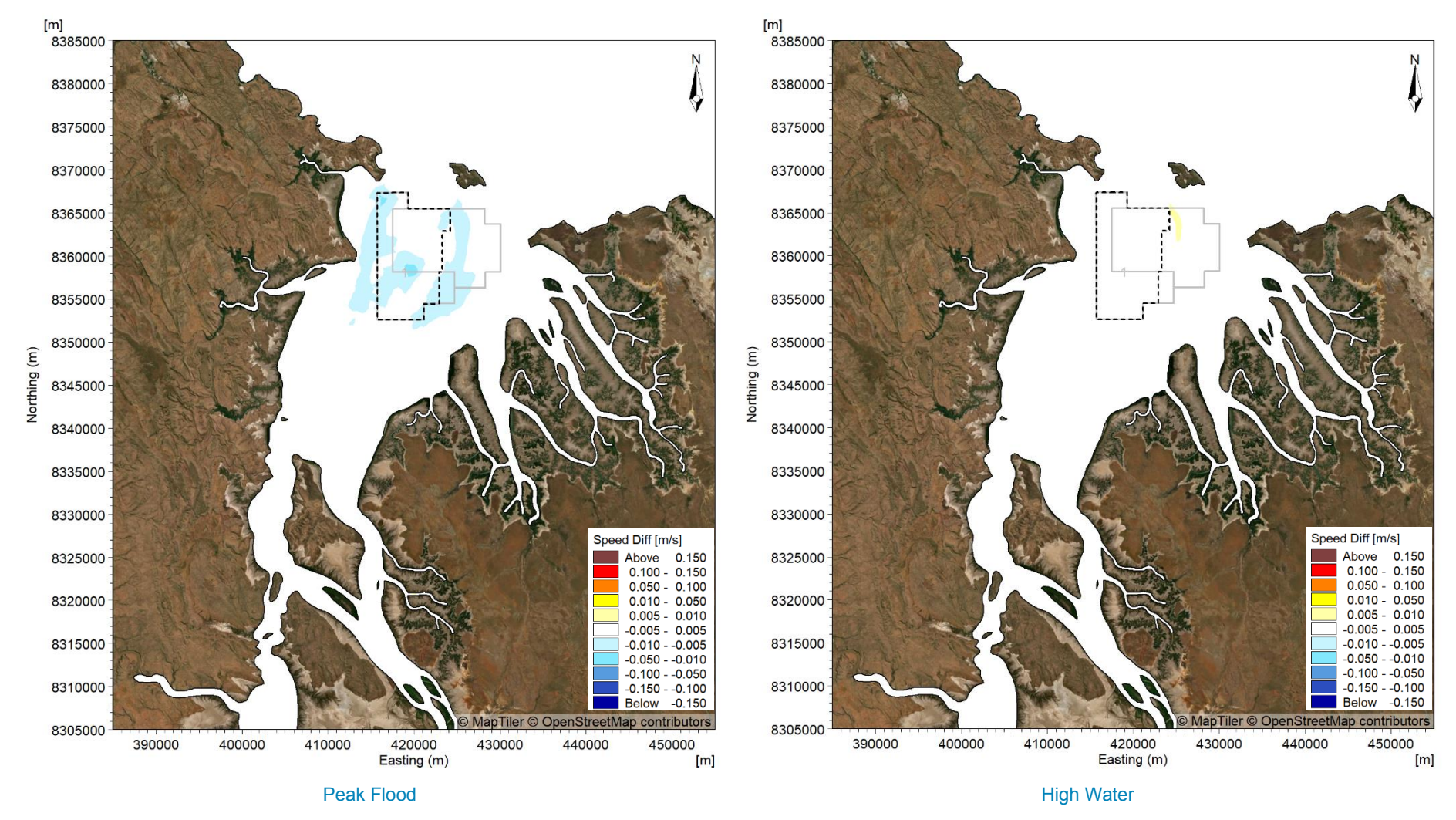


Figure B41. Modelled change in current speed at peak flood (left) and high water (right) after 5 years of sand sourcing during TC Marcus.



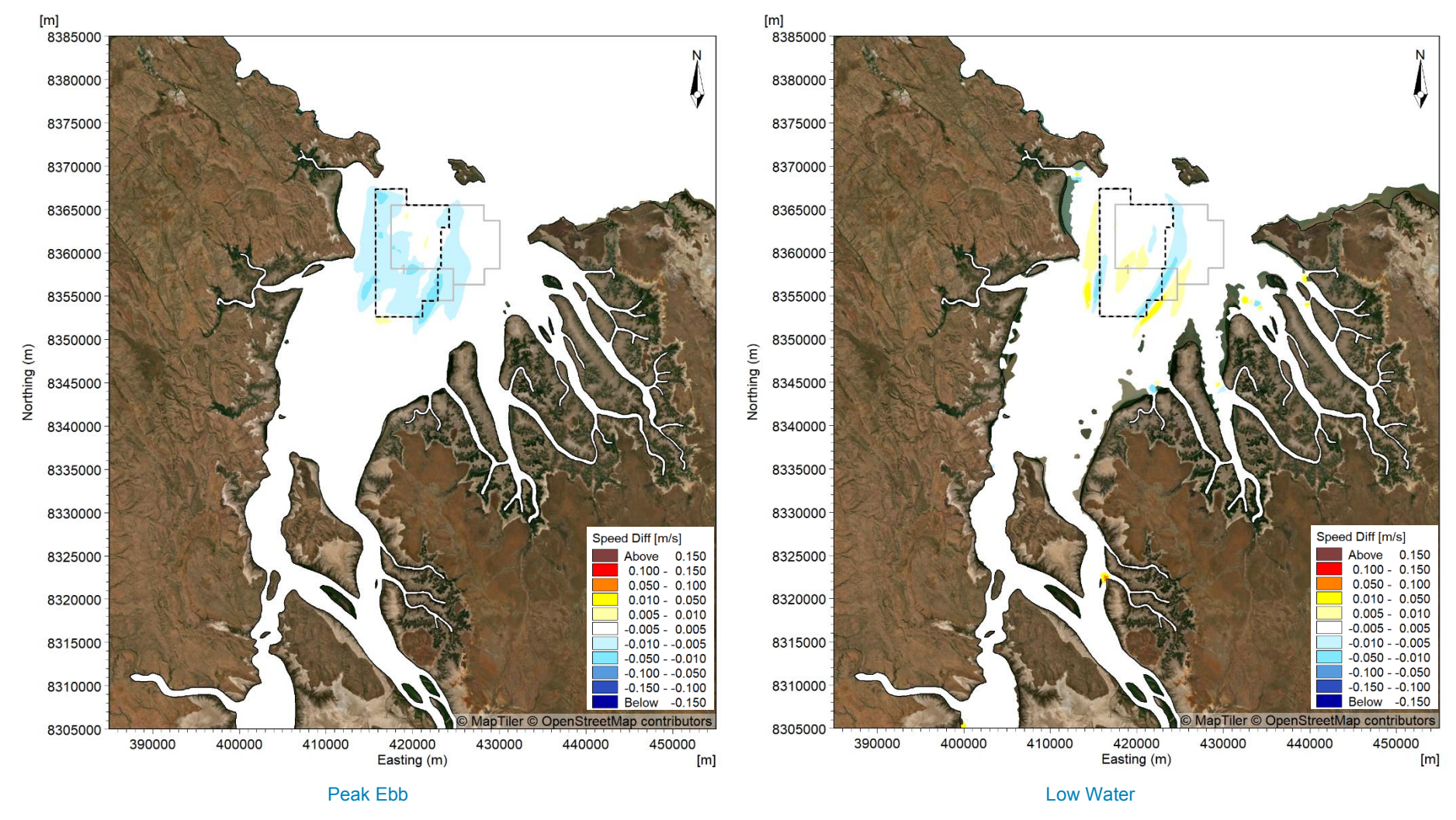


Figure B42. Modelled change in current speed at peak ebb (left) and low water (right) after 5 years of sand sourcing during TC Marcus.



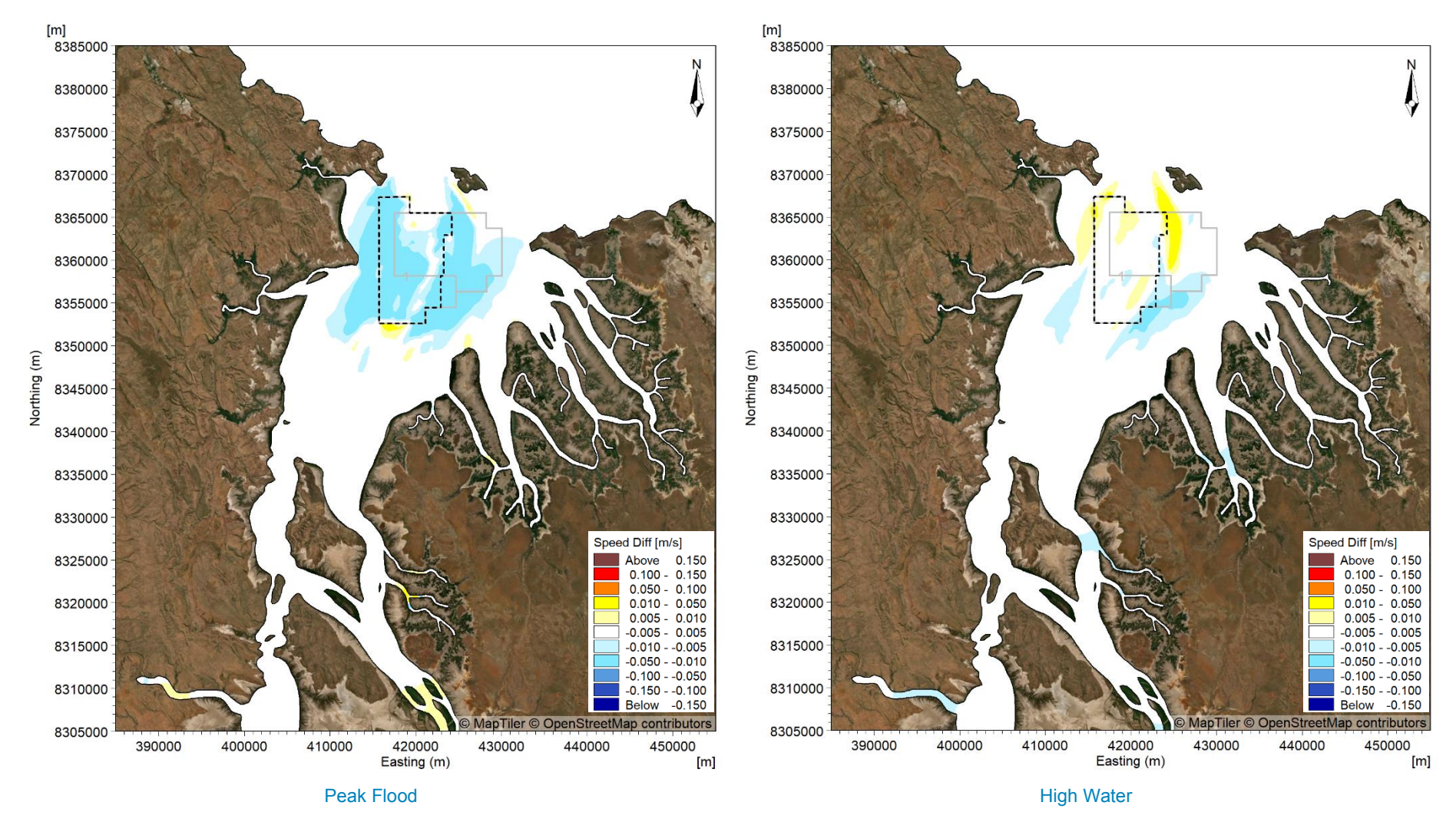


Figure B43. Modelled change in current speed at peak flood (left) and high water (right) after 15 years of sand sourcing during TC Marcus.



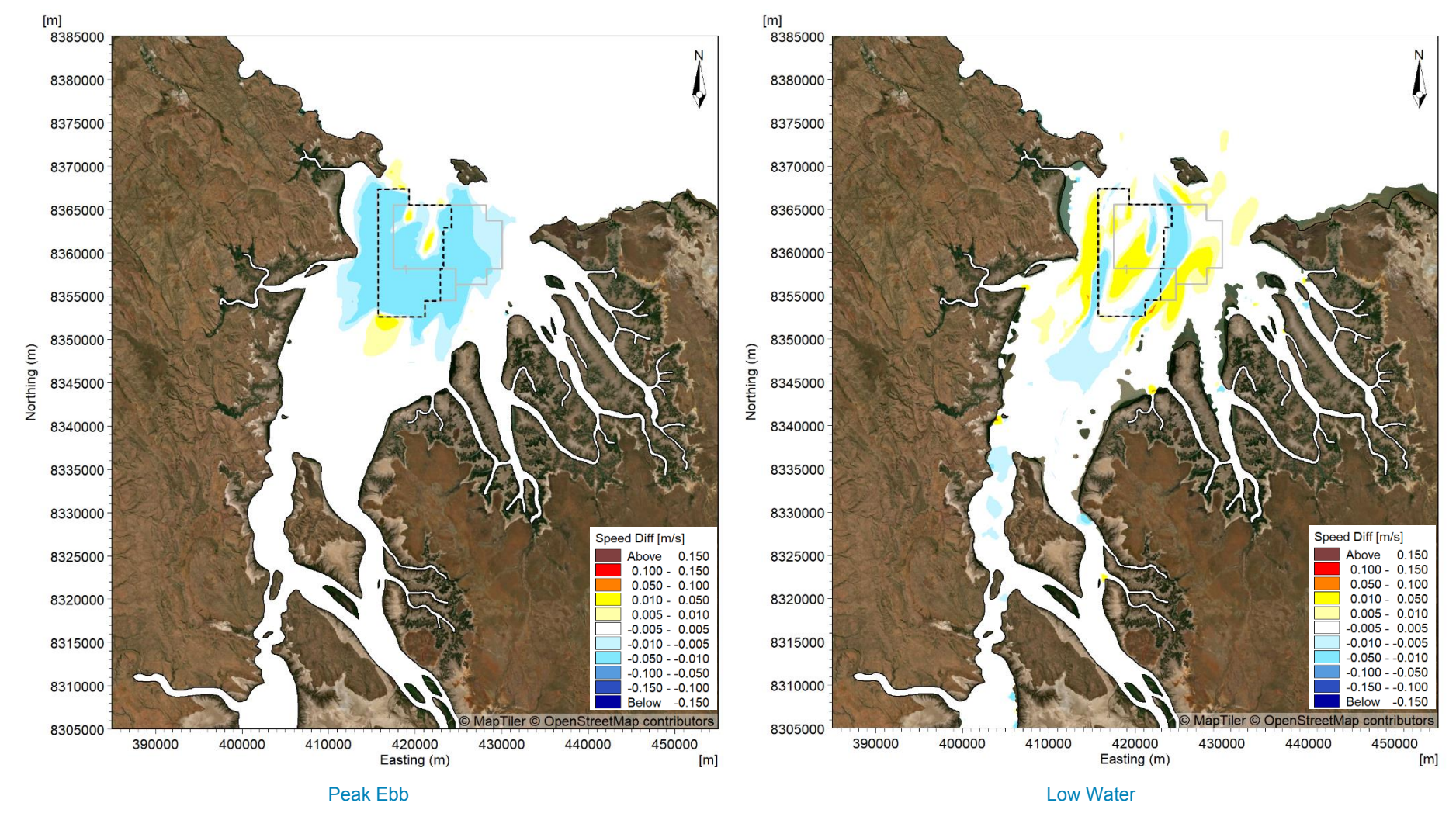


Figure B44. Modelled change in current speed at peak ebb (left) and low water (right) after 15 years of sand sourcing during TC Marcus.



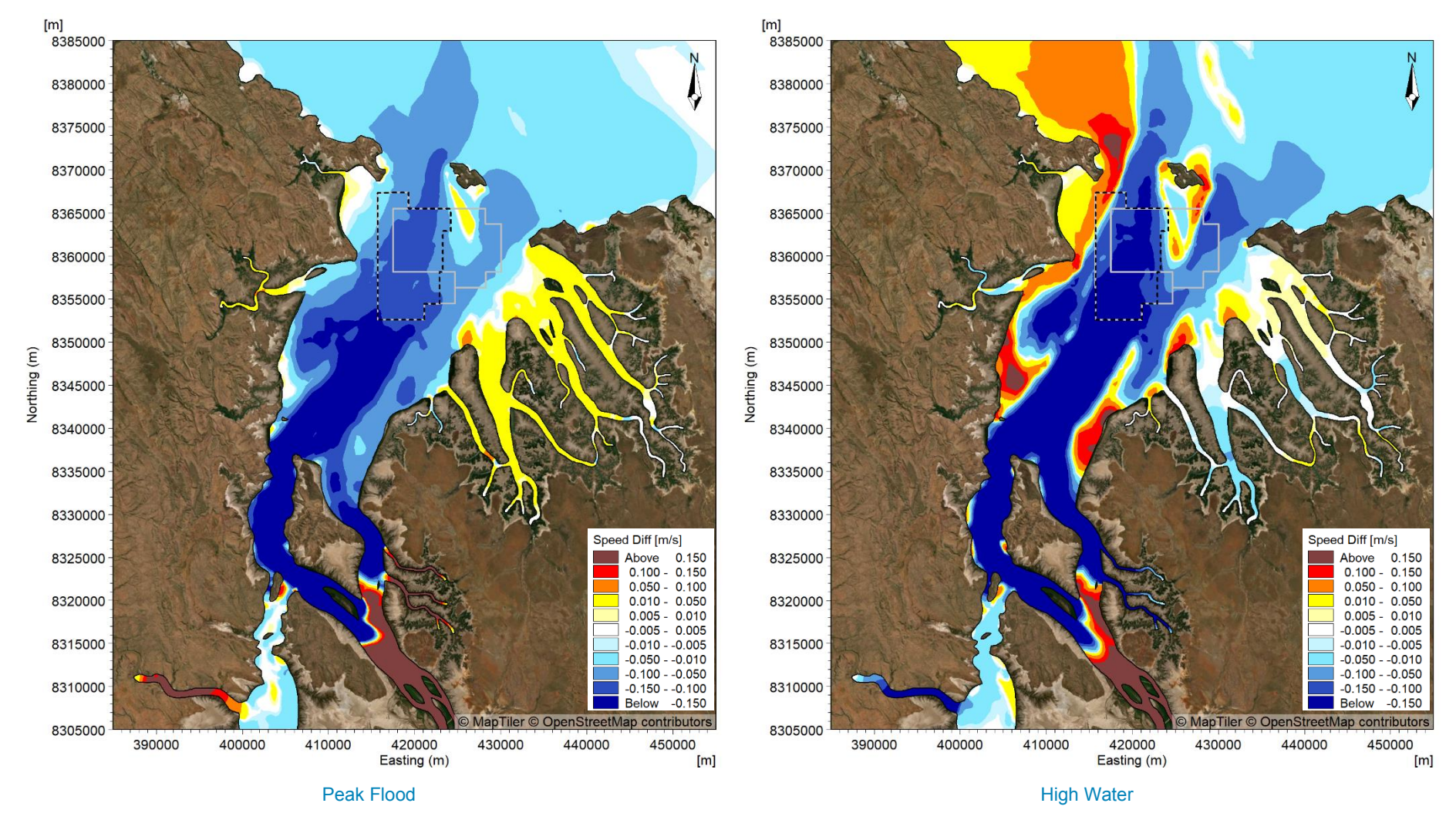


Figure B45. Modelled change in current speed at peak flood (left) and high water (right) for the Pre-European Settlement scenario during a spring tide in the wet season during a high discharge event.



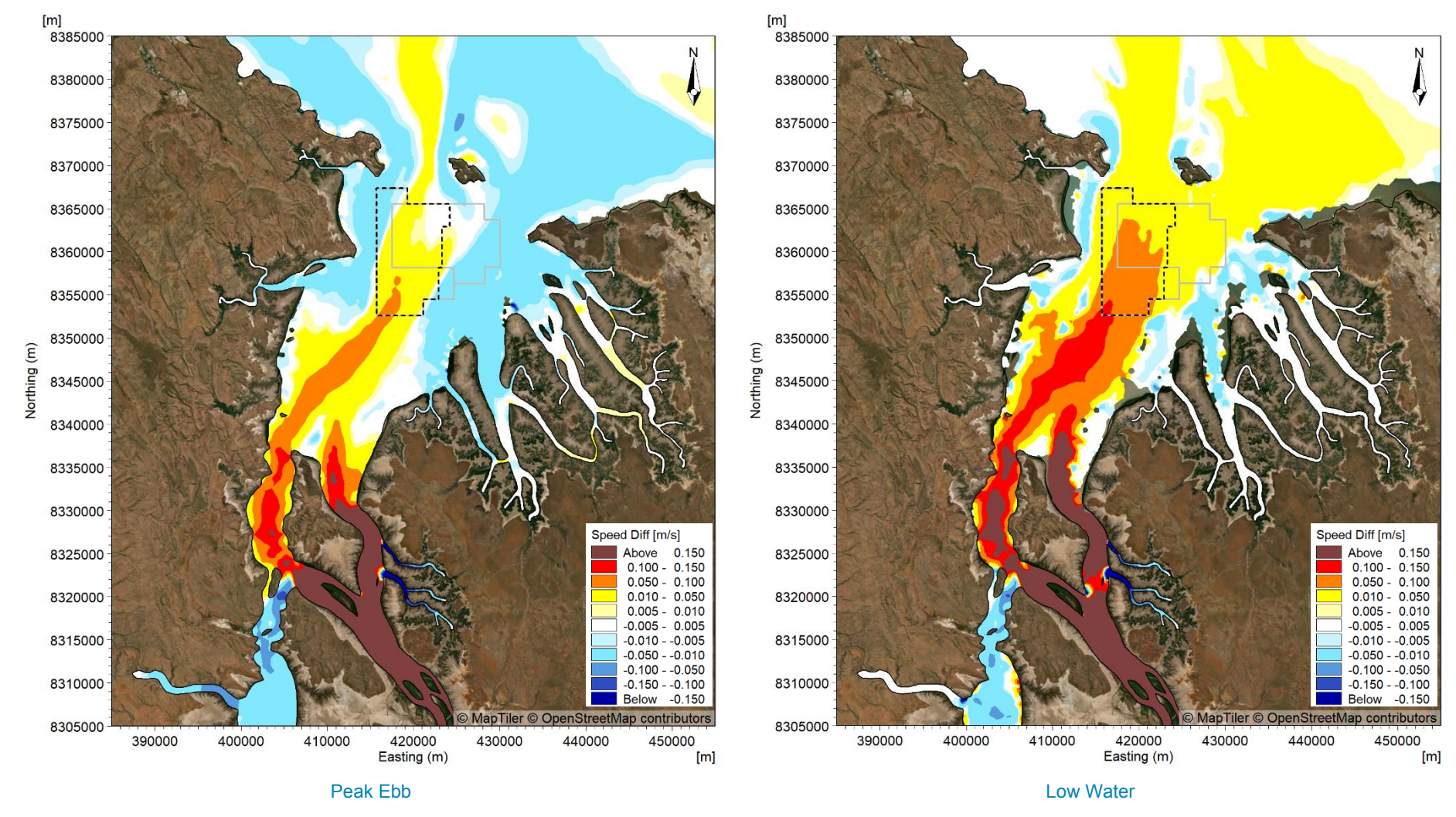


Figure B46. Modelled change in current speed at peak ebb (left) and low water (right) for the Pre-European Settlement scenario during a spring tide in the wet season during a high discharge event.



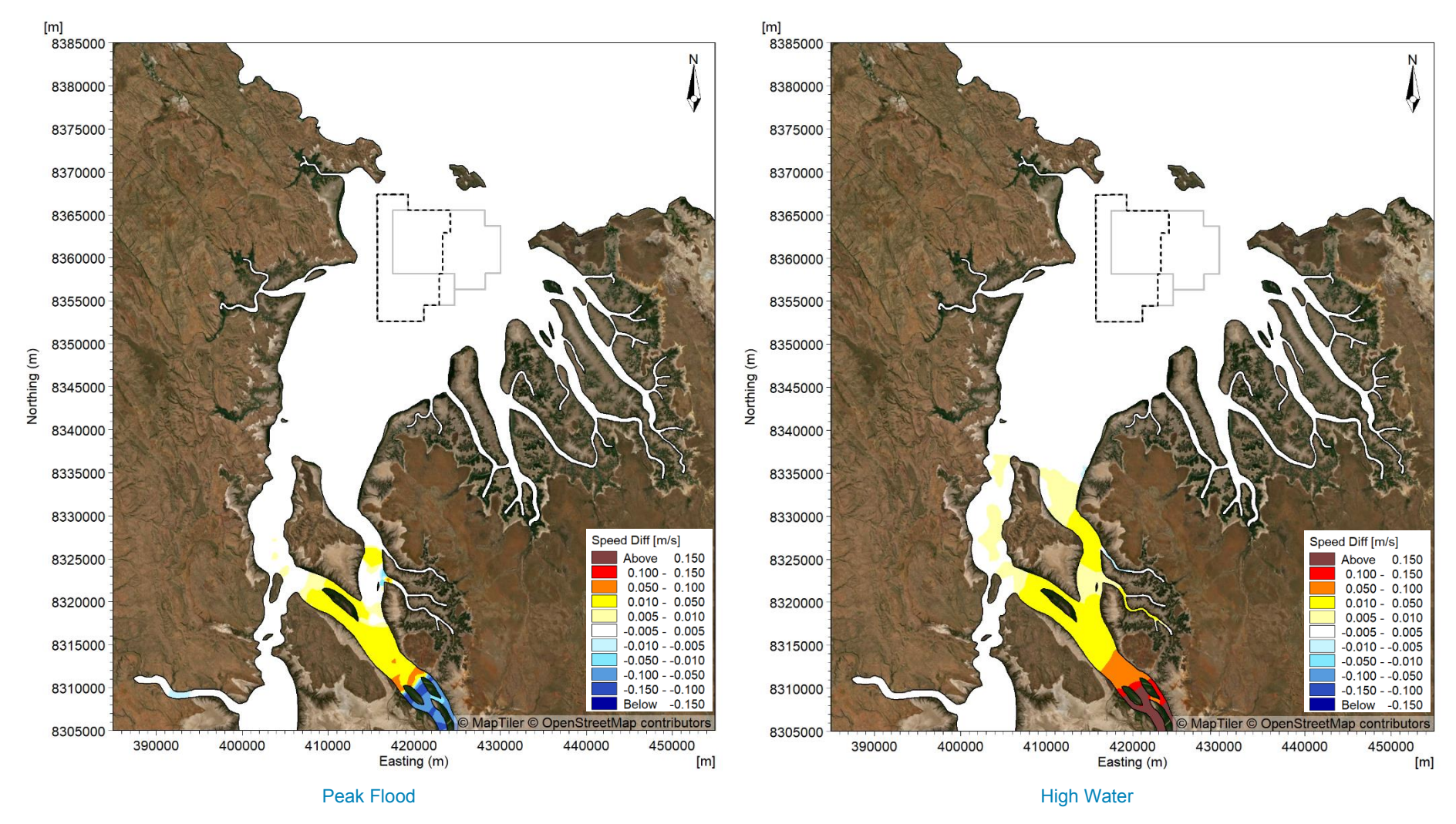


Figure B47. Modelled change in current speed at peak flood (left) and high water (right) for the Pre-European Settlement scenario during a spring tide in the dry season.



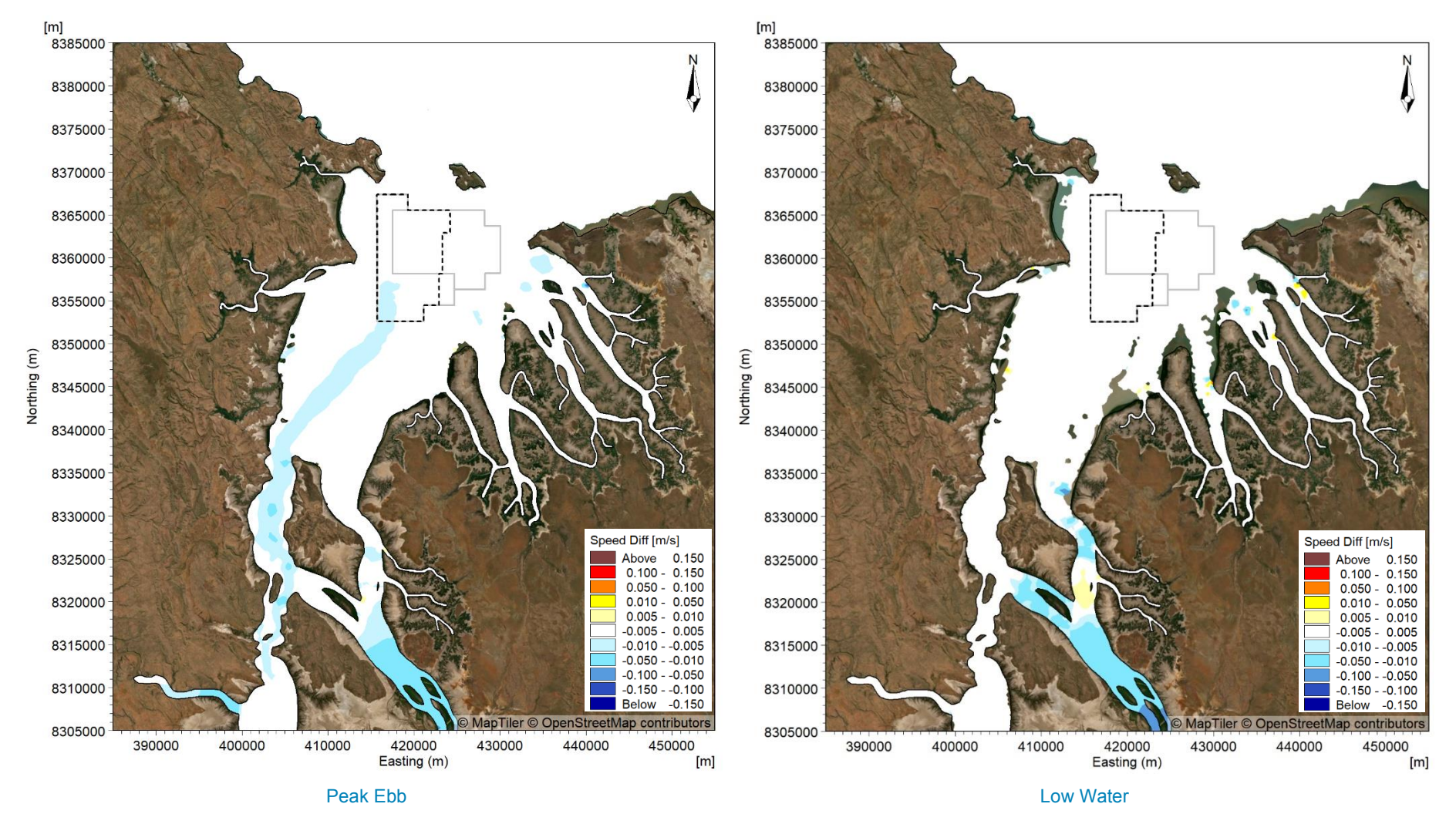


Figure B48. Modelled change in current speed at peak ebb (left) and low water (right) for the Pre-European Settlement scenario during a spring tide in the dry season.



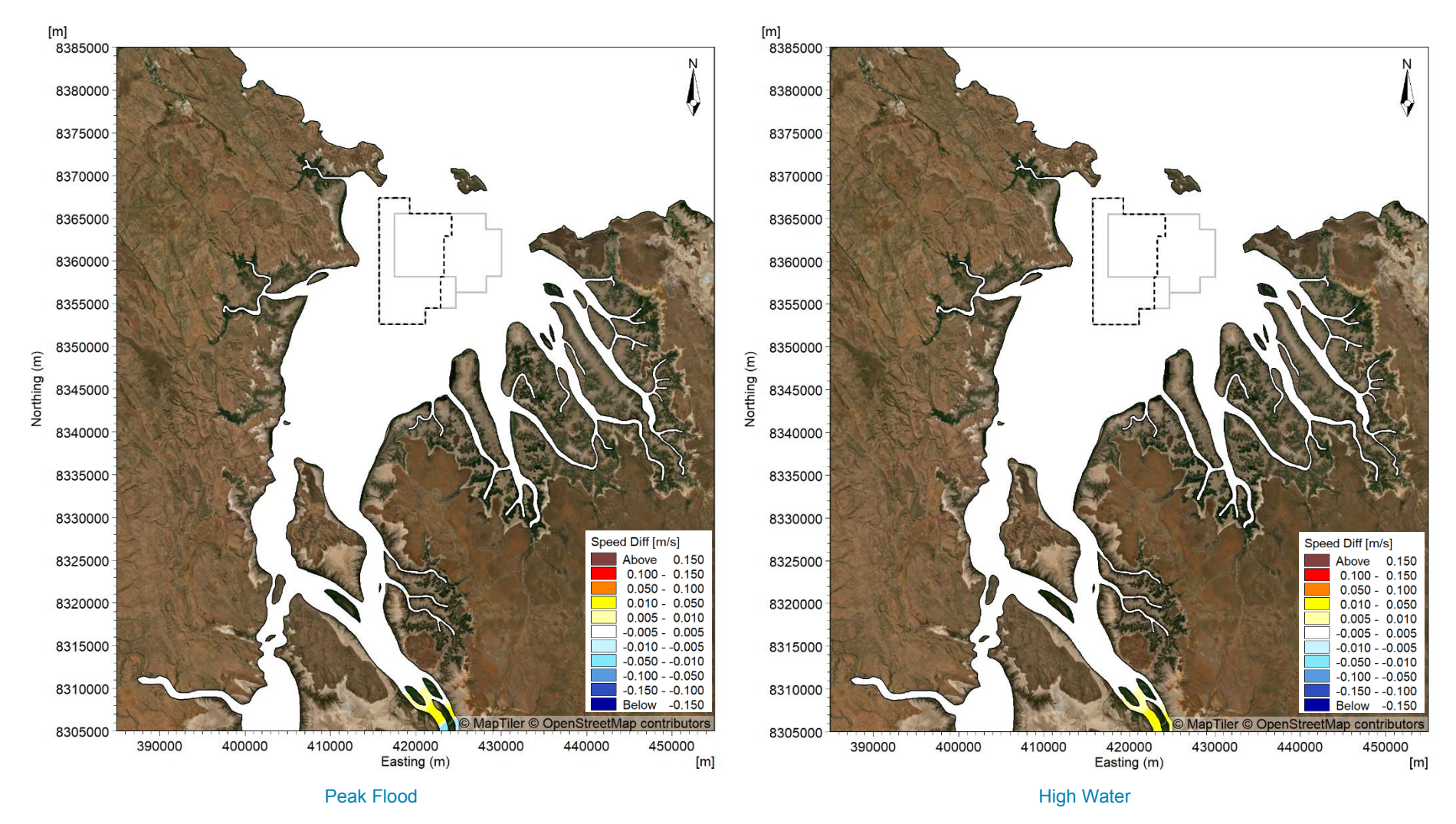


Figure B49. Modelled change in current speed at peak flood (left) and high water (right) for the Pre-European Settlement scenario during a spring tide in the transitional season.



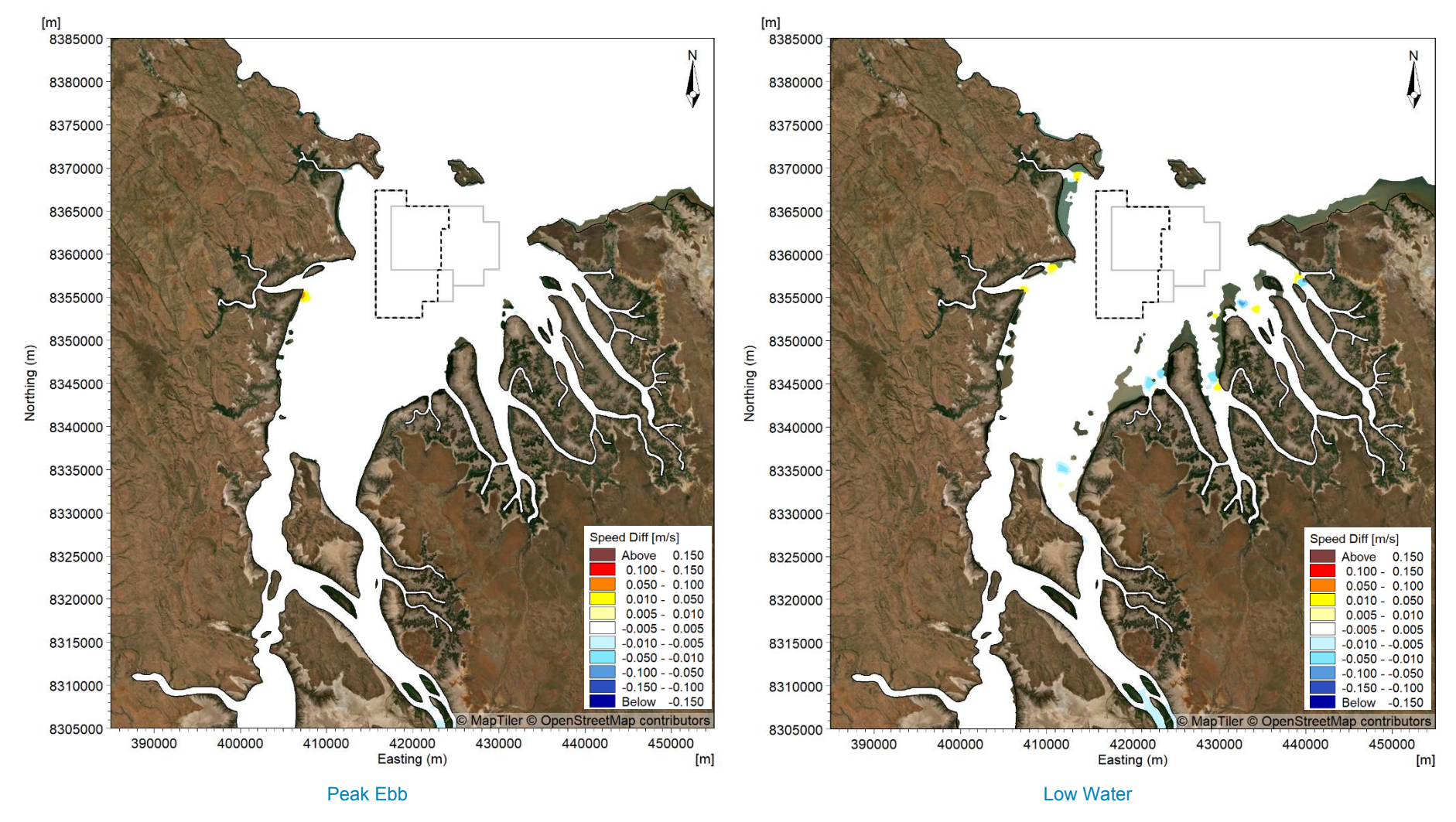


Figure B50. Modelled change in current speed at peak ebb (left) and low water (right) for the Pre-European Settlement scenario during a spring tide in the transitional season.



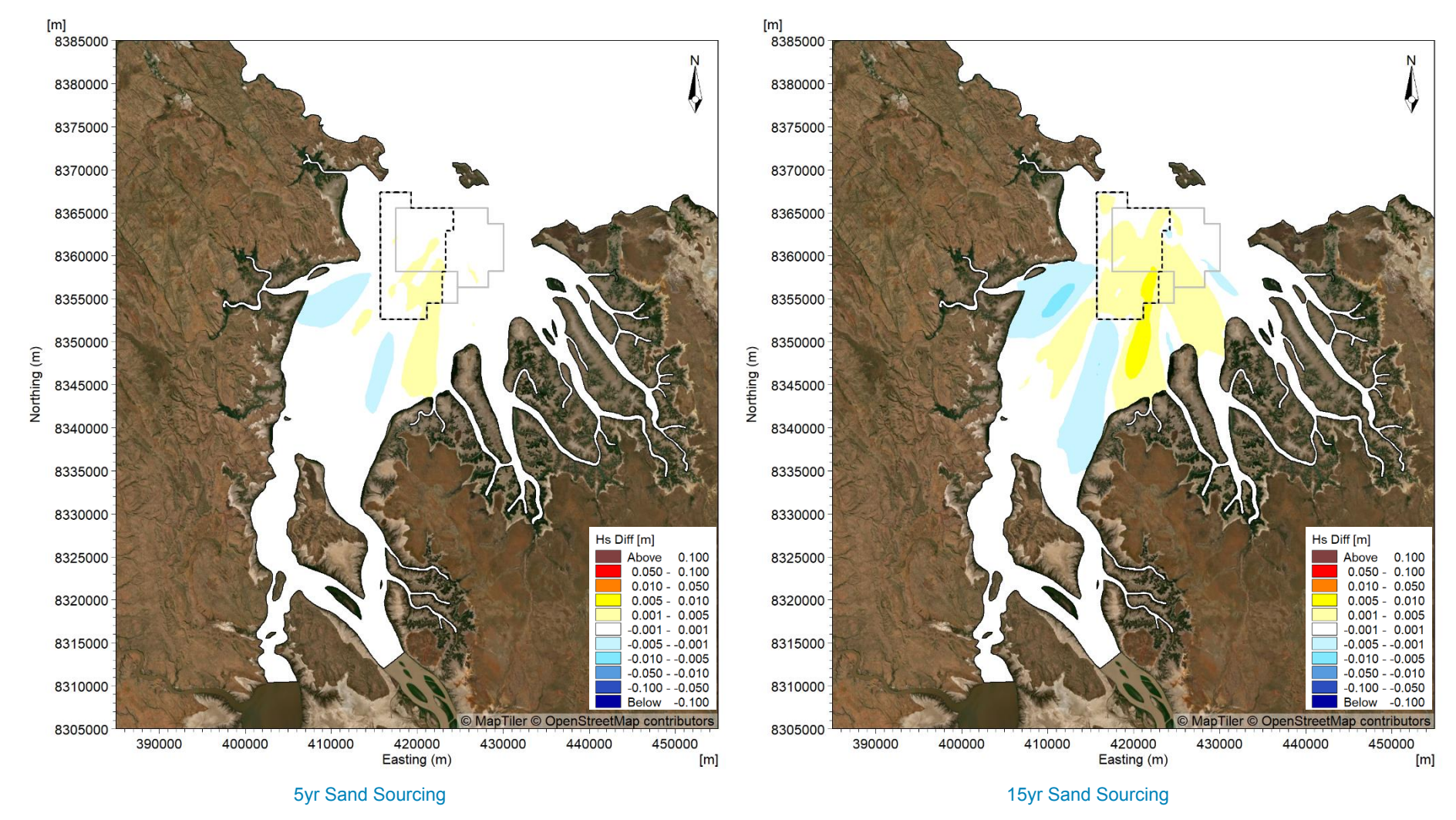


Figure B51. Modelled change in H<sub>s</sub> during the largest wave event in the wet season period due to 5 years of sand sourcing (left) and 15 years of sand sourcing (right).



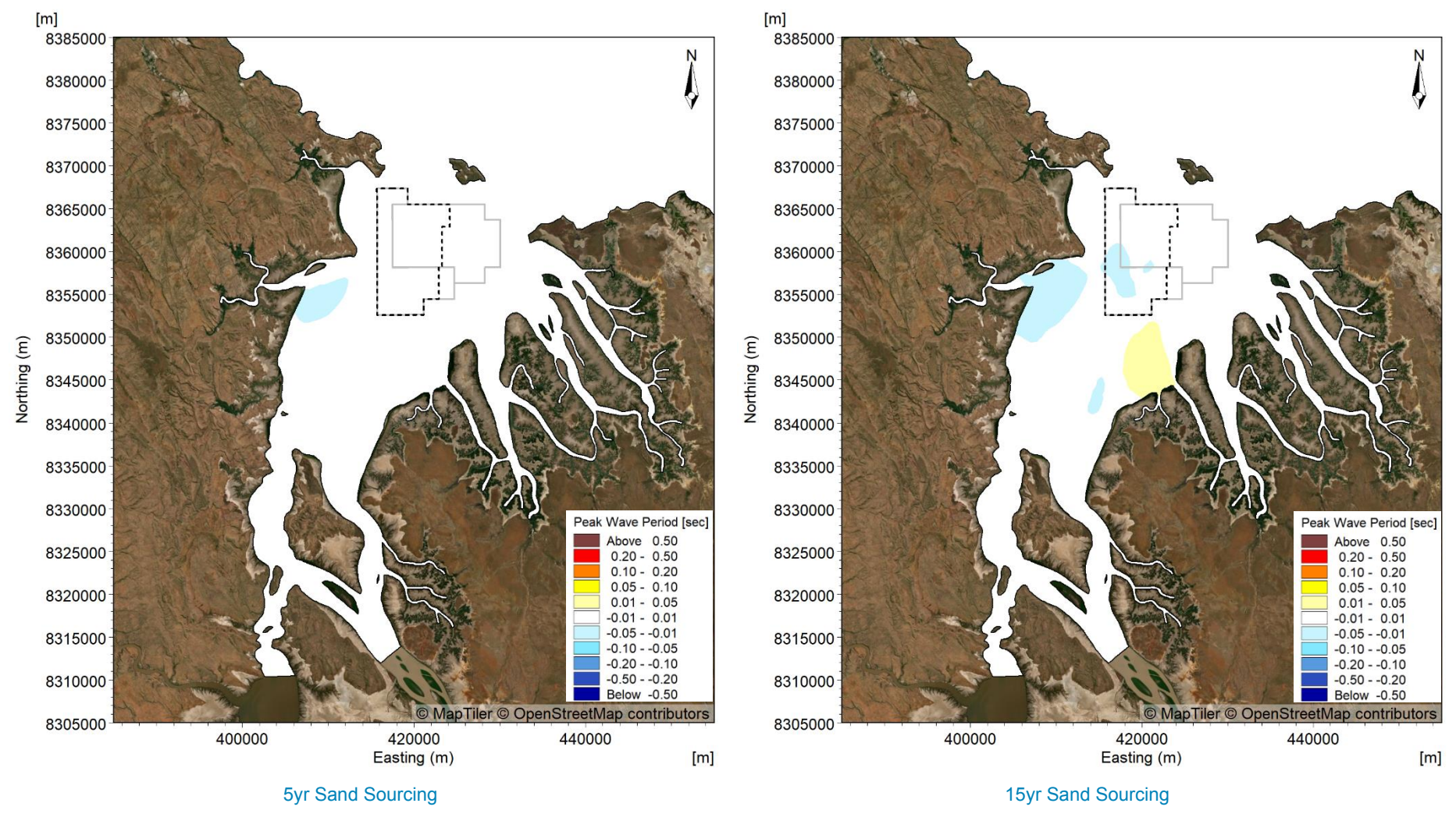


Figure B52. Modelled change in T<sub>p</sub> during the largest wave event in the wet season period due to 5 years of sand sourcing (left) and 15 years of sand sourcing (right).



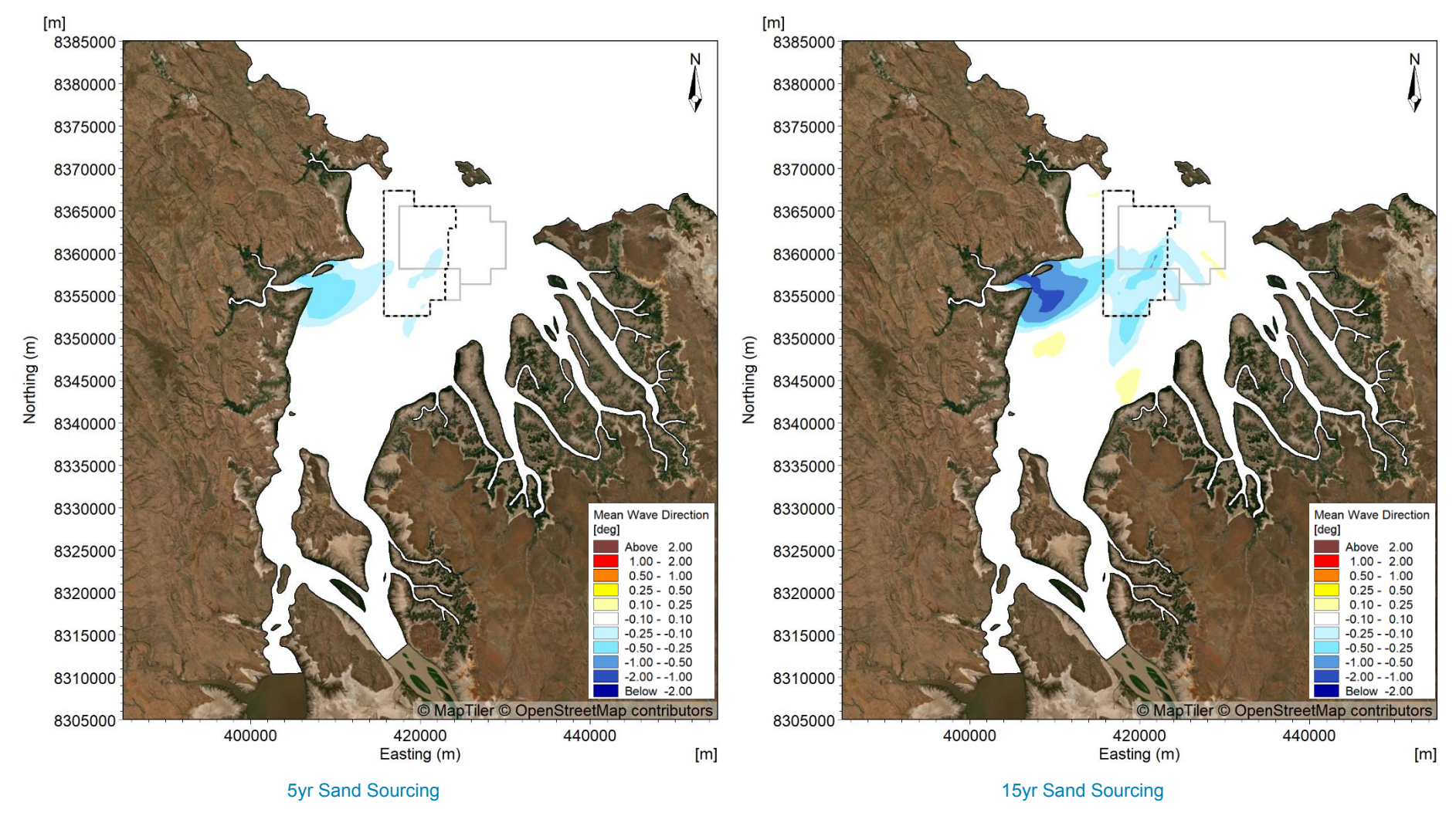


Figure B53. Modelled change in wave direction during the largest wave event in the wet season period due to 5 years of sand sourcing (left) and 15 years of sand sourcing (right).



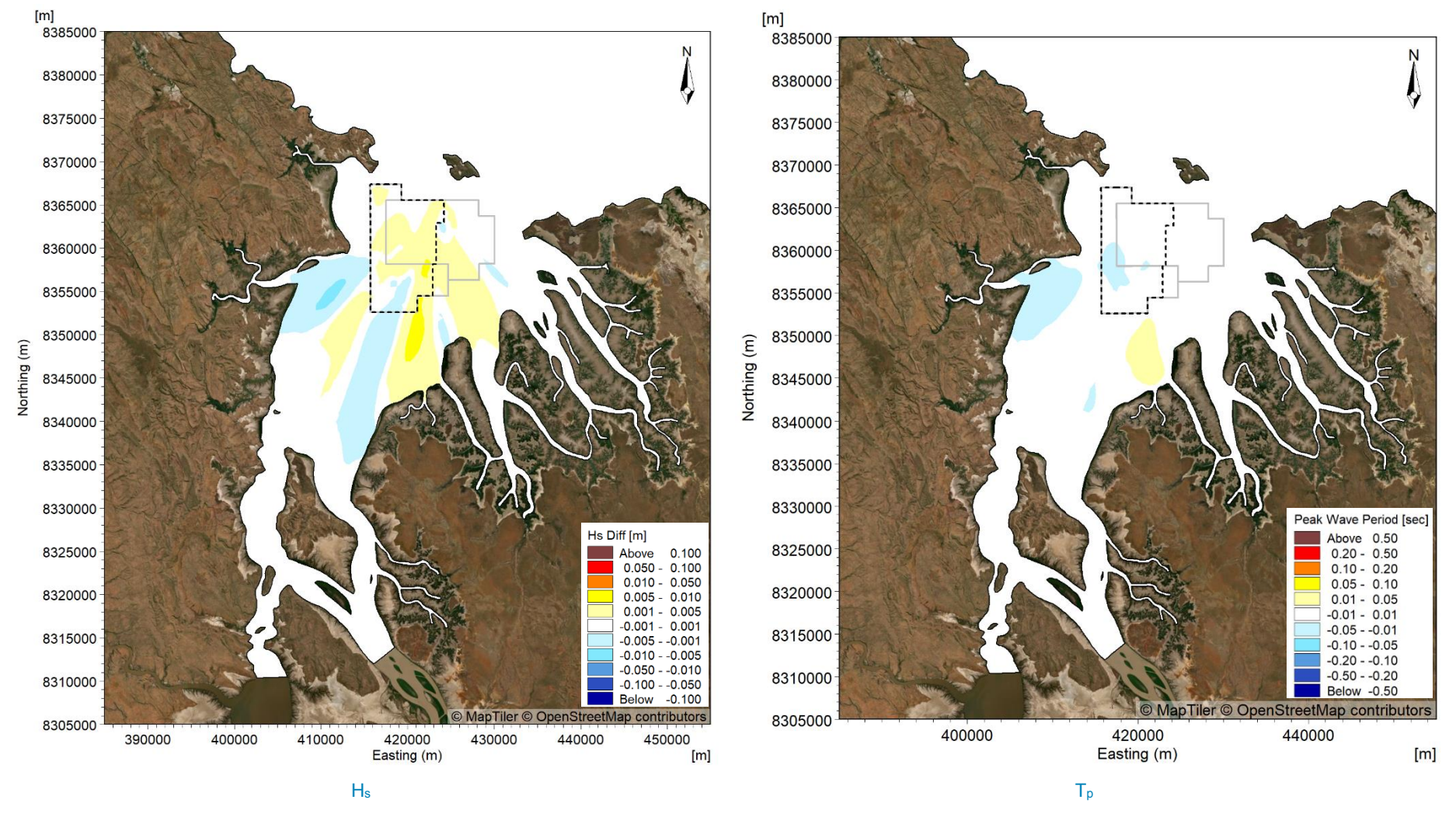


Figure B54. Modelled change in H<sub>s</sub> (left) and T<sub>p</sub> (right) during the largest wave event in the wet season period in 100 years time after 15 years of sand sourcing.



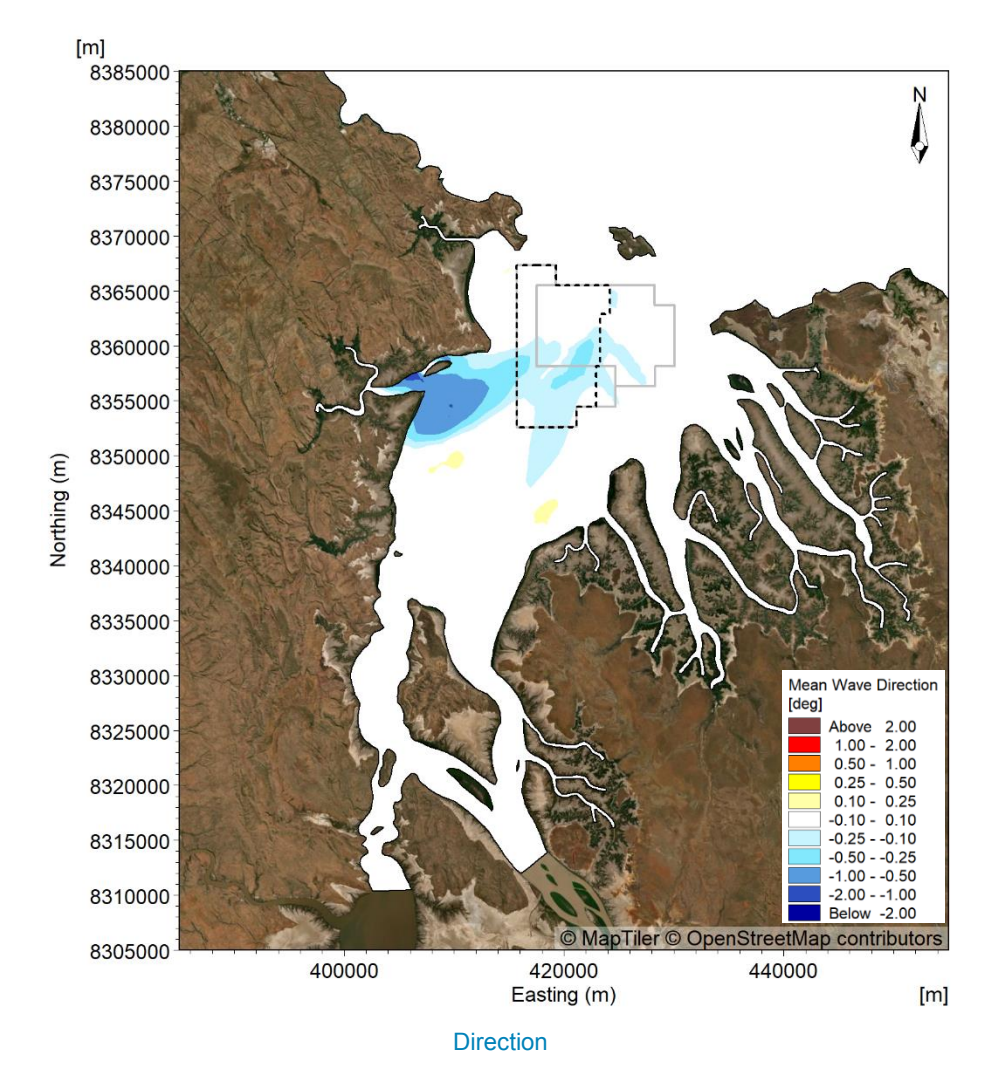


Figure B55. Modelled change in wave direction during the largest wave event in the wet season period in 100 years time after 15 years of sand sourcing.



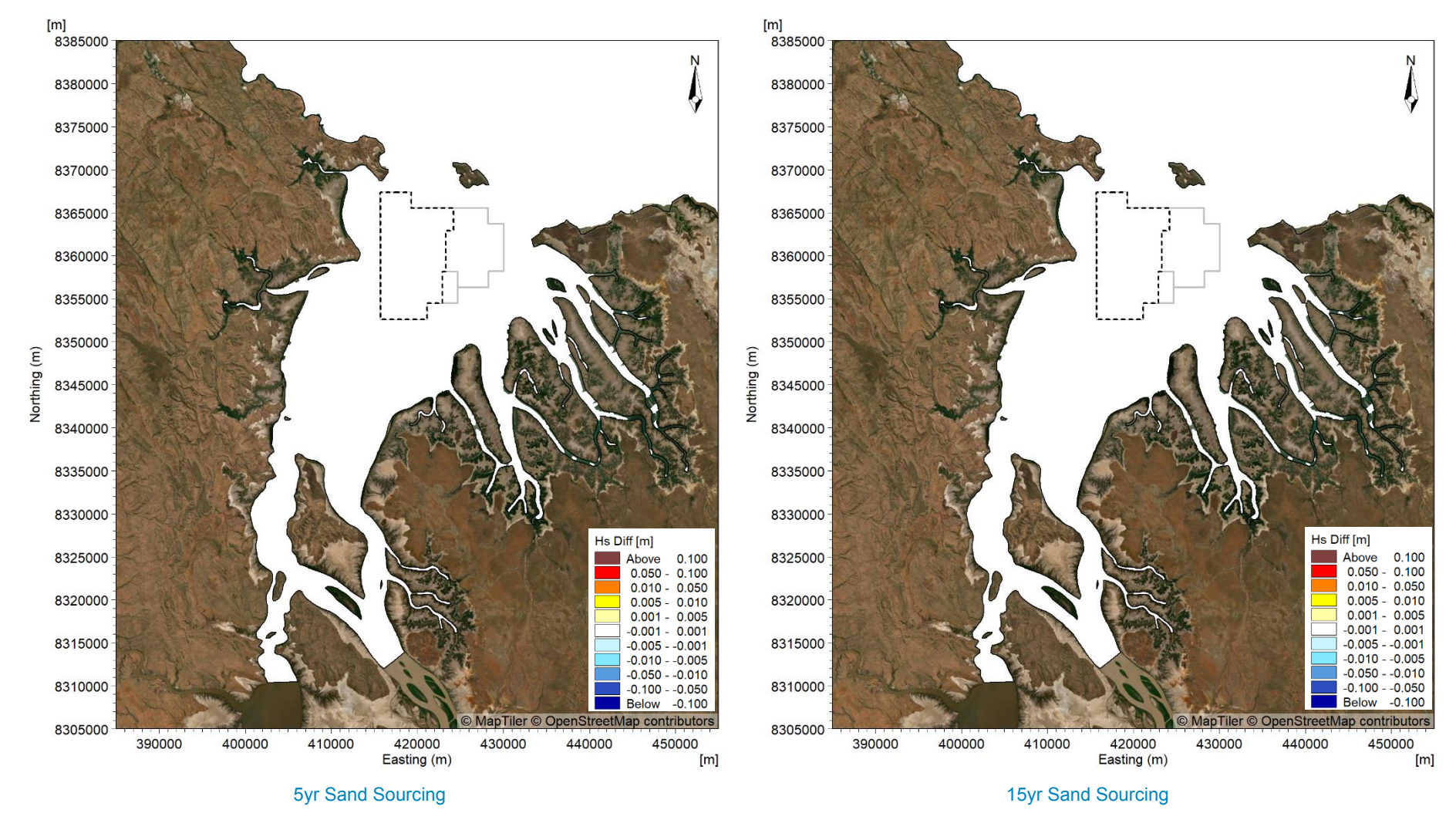


Figure B56. Modelled change in H<sub>s</sub> during the largest wave event in the dry season period due to 5 years of sand sourcing (left) and 15 years of sand sourcing (right).



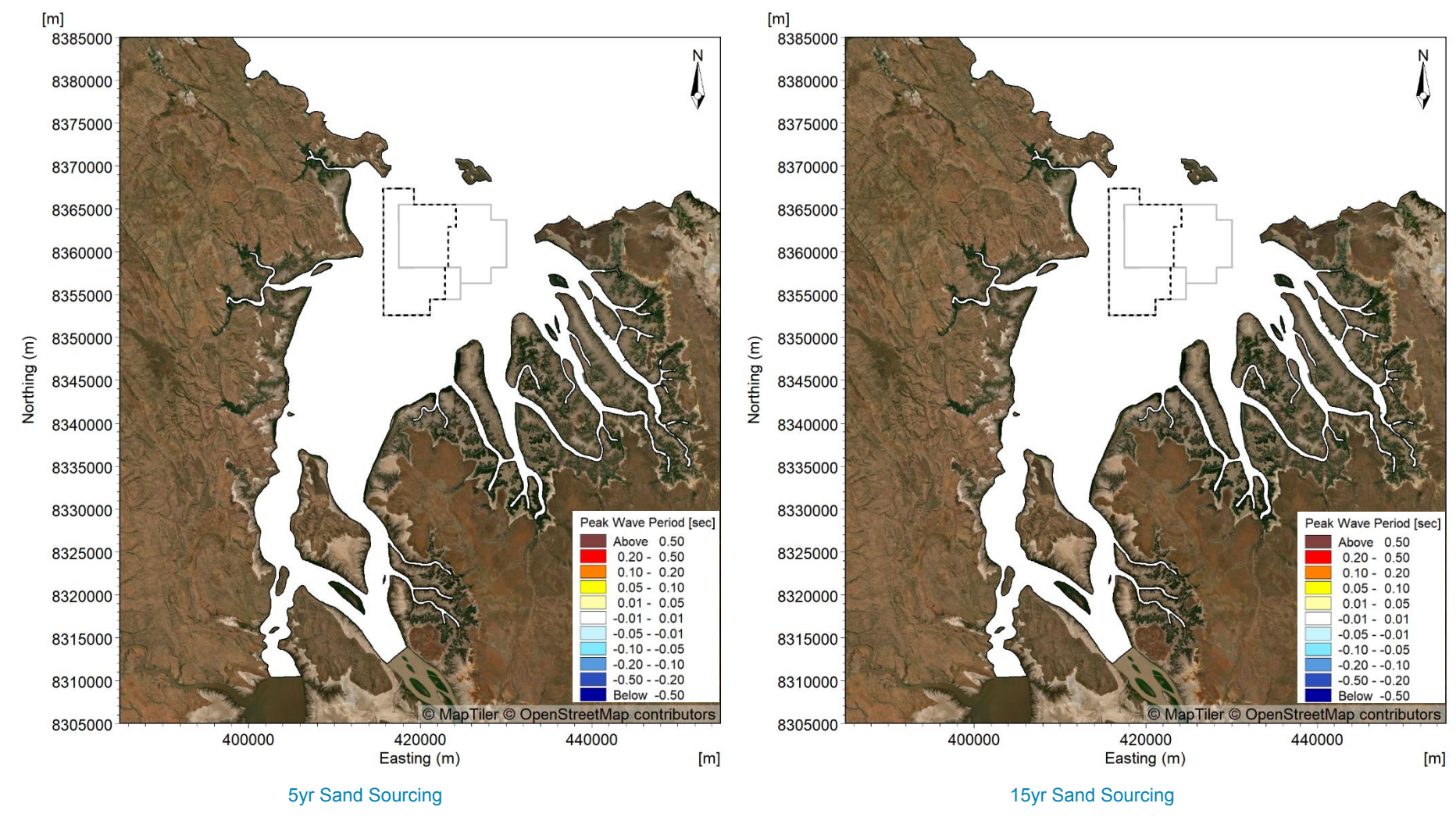


Figure B57. Modelled change in T<sub>p</sub> during the largest wave event in the dry season period due to 5 years of sand sourcing (left) and 15 years of sand sourcing (right).



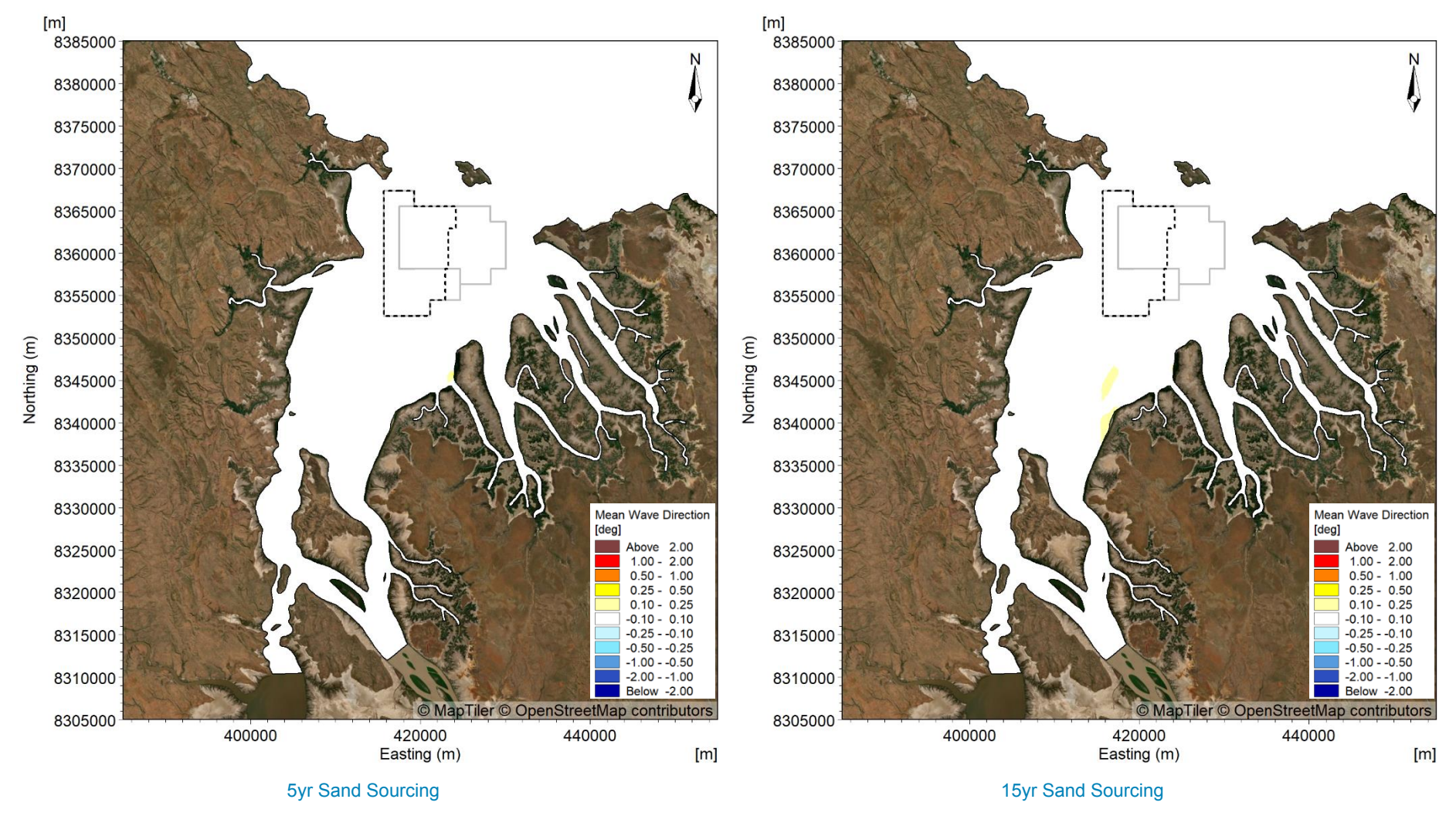


Figure B58. Modelled change in wave direction during the largest wave event in the dry season period due to 5 years of sand sourcing (left) and 15 years of sand sourcing (right).



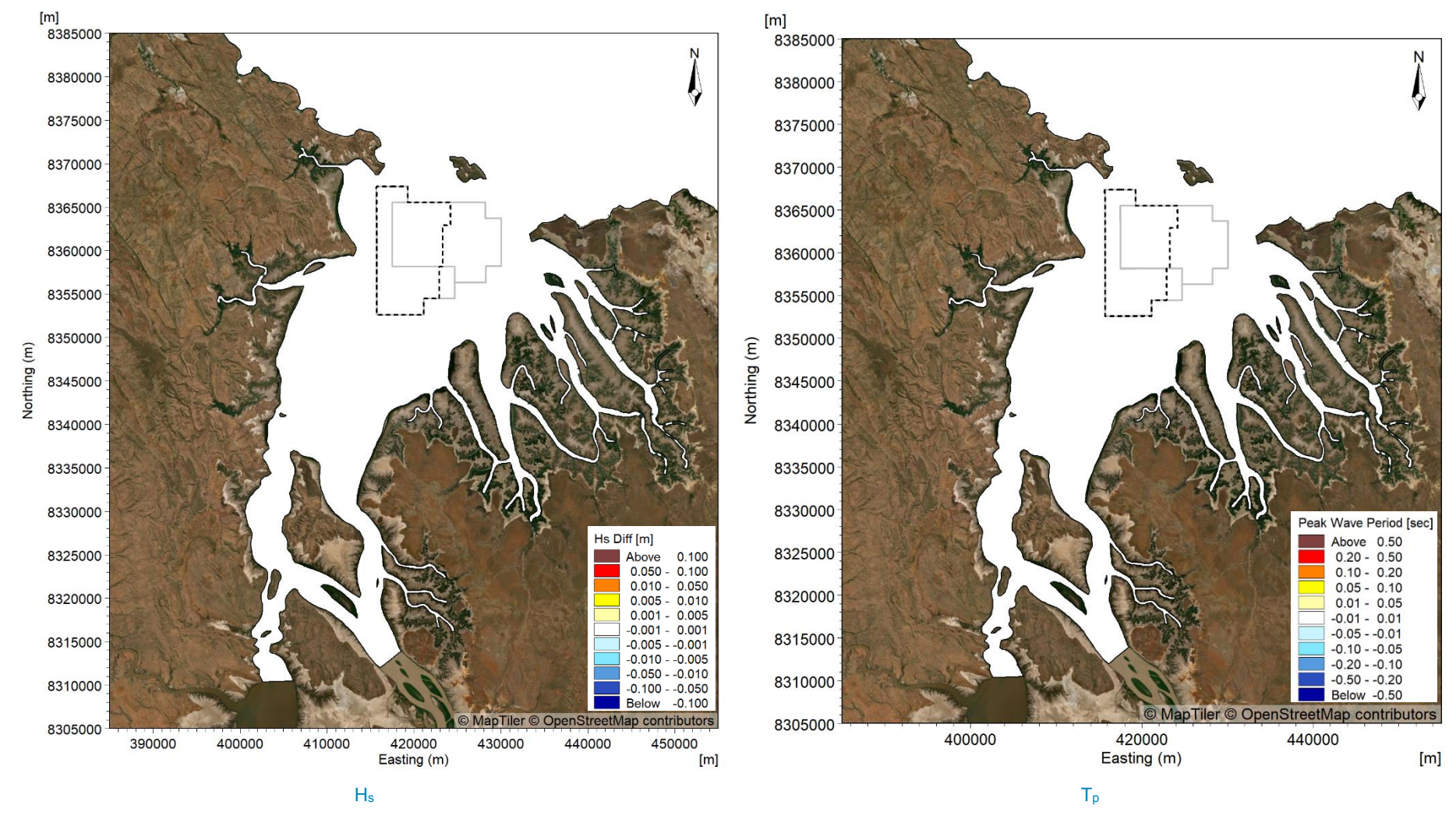


Figure B59. Modelled change in H<sub>s</sub> (left) and T<sub>p</sub> (right) during the largest wave event in the dry season period in 100 years time after 15 years of sand sourcing.



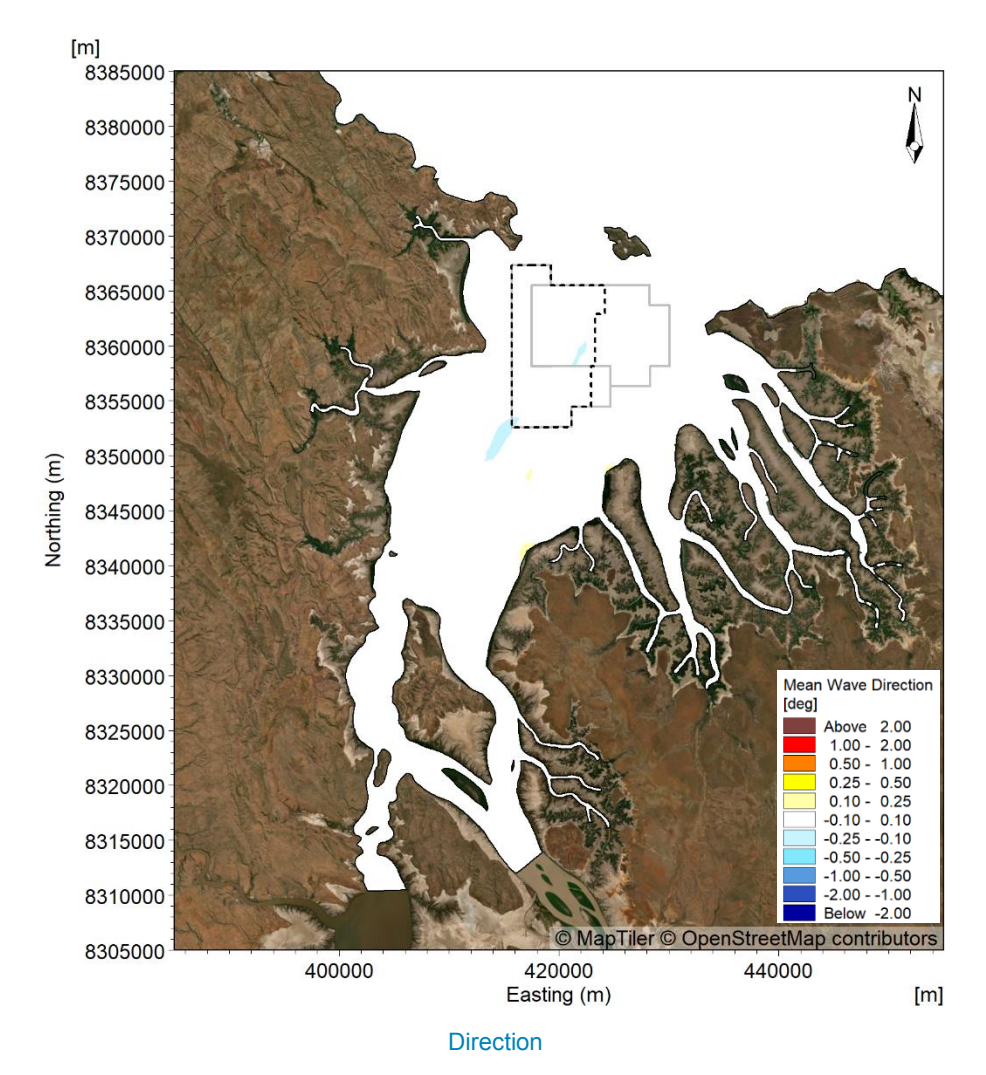


Figure B60. Modelled change in wave direction during the largest wave event in the dry season period in 100 years time after 15 years of sand sourcing.



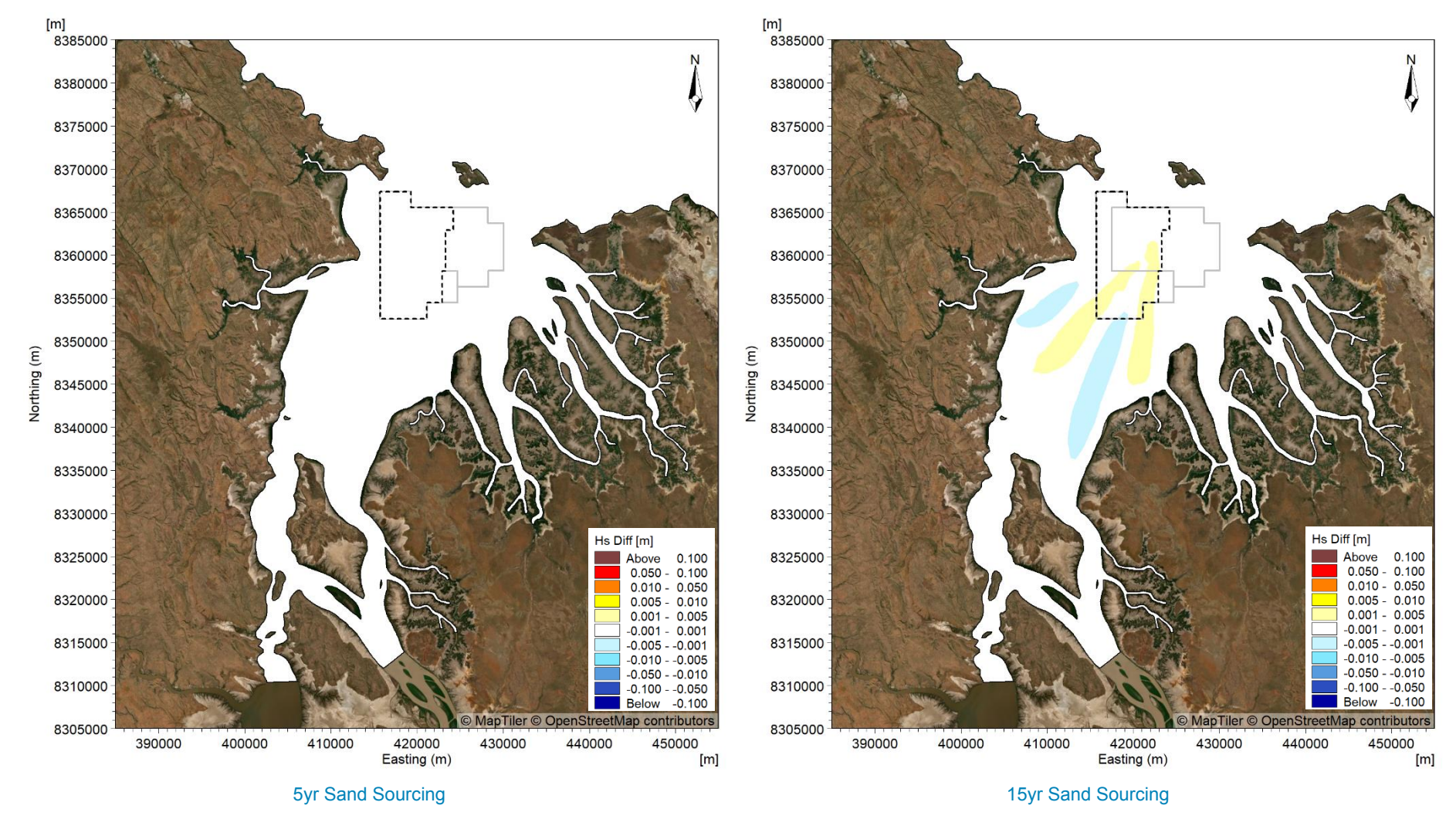


Figure B61. Modelled change in H<sub>s</sub> during the largest wave event in the transitional season period due to 5 years of sand sourcing (left) and 15 years of sand sourcing (right).



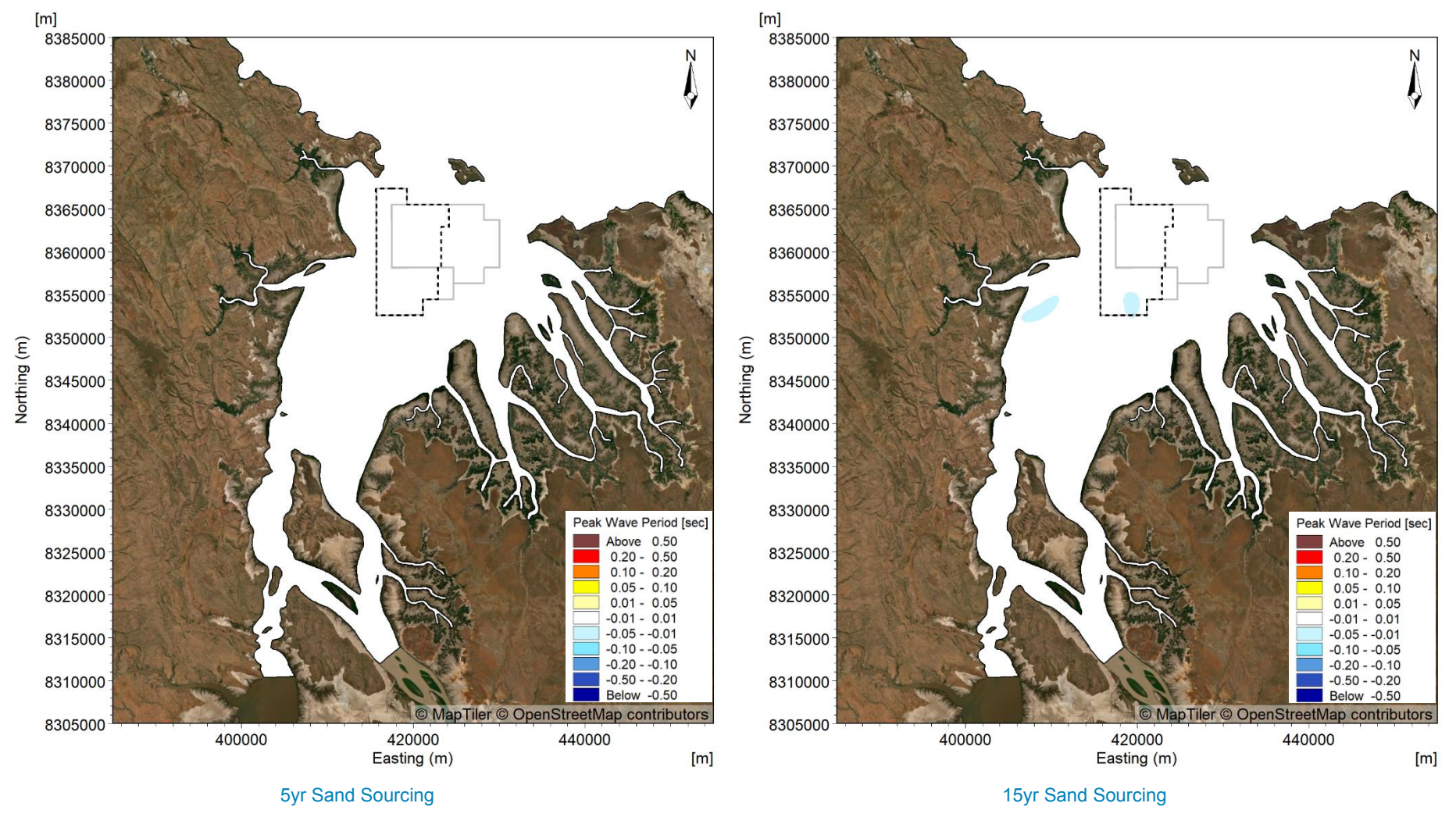


Figure B62. Modelled change in T<sub>p</sub> during the largest wave event in the transitional season period due to 5 years of sand sourcing (left) and 15 years of sand sourcing (right).



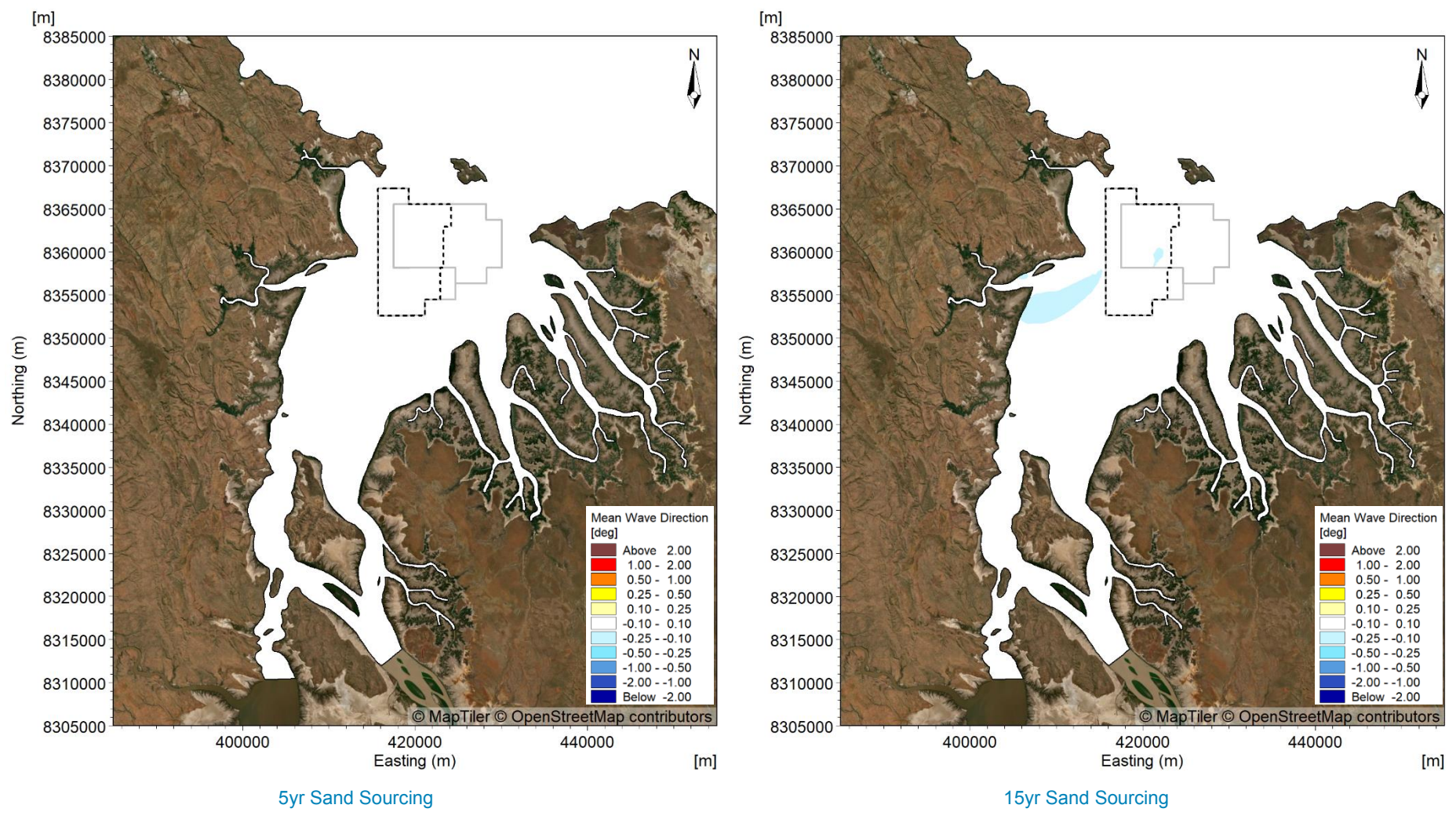


Figure B63. Modelled change in wave direction during the largest wave event in the transitional season period due to 5 years of sand sourcing (left) and 15 years of sand sourcing (right).



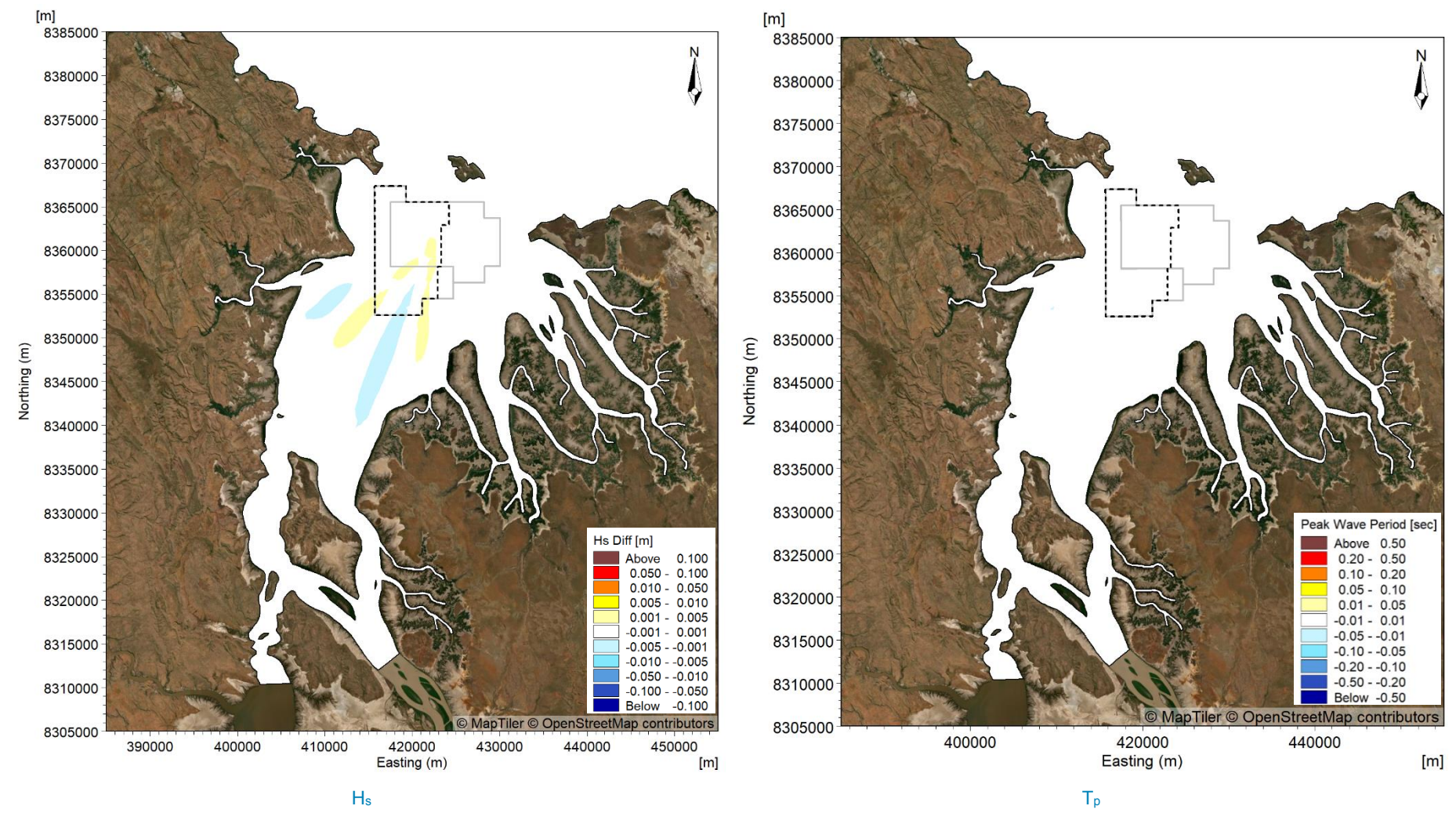


Figure B64. Modelled change in H<sub>s</sub> (left) and T<sub>p</sub> (right) during the largest wave event in the transitional season period in 100 years time after 15 years of sand sourcing.



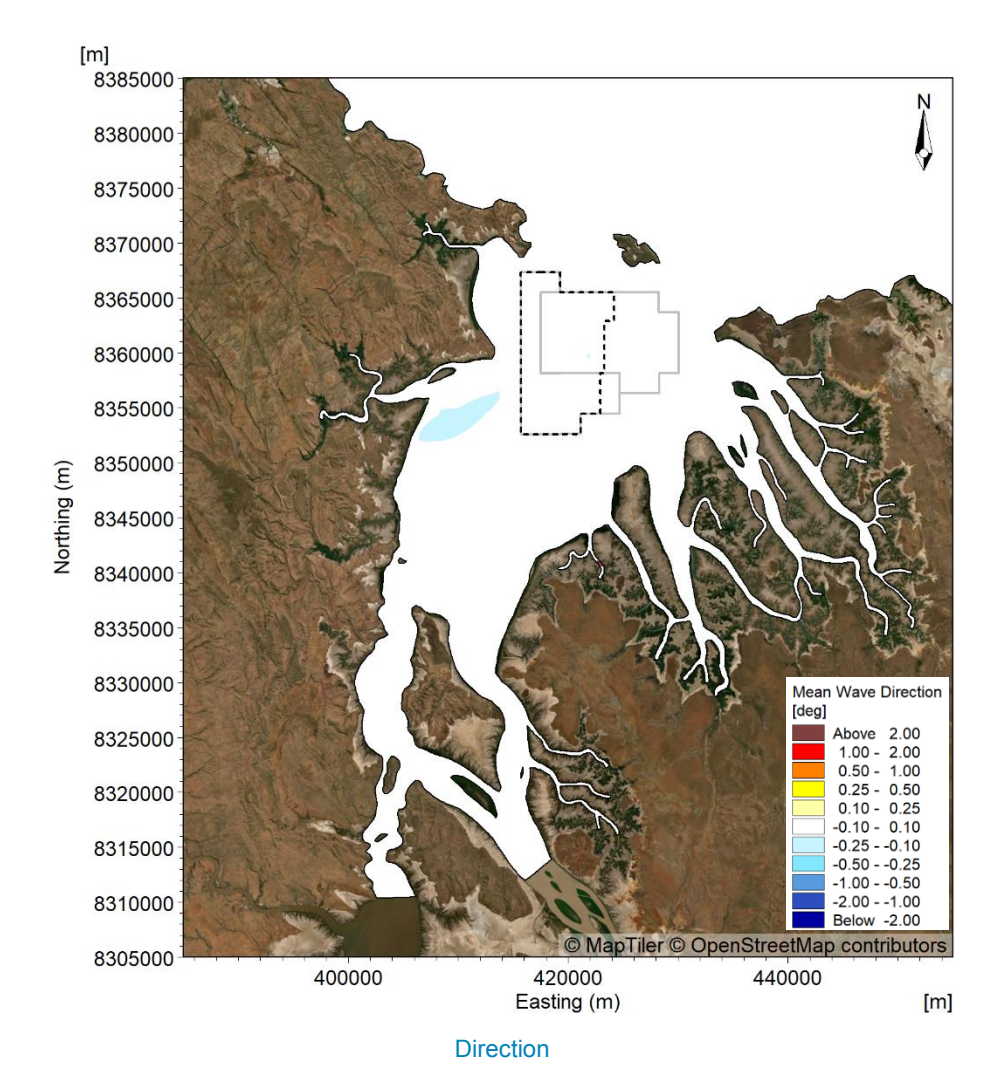


Figure B65. Modelled change in wave direction during the largest wave event in the transitional season period in 100 years time after 15 years of sand sourcing.



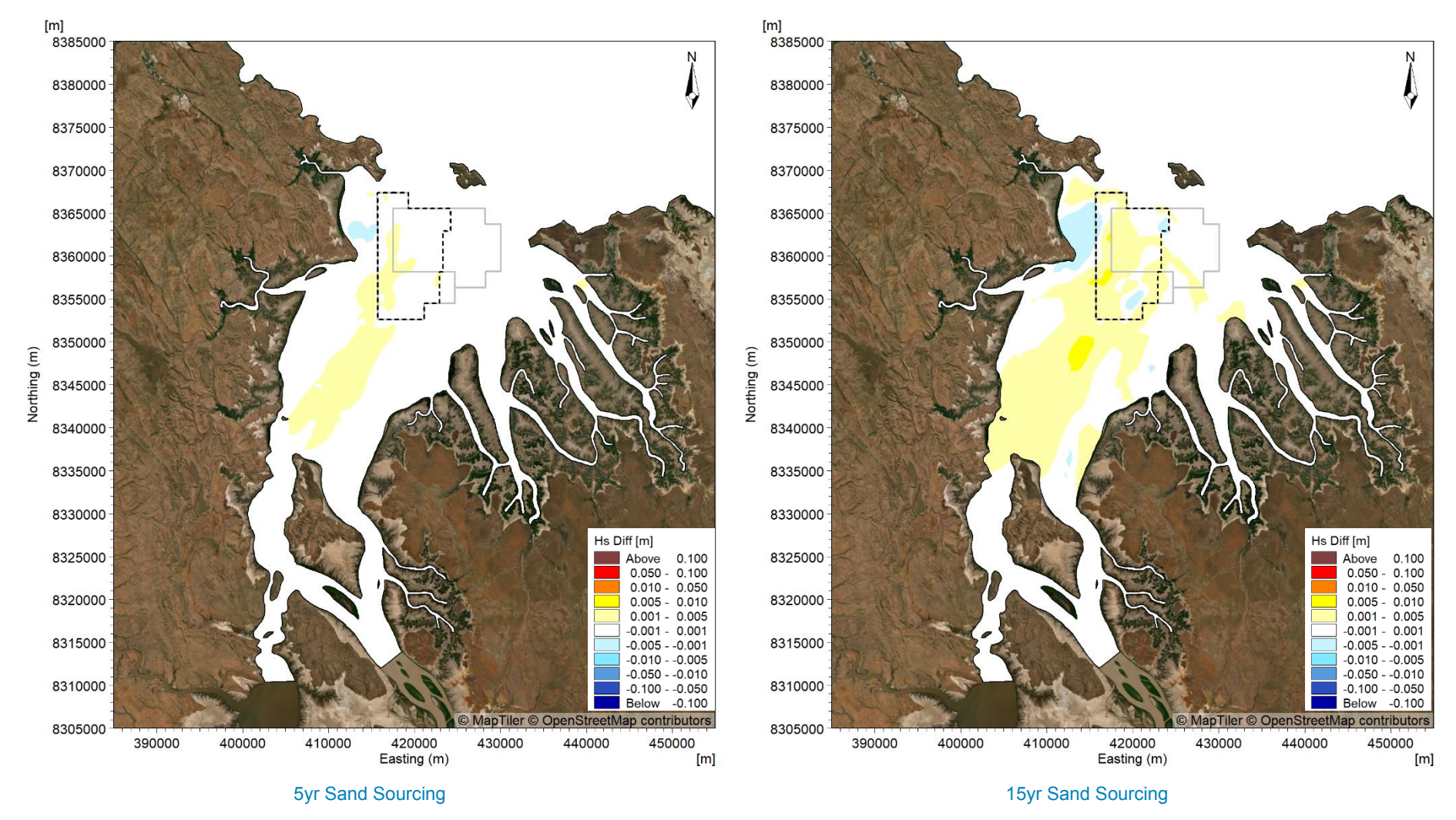


Figure B66. Modelled change in H<sub>s</sub> during the peak of TC Marcus due to 5 years of sand sourcing (left) and 15 years of sand sourcing (right).



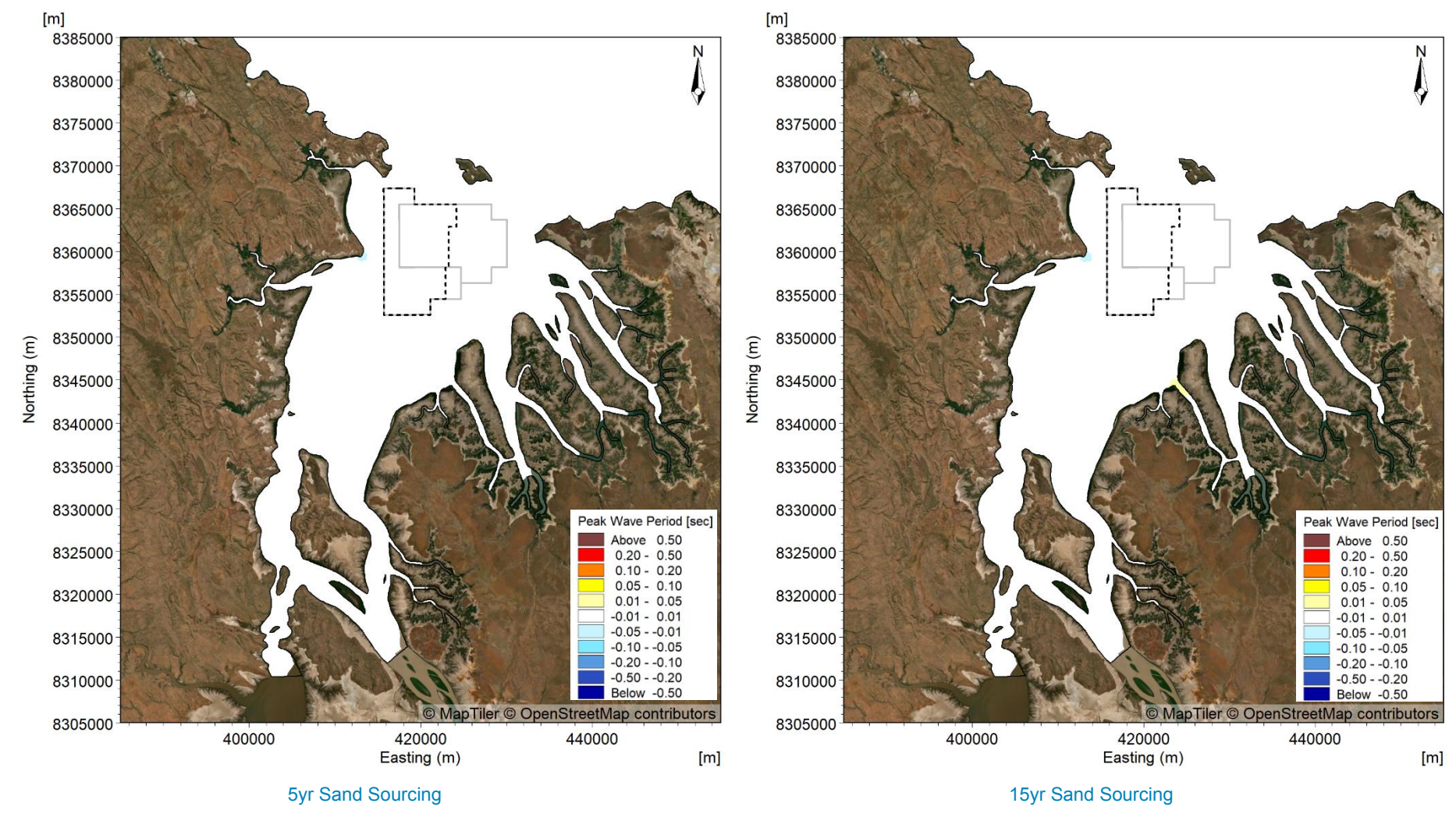


Figure B67. Modelled change in T<sub>p</sub> during the peak of TC Marcus in the wet season period due to 5 years of sand sourcing (left) and 15 years of sand sourcing (right).



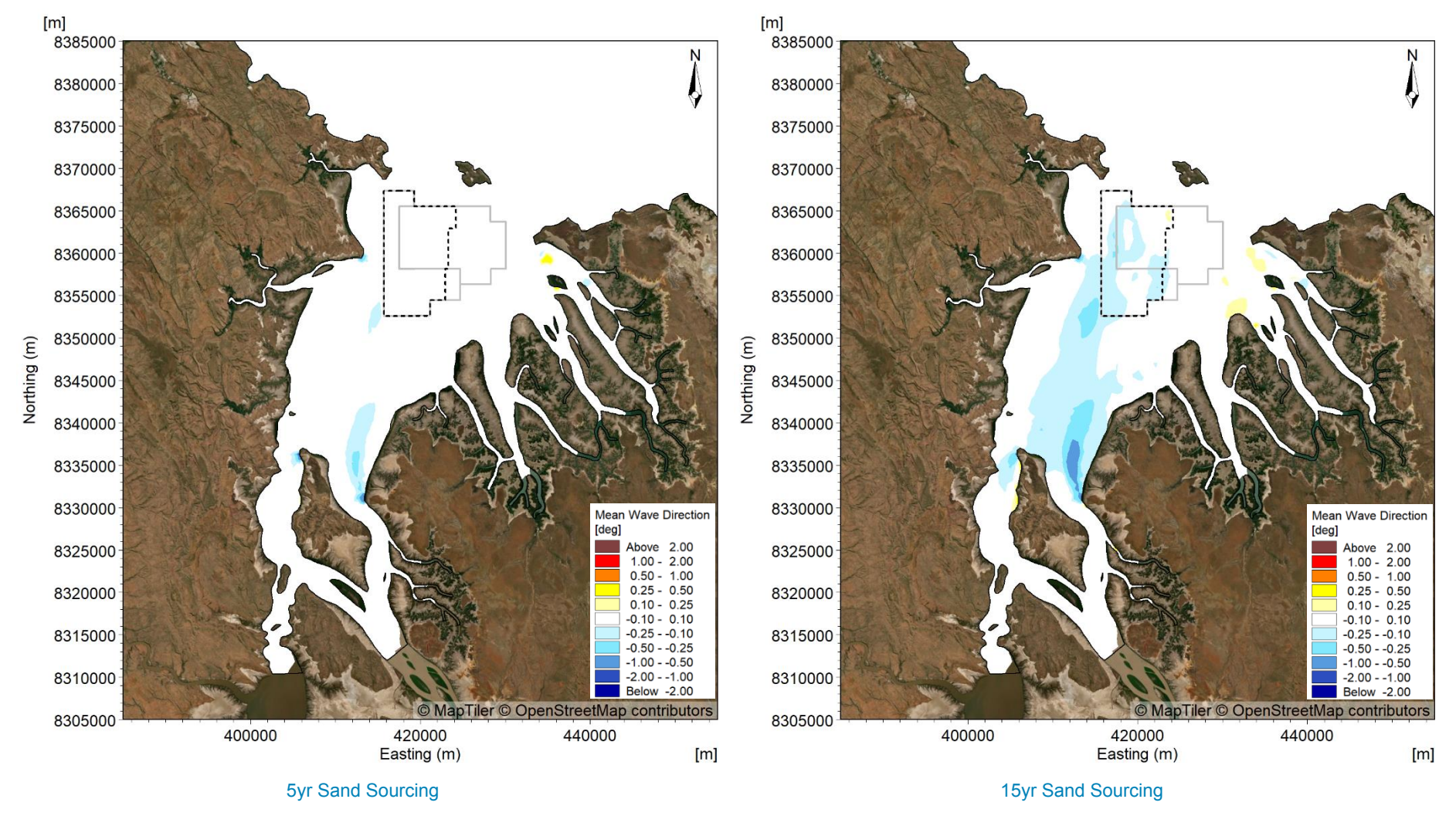


Figure B68. Modelled change in wave direction during the peak of TC Marcus in the wet season period due to 5 years of sand sourcing (left) and 15 years of sand sourcing (right).



## Appendix C – Sediment Transport Impact Plots



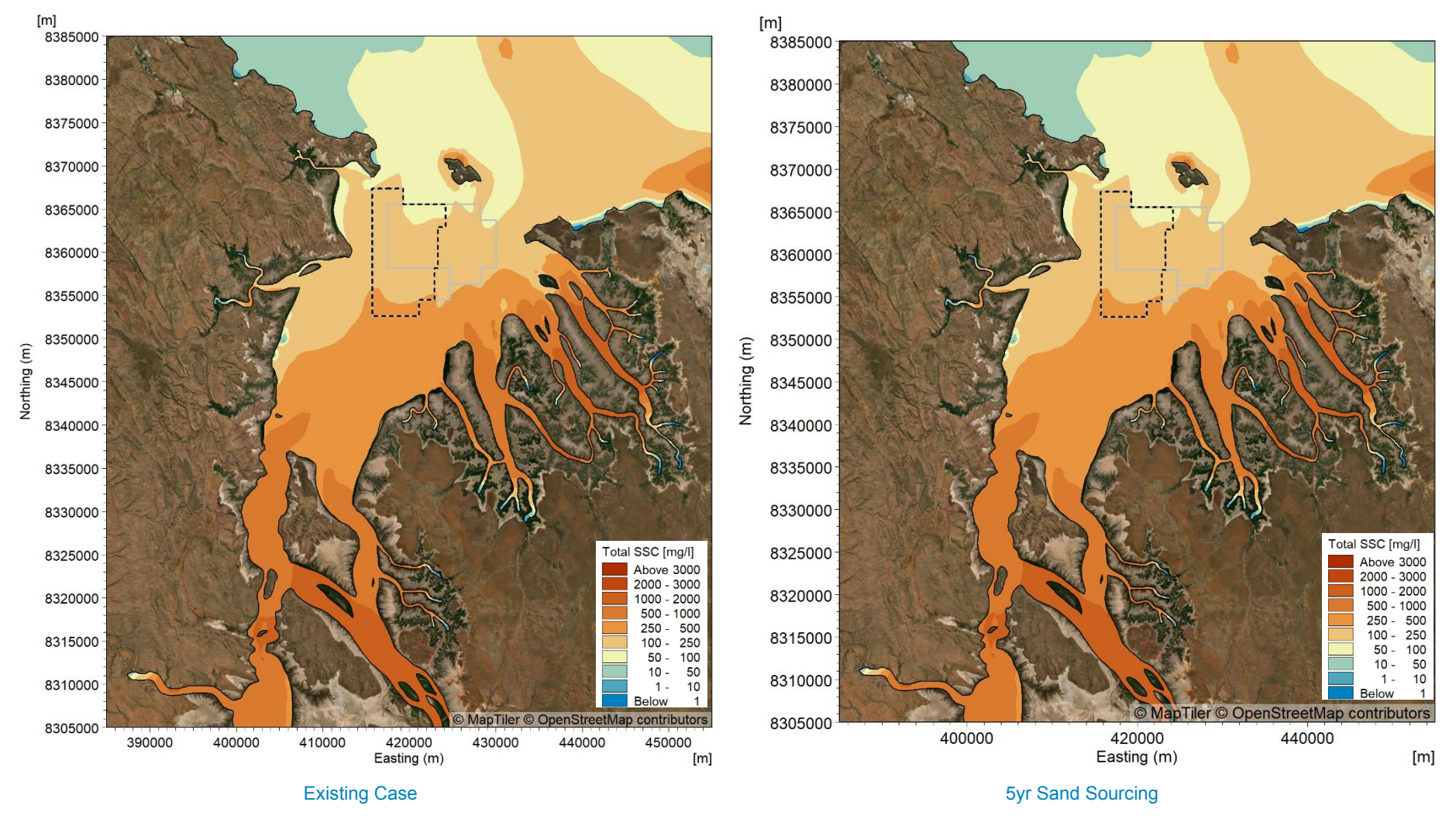


Figure C1. Modelled existing case and 5 years of sand sourcing scenario 50<sup>th</sup> percentile SSC over the 2 month wet season period.



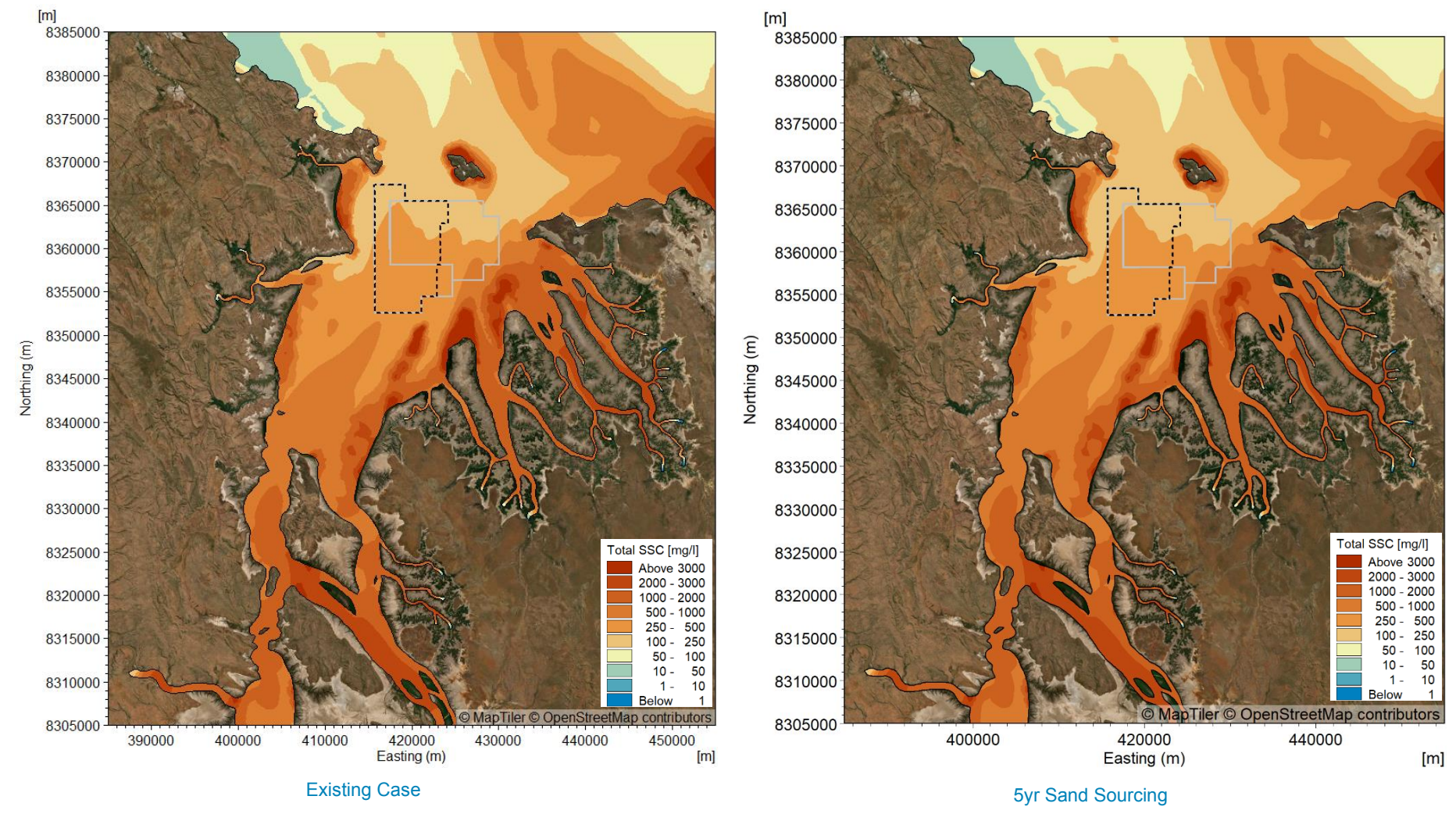


Figure C2. Modelled existing case and 5 years of sand sourcing scenario 95<sup>th</sup> percentile SSC over the 2 month wet season period.



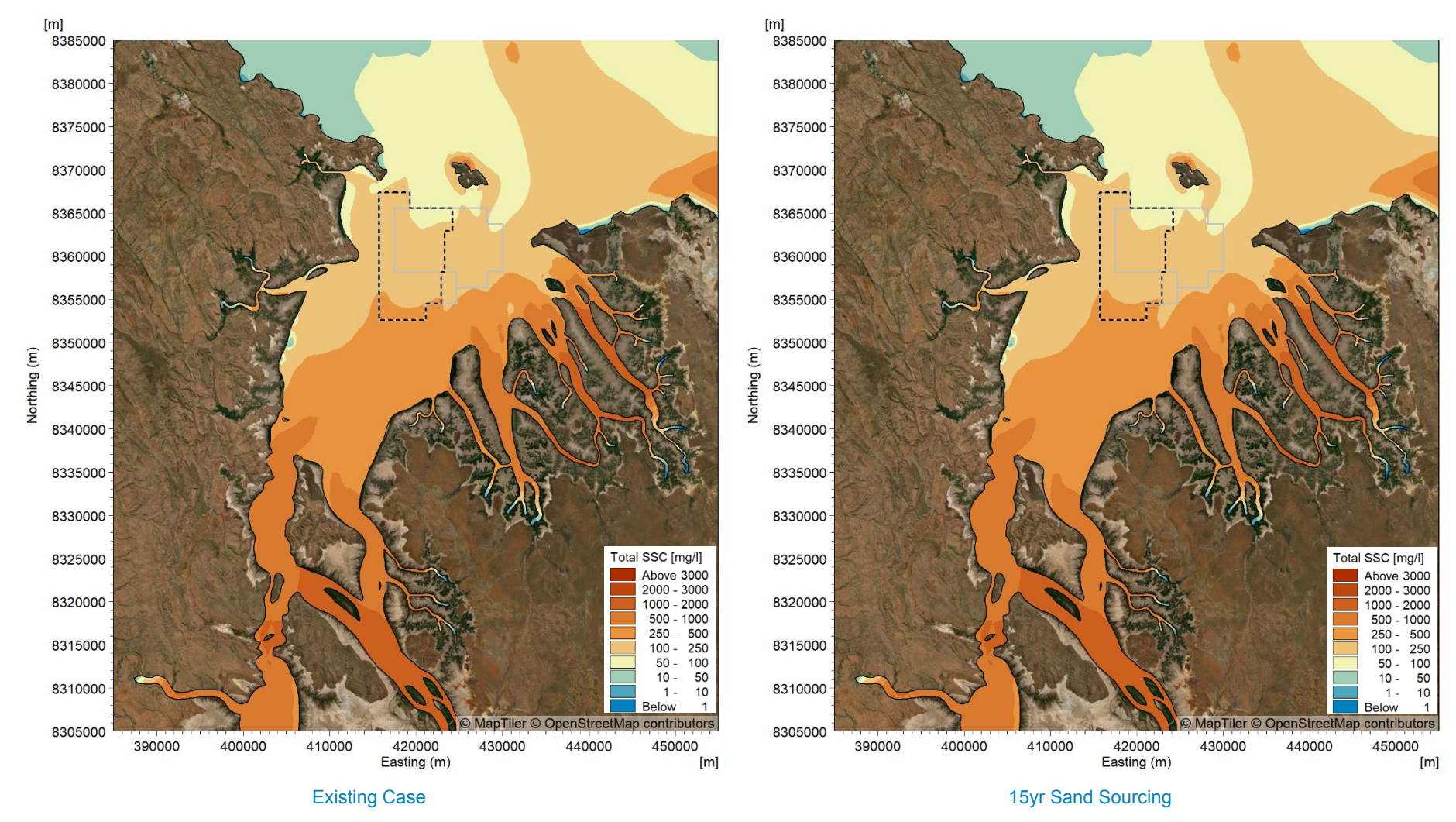


Figure C3. Modelled existing case and 15 years of sand sourcing scenario 50<sup>th</sup> percentile SSC over the 2 month wet season period.



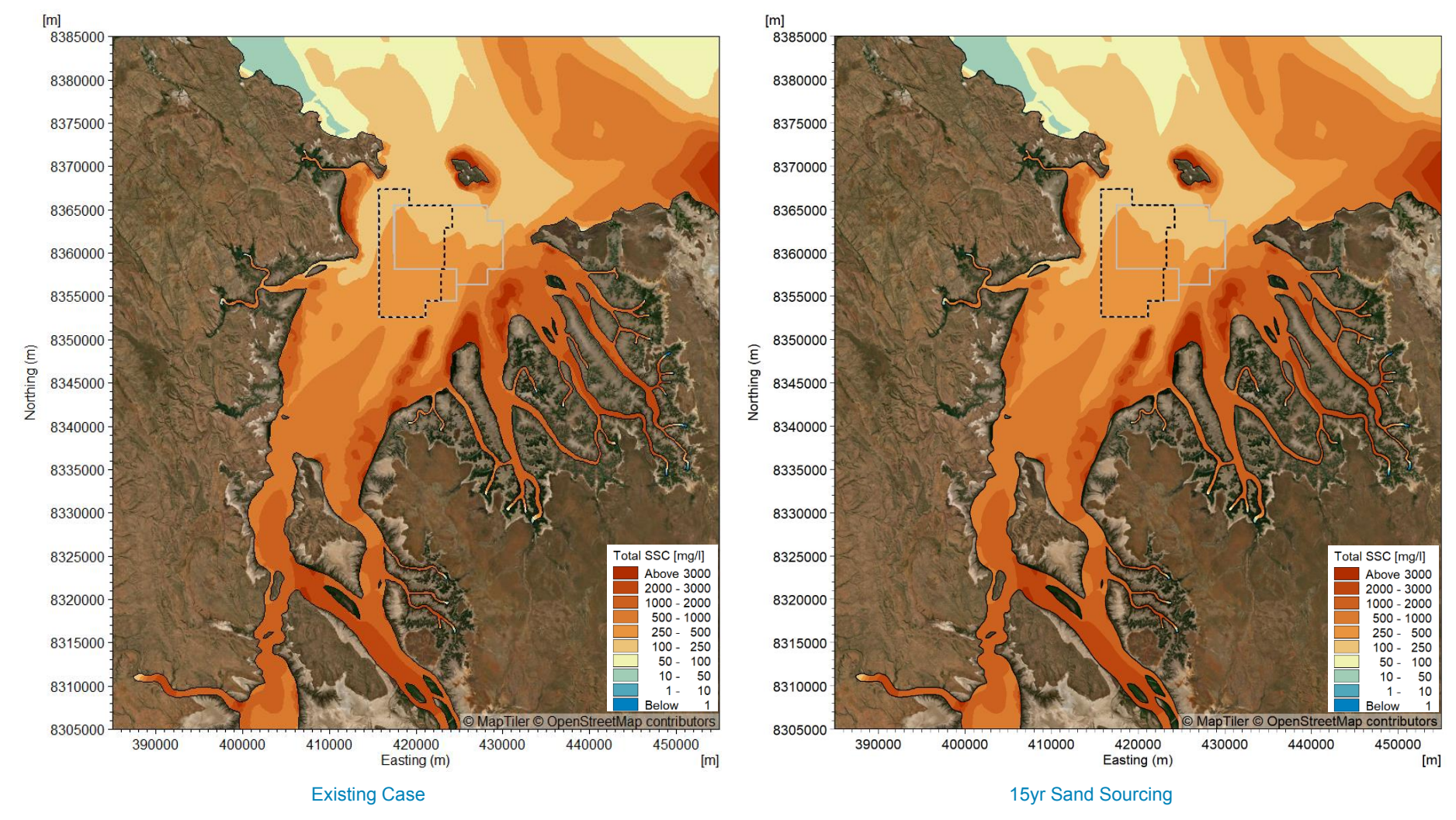


Figure C4. Modelled existing case and 15 years of sand sourcing scenario 95<sup>th</sup> percentile SSC over the 2 month wet season period.



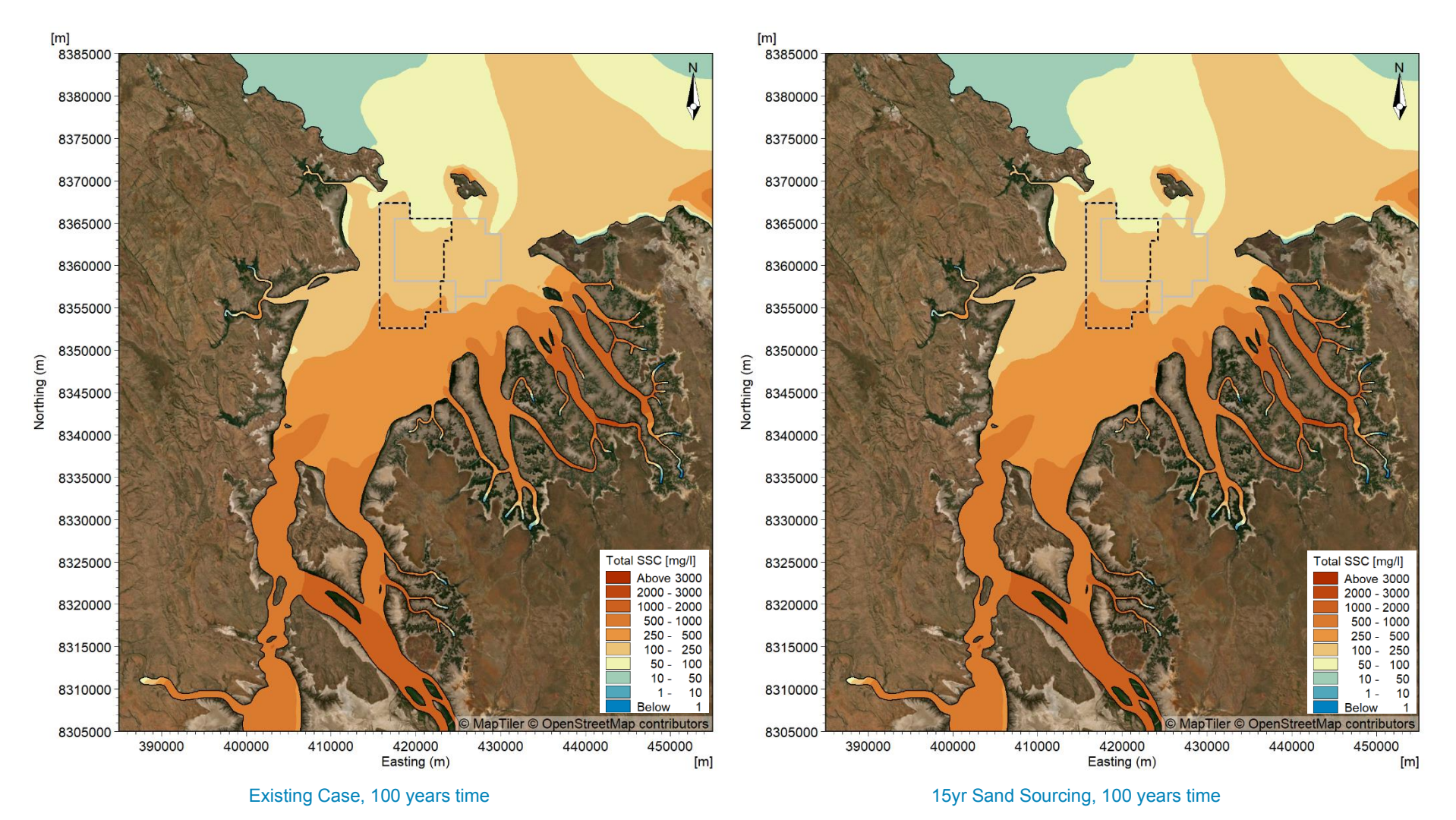


Figure C5. Modelled existing case in 100 years time and 15 years of sand sourcing scenario 50<sup>th</sup> percentile SSC over the 2 month wet season period.



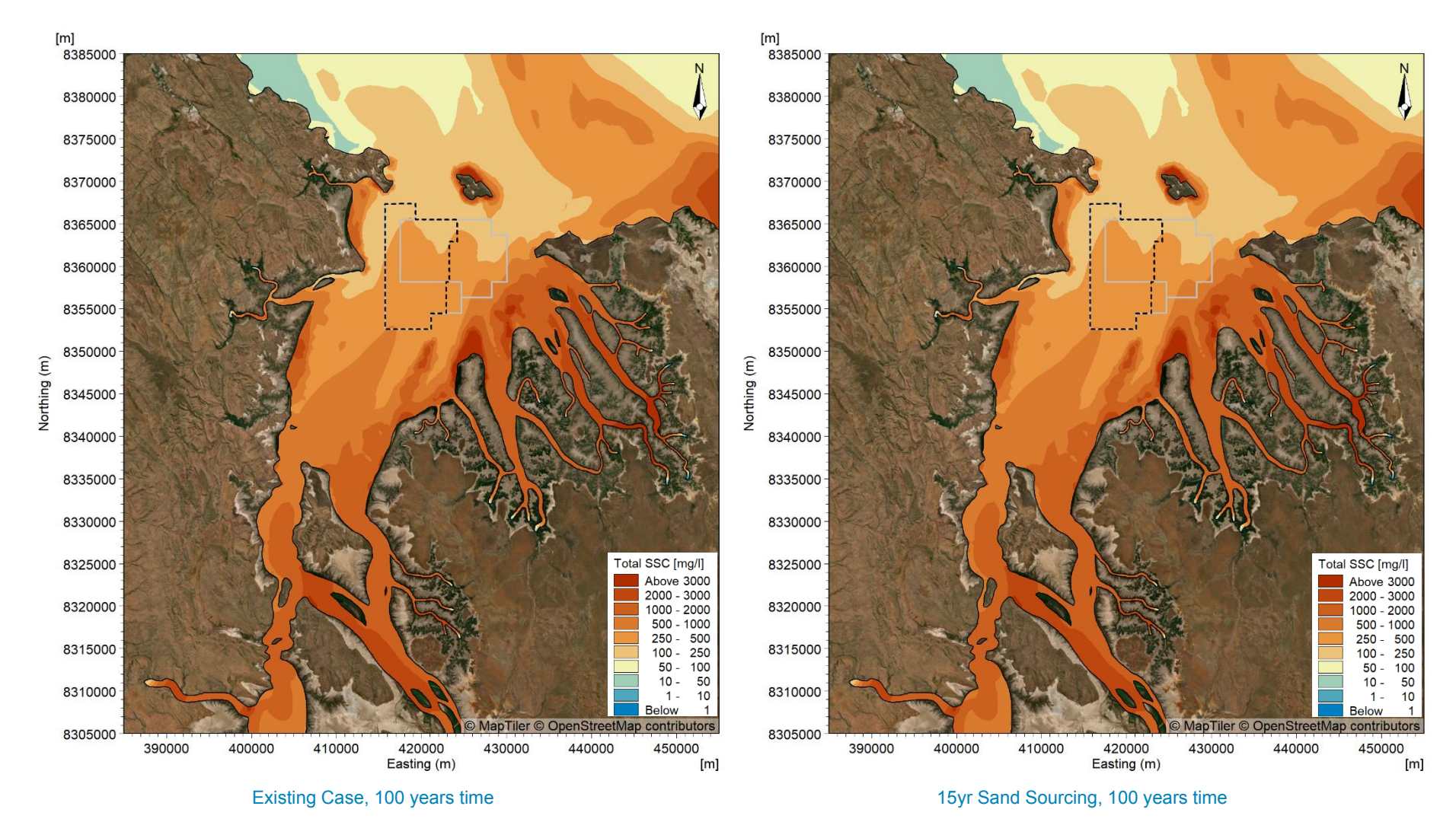


Figure C6. Modelled existing case in 100 years time and 15 years of sand sourcing scenario 95th percentile SSC over the 2 month wet season period.



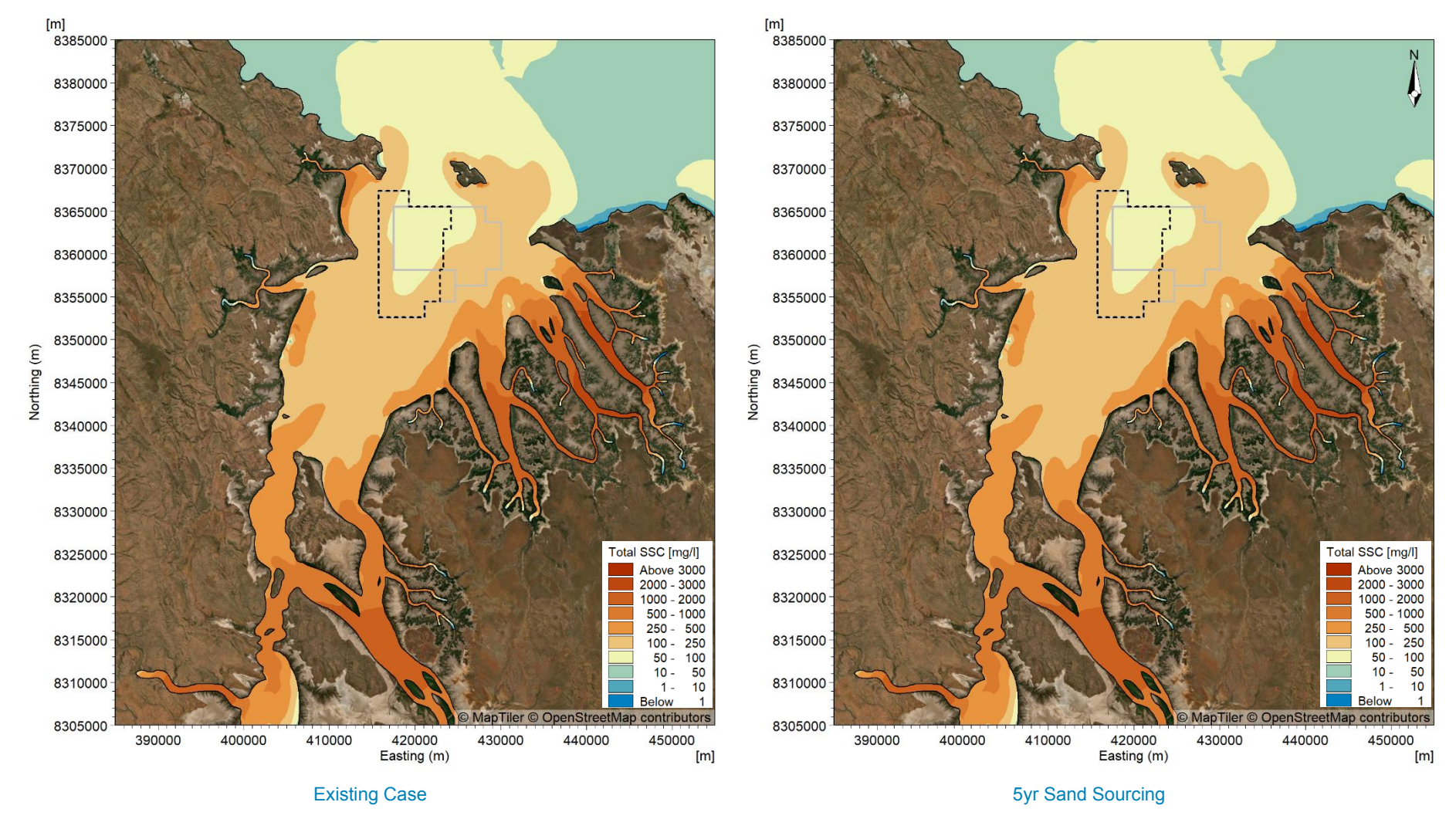


Figure C7. Modelled existing case and 5 years of sand sourcing scenario 50<sup>th</sup> percentile SSC over the 2 month dry season period.



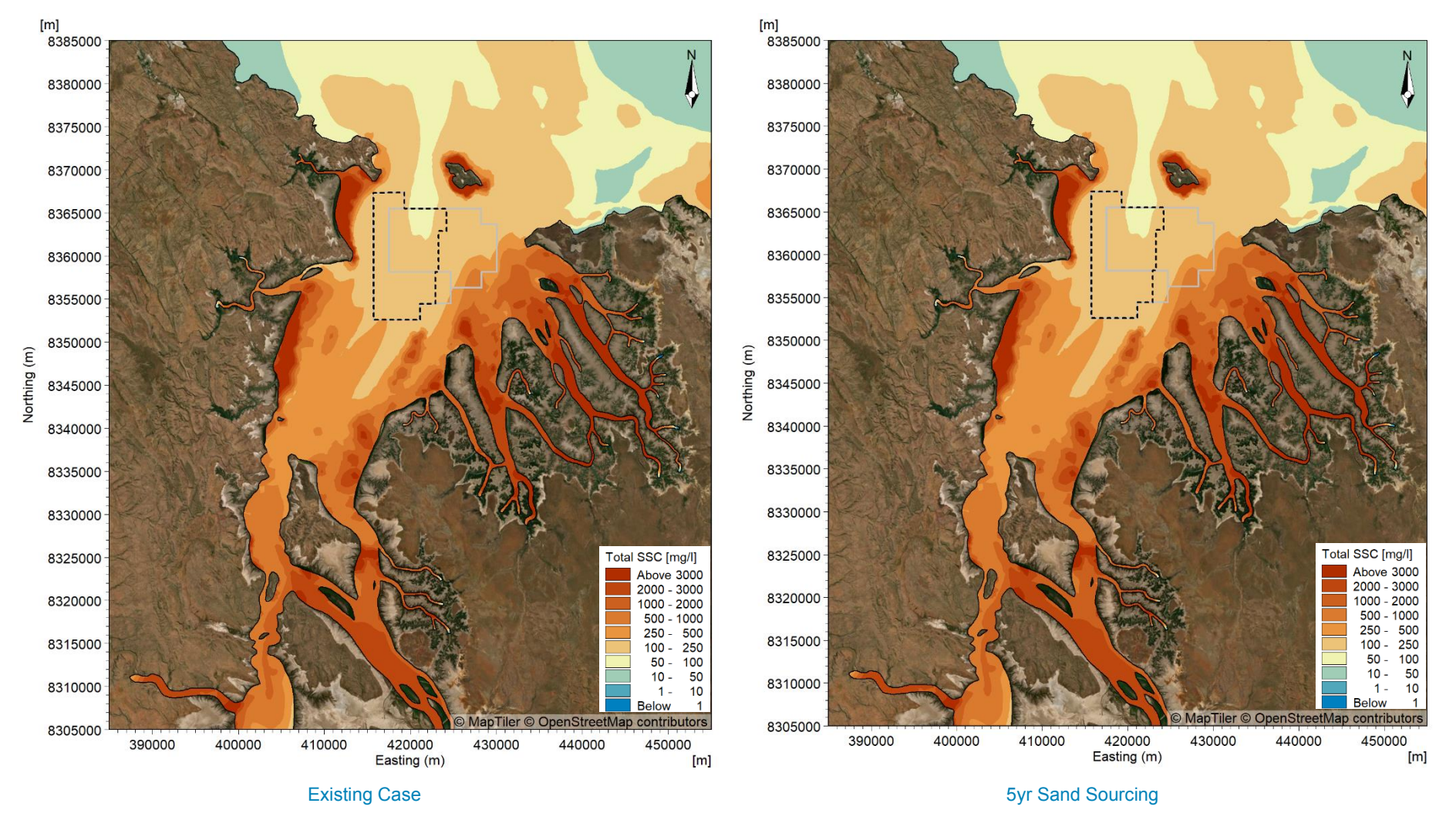


Figure C8. Modelled existing case and 5 years of sand sourcing scenario 95<sup>th</sup> percentile SSC over the 2 month dry season period.



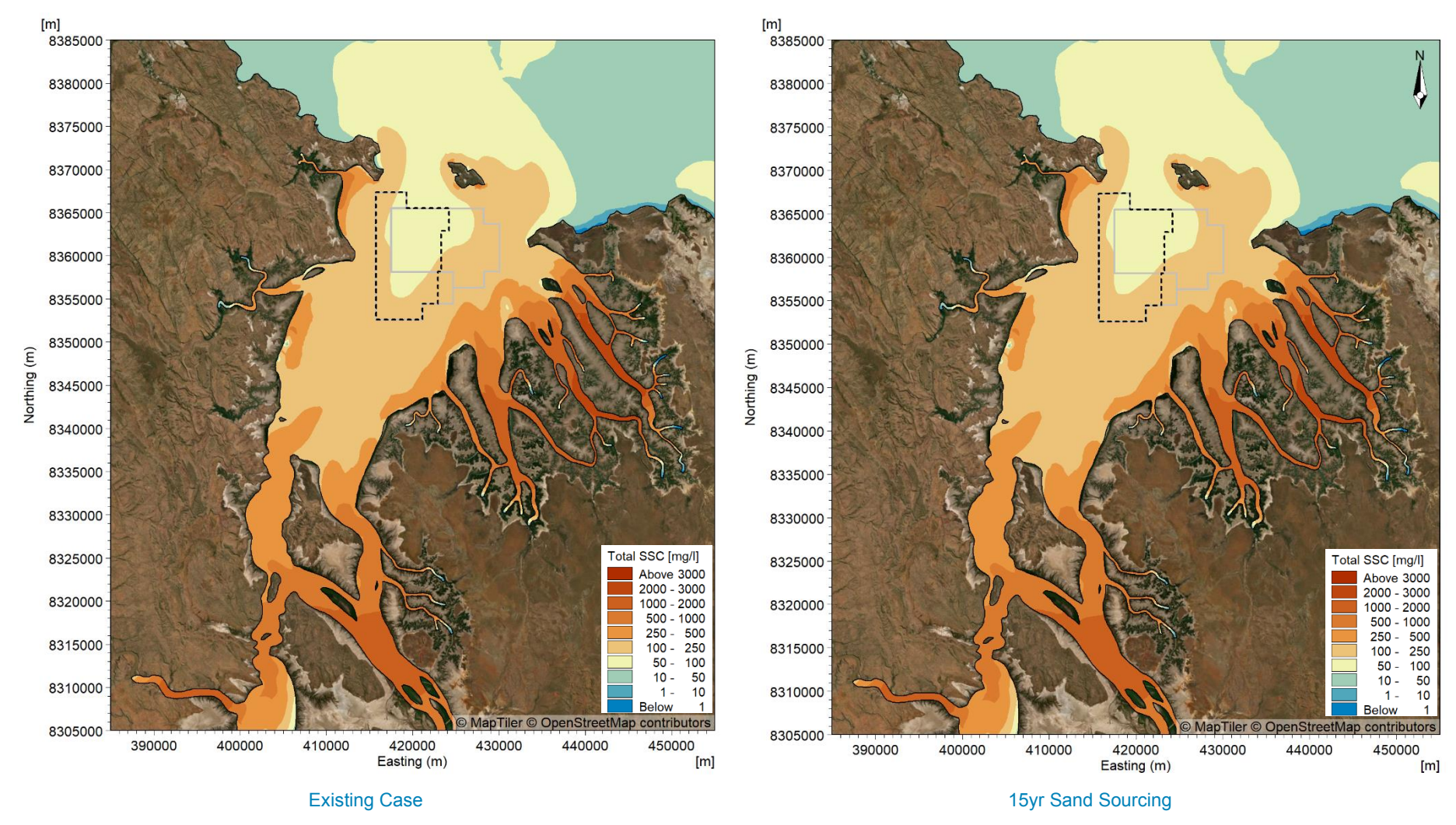


Figure C9. Modelled existing case and 15 years of sand sourcing scenario 50th percentile SSC over the 2 month dry season period.



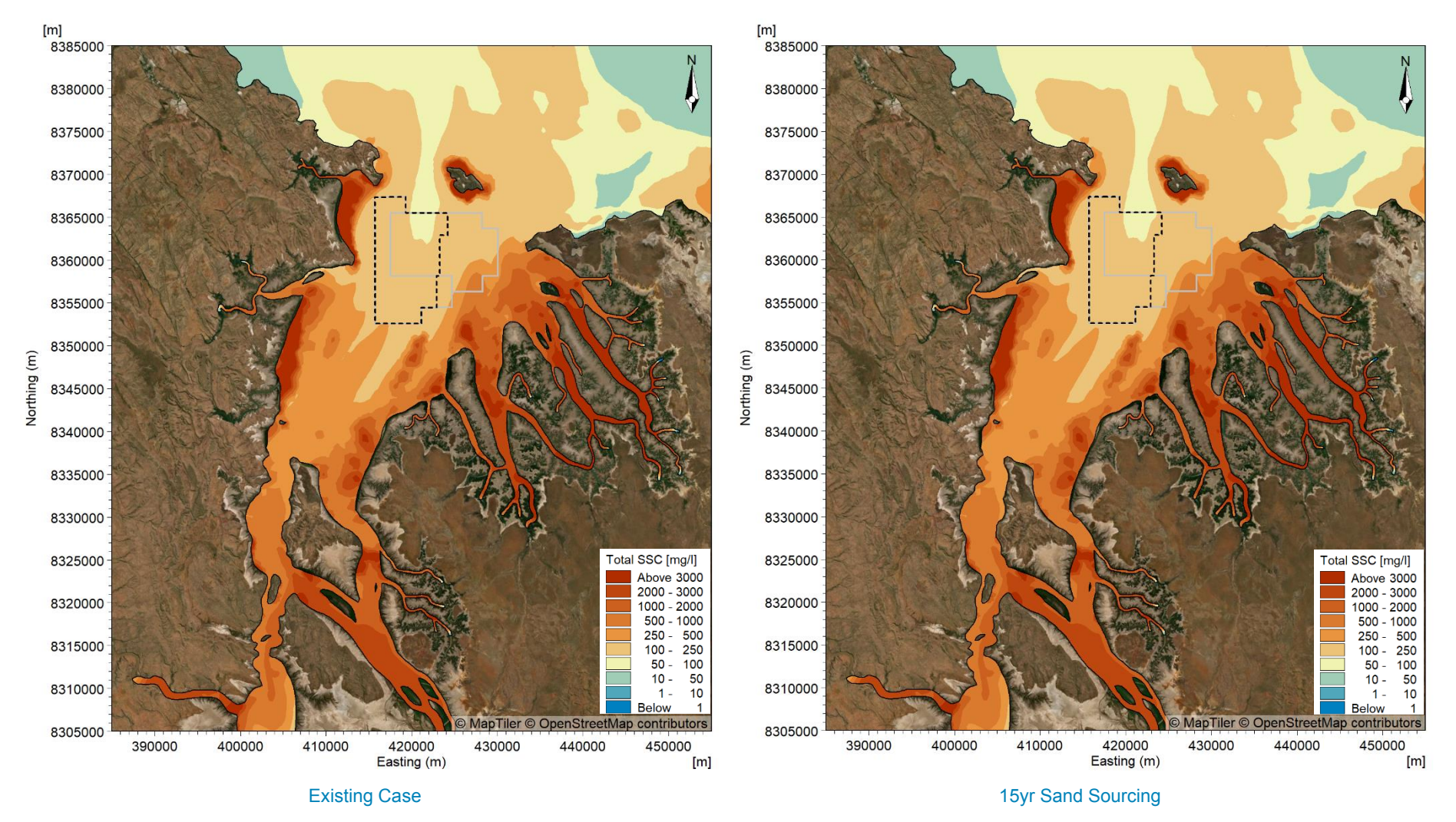


Figure C10. Modelled existing case and 15 years of sand sourcing scenario 95<sup>th</sup> percentile SSC over the 2 month dry season period.



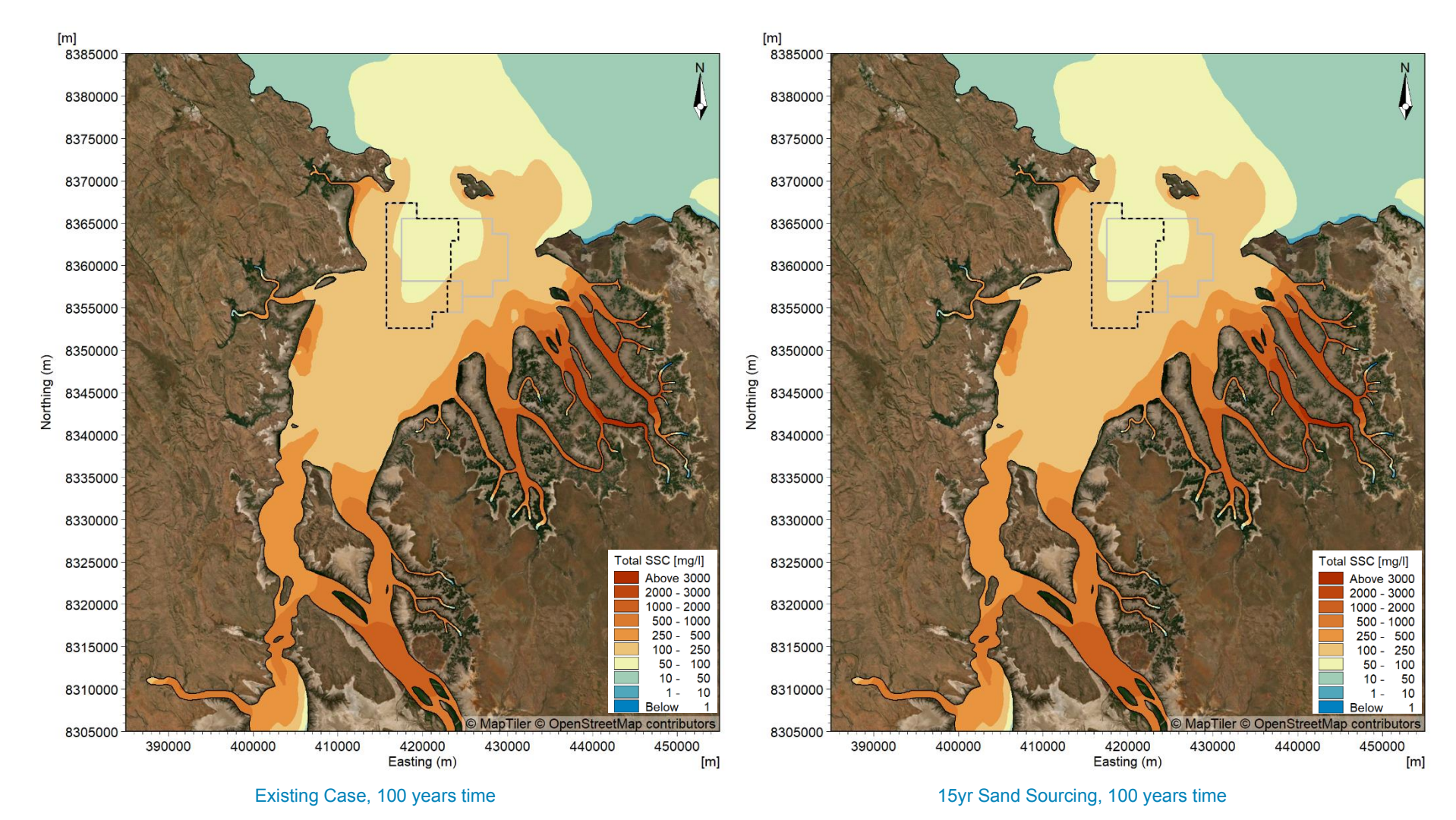


Figure C11. Modelled existing case in 100 years time and 15 years of sand sourcing scenario 50<sup>th</sup> percentile SSC over the 2 month dry season period.



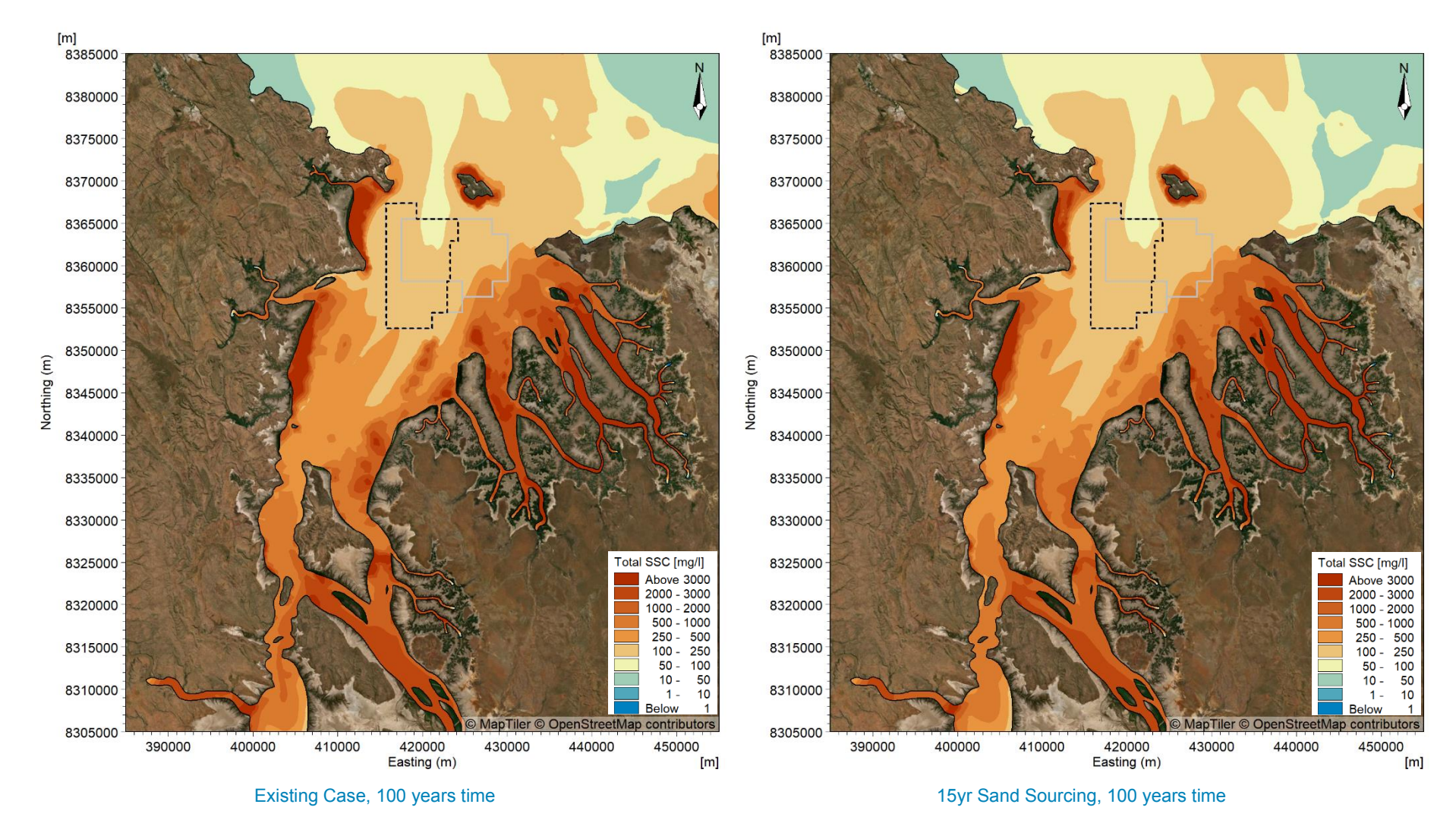


Figure C12. Modelled existing case in 100 years time and 15 years of sand sourcing scenario 95<sup>th</sup> percentile SSC over the 2 month dry season period.



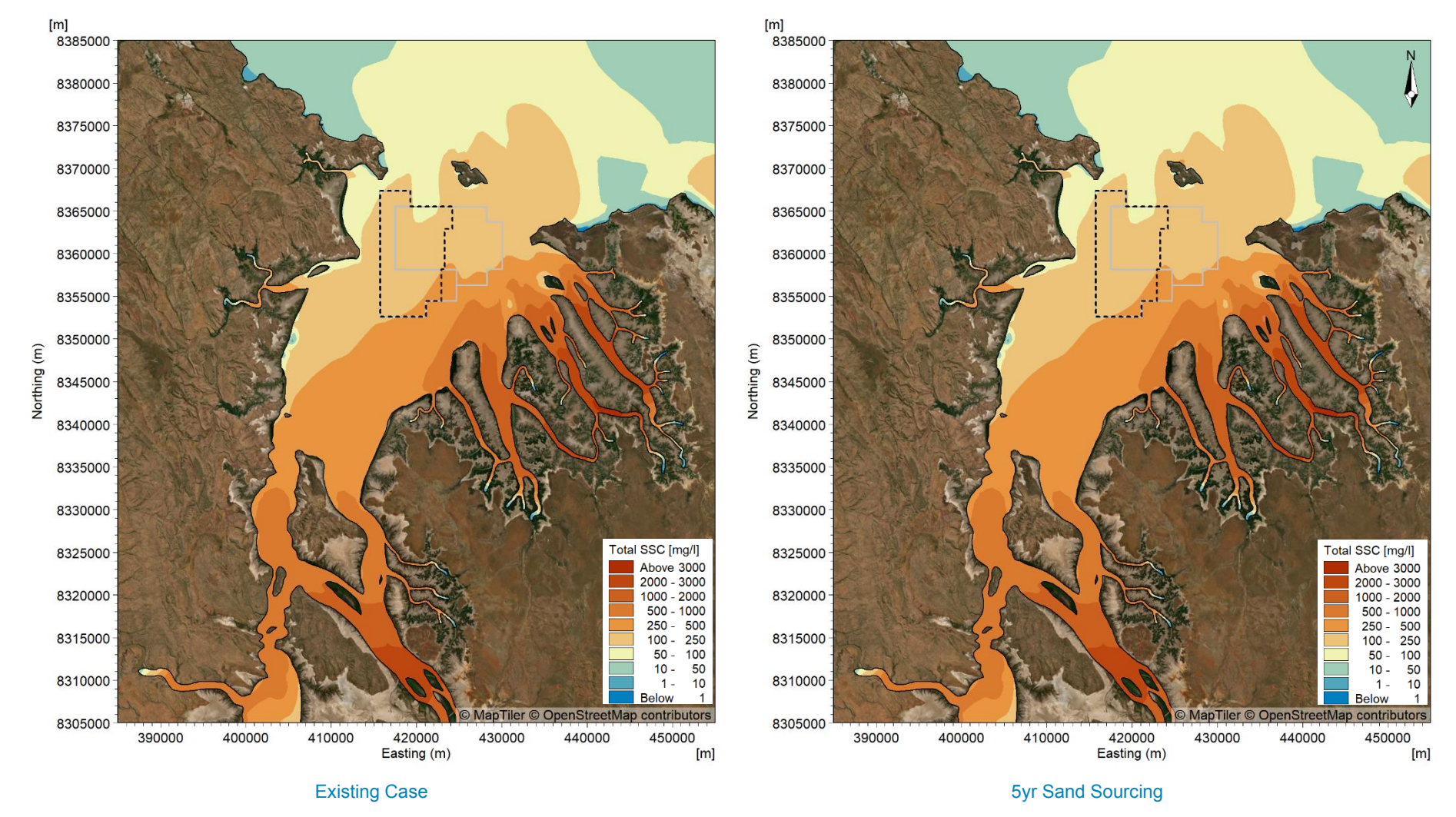


Figure C13. Modelled existing case and 5 years of sand sourcing scenario 50<sup>th</sup> percentile SSC over the 2 month transitional season period.



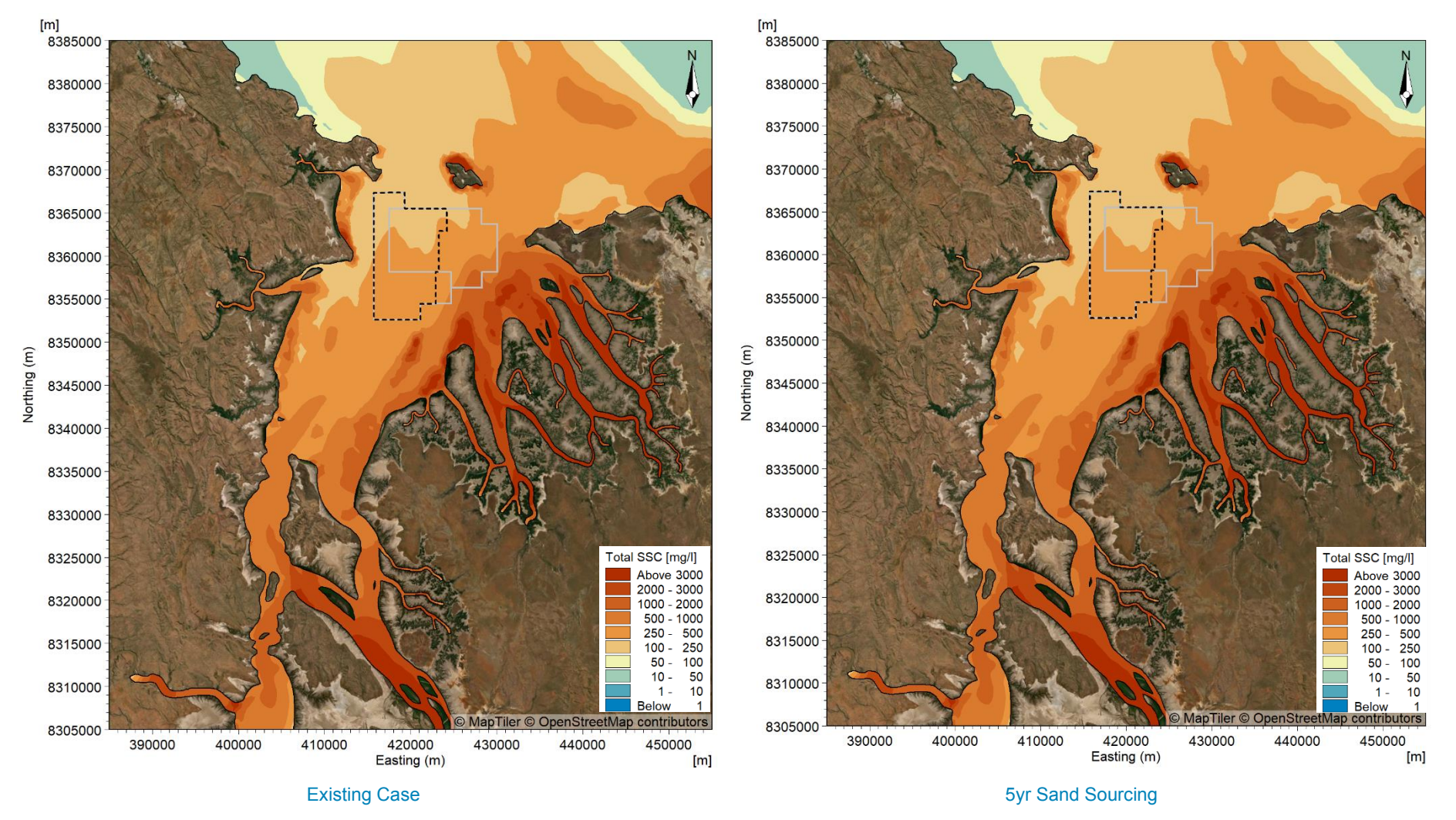


Figure C14. Modelled existing case and 5 years of sand sourcing scenario 95<sup>th</sup> percentile SSC over the 2 month transitional season period.



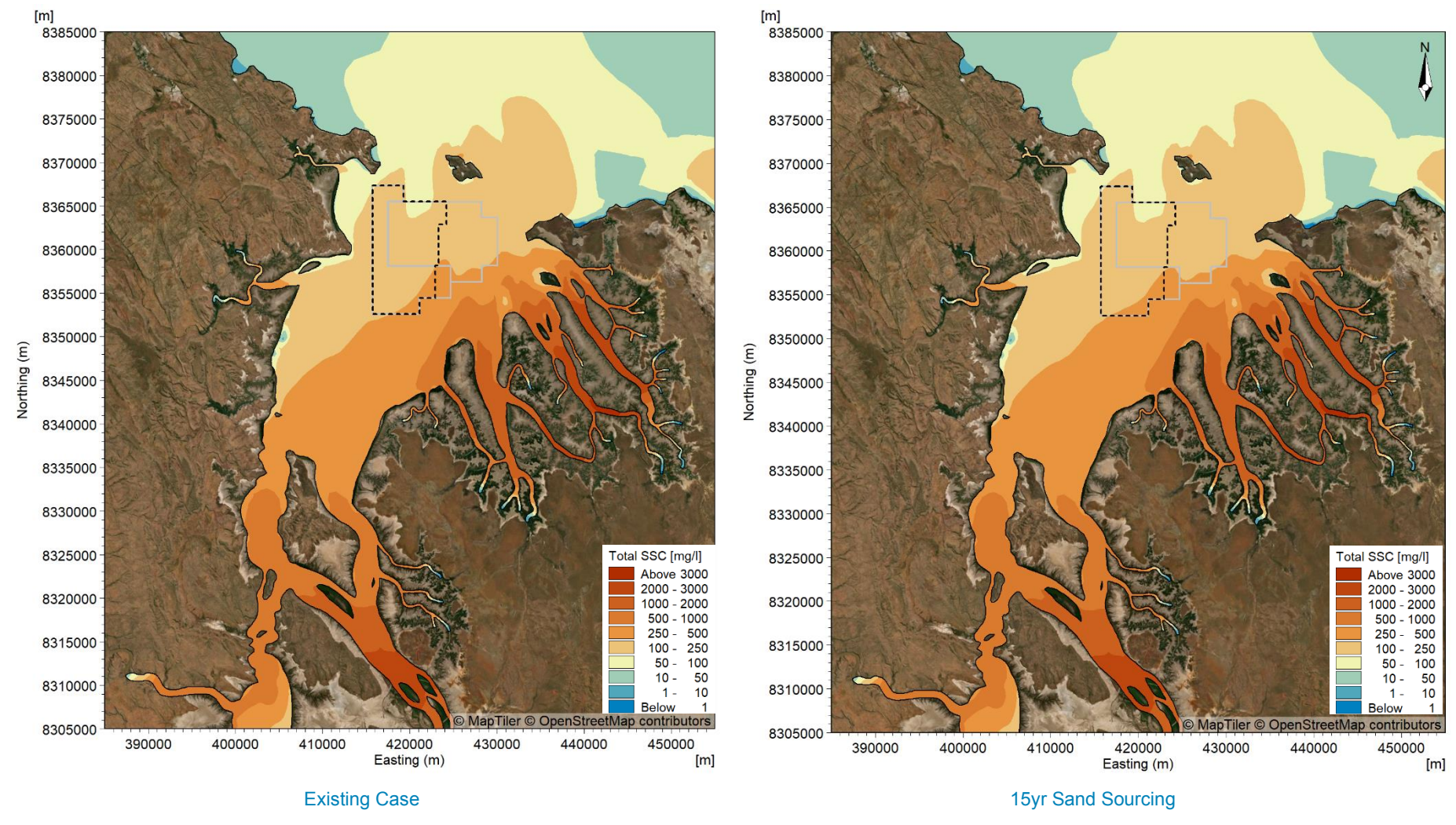


Figure C15. Modelled existing case and 15 years of sand sourcing scenario 50th percentile SSC over the 2 month transitional season period.



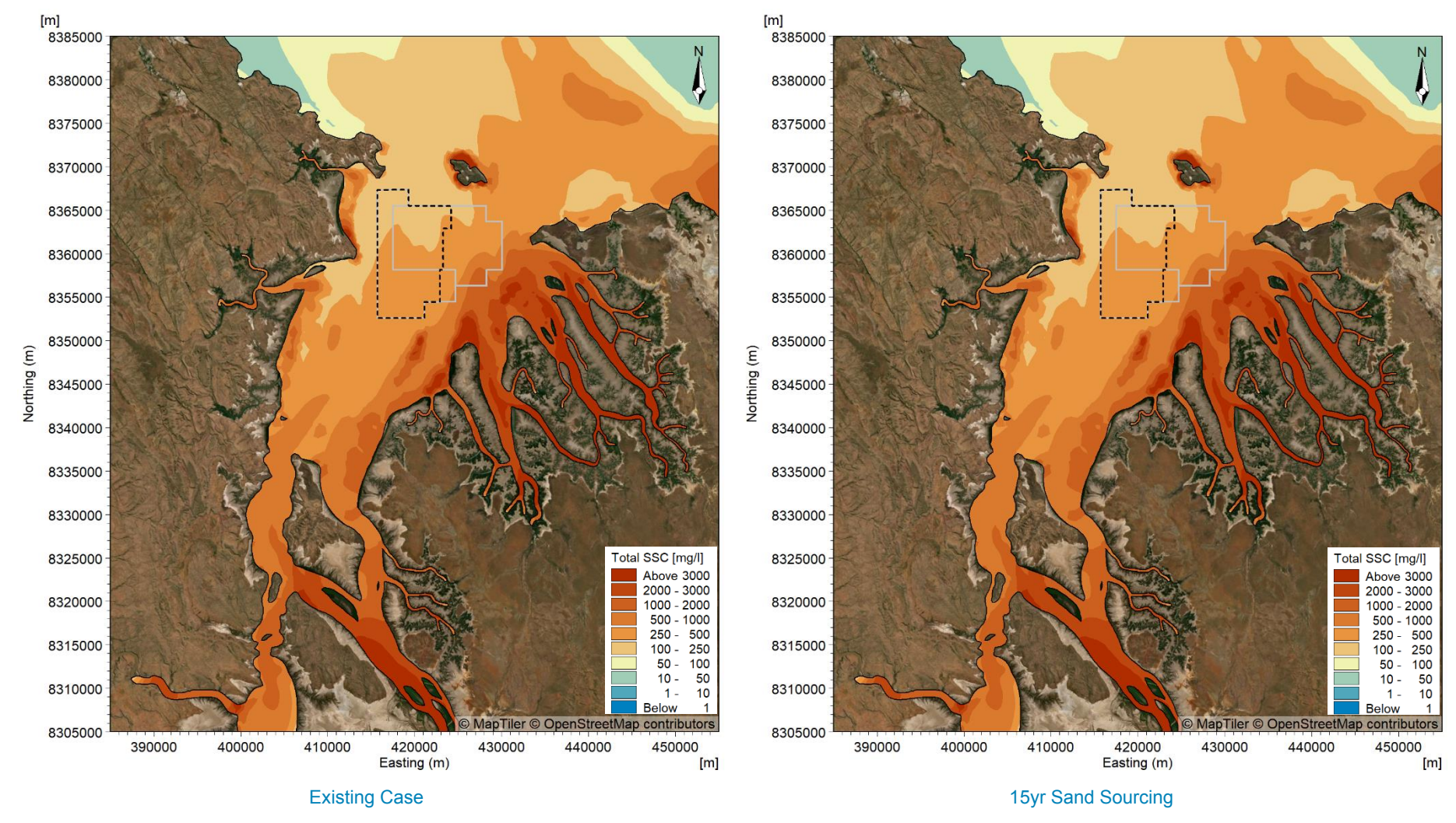


Figure C16. Modelled existing case and 15 years of sand sourcing scenario 95<sup>th</sup> percentile SSC over the 2 month transitional season period.



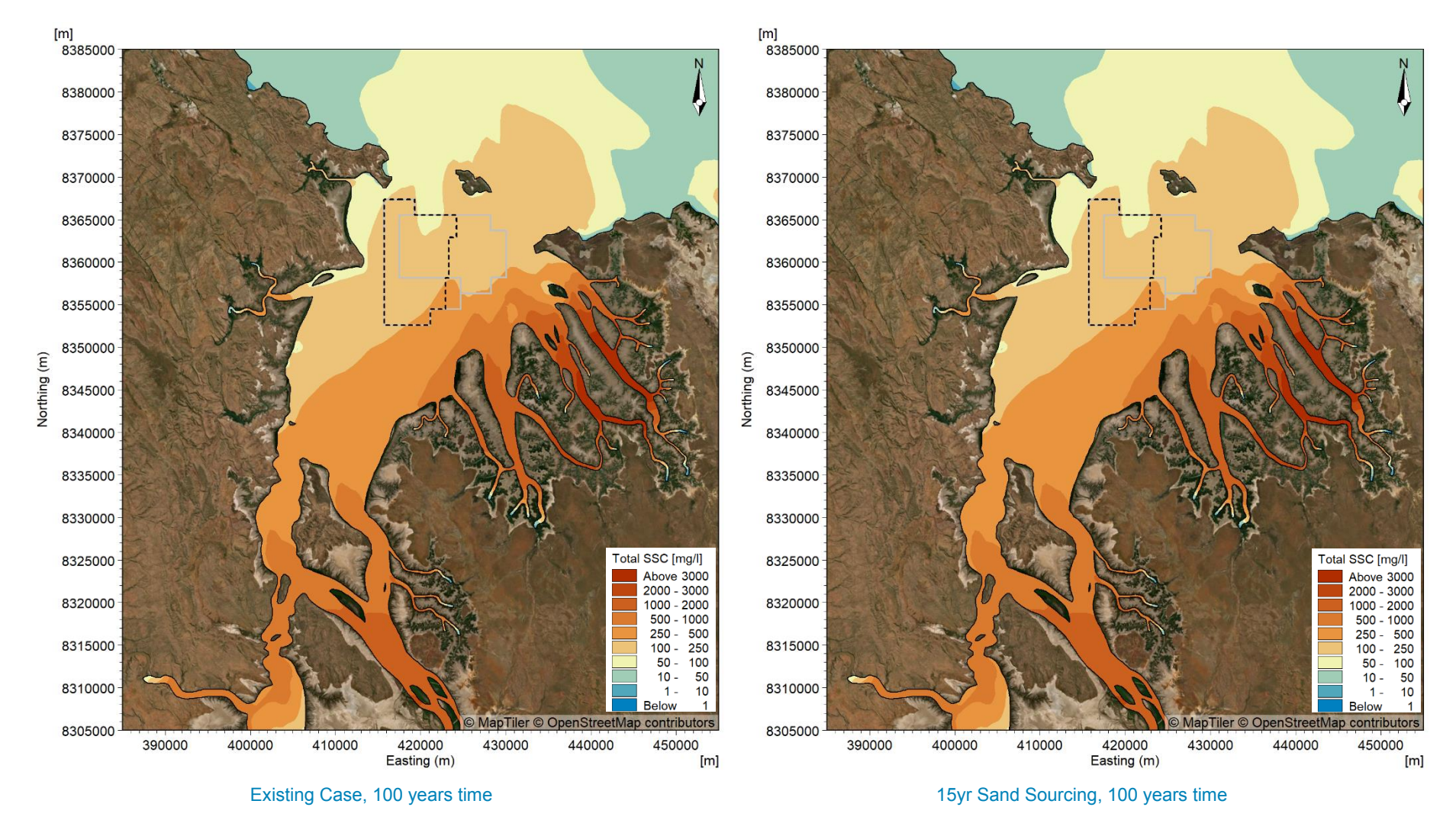


Figure C17. Modelled existing case in 100 years time and 15 years of sand sourcing scenario 50<sup>th</sup> percentile SSC over the 2 month transitional season period.



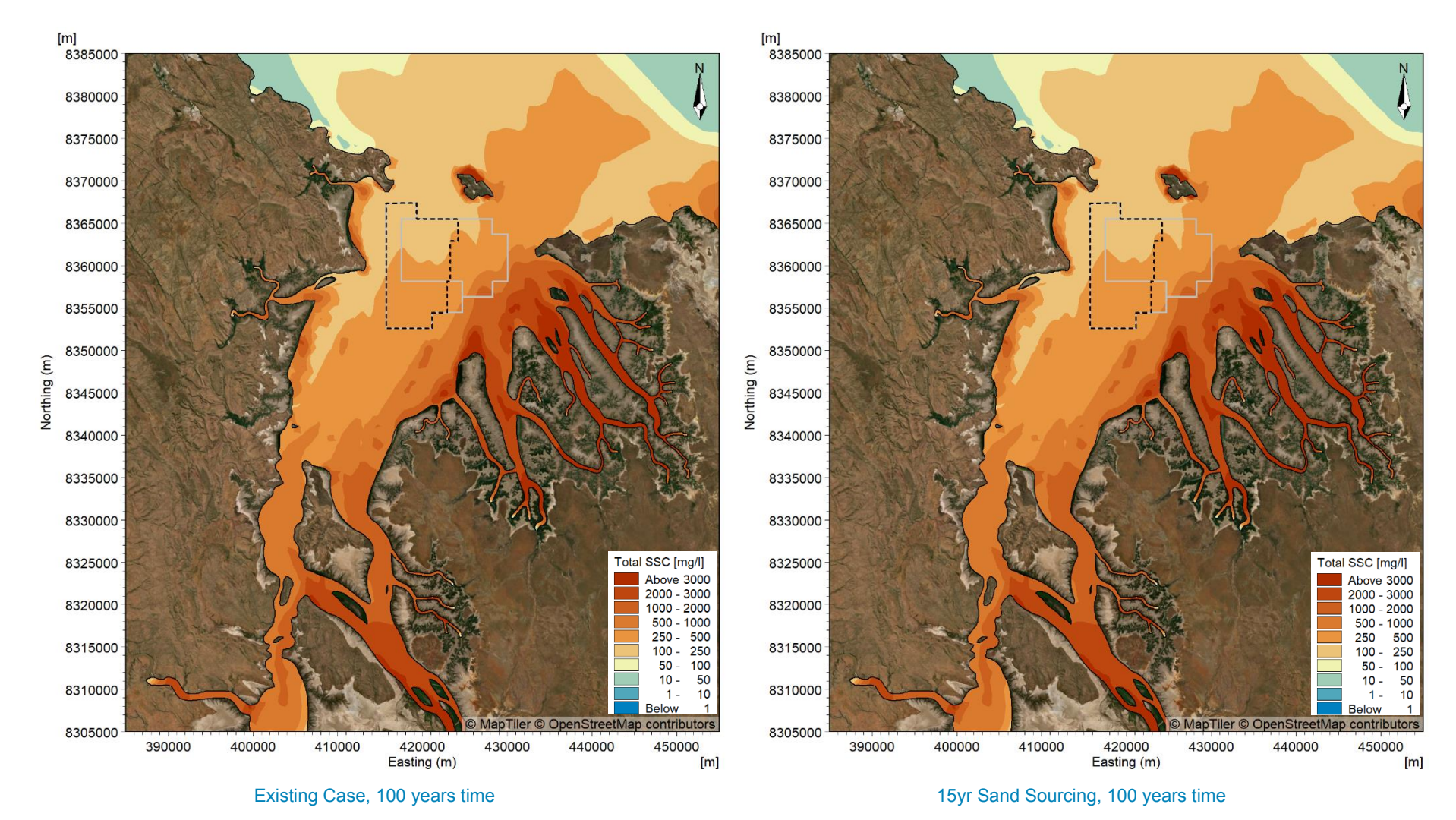


Figure C18. Modelled existing case in 100 years time and 15 years of sand sourcing scenario 95th percentile SSC over the 2 month transitional season period.



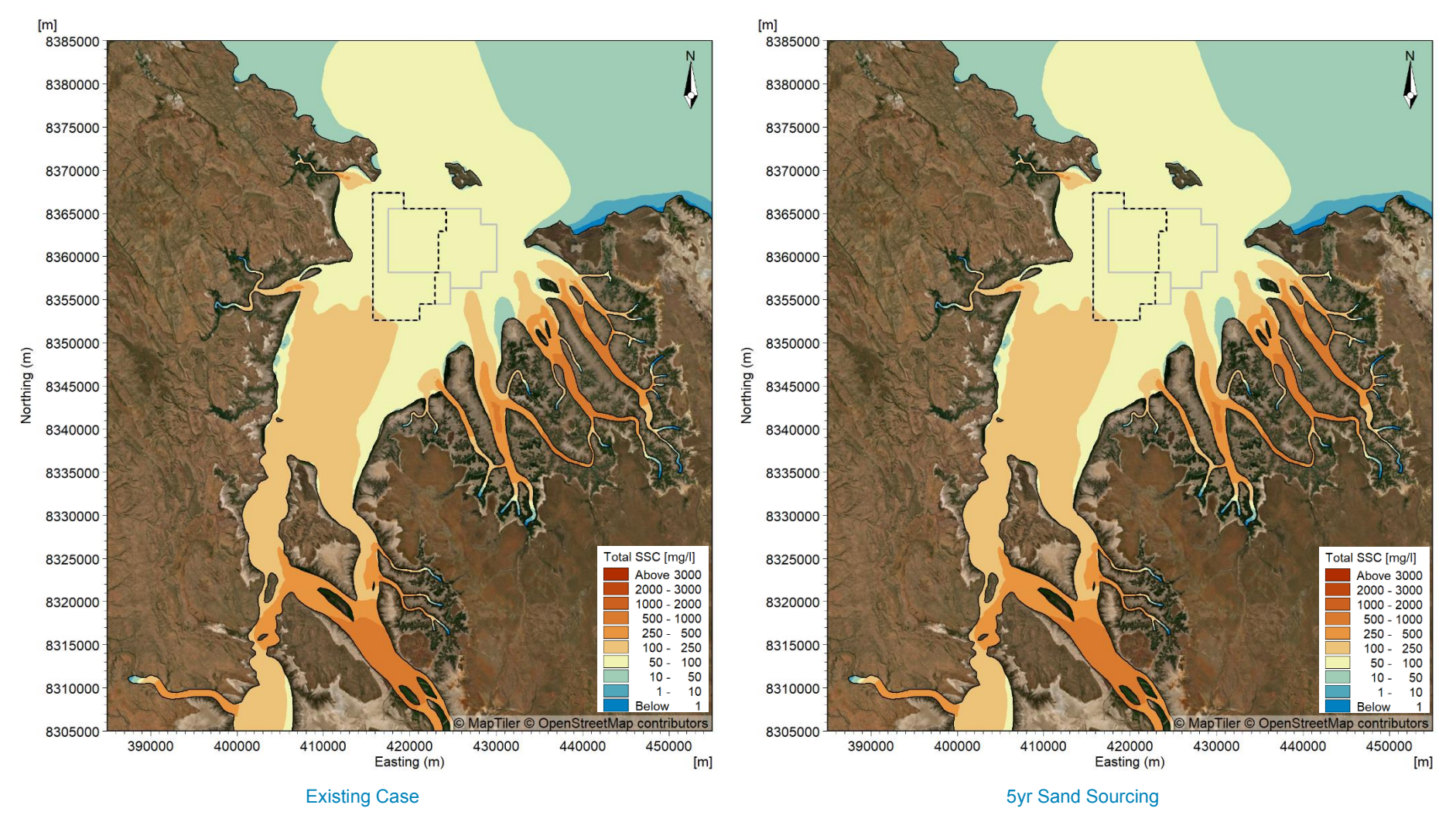


Figure C19. Modelled existing case and 5 years of sand sourcing scenario 50<sup>th</sup> percentile SSC during TC Marcus.



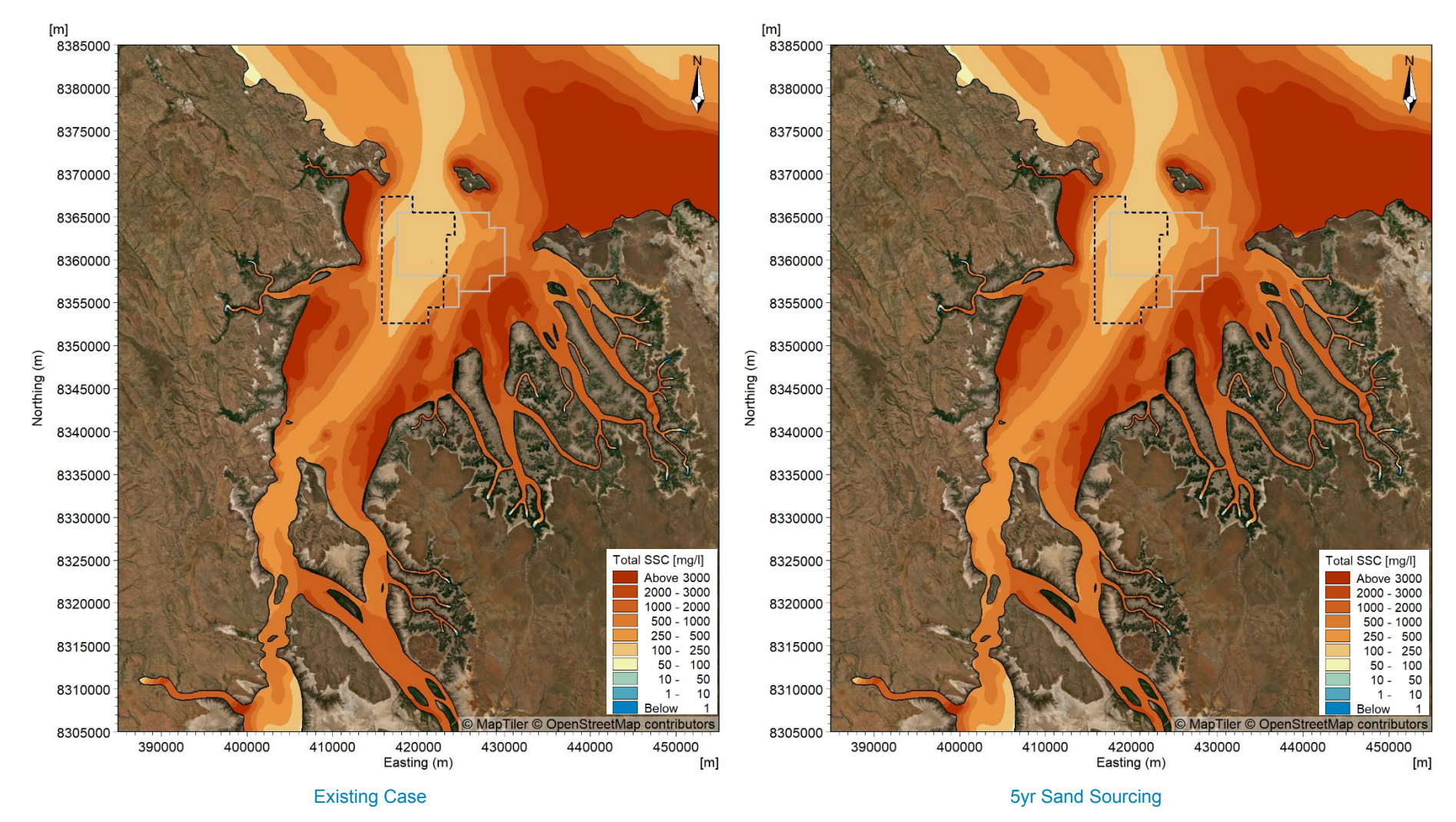


Figure C20. Modelled existing case and 5 years of sand sourcing scenario 95<sup>th</sup> percentile SSC during TC Marcus.



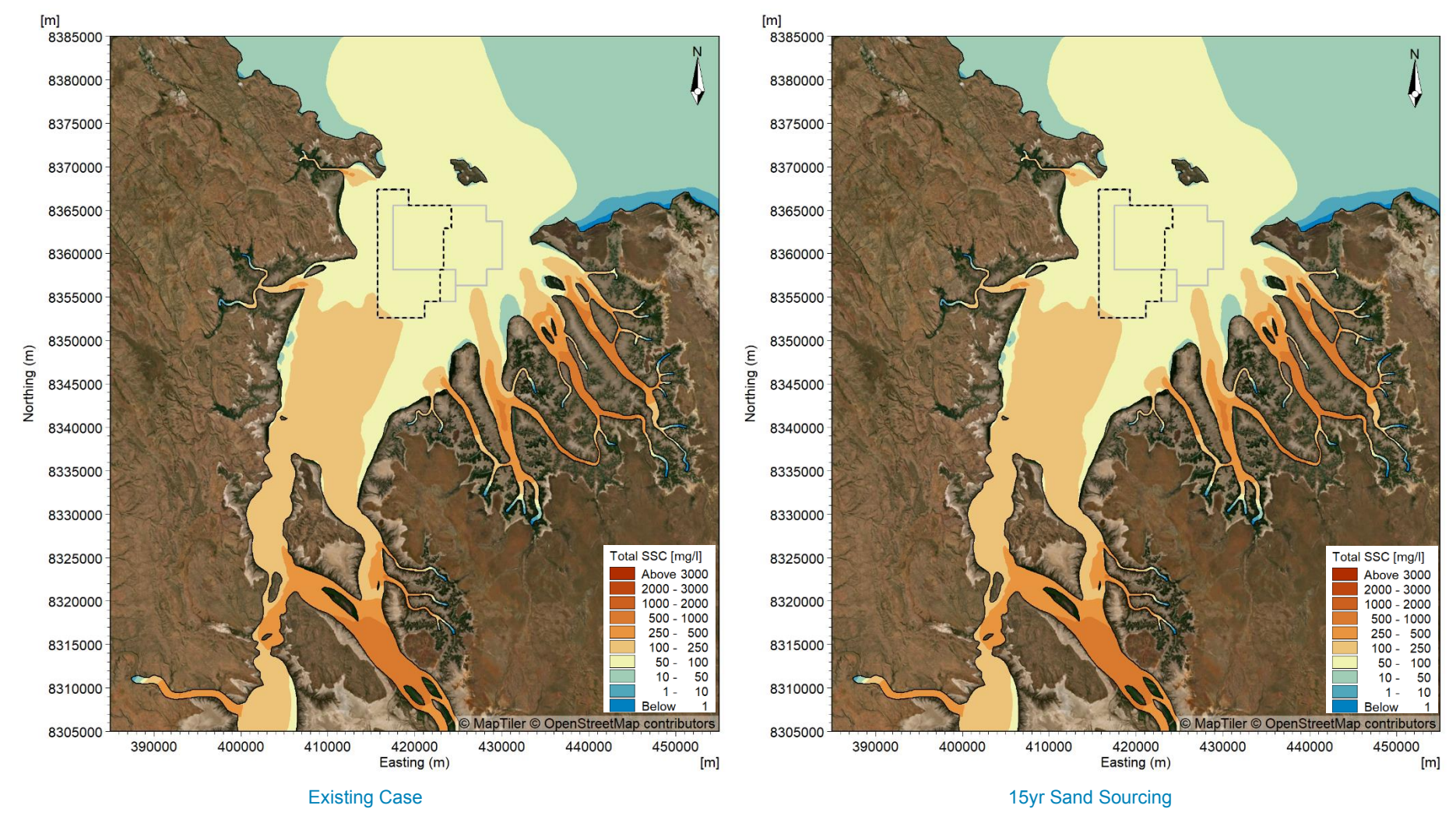


Figure C21. Modelled existing case and 15 years of sand sourcing scenario 50<sup>th</sup> percentile SSC during TC Marcus.



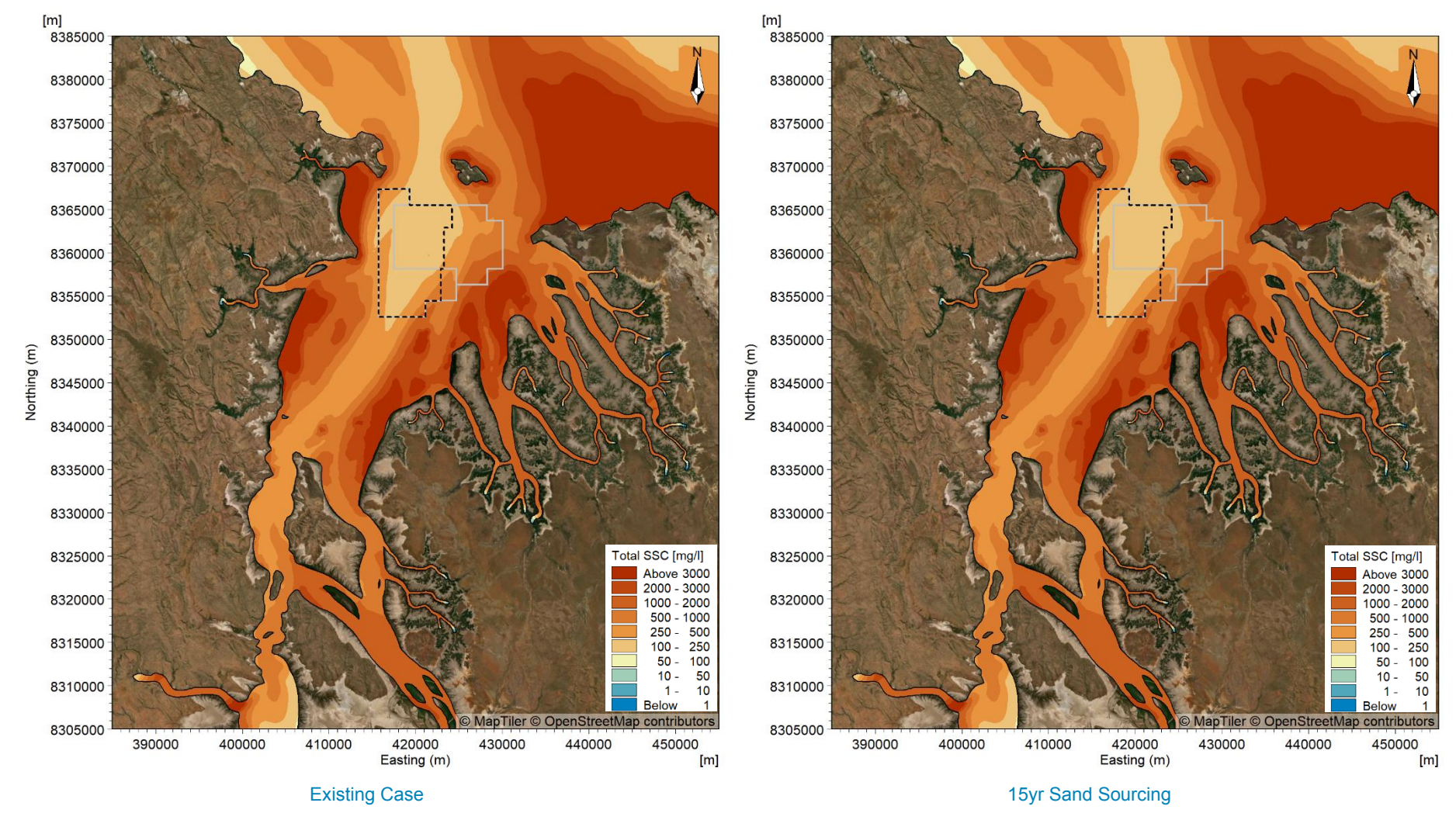


Figure C22. Modelled existing case and 15 years of sand sourcing scenario 95<sup>th</sup> percentile SSC during TC Marcus.



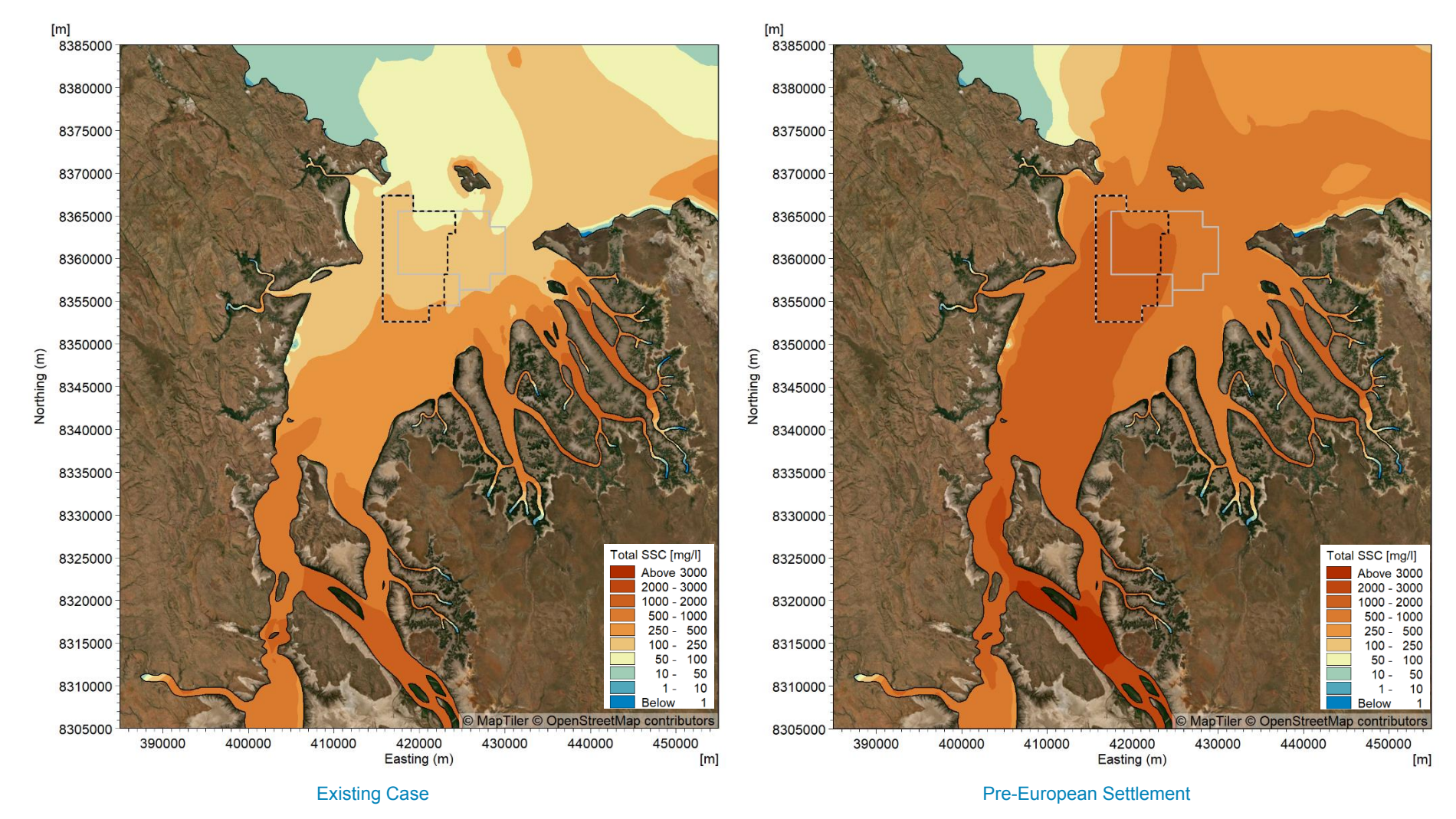


Figure C23. Modelled existing case and the pre-European settlement scenario 50th percentile SSC over the 2 month wet season period.



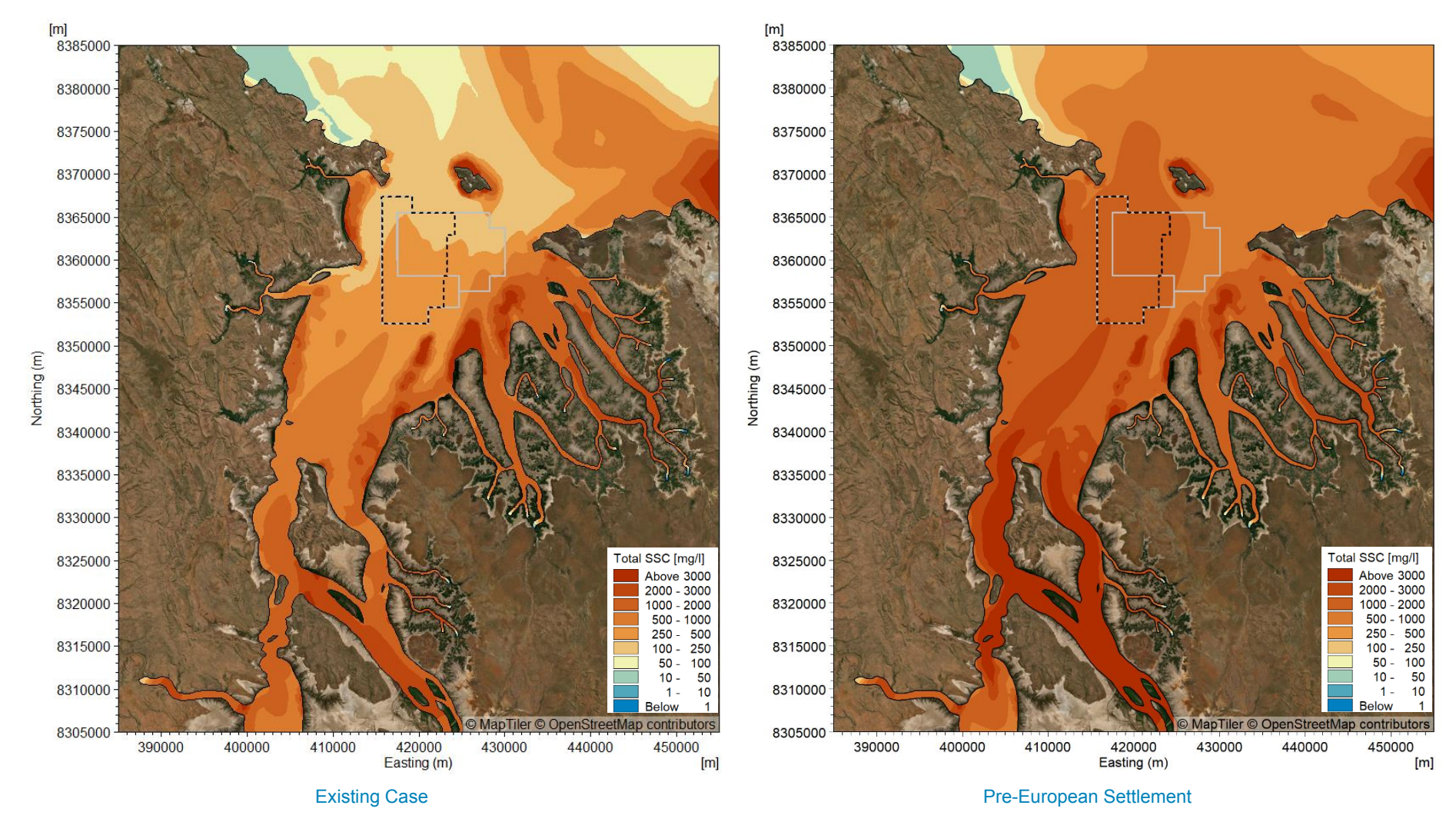


Figure C24. Modelled existing case and the pre-European settlement scenario 95th percentile SSC over the 2 month wet season period.



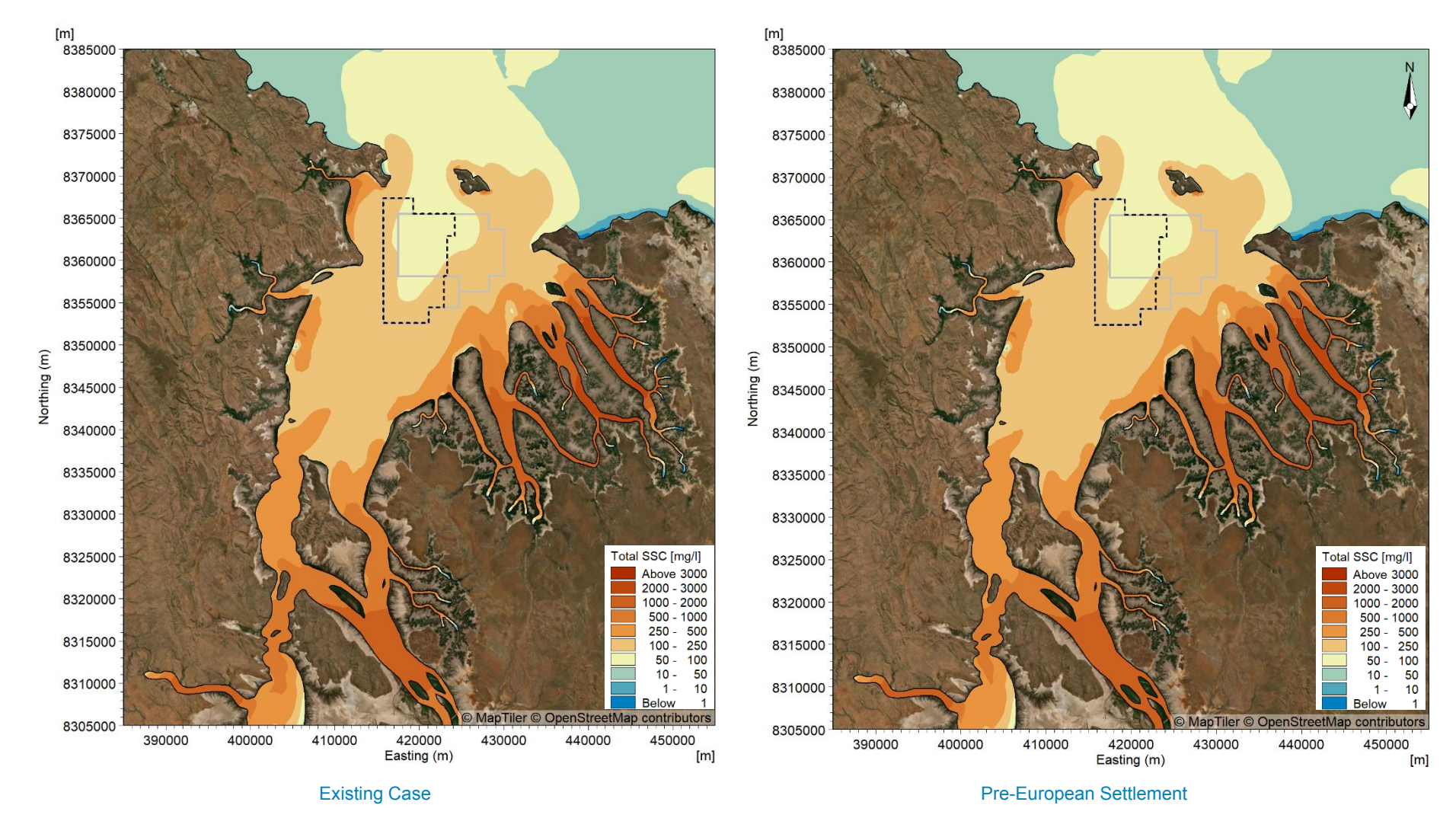


Figure C25. Modelled existing case and the pre-European settlement scenario 50th percentile SSC over the 2 month dry season period.



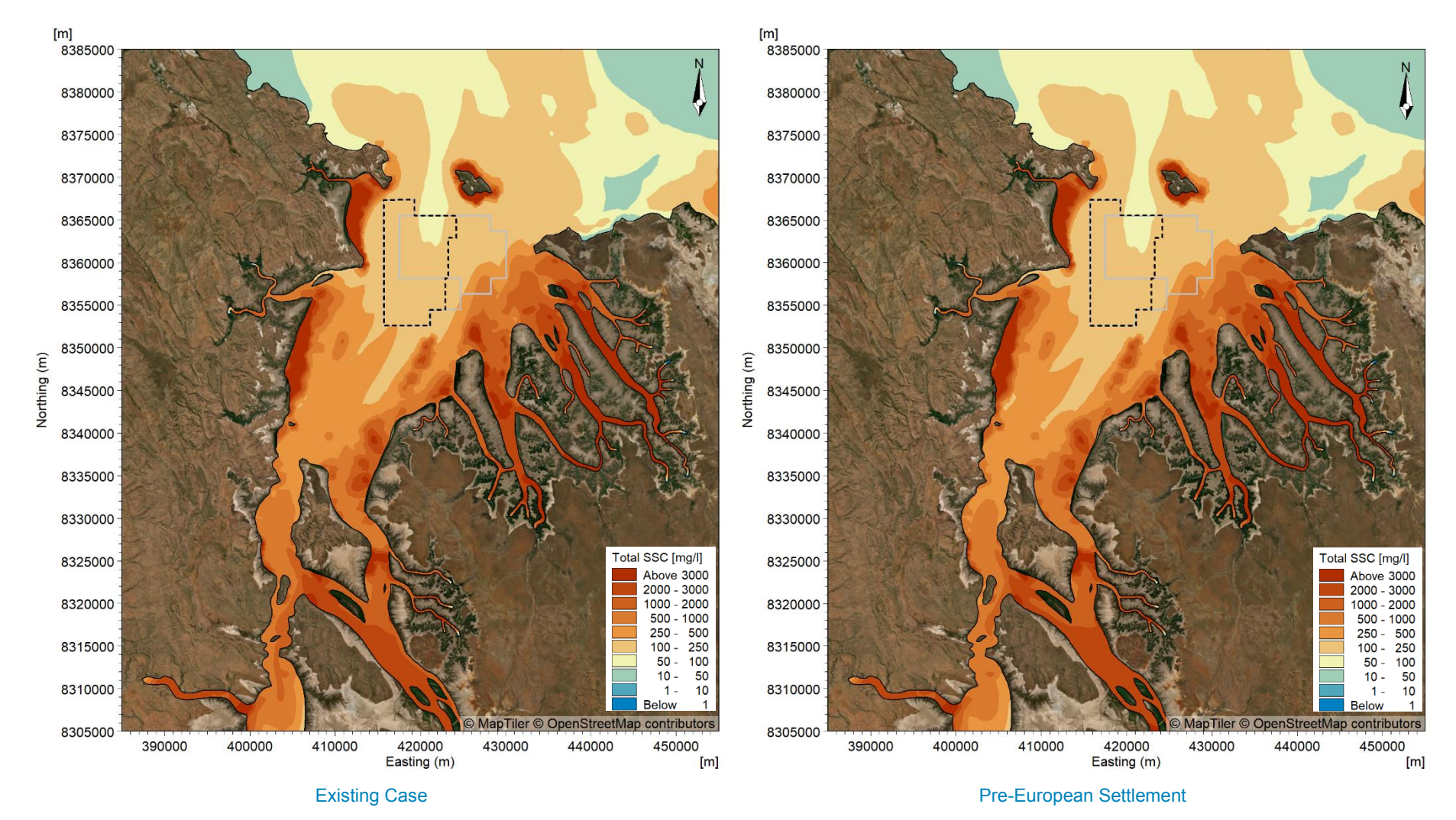


Figure C26. Modelled existing case and the pre-European settlement scenario 95<sup>th</sup> percentile SSC over the 2 month dry season period.



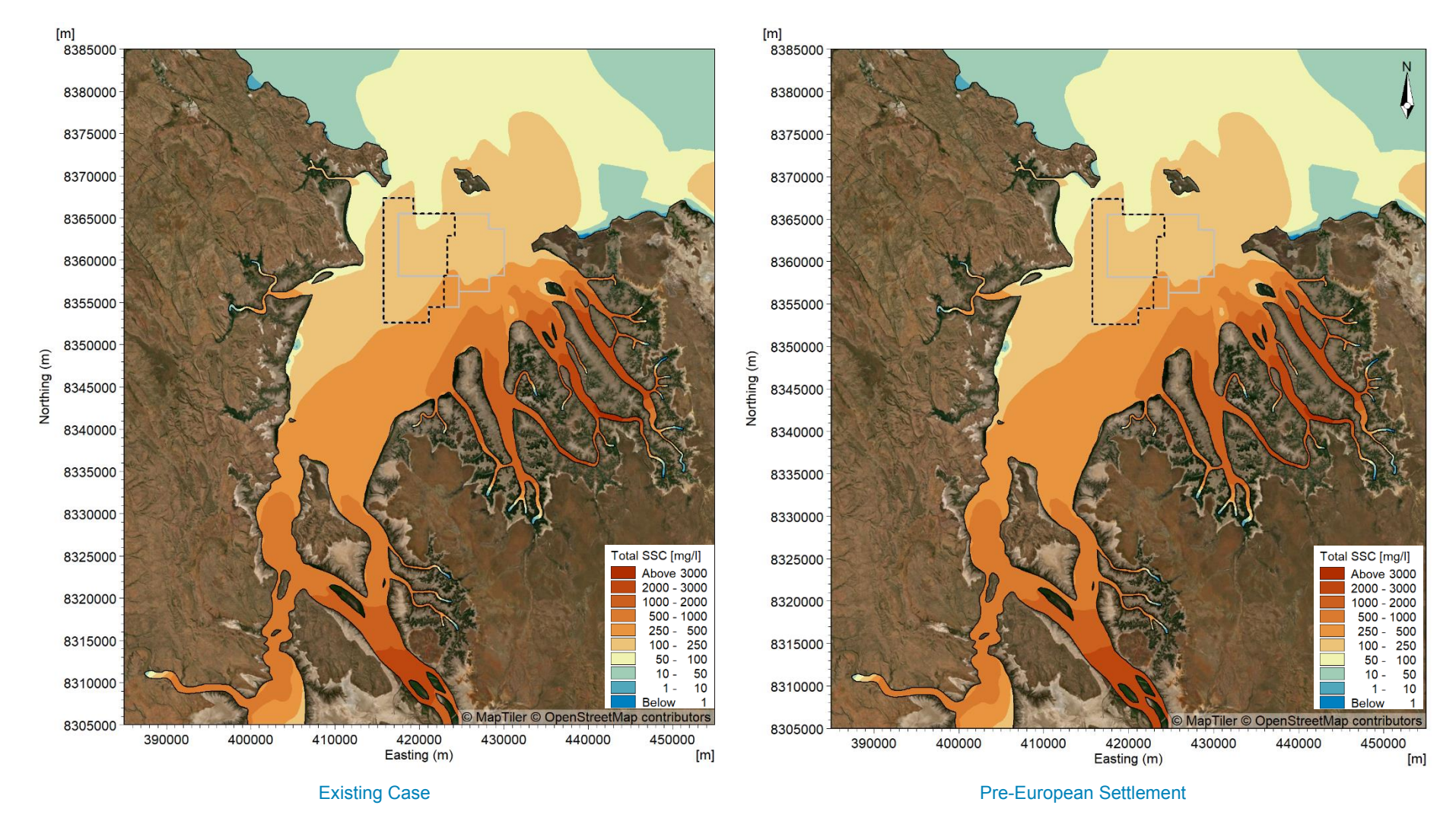


Figure C27. Modelled existing case and the pre-European settlement scenario 50<sup>th</sup> percentile SSC over the 2 month transitional season period.



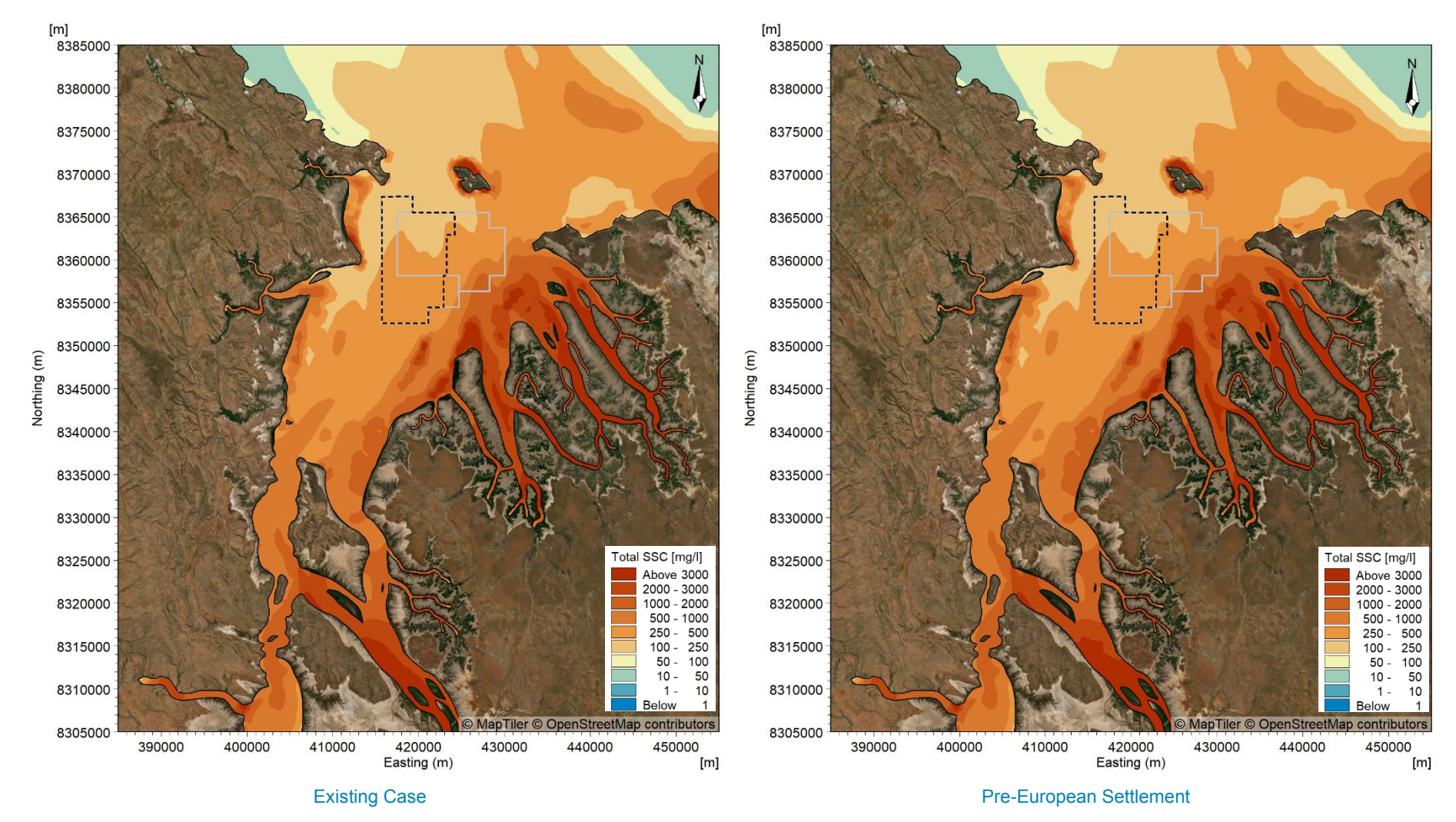


Figure C28. Modelled existing case and the pre-European settlement scenario 95<sup>th</sup> percentile SSC over the 2 month transitional season period.



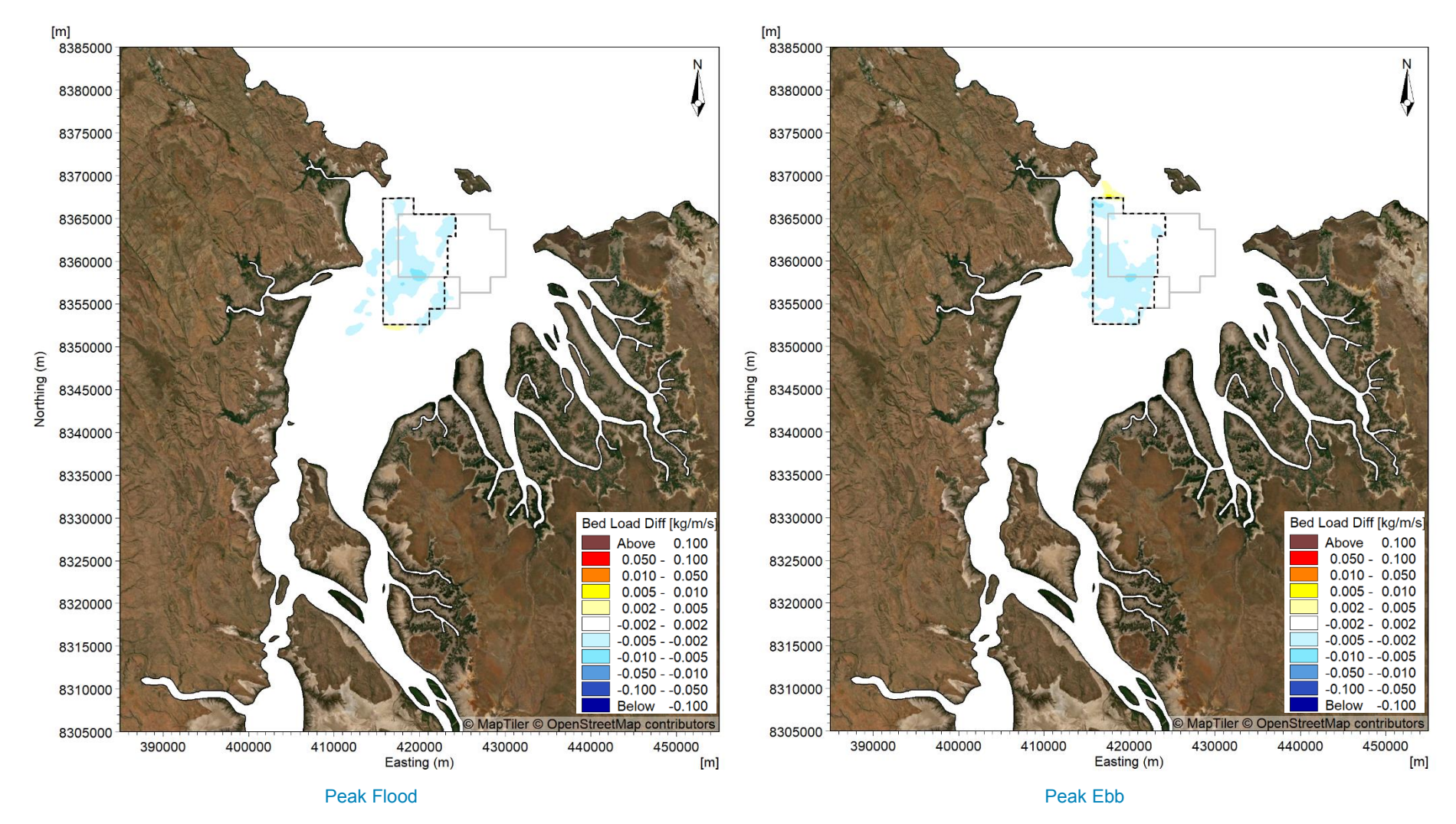


Figure C29. Modelled change in bedload transport rate during a spring tide at peak flood and peak ebb in the wet season due to the 5 year sand sourcing scenario.



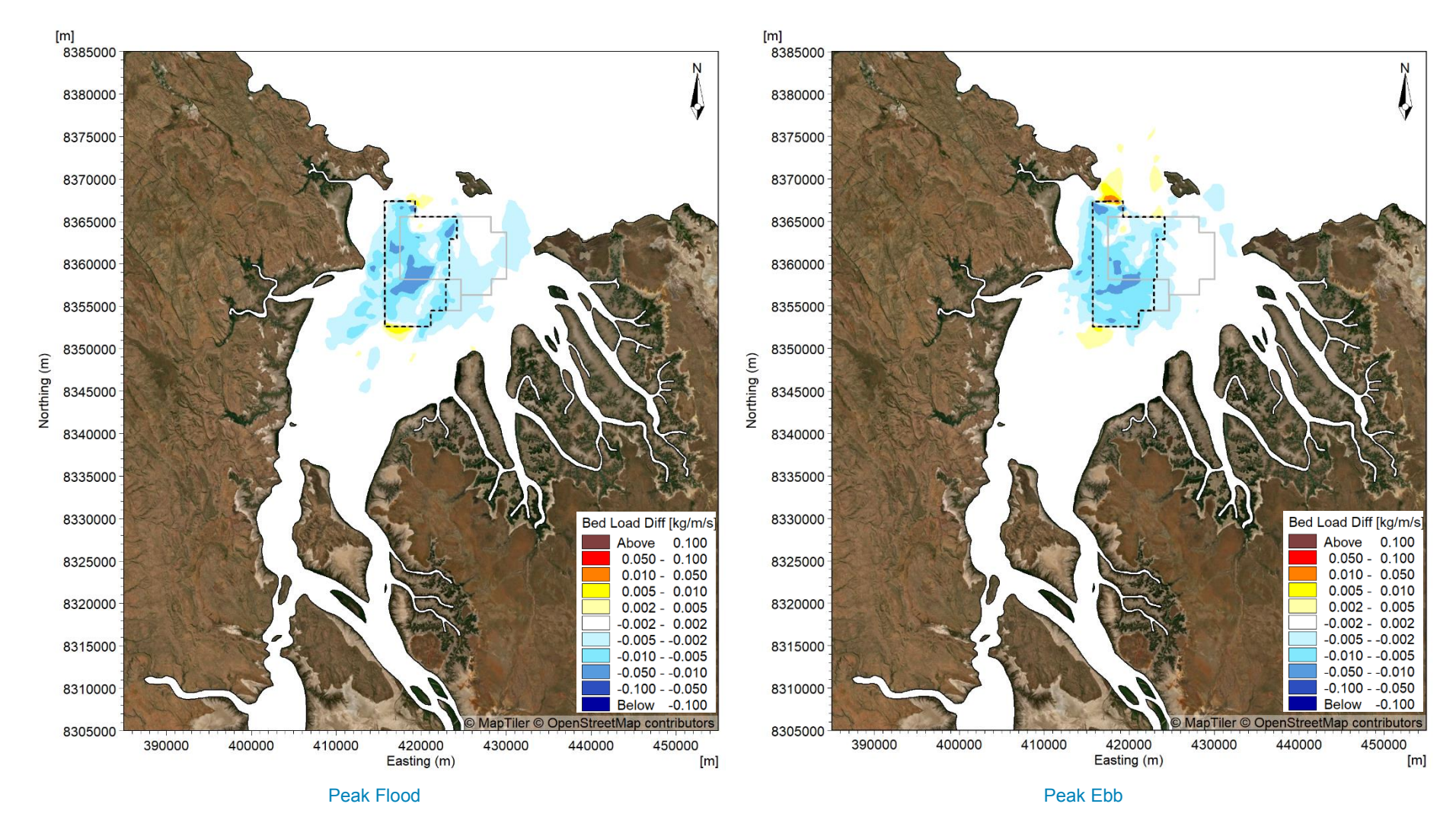


Figure C30. Modelled change in bedload transport rate during a spring tide at peak flood and peak ebb in the wet season due to the 15 year sand sourcing scenario.



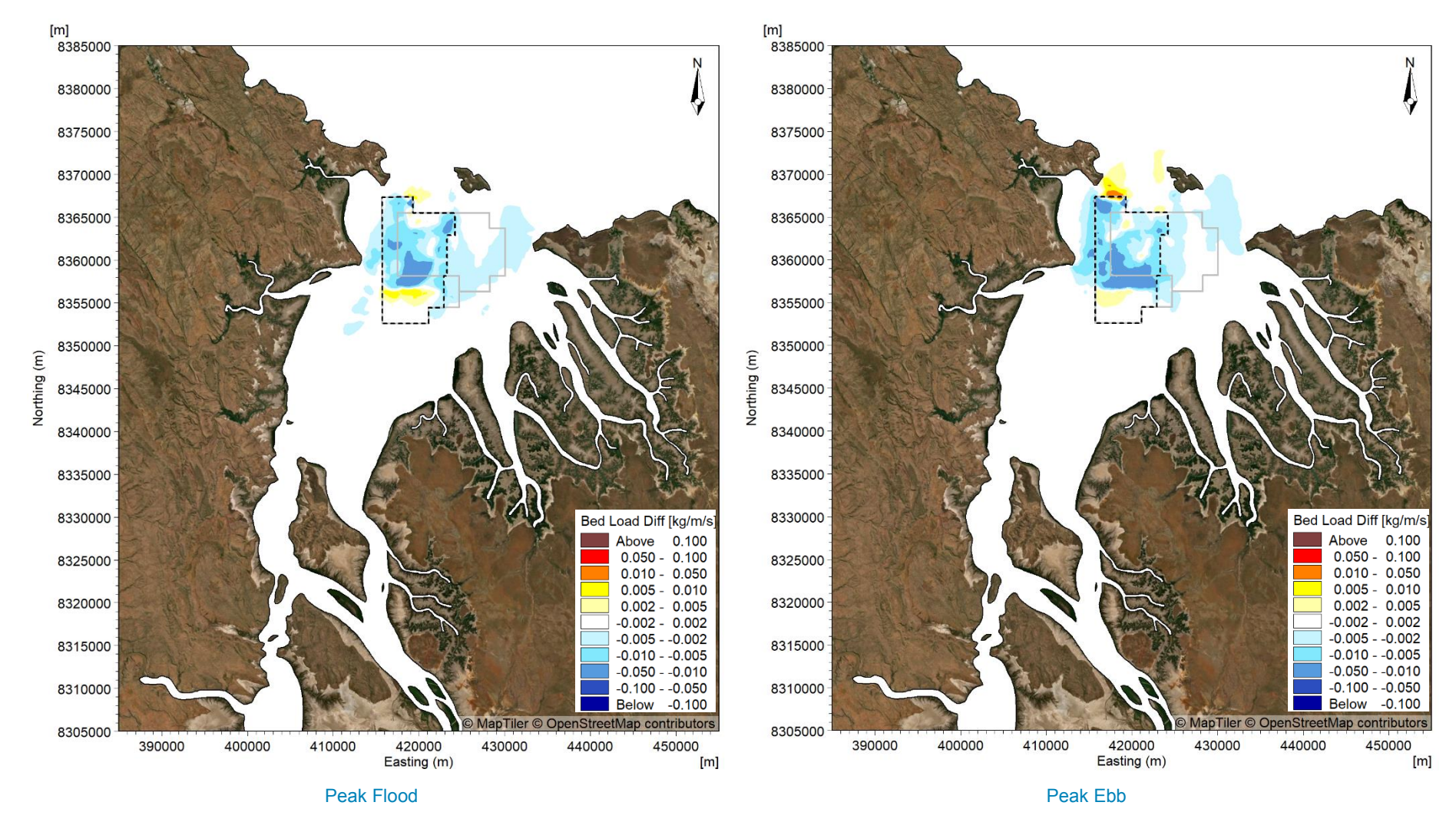


Figure C31. Modelled change in bedload transport rate during a spring tide at peak flood and peak ebb in the wet season due to the 15 year sand sourcing in 100 years time scenario.



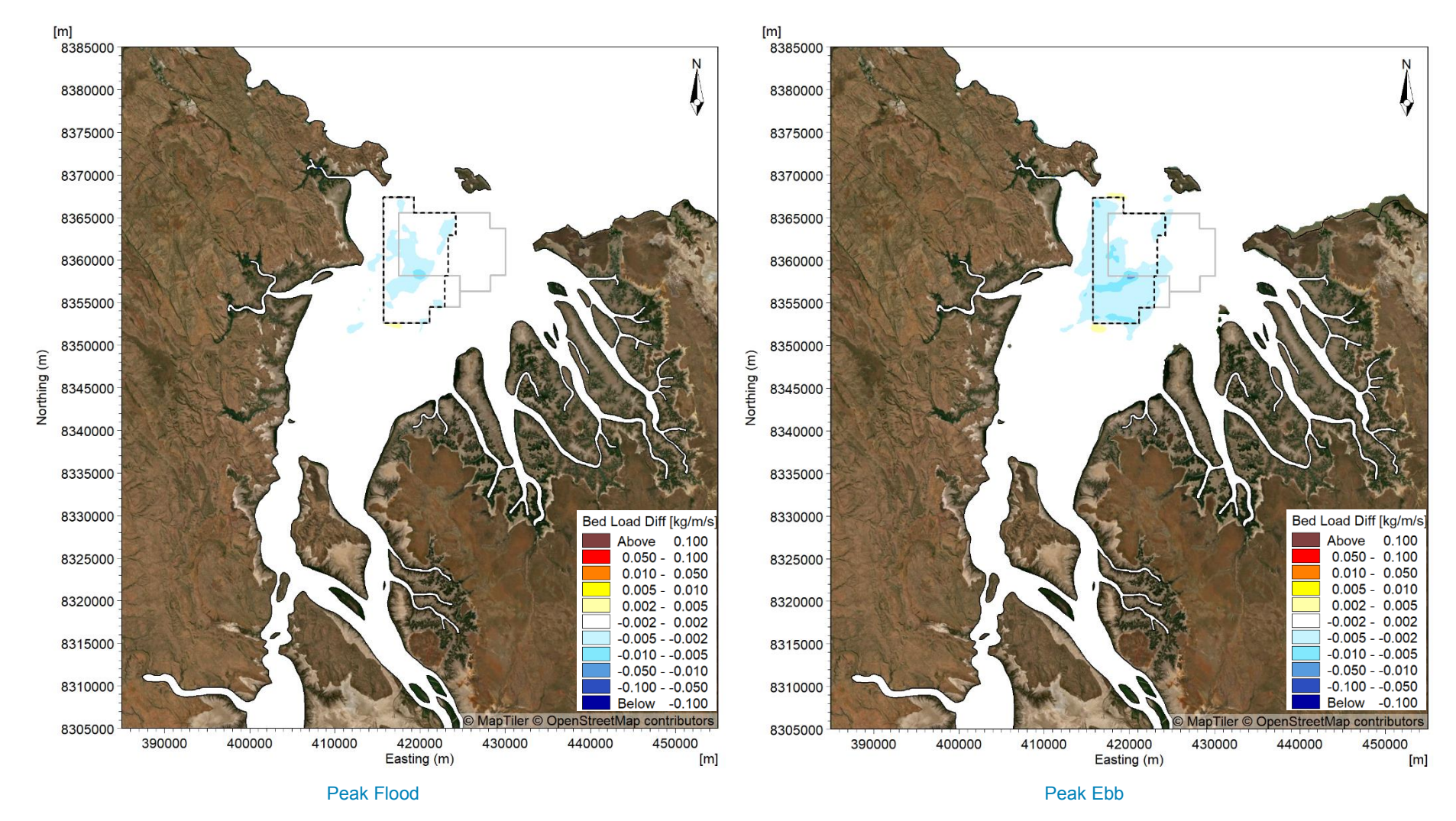


Figure C32. Modelled change in bedload transport rate during a spring tide at peak flood and peak ebb in the dry season due to the 5 year sand sourcing scenario.



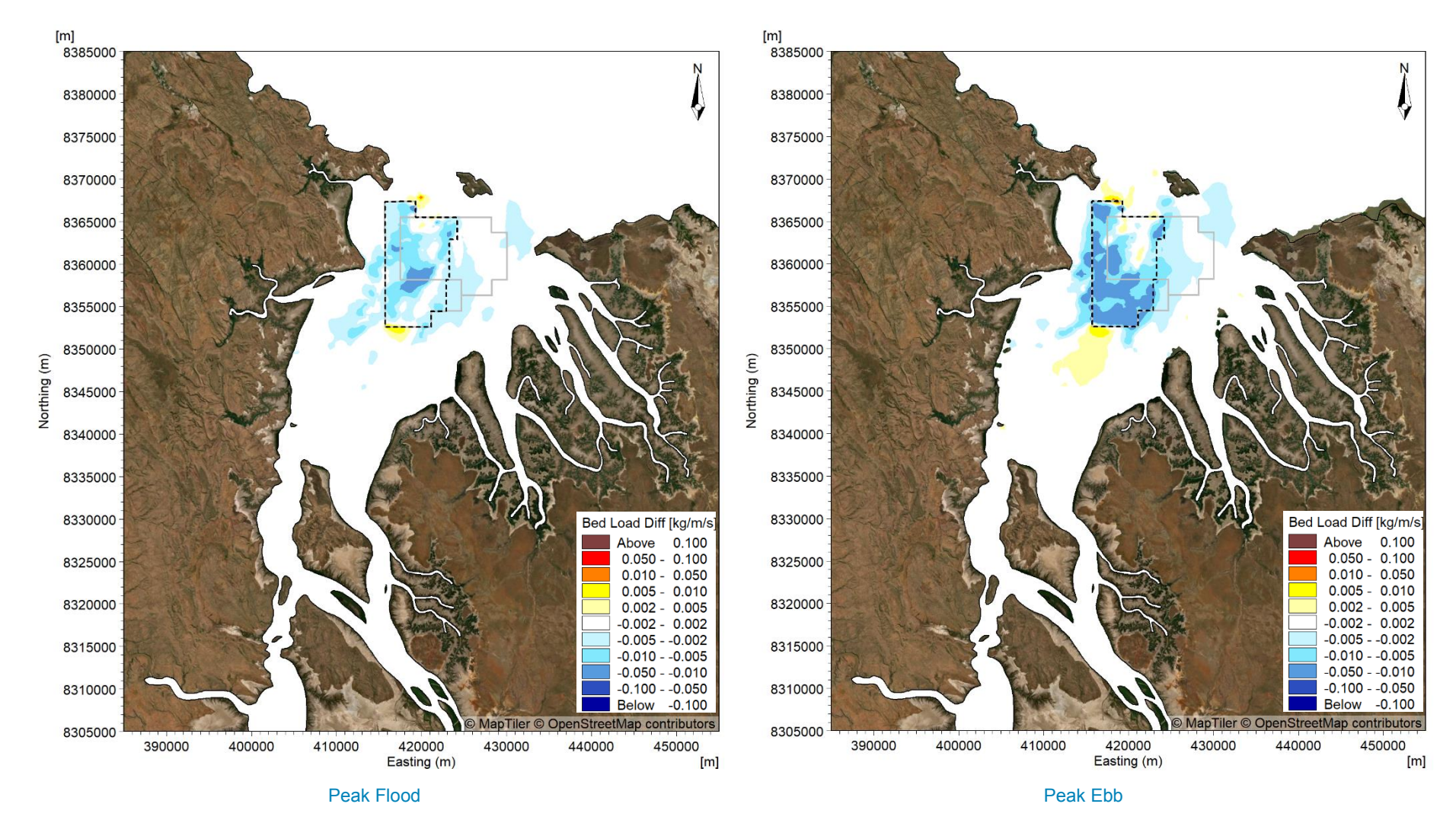


Figure C33. Modelled change in bedload transport rate during a spring tide at peak flood and peak ebb in the dry season due to the 15 year sand sourcing scenario.



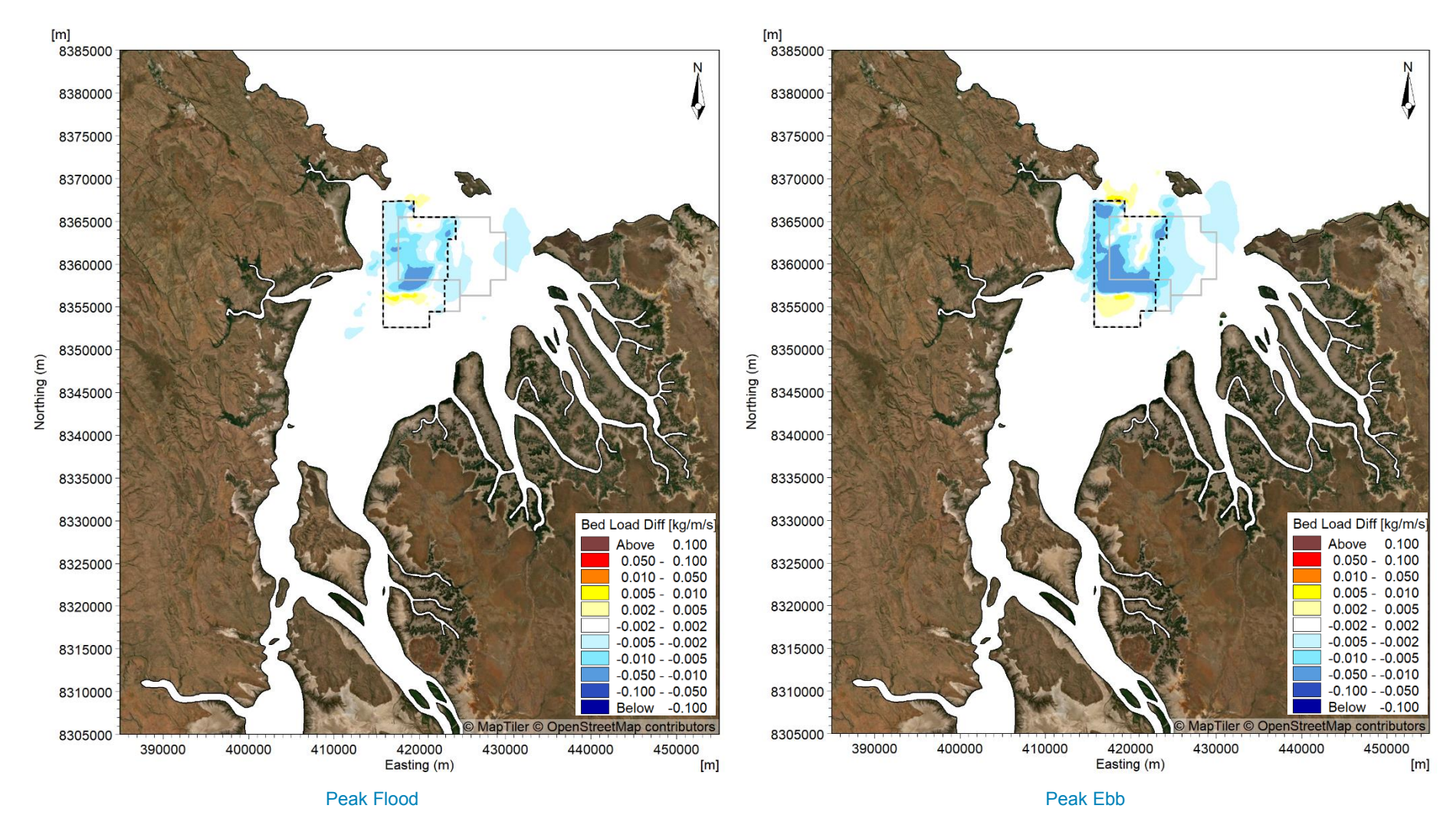


Figure C34. Modelled change in bedload transport rate during a spring tide at peak flood and peak ebb in the dry season due to the 15 year sand sourcing in 100 years time scenario.



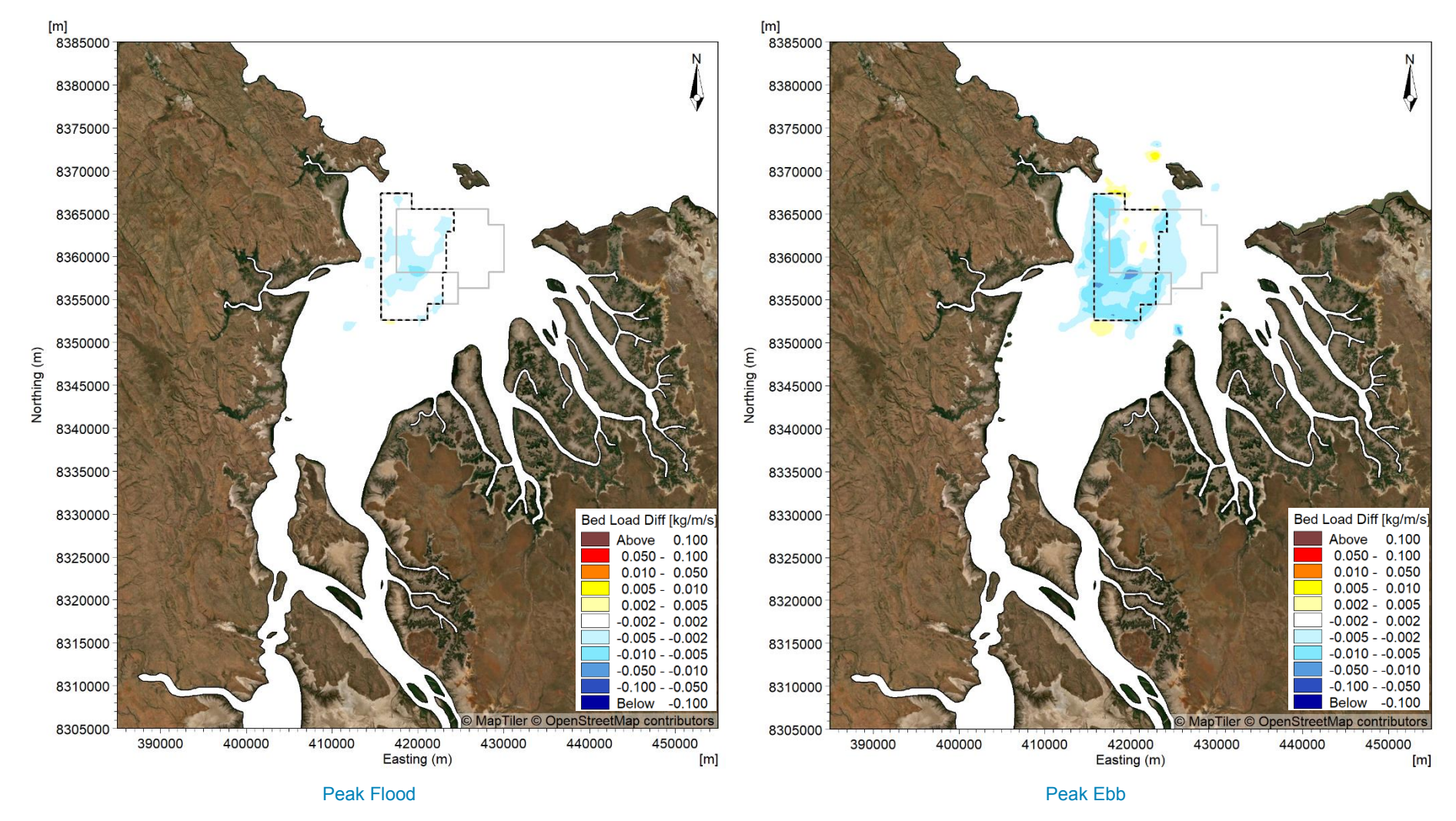


Figure C35. Modelled change in bedload transport rate during a spring tide at peak flood and peak ebb in the transitional season due to the 5 year sand sourcing scenario.



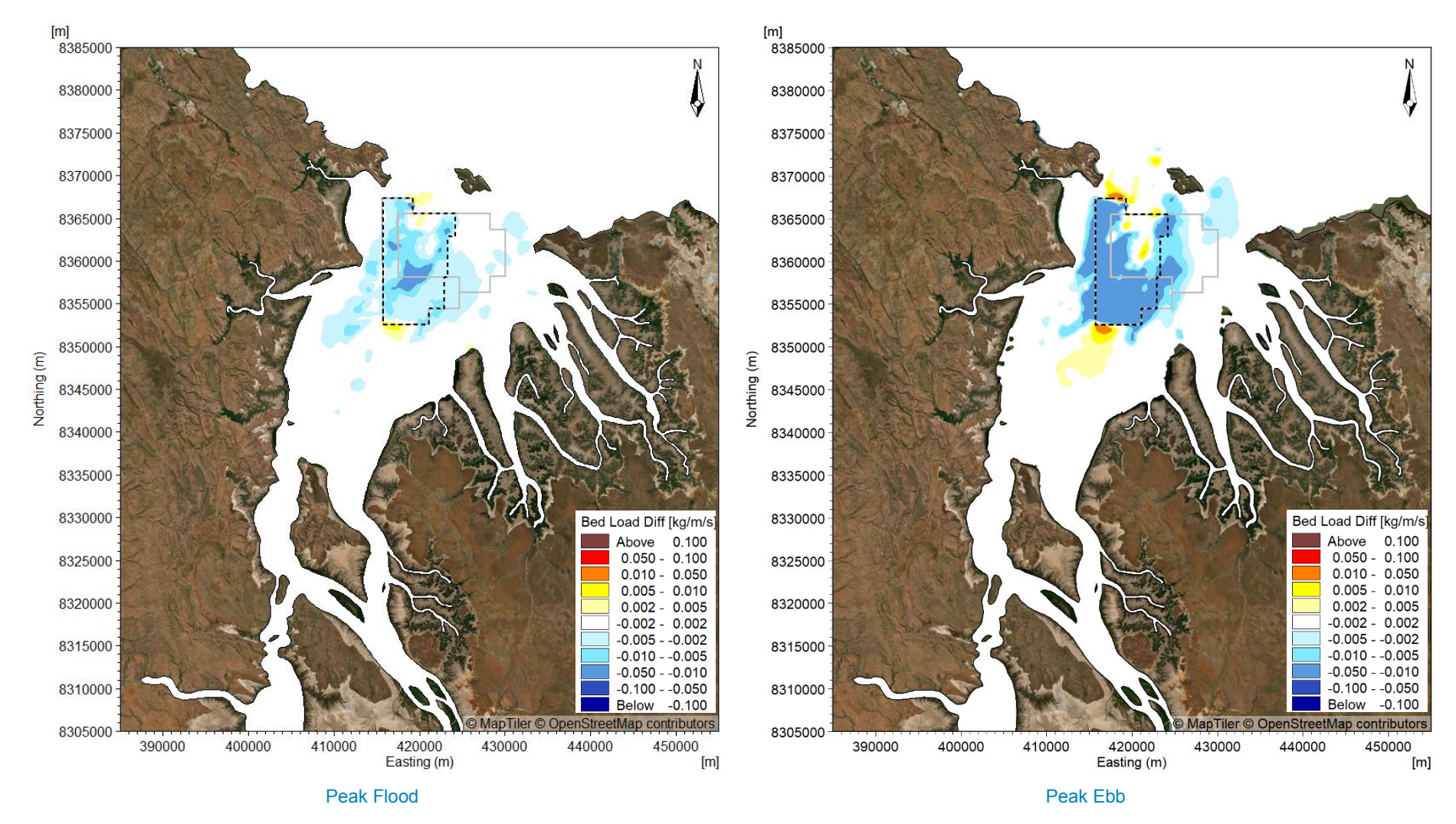


Figure C36. Modelled change in bedload transport rate during a spring tide at peak flood and peak ebb in the transitional season due to the 15 year sand sourcing scenario.



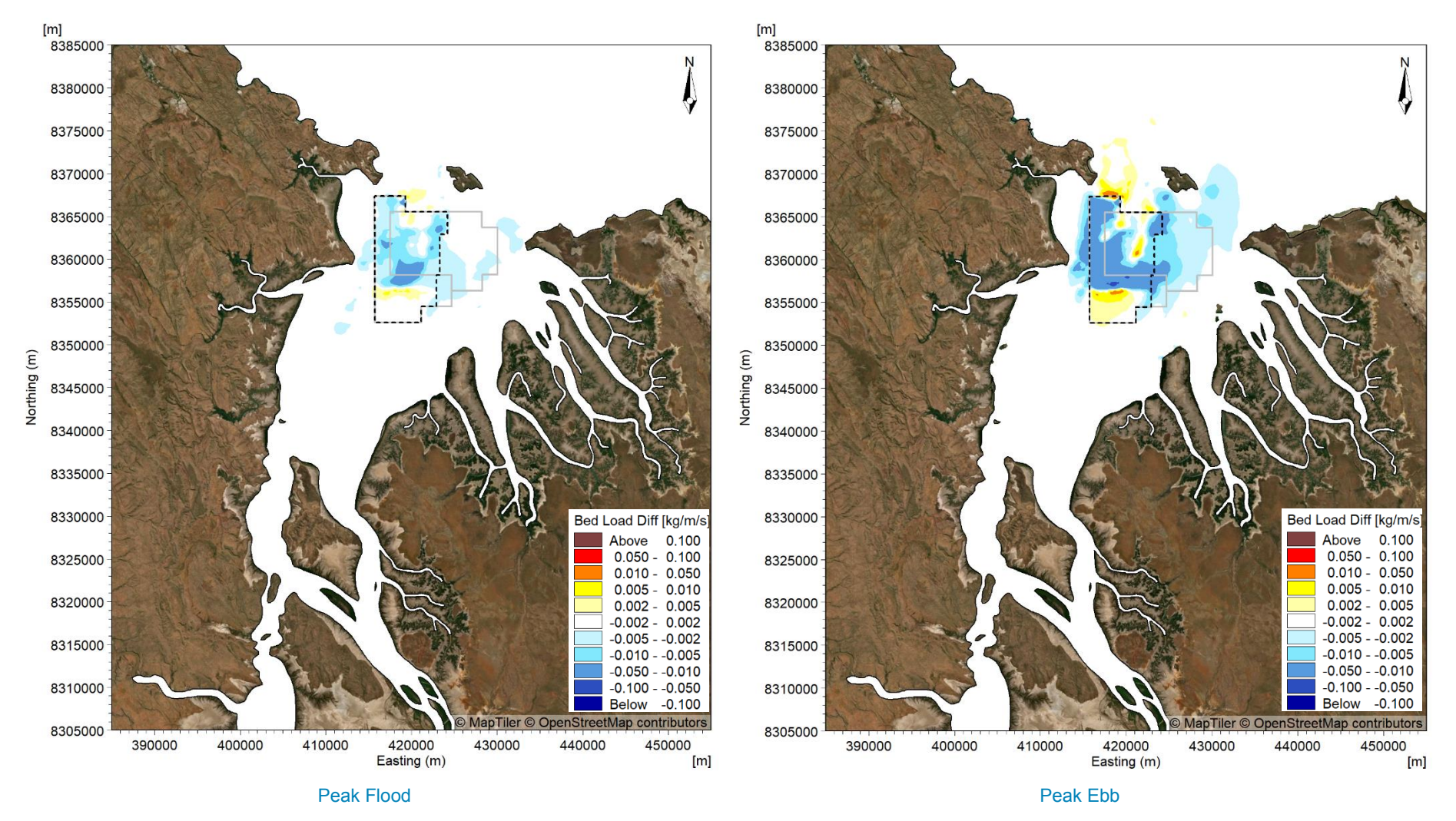


Figure C37. Modelled change in bedload transport rate during a spring tide at peak flood and peak ebb in the transitional season due to the 15 year sand sourcing in 100 years time scenario.



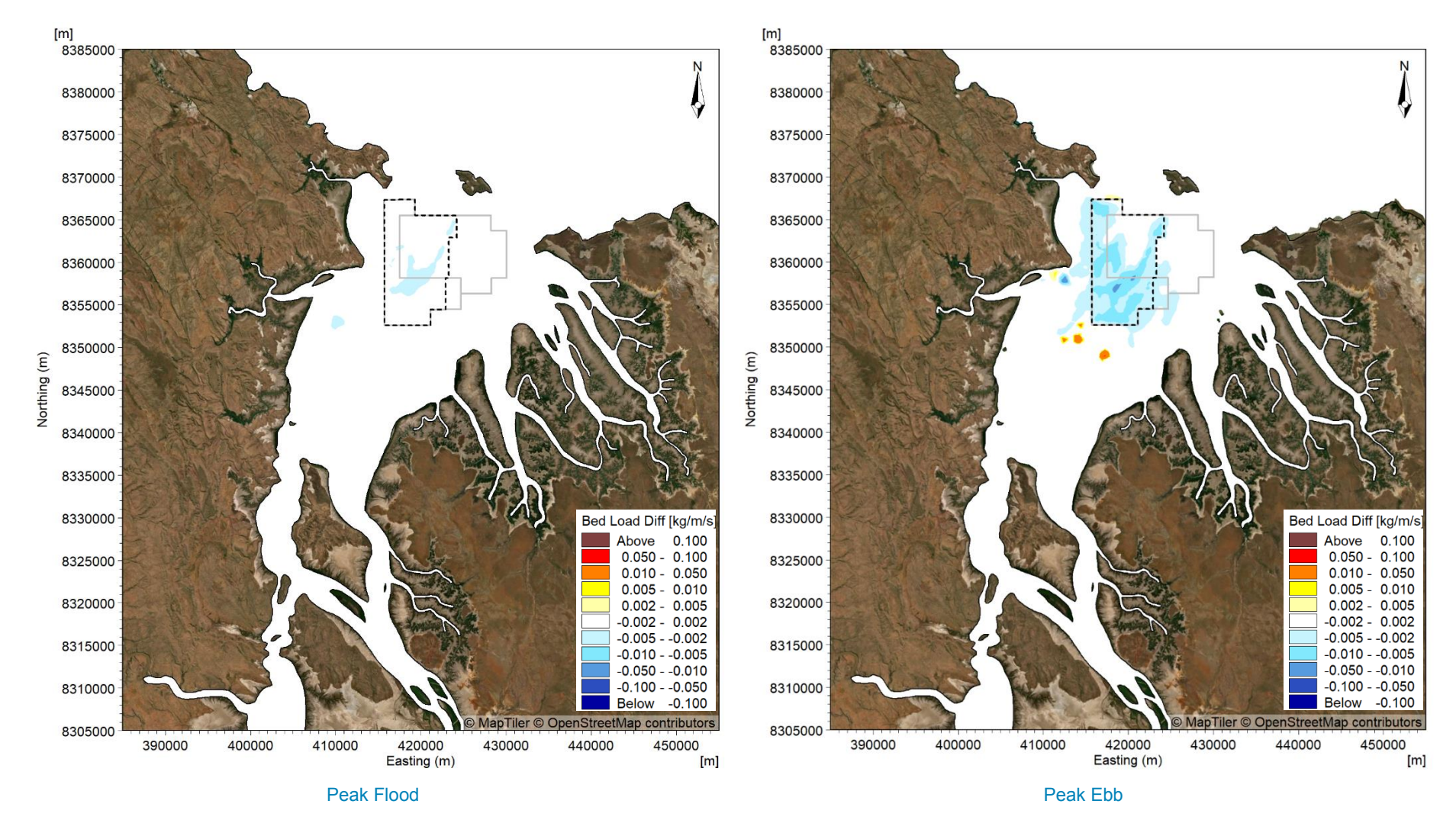


Figure C38. Modelled change in bedload transport rate at peak flood and peak ebb during TC Marcus due to the 5 year sand sourcing scenario.



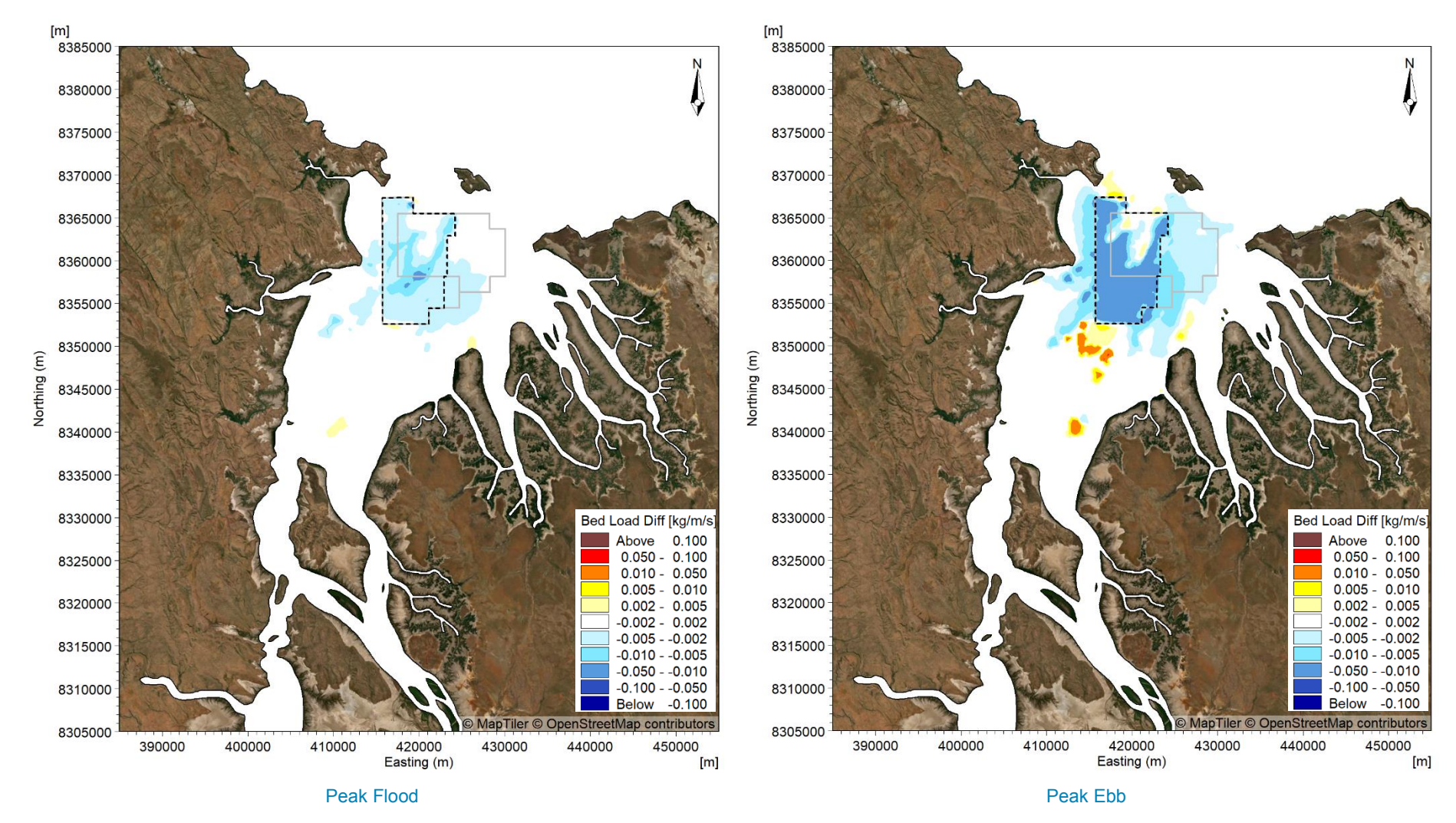


Figure C39. Modelled change in bedload transport rate at peak flood and peak ebb during TC Marcus due to the 15 year sand sourcing scenario.



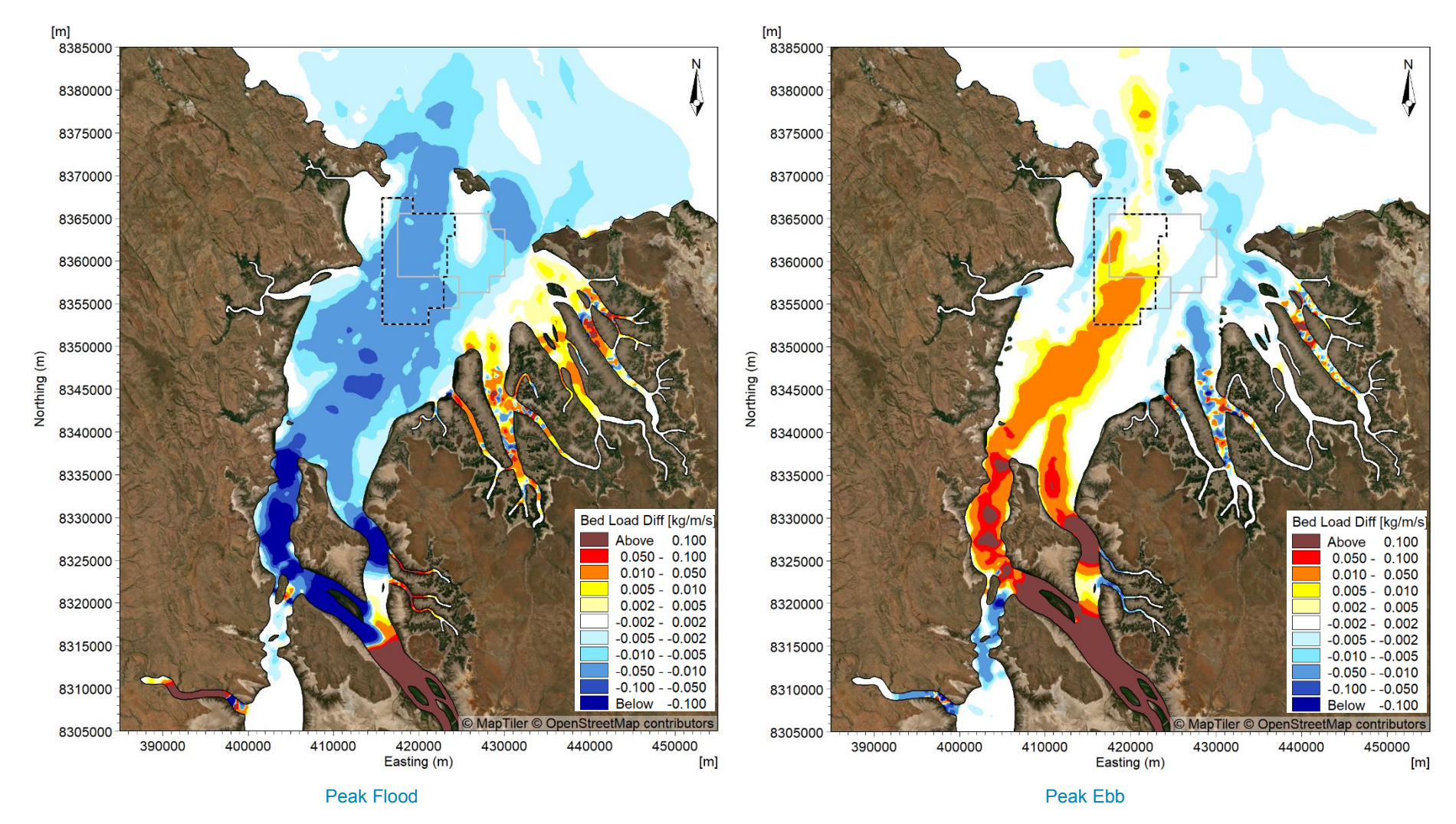


Figure C40. Modelled change in bedload transport rate during a spring tide at peak flood and peak ebb in the wet season for the pre-European settlement scenario.



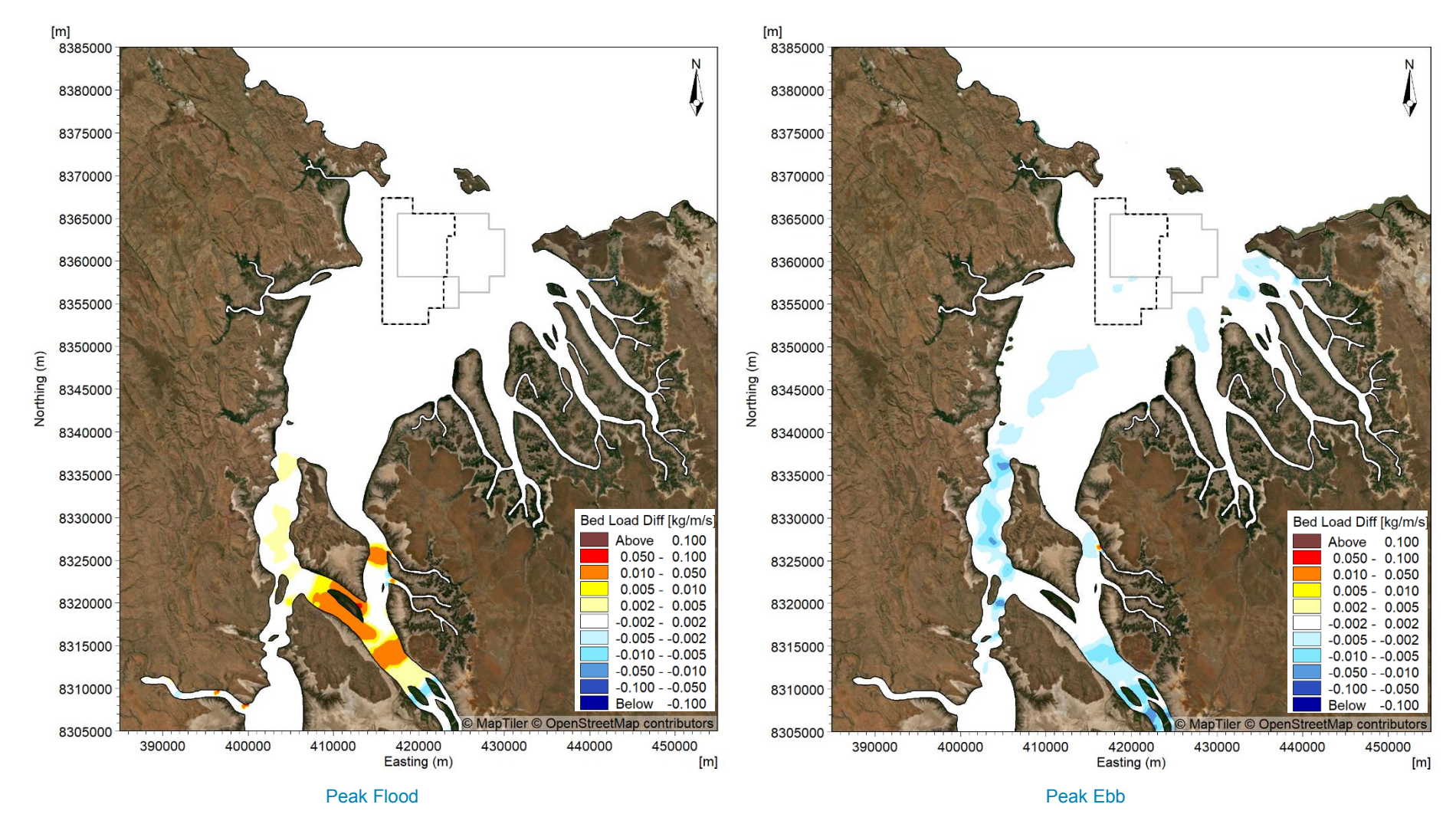


Figure C41. Modelled change in bedload transport rate during a spring tide at peak flood and peak ebb in the dry season for the pre-European settlement scenario.



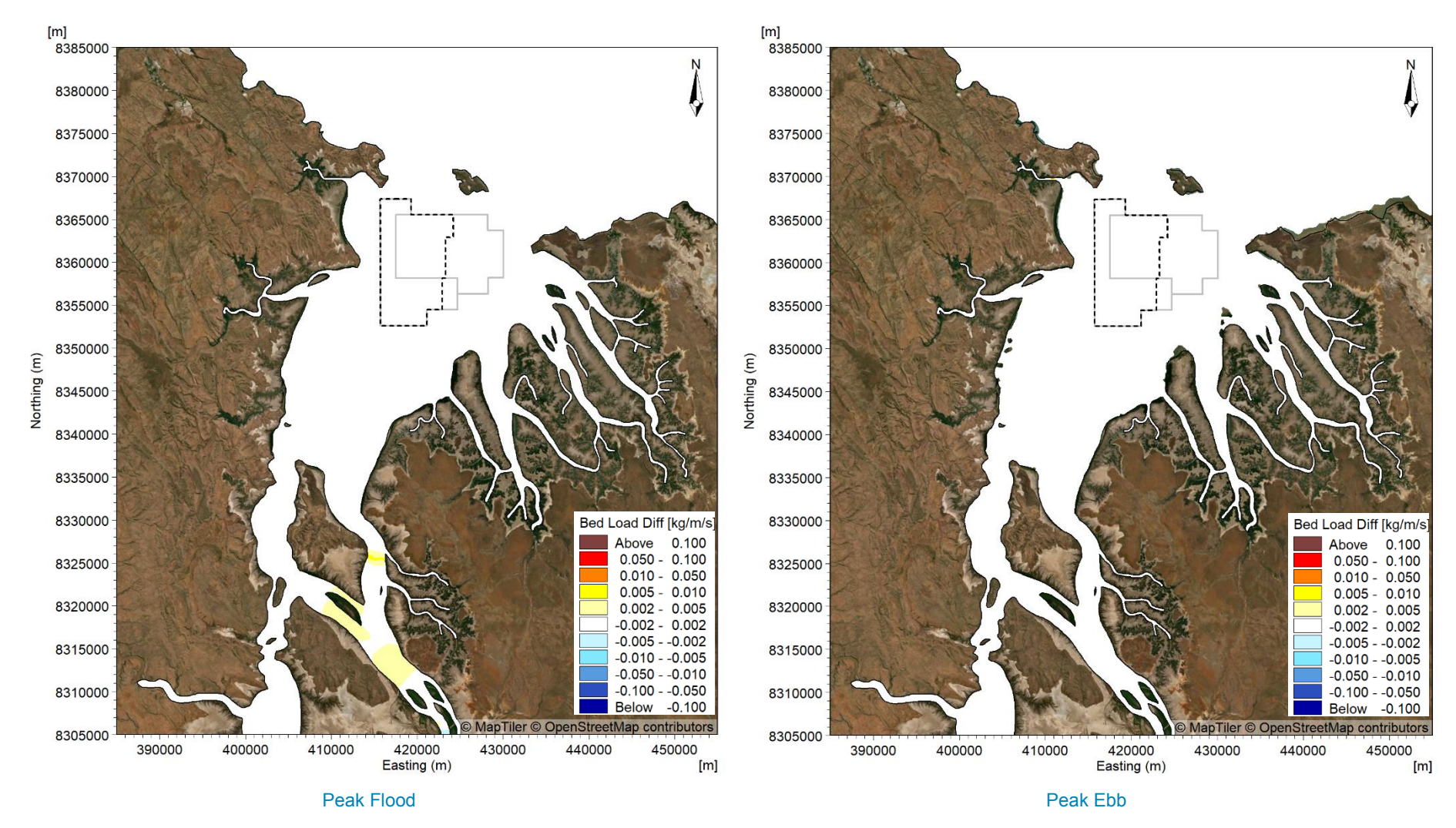


Figure C42. Modelled change in bedload transport rate during a spring tide at peak flood and peak ebb in the transitional season for the pre-European settlement scenario.



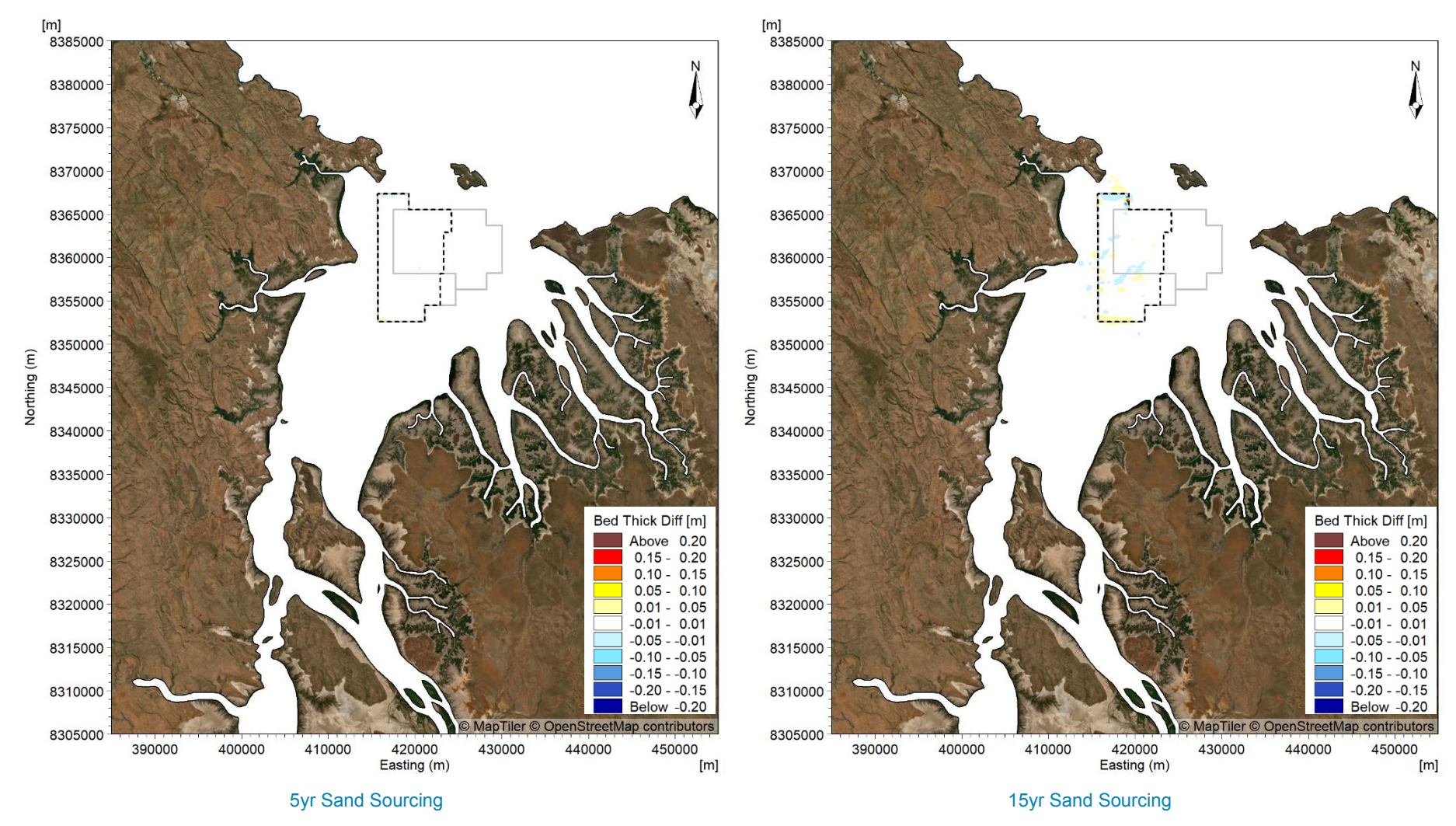
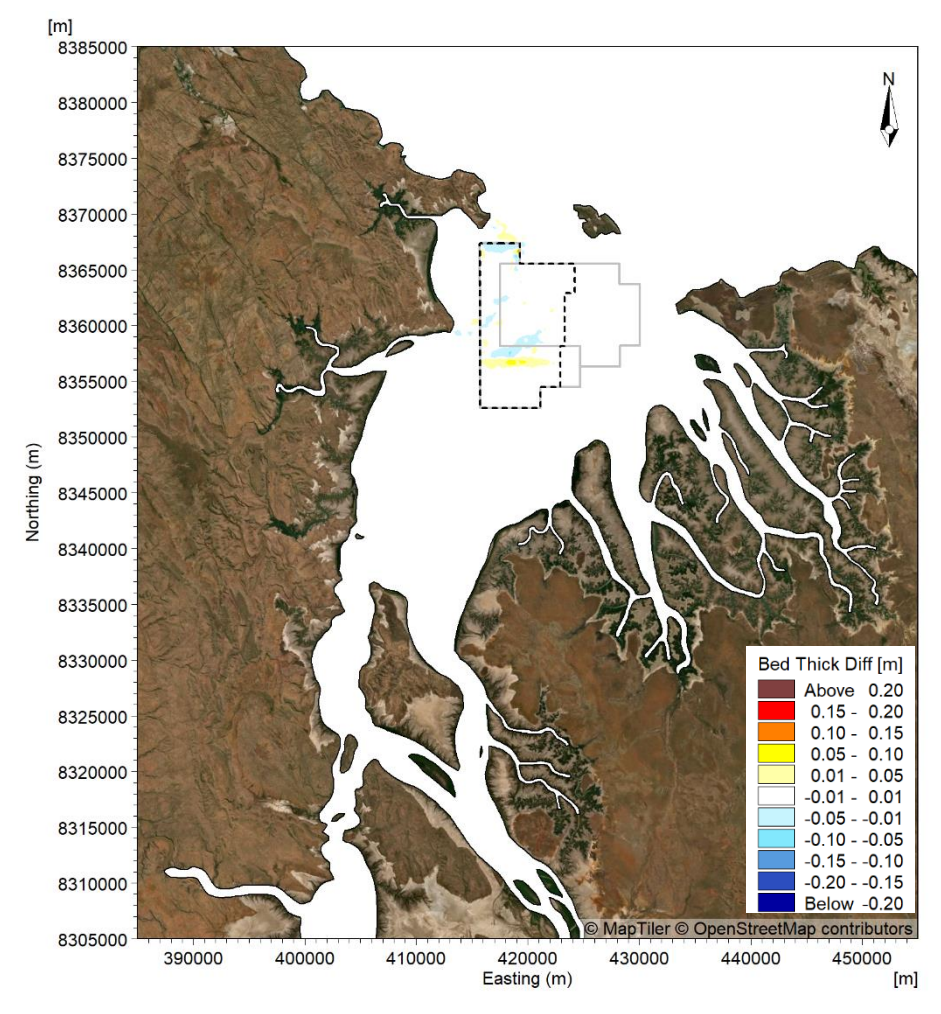


Figure C43. Modelled change in bed thickness due to the 5 and 15 years of sand sourcing scenarios over the 2 month wet season period.





15yr Sand Sourcing, 100 years time

Figure C44. Modelled change in bed thickness due to the 15 year sand sourcing in 100 years time scenario over the 2 month wet season period.



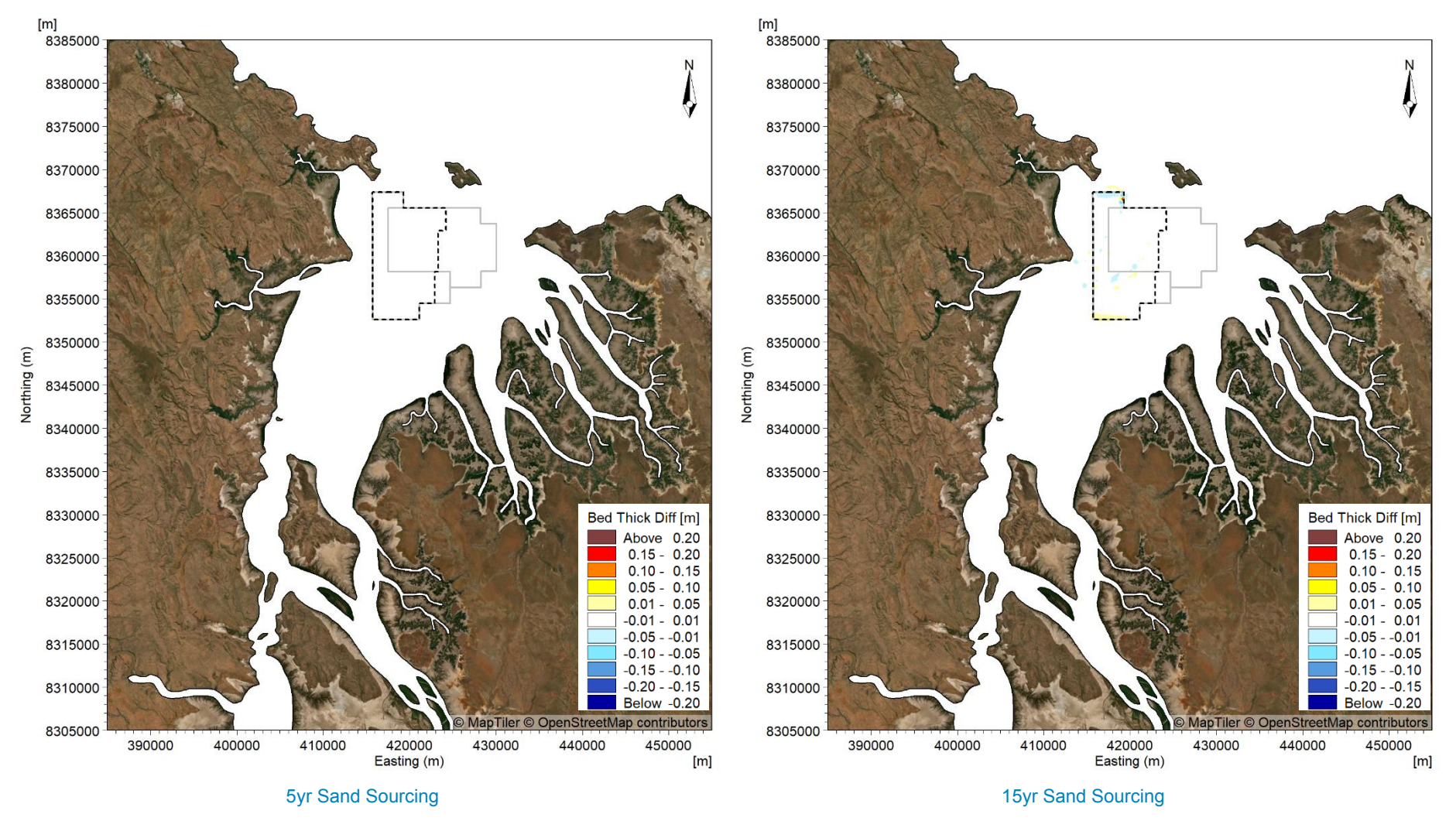
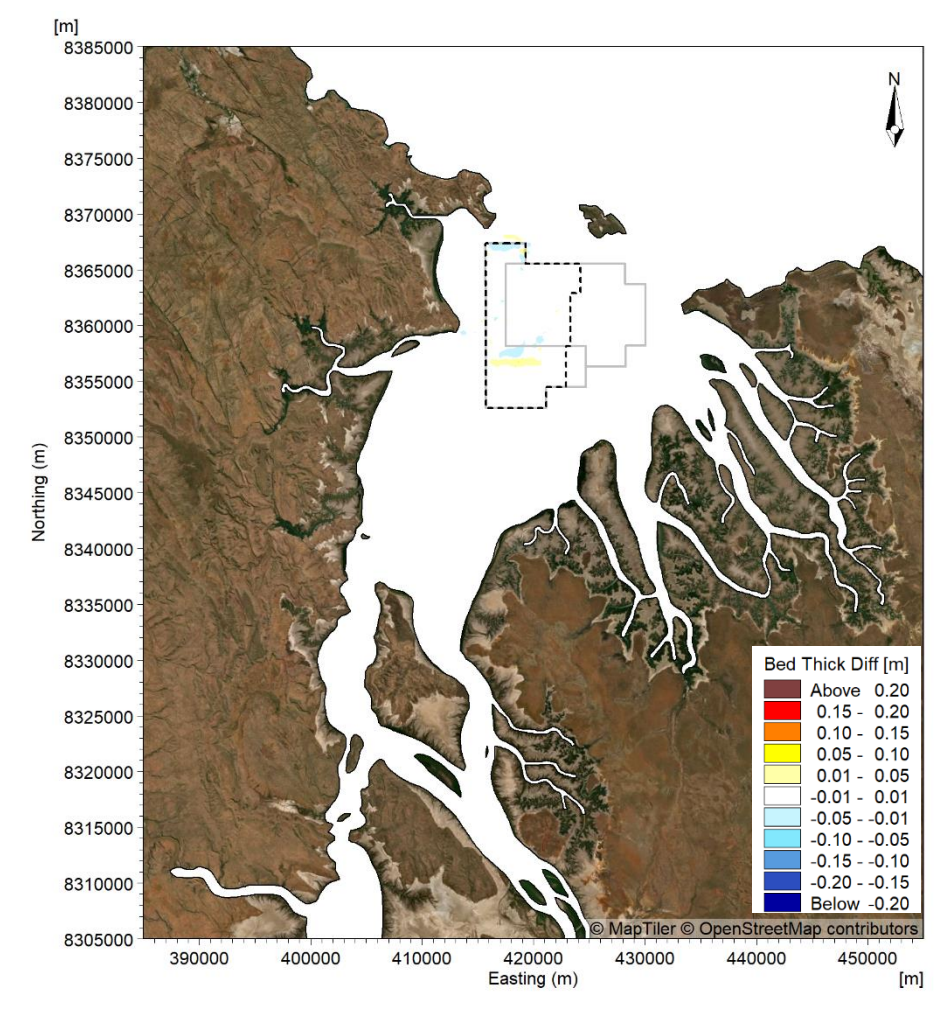


Figure C45. Modelled difference in bed thickness due to the 5 and 15 years of sand sourcing scenarios over the 2 month dry season period.





15yr Sand Sourcing, 100 years time

Figure C46. Modelled change in bed thickness due to the 15 year sand sourcing in 100 years time scenario over the 2 month dry season period.



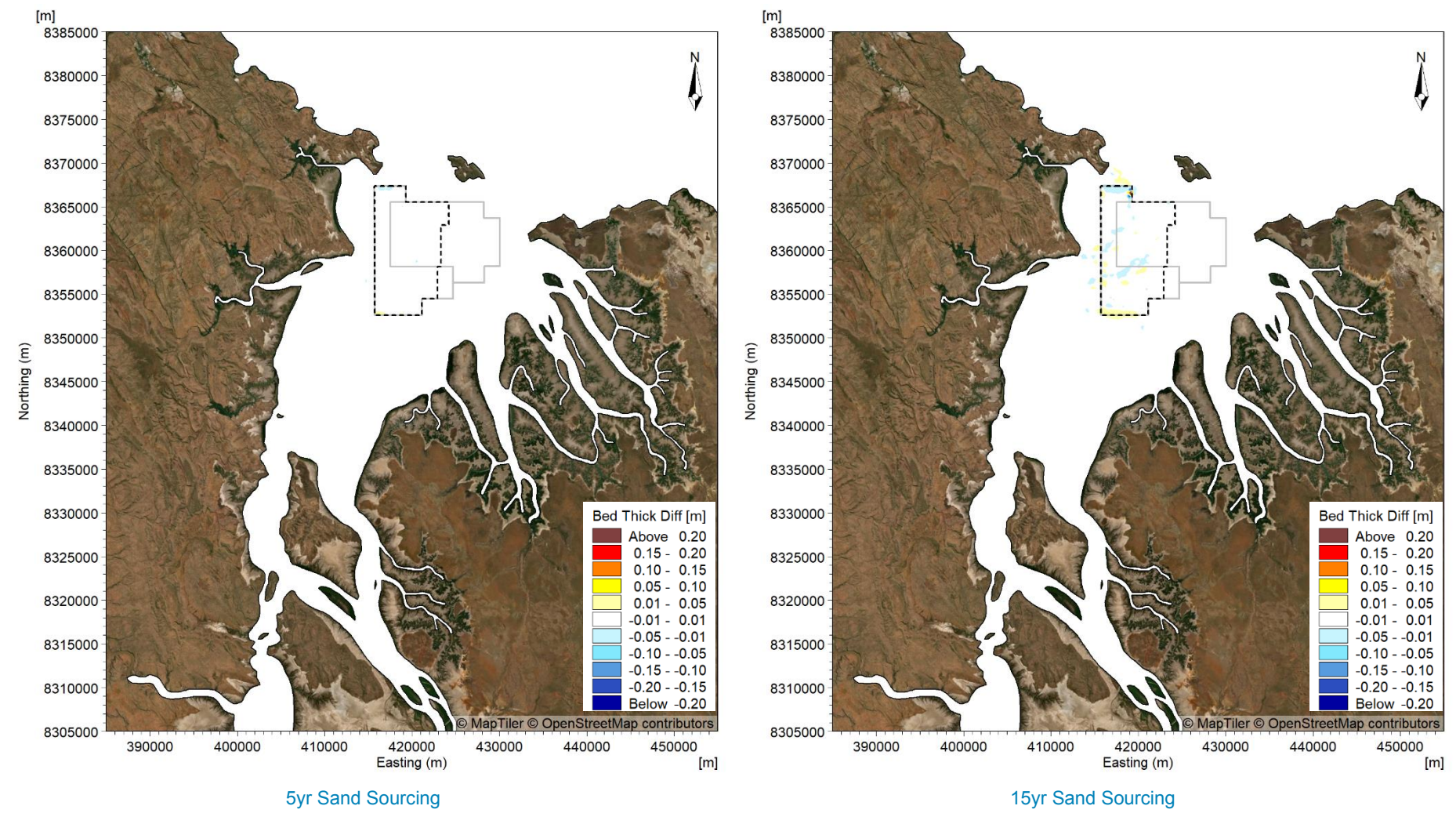
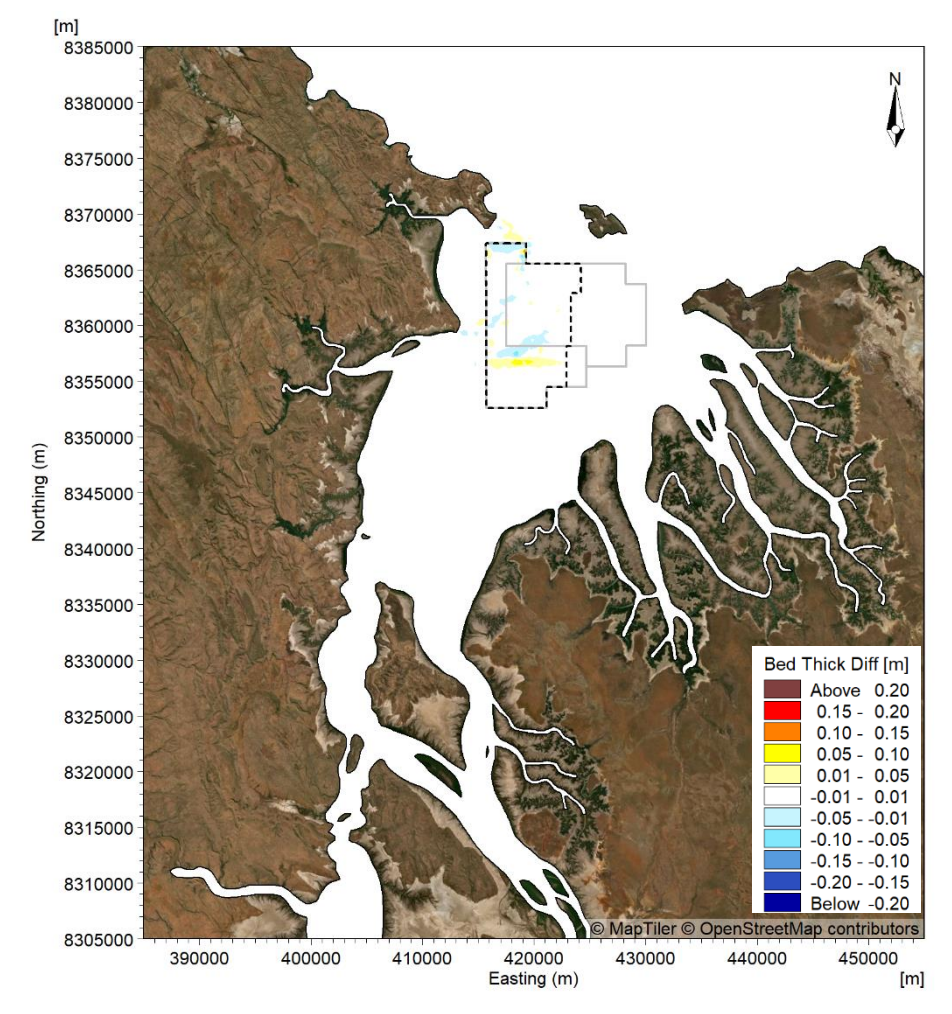


Figure C47. Modelled difference in bed thickness due to the 5 and 15 years of sand sourcing scenarios over the 2 month transitional season period.





15yr Sand Sourcing, 100 years time

Figure C48. Modelled change in bed thickness due to the 15 year sand sourcing in 100 years time scenario over the 2 month transitional season period.



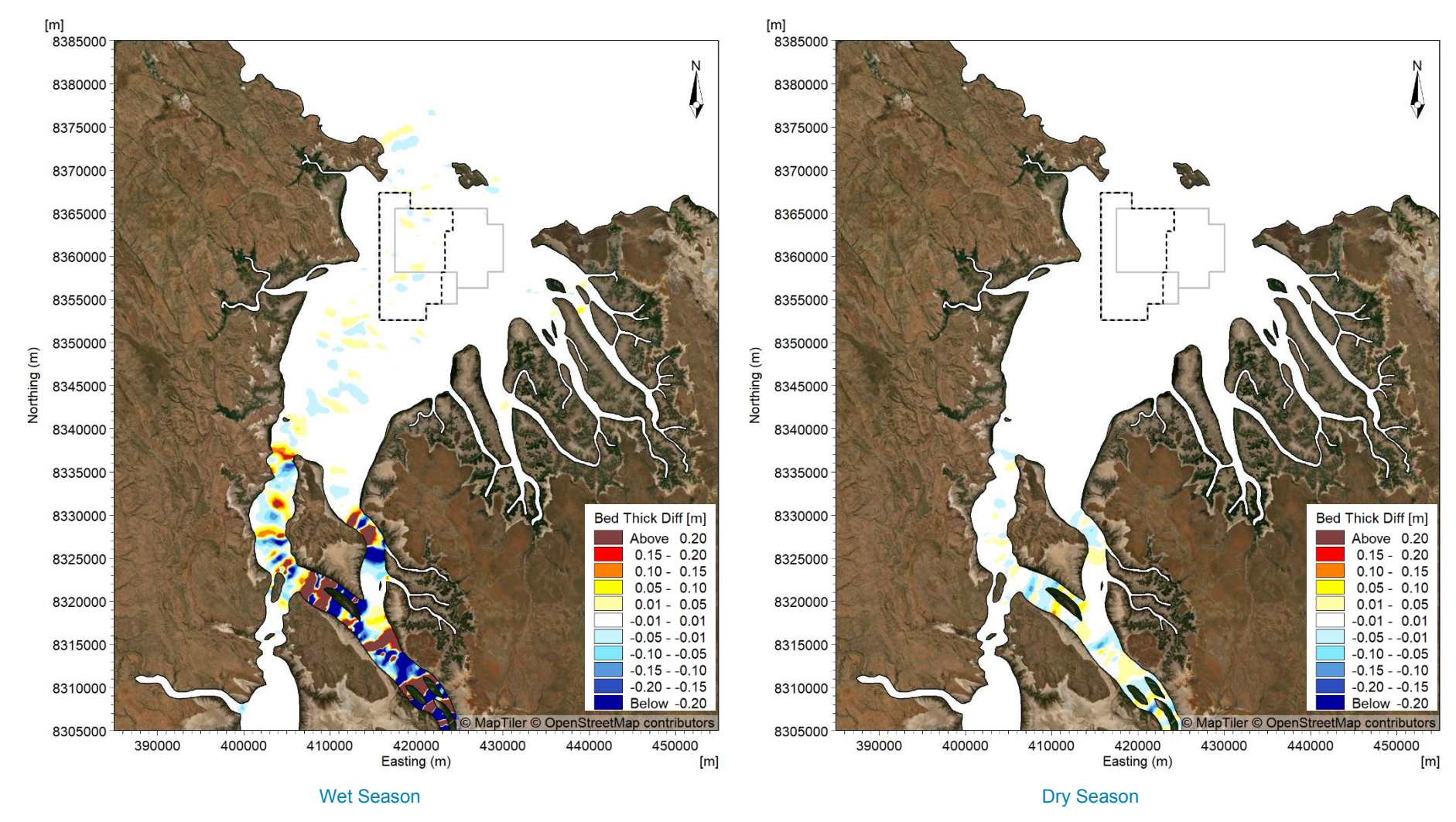


Figure C49. Modelled difference in bed thickness between the existing case and the pre-European settlement scenario over the 2 month wet and dry season periods.



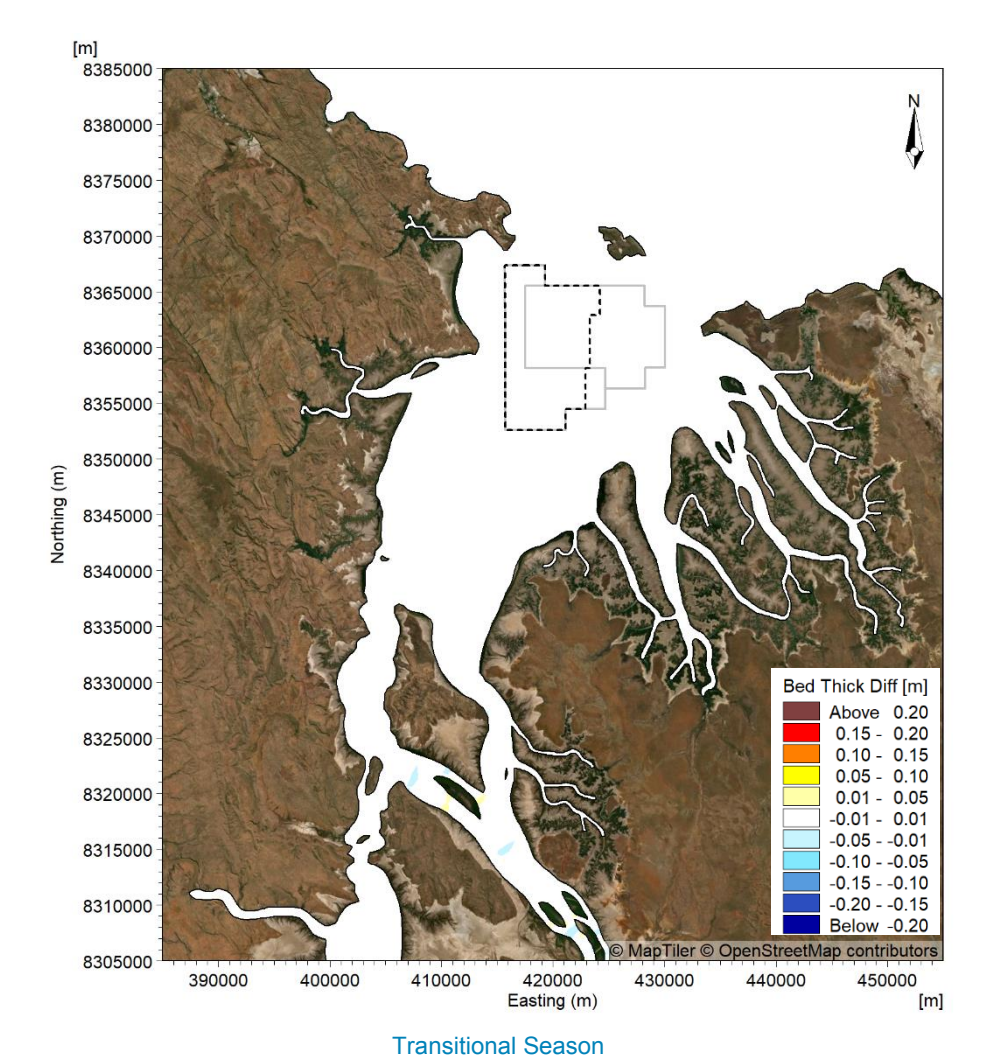


Figure C50. Modelled difference in bed thickness between the existing case and the pre-European settlement scenario over the 2 month transitional season period.



## Appendix D – Sediment Plume Modelling Plots



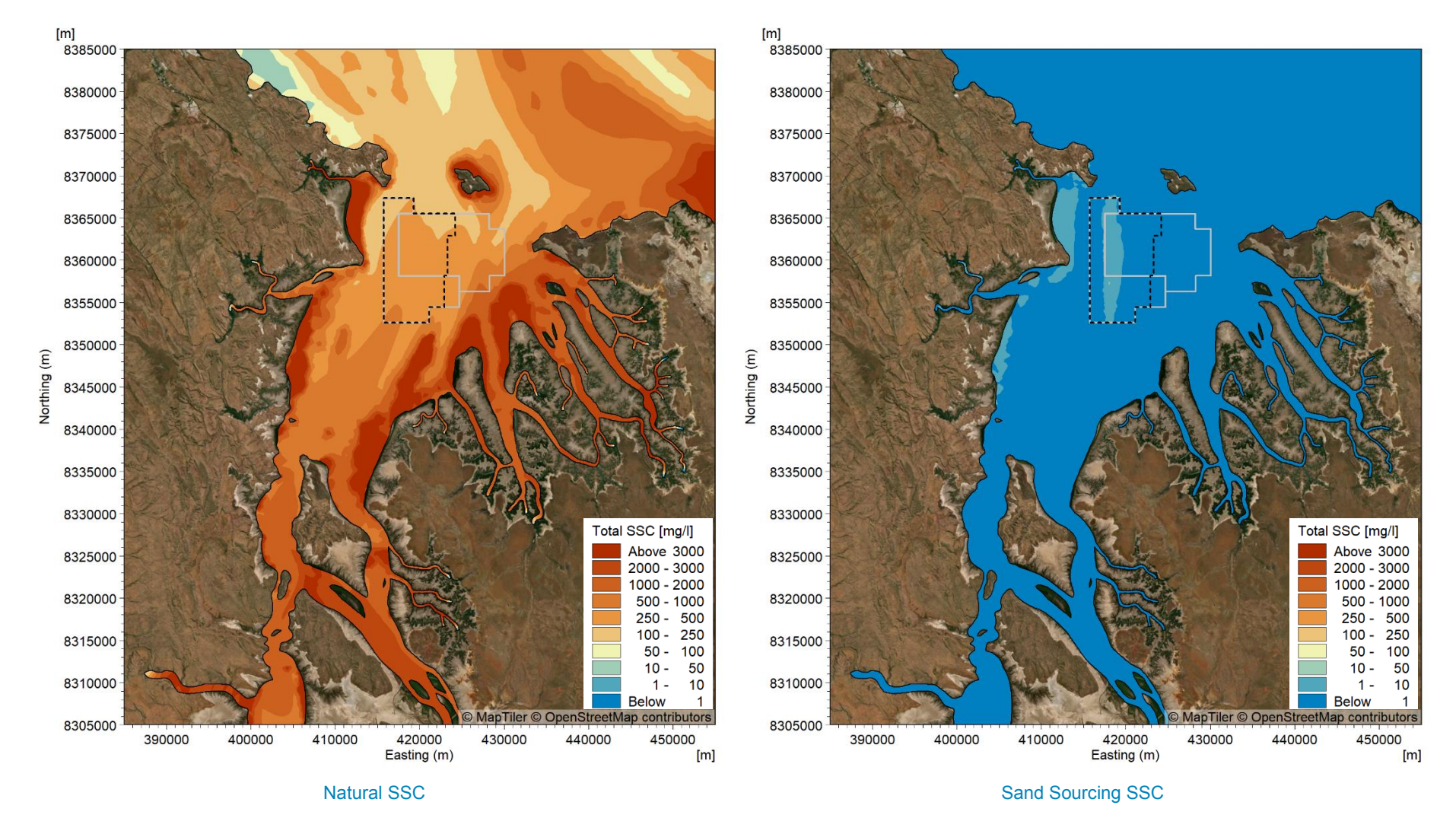


Figure D1. Modelled maximum natural SSC and maximum sand sourcing SSC for the mid-depth layer when sand sourcing during neap tides over a two-month (60 days) period in the wet season for Scenario 1.

20/01/2025 D2 Cambridge Gulf: Modelling Report



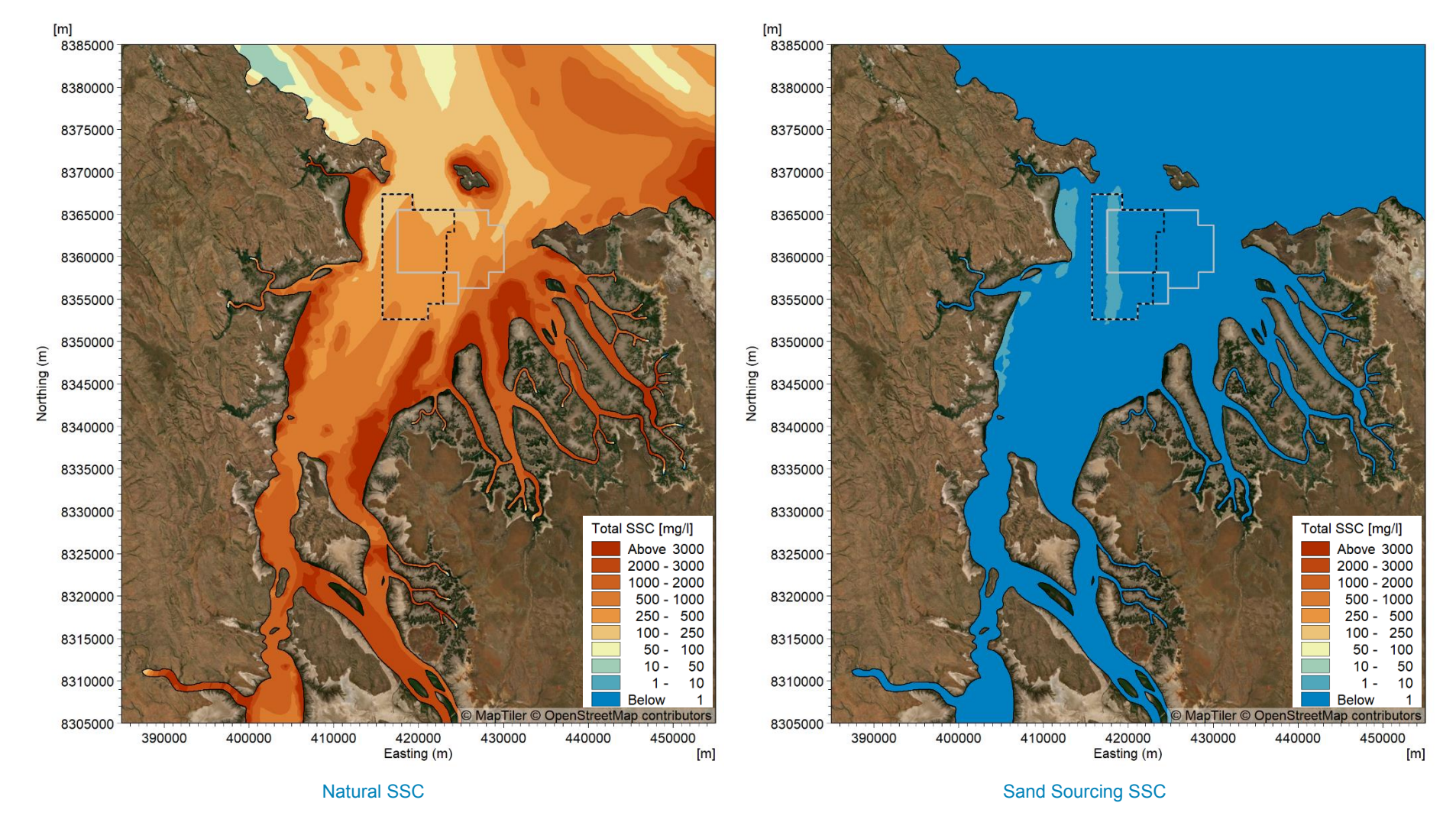


Figure D2. Modelled maximum natural SSC and maximum sand sourcing SSC for the mid-depth layer when sand sourcing during spring tides over a two-month (60 days) period in the wet season for Scenario 1.

20/01/2025 D3 Cambridge Gulf: Modelling Report



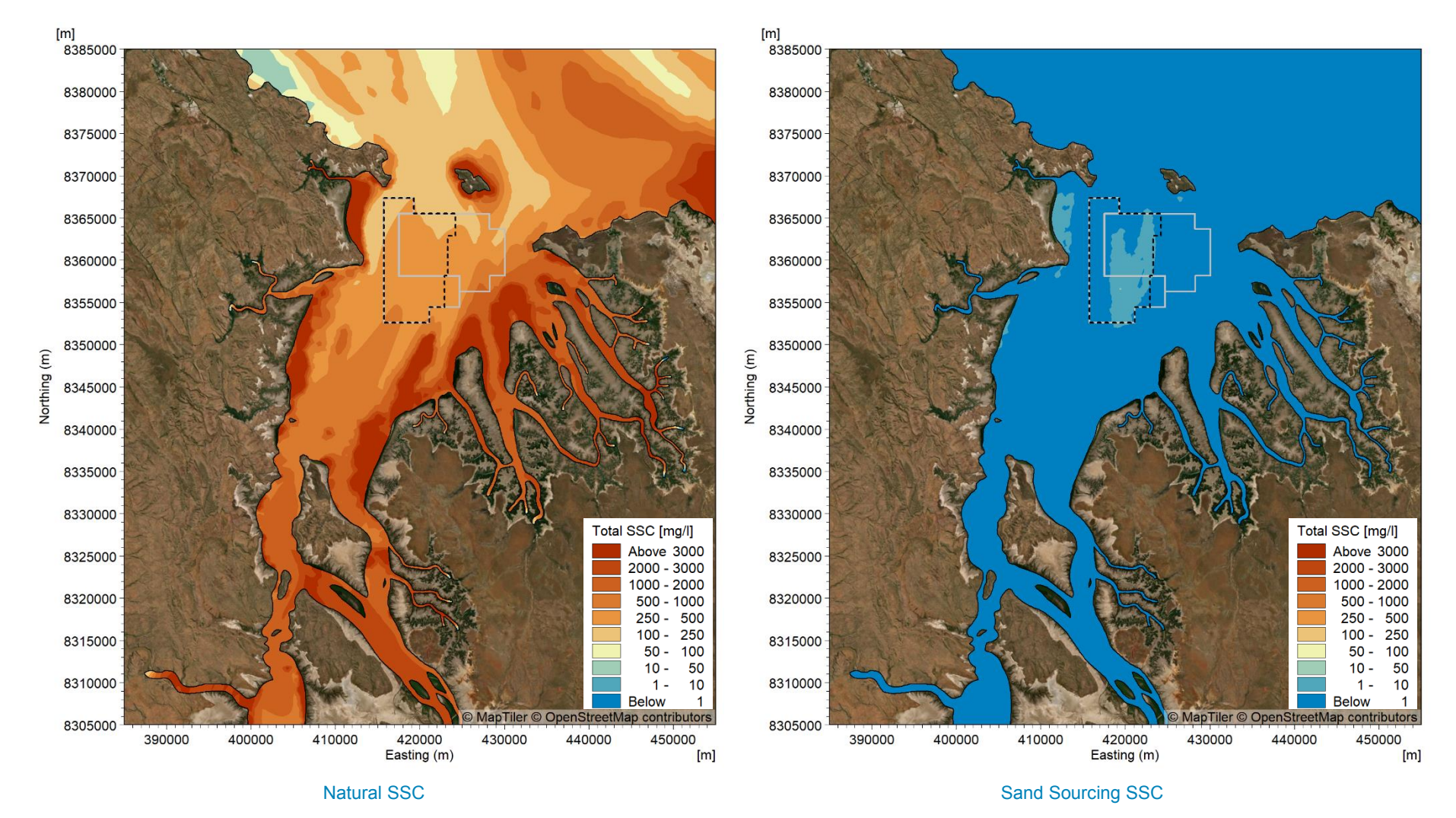


Figure D3. Modelled maximum natural SSC and maximum sand sourcing SSC for the mid-depth layer when sand sourcing during neap tides over a two-month (60 days) period in the wet season for Scenario 2.

20/01/2025 D4 Cambridge Gulf: Modelling Report



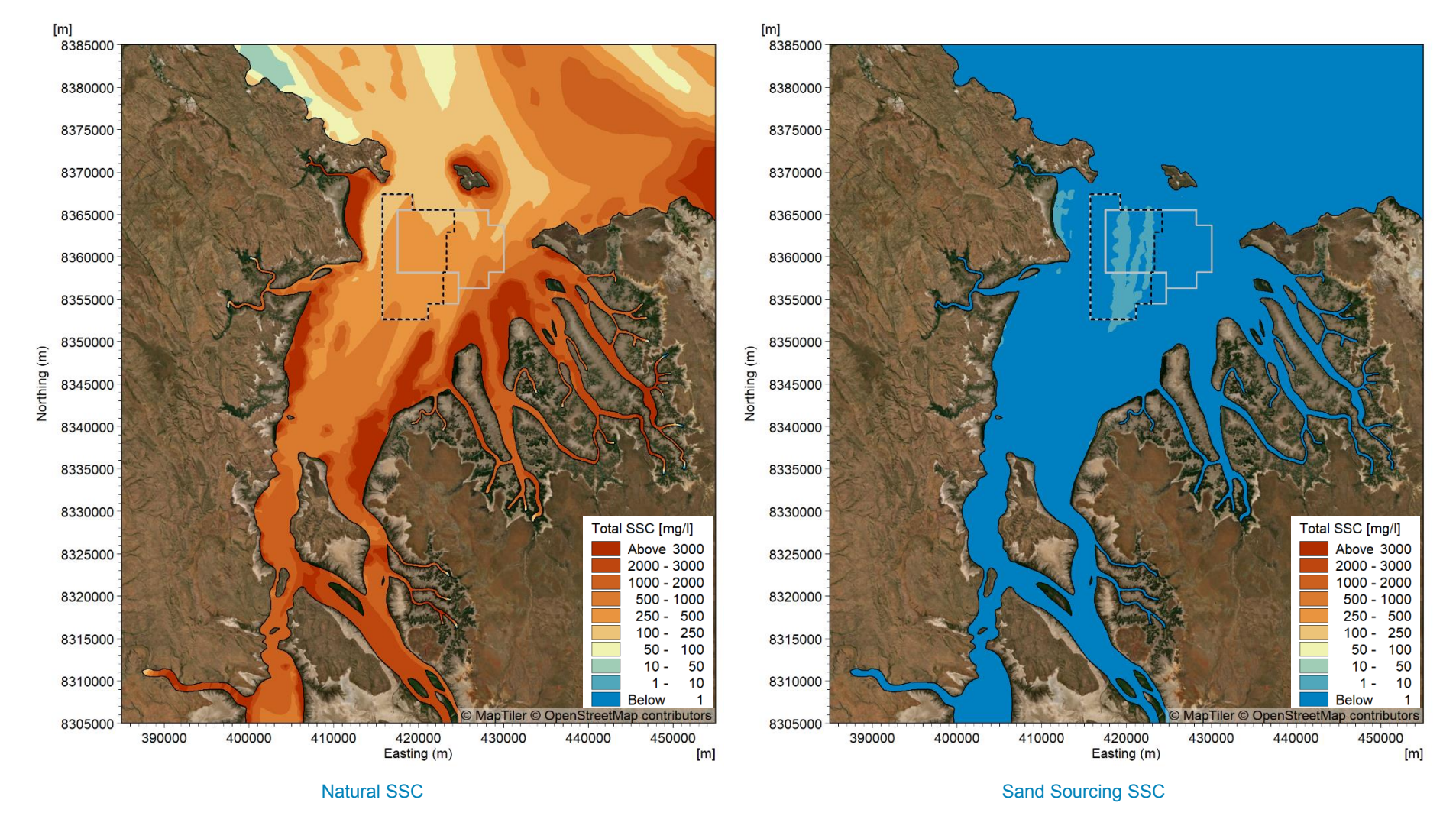


Figure D4. Modelled maximum natural SSC and maximum sand sourcing SSC for the mid-depth layer when sand sourcing during spring tides over a two-month (60 days) period in the wet season for Scenario 2.

20/01/2025 D5 Cambridge Gulf: Modelling Report



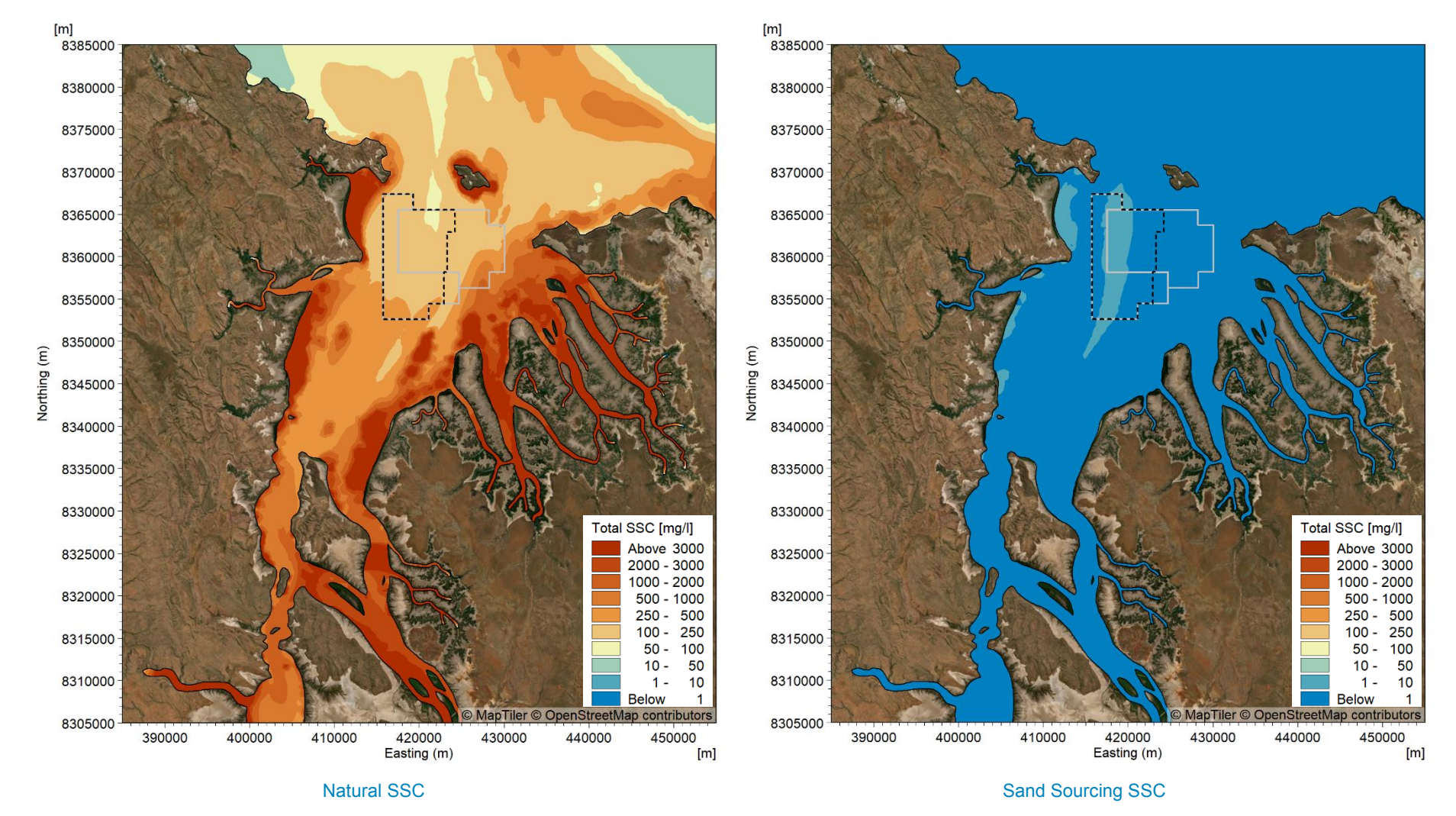


Figure D5. Modelled maximum natural SSC and maximum sand sourcing SSC for the mid-depth layer when sand sourcing during neap tides over a two-month (61 days) period in the dry season for Scenario 1.

20/01/2025 D6 Cambridge Gulf: Modelling Report



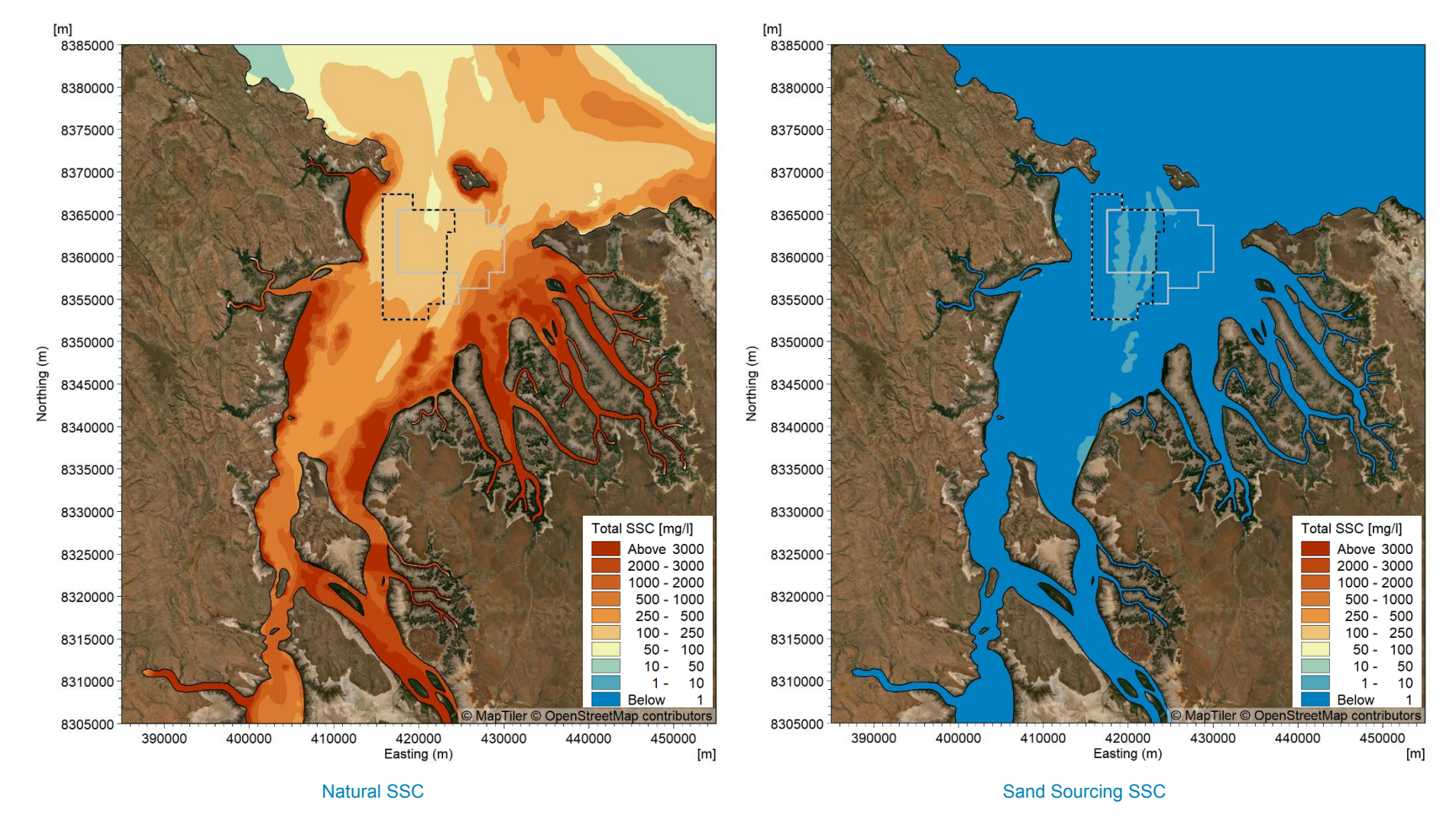


Figure D6. Modelled maximum natural SSC and maximum sand sourcing SSC for the mid-depth layer when sand sourcing during spring tides over a two-month (61 days) period in the dry season for Scenario 1.

20/01/2025 D7 Cambridge Gulf: Modelling Report



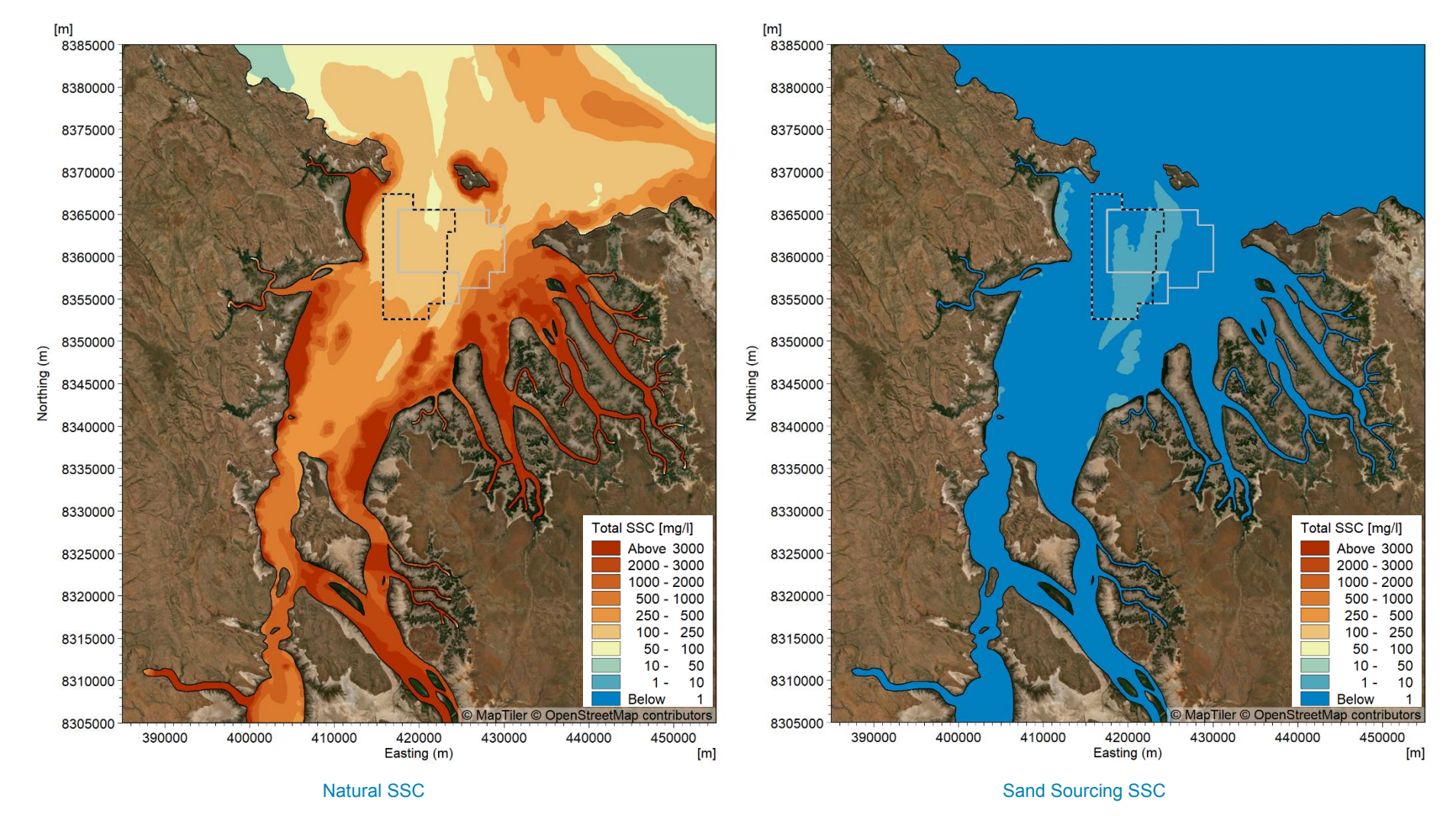


Figure D7. Modelled maximum natural SSC and maximum sand sourcing SSC for the mid-depth layer when sand sourcing during neap tides over a two-month (61 days) period in the dry season for Scenario 2.

20/01/2025 D8 Cambridge Gulf: Modelling Report



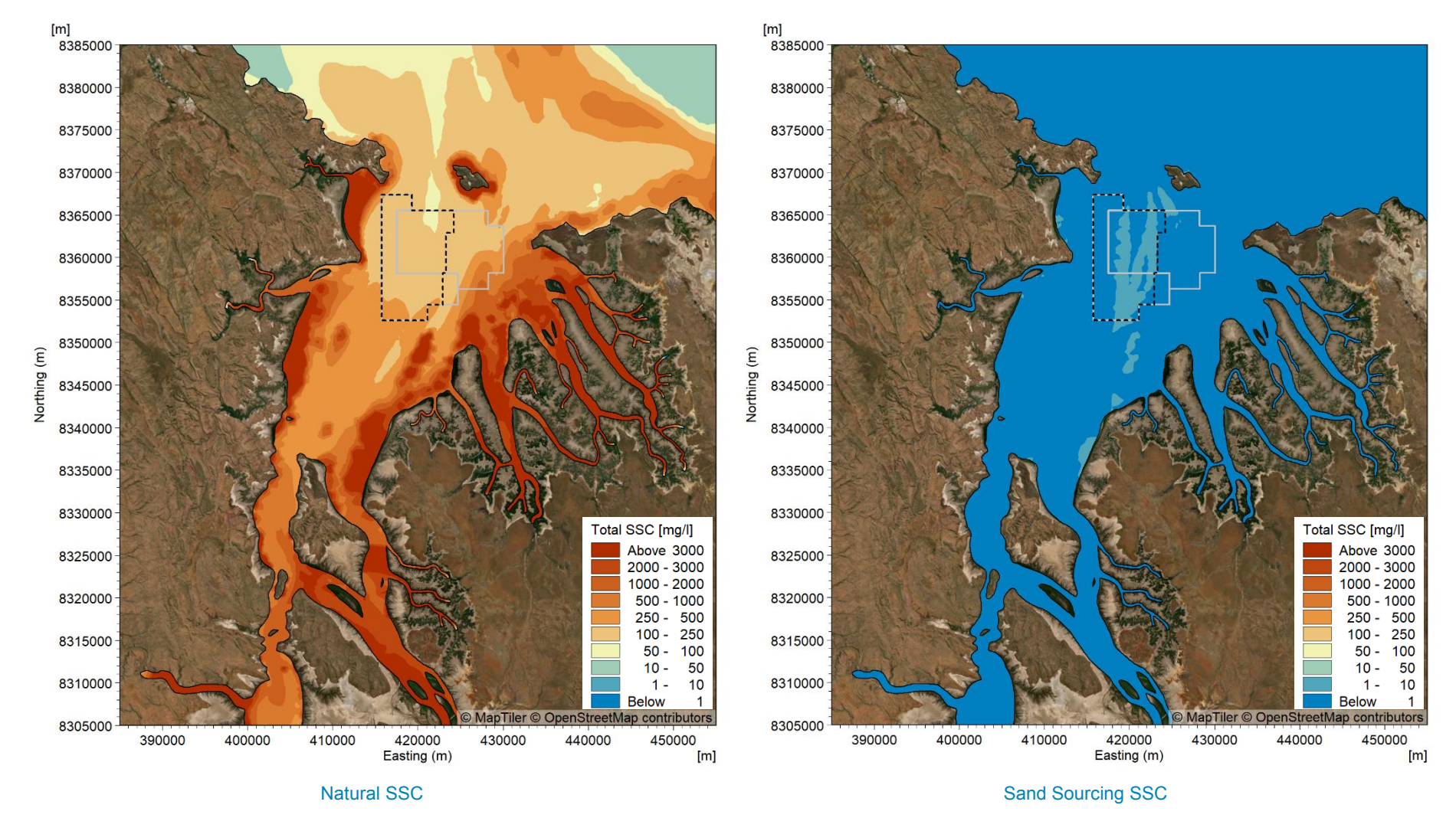


Figure D8. Modelled maximum natural SSC and maximum sand sourcing SSC for the mid-depth layer when sand sourcing during spring tides over a two-month (61 days) period in the dry season for Scenario 2.

20/01/2025 D9 Cambridge Gulf: Modelling Report



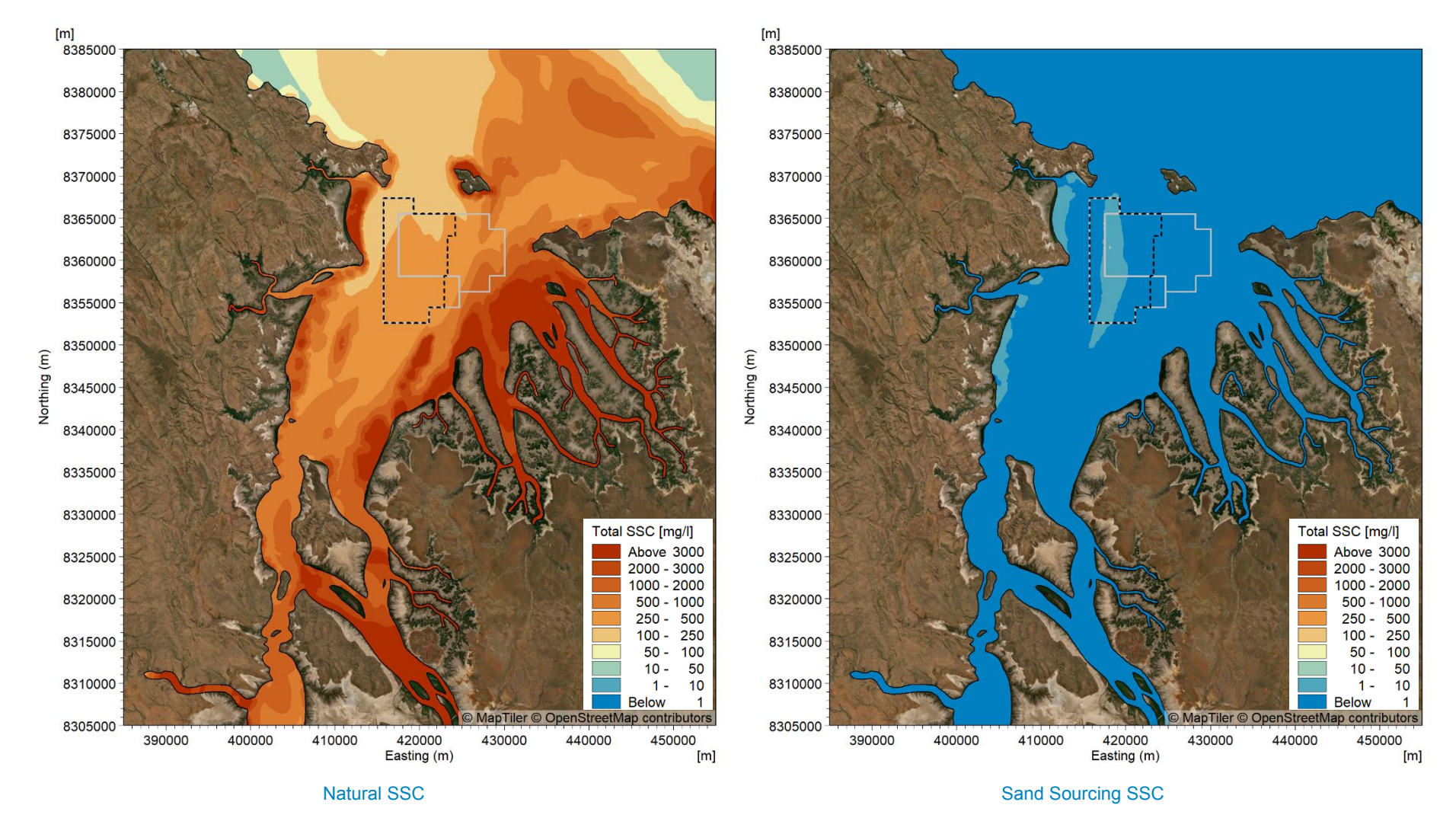


Figure D9. Modelled maximum natural SSC and maximum sand sourcing SSC for the mid-depth layer when sand sourcing during neap tides over a two-month (61 days) period in the transitional season for Scenario 1.

20/01/2025 D10 Cambridge Gulf: Modelling Report



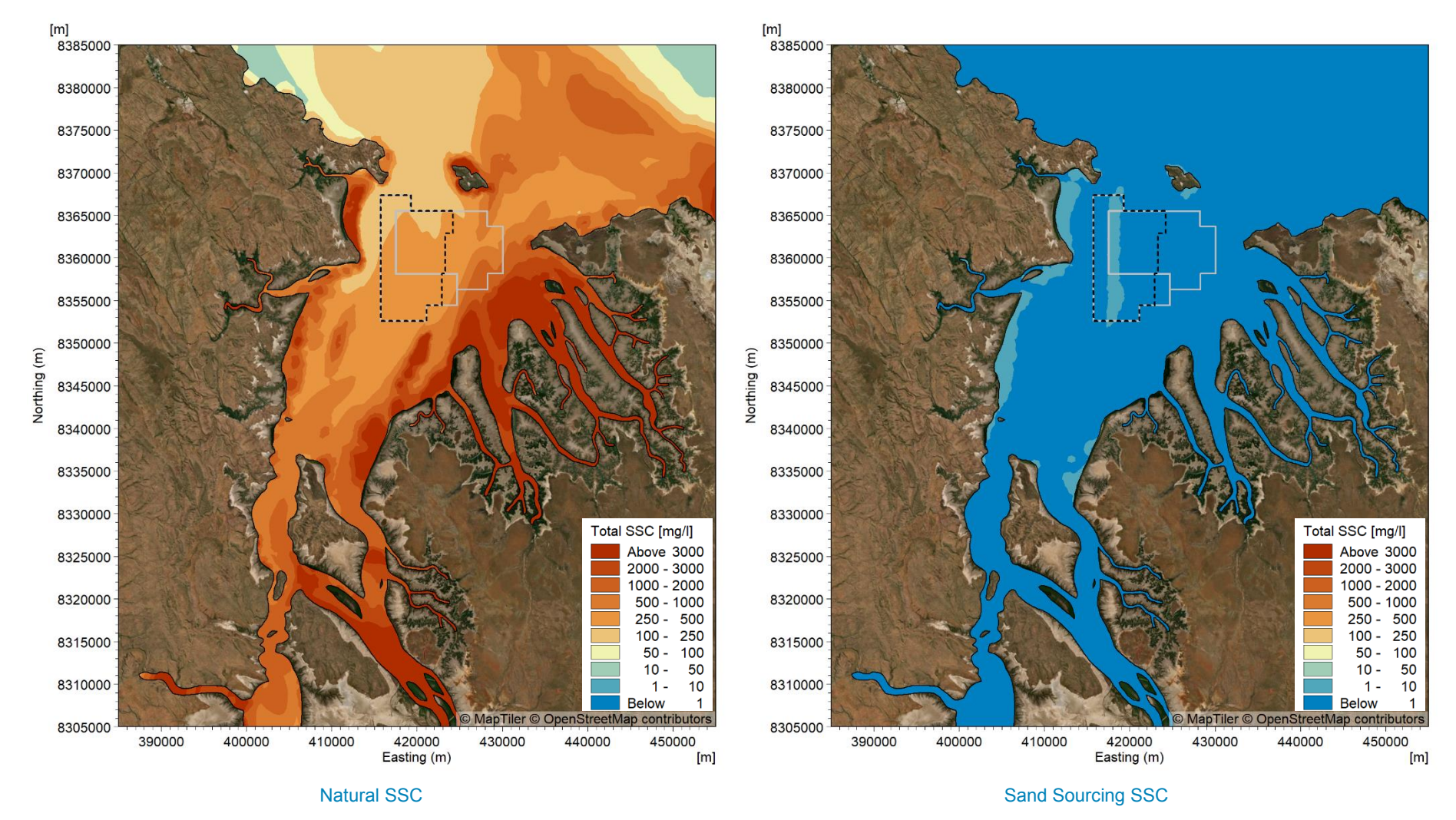


Figure D10. Modelled maximum natural SSC and maximum sand sourcing SSC for the mid-depth layer when sand sourcing during spring tides over a two-month (61 days) period in the transitional season for Scenario 1.

20/01/2025 D11 Cambridge Gulf: Modelling Report



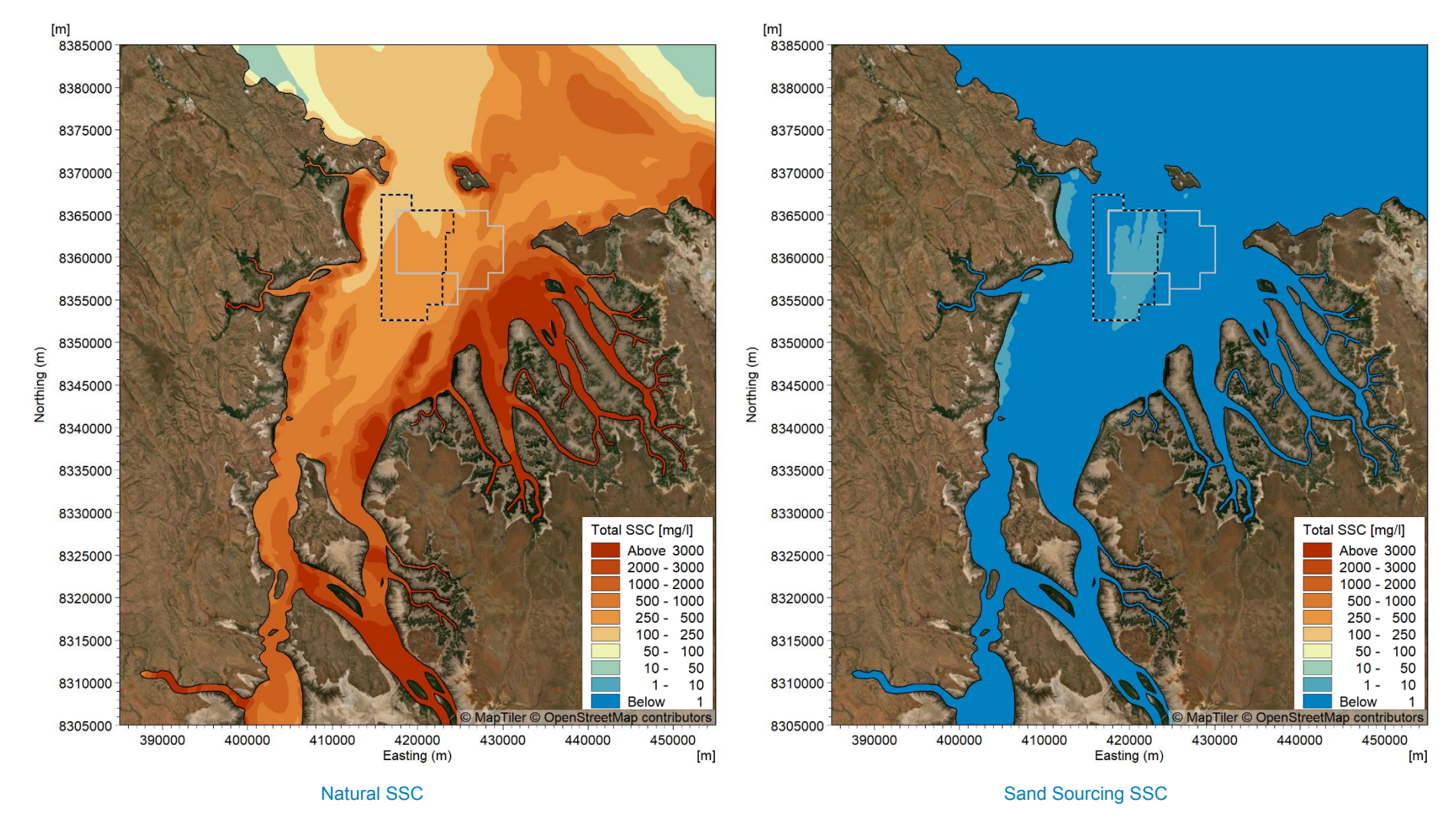


Figure D11. Modelled maximum natural SSC and maximum sand sourcing SSC for the mid-depth layer when sand sourcing during neap tides over a two-month (61 days) period in the transitional season for Scenario 2.

20/01/2025 D12 Cambridge Gulf: Modelling Report



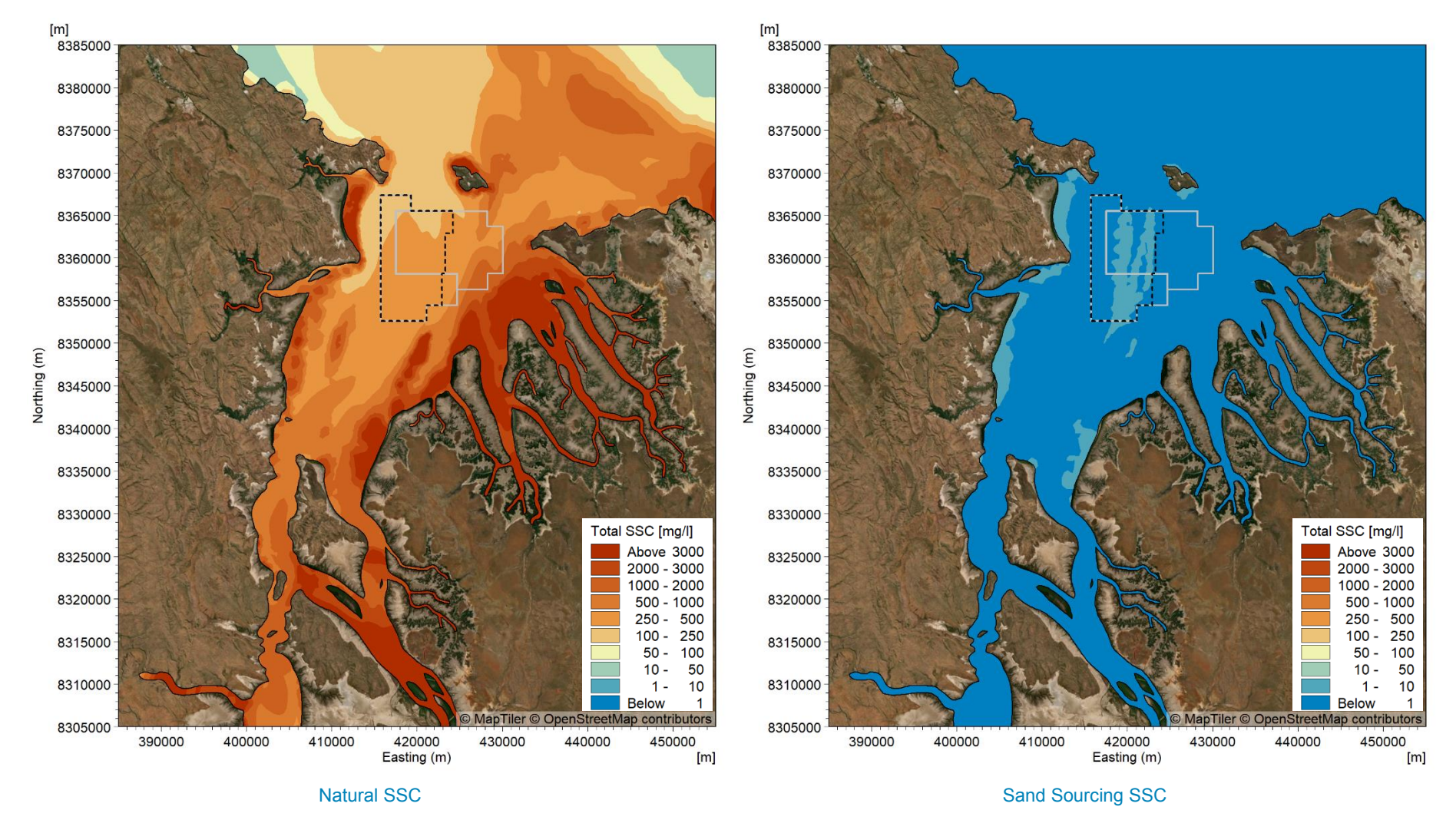


Figure D12. Modelled maximum natural SSC and maximum sand sourcing SSC for the mid-depth layer when sand sourcing during spring tides over a two-month (61 days) period in the transitional season for Scenario 2.

20/01/2025 D13 Cambridge Gulf: Modelling Report



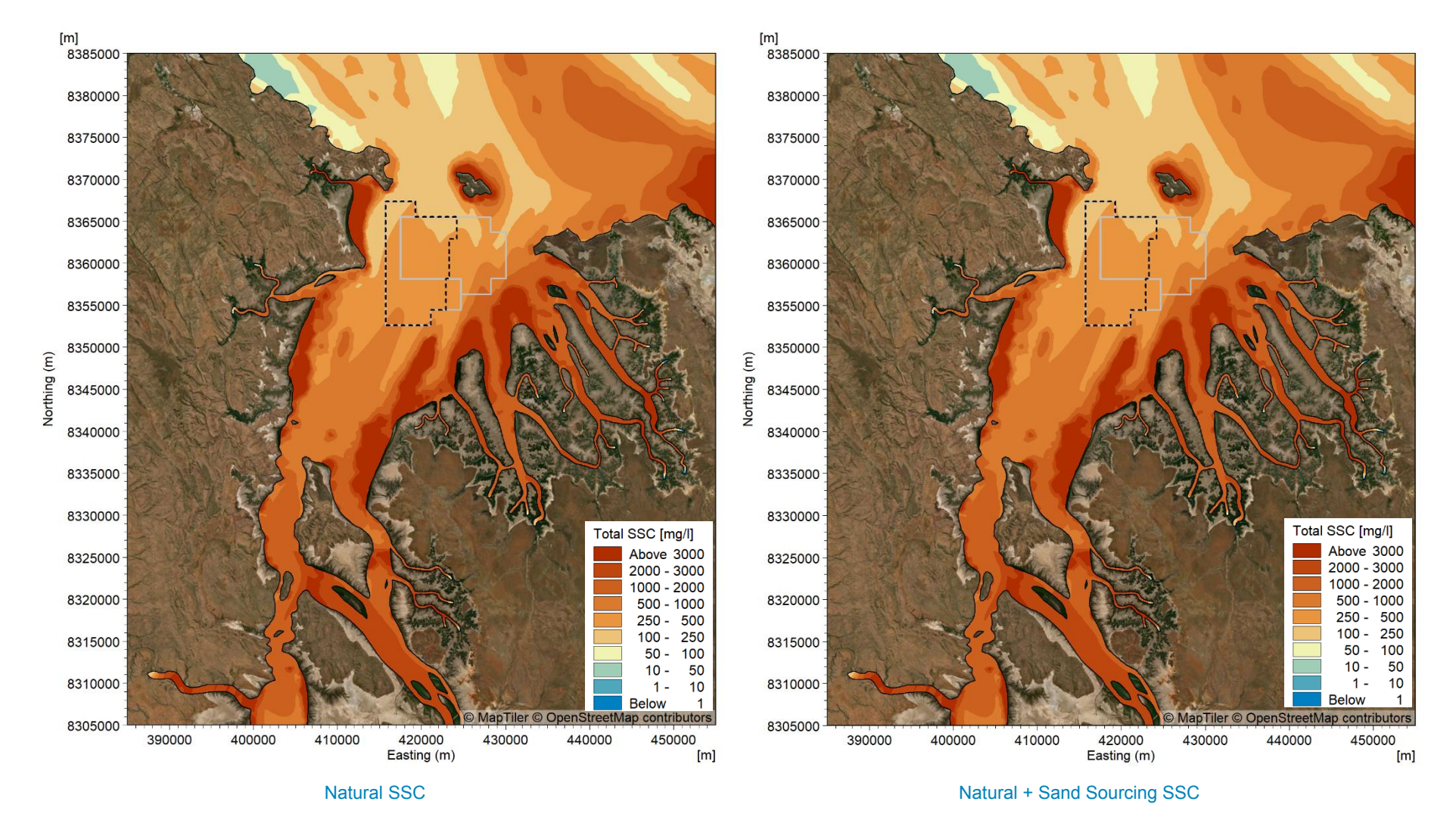


Figure D13. Modelled maximum natural SSC and maximum natural plus sand sourcing SSC for the mid-depth layer when sand sourcing during neap tides over a two-month (60 days) period in the wet season for Scenario 1.



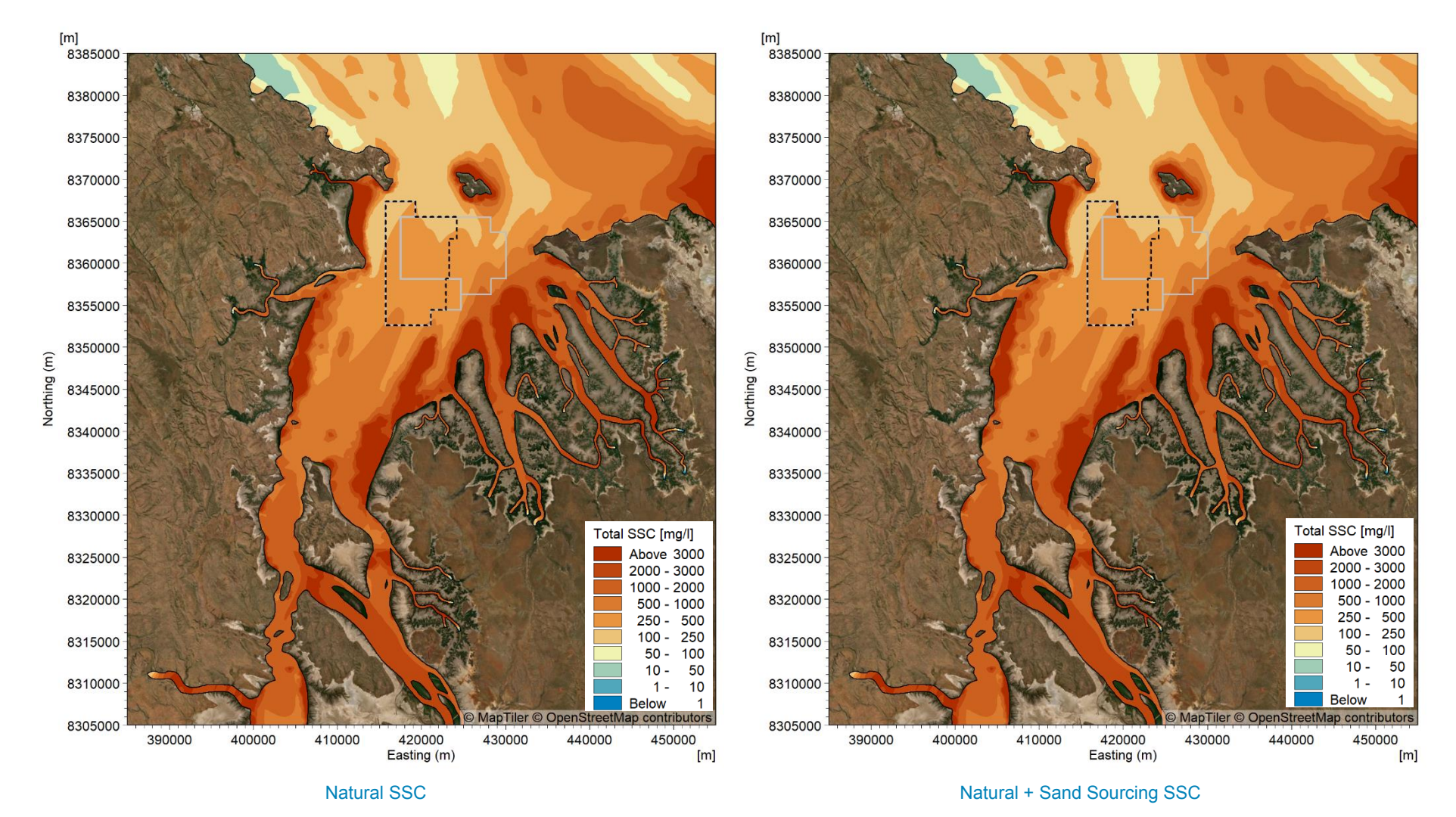


Figure D14. Modelled maximum natural SSC and maximum natural plus sand sourcing SSC for the mid-depth layer when sand sourcing during spring tides over a two-month (60 days) period in the wet season for Scenario 1.

20/01/2025 Cambridge Gulf: Modelling Report



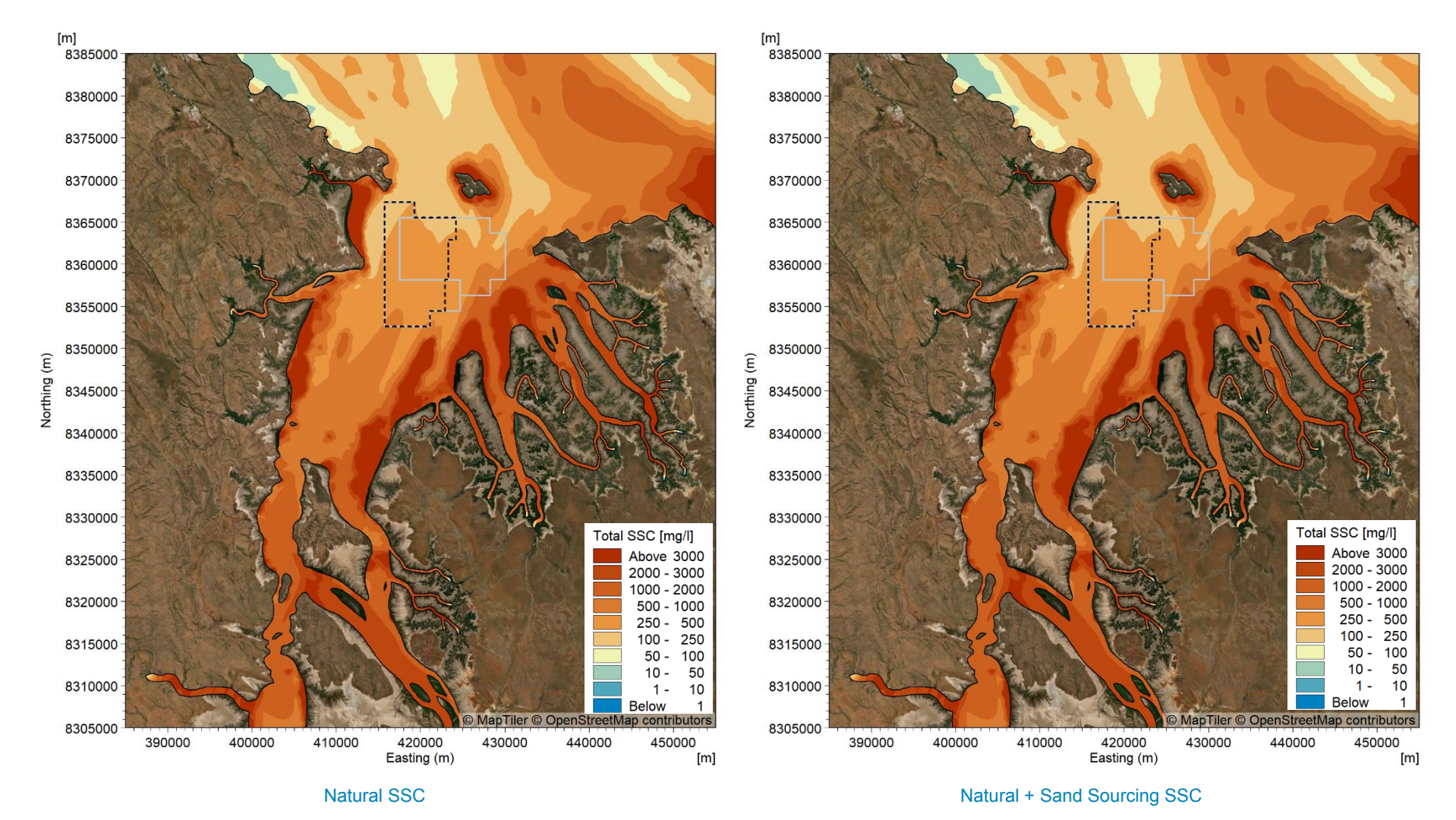


Figure D15. Modelled maximum natural SSC and maximum natural plus sand sourcing SSC for the mid-depth layer when sand sourcing during neap tides over a two-month (61 days) period in the wet season for Scenario 2.

20/01/2025 D16 Cambridge Gulf: Modelling Report



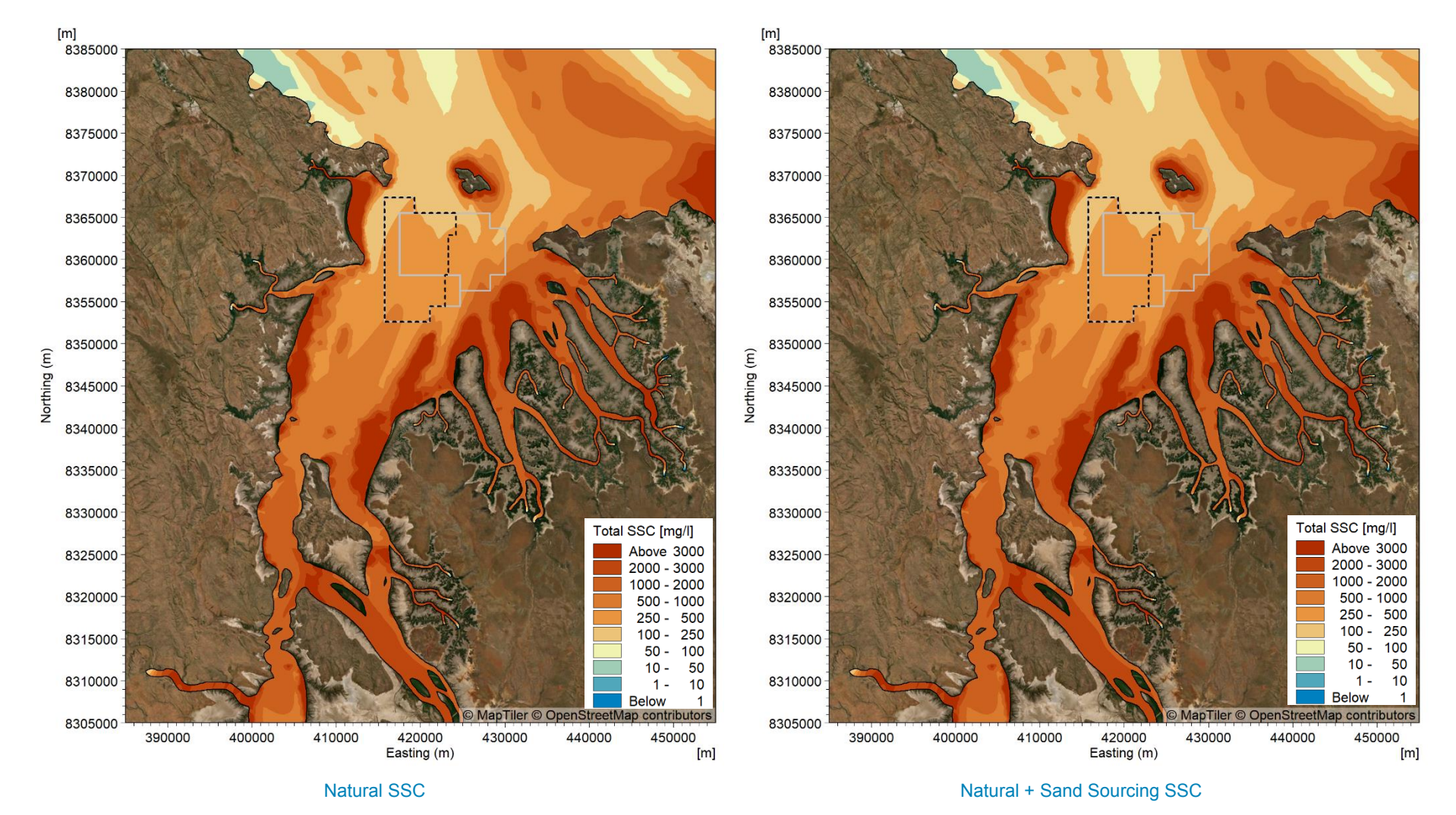


Figure D16. Modelled maximum natural SSC and maximum natural plus sand sourcing SSC for the mid-depth layer when sand sourcing during spring tides over a two-month (61 days) period in the wet season for Scenario 2.

20/01/2025 D17 Cambridge Gulf: Modelling Report



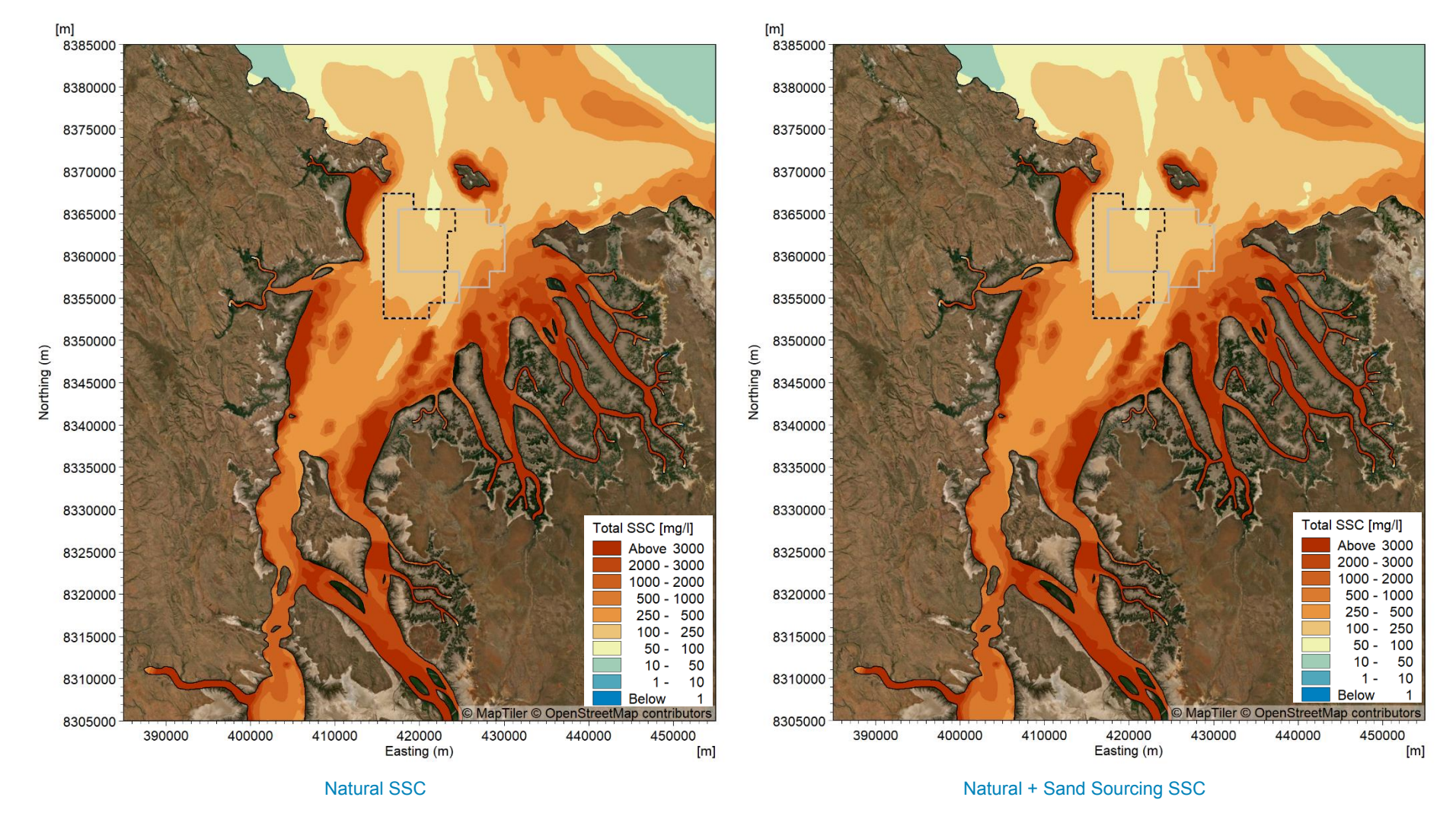


Figure D17. Modelled maximum natural SSC and maximum natural plus sand sourcing SSC for the mid-depth layer when sand sourcing during neap tides over a two-month (60 days) period in the dry season for Scenario 1.

20/01/2025 D18 Cambridge Gulf: Modelling Report



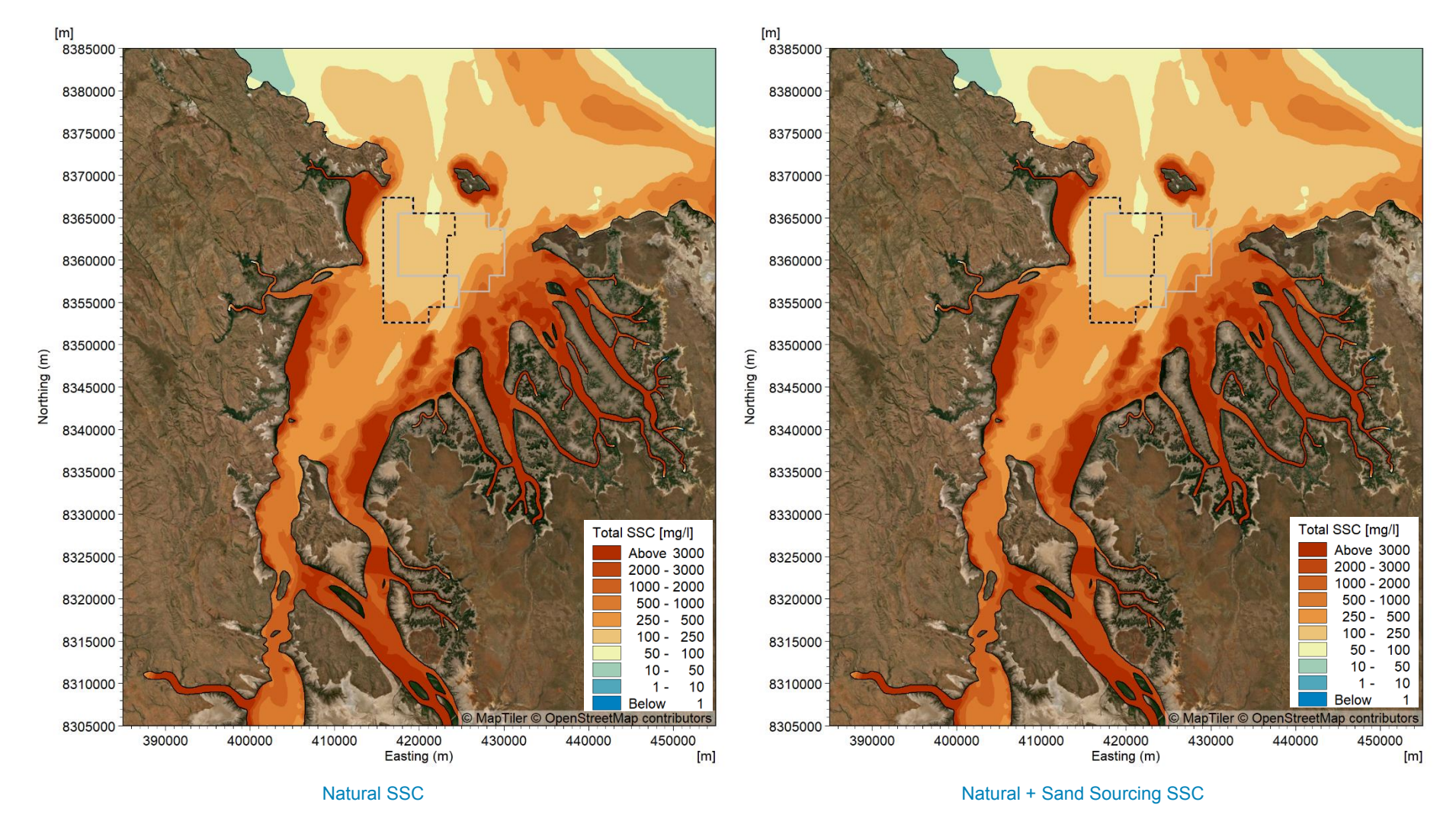


Figure D18. Modelled maximum natural SSC and maximum natural plus sand sourcing SSC for the mid-depth layer when sand sourcing during spring tides over a two-month (60 days) period in the dry season for Scenario 1.

20/01/2025 D19 Cambridge Gulf: Modelling Report



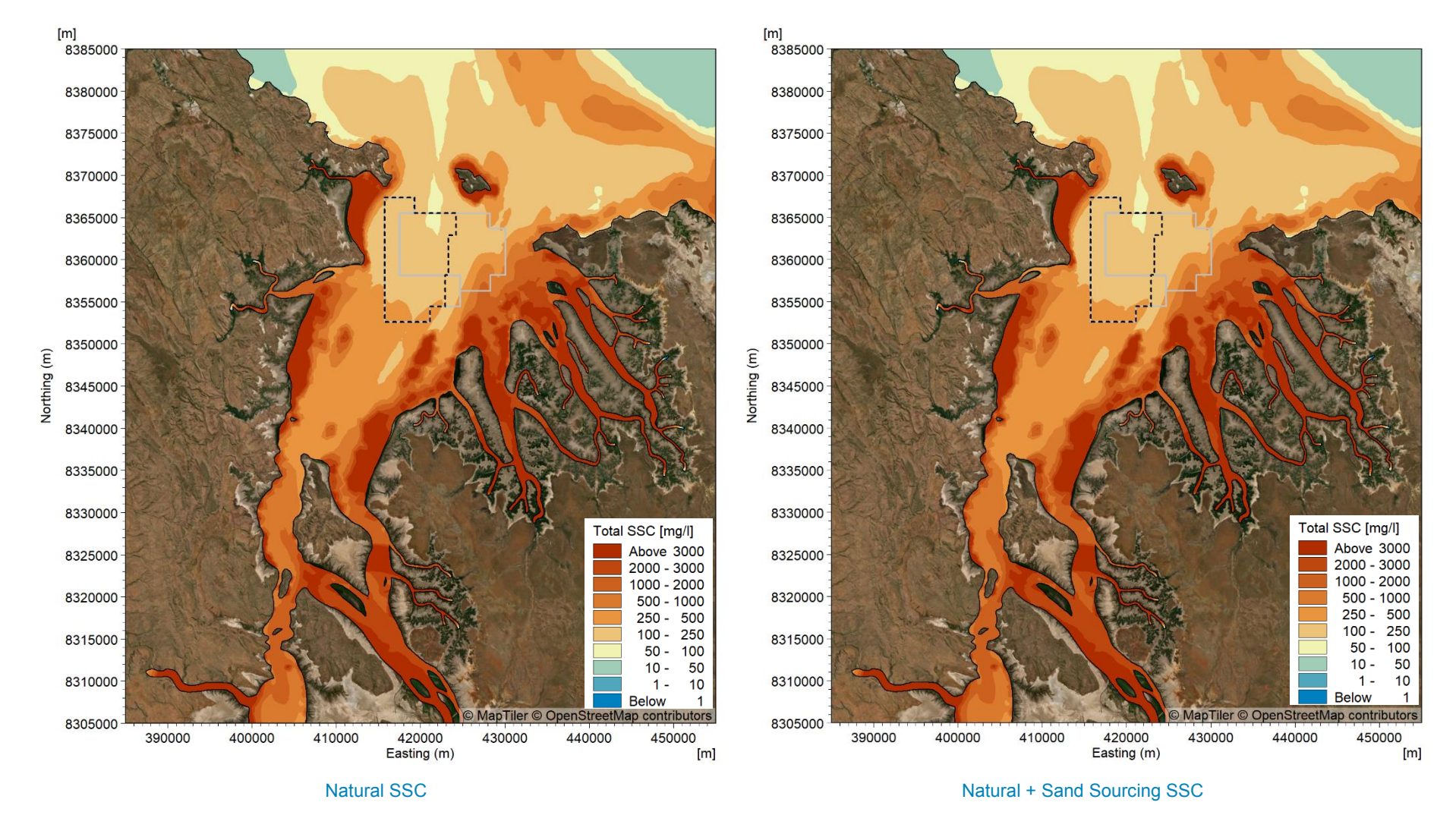


Figure D19. Modelled maximum natural SSC and maximum natural plus sand sourcing SSC for the mid-depth layer when sand sourcing during neap tides over a two-month (61 days) period in the dry season for Scenario 2.

20/01/2025 D20 Cambridge Gulf: Modelling Report



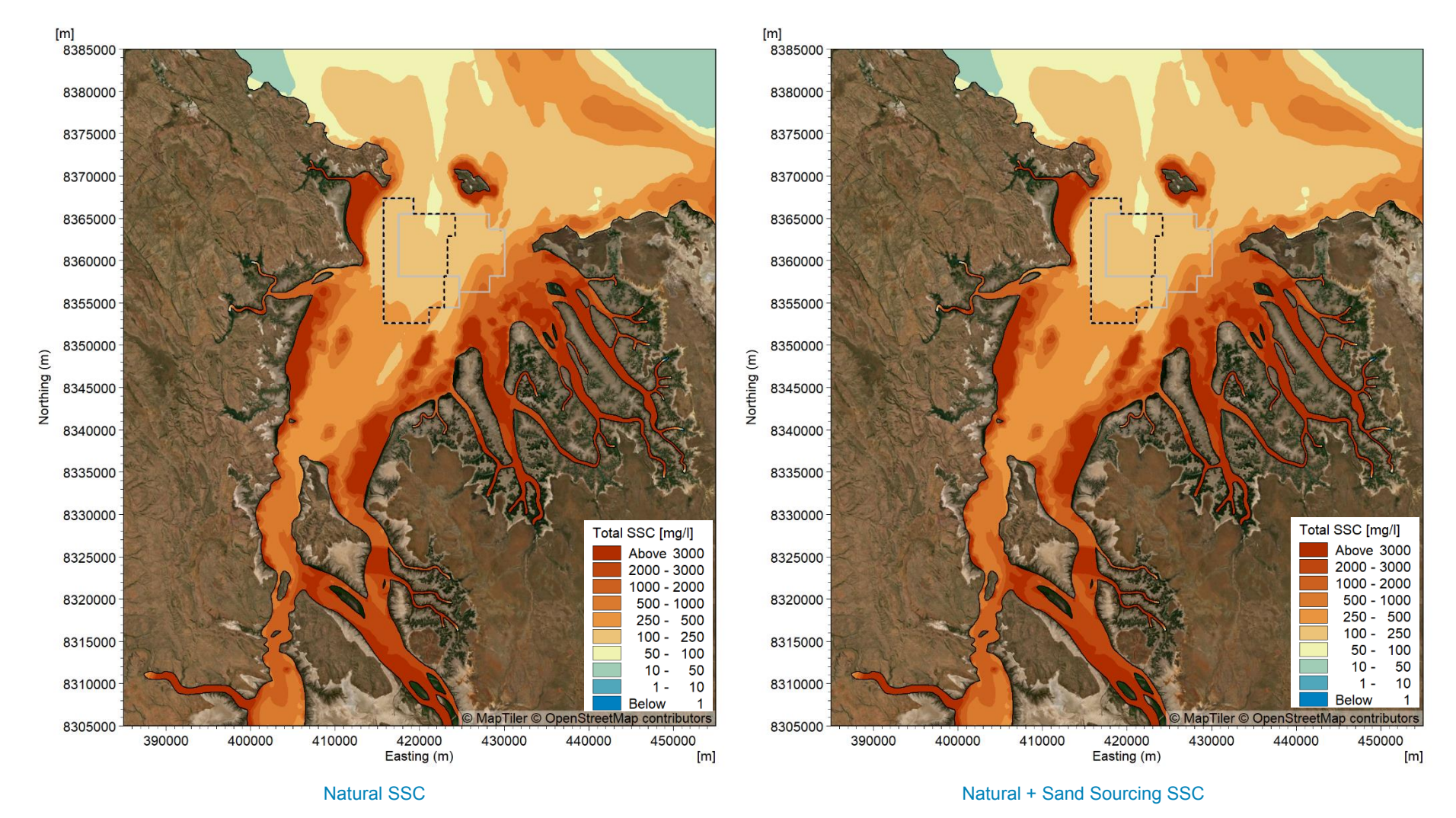


Figure D20. Modelled maximum natural SSC and maximum natural plus sand sourcing SSC for the mid-depth layer when sand sourcing during spring tides over a two-month (61 days) period in the dry season for Scenario 2.

20/01/2025 D21 Cambridge Gulf: Modelling Report



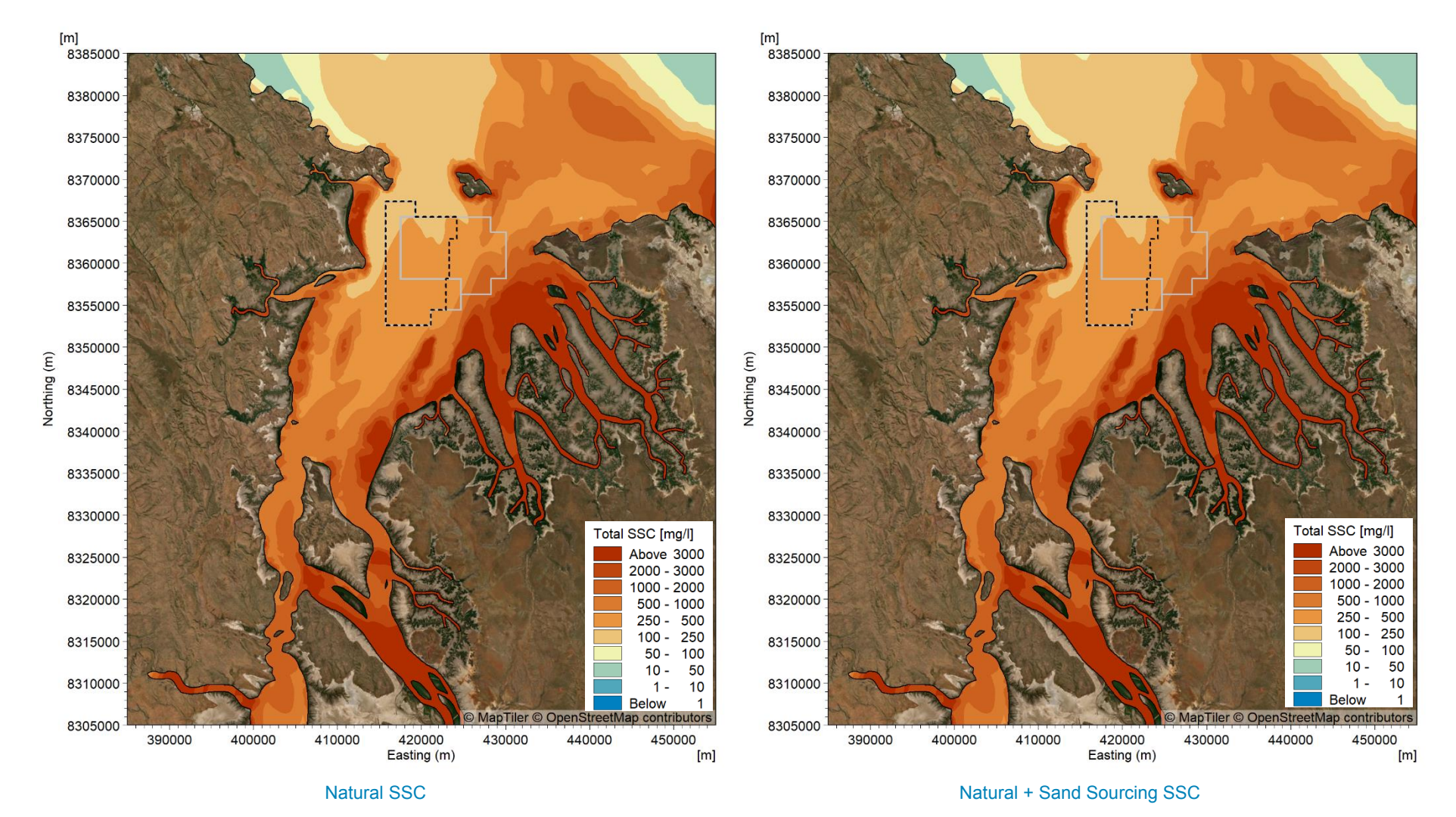


Figure D17. Modelled maximum natural SSC and maximum natural plus sand sourcing SSC for the mid-depth layer when sand sourcing during neap tides over a two-month (61 days) period in the transitional season for Scenario 1.

20/01/2025 Cambridge Gulf: Modelling Report



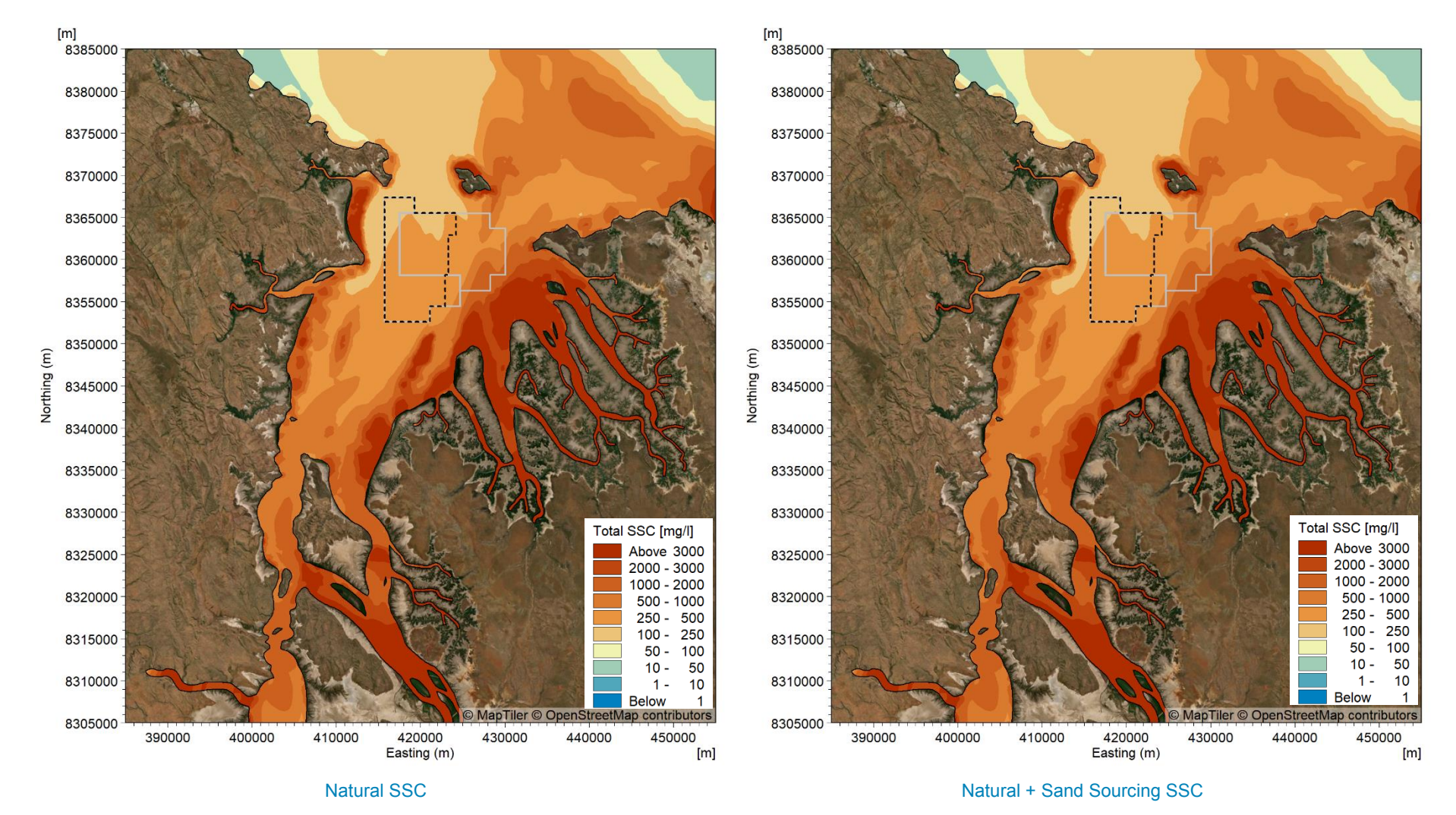


Figure D18. Modelled maximum natural SSC and maximum natural plus sand sourcing SSC for the mid-depth layer when sand sourcing during spring tides over a two-month (61 days) period in the transitional season for Scenario 1.

20/01/2025 D23 Cambridge Gulf: Modelling Report



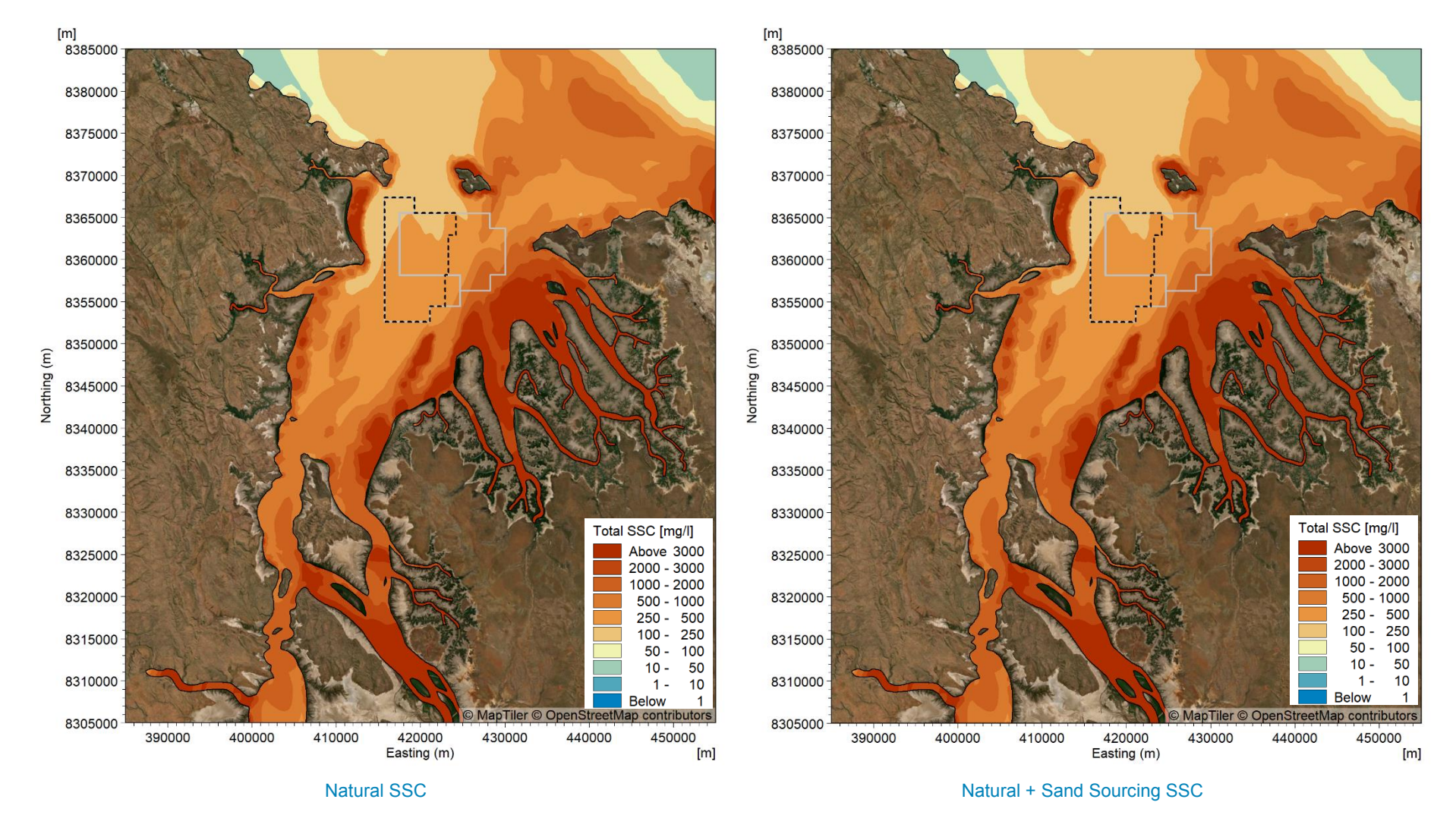


Figure D19. Modelled maximum natural SSC and maximum natural plus sand sourcing SSC for the mid-depth layer when sand sourcing during neap tides over a two-month (61 days) period in the transitional season for Scenario 2.

20/01/2025 D24 Cambridge Gulf: Modelling Report



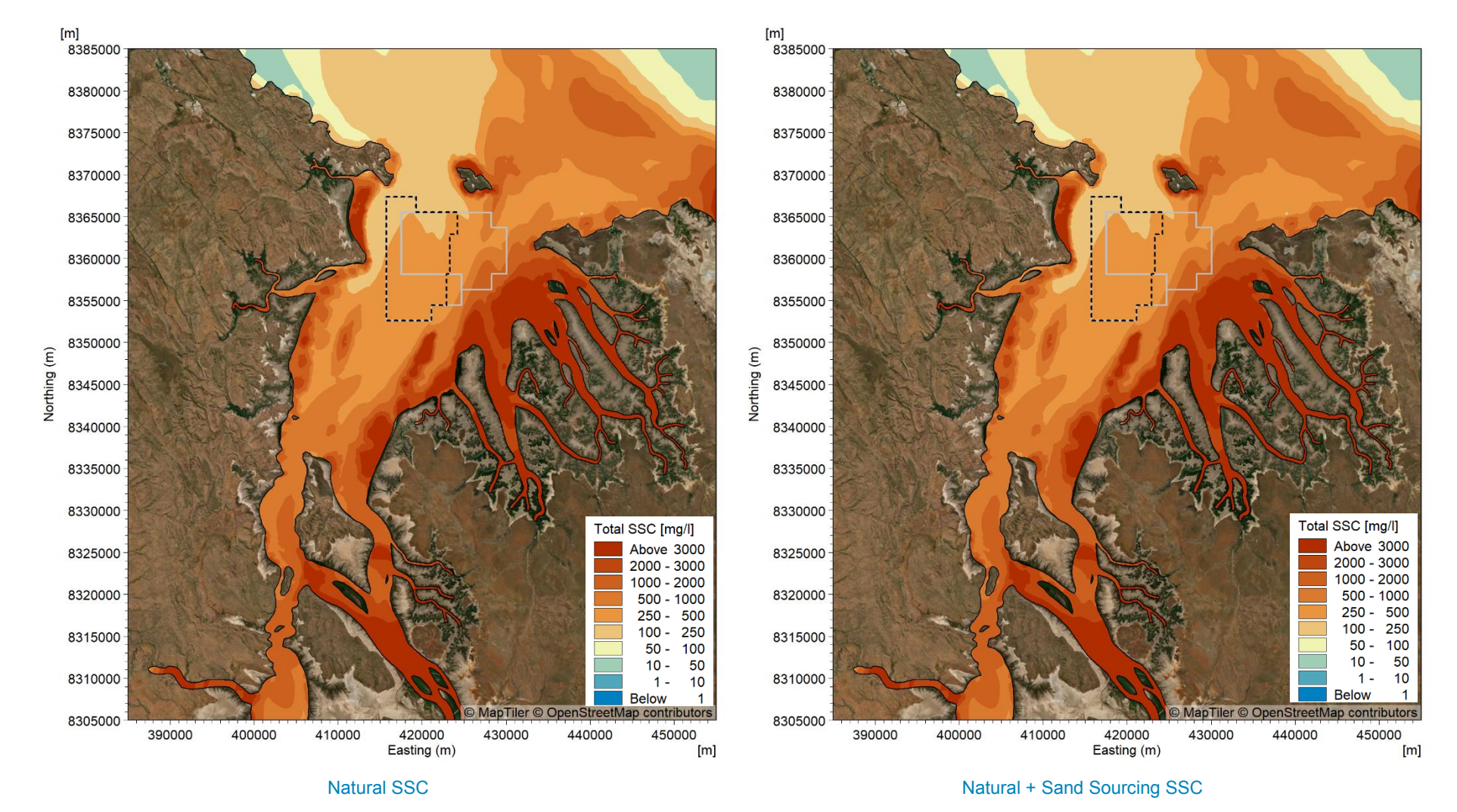


Figure D20. Modelled maximum natural SSC and maximum natural plus sand sourcing SSC for the mid-depth layer when sand sourcing during spring tides over a two-month (61 days) period in the transitional season for Scenario 2.

20/01/2025 Cambridge Gulf: Modelling Report